DEVELOPMENT OF NOVEL STRATEGIES FOR HIV-1 VACCINES

BELKIS MERVE AKIS YILDIRIM, MD

A THESIS SUBMITTED FOR THE DEGREE OF

DOCTOR OF PHILOSOPHY

MICHAELMAS TERM 2025

ST CROSS COLLEGE
UNIVERSITY OF OXFORD

TABLE OF CONTENTS

ABBREVIATIONS

AA	Amino Acid
ADCC	Antibody-Dependent Cellular Cytotoxicity
AddaVax	Squalene-Based Oil-in-Water Adjuvant
AIDS	Acquired Immunodeficiency Syndrome
AMP	Antibody-Mediated Prevention
APC	Antigen-Presenting Cell
ART	Antiretroviral Therapy
BALB/c	Bagg Albino Laboratory-Bred Mice, Substrain c
bNAb	Broadly Neutralizing Antibody
bp	Base Pair
CA	Capsid
CAP256-VRC26.25	Broadly Neutralizing Antibody Targeting the V2 Apex
CAPRISA	Centre for the AIDS Programme of Research in South Africa
cART	Combined Antiretroviral Therapy
CCR5	C-C Chemokine Receptor Type 5
CD4	Cluster of Differentiation 4
CD8	Cluster of Differentiation 8
CD4bs	CD4 Binding Site of the HIV-1 Envelope Glycoprotein
CE	Conserved Elements
CMV	Cytomegalovirus
COVID-19	Coronavirus Disease 2019
CRF	Circulating Recombinant Form
CTL	Cytotoxic T Lymphocyte
CXCR4	C-X-C Chemokine Receptor Type 4
DC	Dendritic Cell
DDD	Triple DNA Vaccine Regimen
DMSO	Dimethyl Sulfoxide
DNA	Deoxyribonucleic Acid
dsDNA	Double-Stranded Deoxyribonucleic Acid
ELISA	Enzyme-Linked Immunosorbent Assay
ELISpot	Enzyme-Linked Immunospot Assay
Env	Envelope Glycoprotein
eOD-GT8	Engineered Outer Domain Germline-Targeting Immunogen
ER	Endoplasmic Reticulum
FBS	Foetal Bovine Serum
FcR	Fragment Crystallizable Receptor
Gag	Group-Specific Antigen
GLA-SE	Glucopyranosyl Lipid A in Stable Emulsion (TLR4 Agonist Adjuvant)
GMP	Good Manufacturing Practice
gp120	Glycoprotein 120
gp140	Glycoprotein 140
gp41	Glycoprotein 41
HBsAg	Hepatitis B Surface Antigen
HBV	Hepatitis B Virus
HCDR3	Heavy Chain Complementarity Determining Region 3

HEPES	4-(2-Hydroxyethyl)-1-Piperazineethanesulfonic Acid
HIV	Human Immunodeficiency Virus
HIV-1	Human Immunodeficiency Virus Type 1
HIV-2	Human Immunodeficiency Virus Type 2
HLA	Human Leukocyte Antigen
HLA-I	Human Leukocyte Antigen Class I
HLA-II	Human Leukocyte Antigen Class II
HPLC	High-Performance Liquid Chromatography
HRP	Horseradish Peroxidase
HVTN	HIV Vaccine Trials Network
ICS	Intracellular Cytokine Staining
IFN-γ	Interferon Gamma
IgA	Immunoglobulin A
IgG	Immunoglobulin G
IgM	Immunoglobulin M
IL-2	Interleukin 2
IN	Integrase , Intranasal
INSTI	Integrase Strand Transfer Inhibitor
IV	Intravenous
kbp	Kilobase Pair
kDa	Kilodalton
LANL	Los Alamos National Laboratory
LEN	Lenacapavir
LTR	Long Terminal Repeat
MA	Matrix Protein
MAb	Monoclonal Antibody
MF59	Squalene-Based Oil-in-Water Emulsion Adjuvant
MHC	Major Histocompatibility Complex
MIP-1α	Macrophage Inflammatory Protein 1 Alpha
MIP-1β	Macrophage Inflammatory Protein 1 Beta
MPER	Membrane-Proximal External Region
mRNA	Messenger Ribonucleic Acid
MVA	Modified Vaccinia Ankara
N6	Broadly Neutralizing Antibody Targeting the CD4 Binding Site
NAb	Neutralizing Antibody
$NaHCO_3$	Sodium Bicarbonate
NALT	Nasopharyngeal-Associated Lymphoreticular Tissue
Nef	Negative Regulatory Factor
NNRTI	Non-Nucleoside Reverse Transcriptase Inhibitor
NPC	Nuclear Pore Complex
NRTI	Nucleoside Reverse Transcriptase Inhibitor
OD	Optical Density
PBMC	Peripheral Blood Mononuclear Cell
PBS	Phosphate-Buffered Saline
PCR	Polymerase Chain Reaction
PFU	Plaque-Forming Unit
PG16	Broadly Neutralizing Antibody Targeting the Variable Loop 2 Apex
PG9	Broadly Neutralizing Antibody Targeting the Variable Loop 2 Apex
PGT121	Broadly Neutralizing Antibody Targeting the Variable Loop 3 Glycan Supersite

PGT145	Broadly Neutralizing Antibody Targeting the Variable Loop 2 Apex
PGT151	Broadly Neutralizing Antibody Targeting the gp120–gp41 Interface
PI	Protease Inhibitor
PIC	Pre-Integration Complex
PIV5	Parainfluenza Virus Type 5
Pol	Polymerase
PrEP	Pre-Exposure Prophylaxis
PRR	Pattern Recognition Receptor
Rev	Regulator of Virion Expression
RNA	Ribonucleic Acid
RPMI	Roswell Park Memorial Institute Medium
RRE	Rev Response Element
RT	Reverse Transcriptase
RTS,S/AS01	Recombinant Hepatitis B Virus Surface Antigen Malaria Vaccine
RV144	Thai HIV Vaccine Trial (ALVAC-HIV/gp120)
SC	Single Chain
SFU	Spot-Forming Unit
SIV	Simian Immunodeficiency Virus
SOSIP	Stabilized Soluble Native-Like gp140 Envelope Trimer
STCL	Short-Term Cell Line
STEP	HVTN 502 HIV Vaccine Clinical Trial
TAP	Transporter Associated with Antigen Presentation
TAT	Trans-Activator of Transcription
TCR	T Cell Receptor
Tfh	Follicular Helper T Cell
Th1	T Helper 1 Cell
Th2	T Helper 2 Cell
TLR4	Toll-Like Receptor 4
TMB	Tetramethylbenzidine
TNF-α	Tumour Necrosis Factor Alpha
Tregs	Regulatory T Cells
TTT	Triple Tandem Trimer
UK	United Kingdom
USA	United States of America
Vif	Virion Infectivity Factor
VLP	Virus-Like Particle
Vpr	Viral Protein R
Vpu	Viral Protein U
VRC01	Broadly Neutralizing Antibody Targeting the CD4 Binding Site
WHO	World Health Organization
10-1074	Broadly Neutralizing Antibody Targeting the Variable Loop 3 Glycan Supersite
10E8	Broadly Neutralizing Antibody Targeting the MPER of gp41
2F5	Broadly Neutralizing Antibody Targeting the MPER of gp41
2G12	Broadly Neutralizing Antibody Targeting High-Mannose Glycans on Env
3BNC117	Broadly Neutralizing Antibody Targeting the CD4 Binding Site
4E10	Broadly Neutralizing Antibody Targeting the MPER of gp41
8ANC195	Broadly Neutralizing Antibody Targeting the gp120-gp41 Interface

LIST OF FIGURES

LIST OF TABLES

ACKNOWLEDGEMENTS

I would like to express my sincere gratitude to my supervisor, Professor Tomáš Hanke, for his invaluable guidance, constructive feedback, and support throughout my D.Phil studies. I am also grateful to my supervisor, Dr. Nicola Borthwick, and to Dr. Edmund Wee for everything they have taught me. Their mentorship contributed greatly to where I am today.

I would also like to acknowledge the postdoctoral fellows, D.Phil students, and research scientists at the Jenner Institute for their generous assistance and insightful discussions.

I am thankful to my family for their endless love and encouragement. My husband, Dr. Muhammed Raşit Yıldırım, has always supported me. I am deeply grateful for his love and all his efforts. I began my doctorate when our daughter, Zeynep Meva, was just three months old. She is now four years old, the sweetest child in the world for me, and my little friend.

I would like to express my heartfelt thanks to my father, Prof. Dr. Metin Akis, and my mother, Yasemin Akis, for always believing in me, standing by me, and inspiring me to achieve more. You have played an enormous role in every success I have had since childhood.

I also sincerely thank my brothers, Dr. Ahmet Sefa Akis and Muhammed Kayra Akis, for their love and support. My gratitude also extends to my brother's wonderful wife, Fatma Nur Ergin Akis, and to my sweet, beloved nephew, Metin Yiğit, who is a constant source of joy.

I am deeply grateful to my dear father-in-law, Prof. Dr. Ahmet Yıldırım, and dear my mother-in-law, Meral Yıldırım, for their love, support, help, and prayers.

My heartfelt thanks go to my dear friends Beatrice Nassanga, Sarah Batawi, and Merve Nur Semiz Almalıoğlu for their love, support, the time they shared with me.

Finally, I gratefully acknowledge the Turkish Ministry of National Education; this doctoral research was conducted under the Ministry's sponsorship.

This thesis is dedicated to my beloved daughter, Zeynep Meva Yıldırım…

PUBLICATIONS ARISING FROM THIS THESIS

- **Belkis M Akis Yildirim, MD***, Chama Chanda, MBChB* , Freddie Kibengo, MD* , Michael Mutua, MBChB* , Fred Ogada, MSc* , Vincent Muturi-Kioi, MBChB* *et al*. Safety and Broad Immunogenicity of HIVconsvX Conserved Mosaic Candidate T-Cell Vaccines Vectored by ChAdOx1 and MVA in HIV-CORE 006: A Double-Blind, Randomized, Placebo-Controlled Phase 1 Trial in Healthy Adults Living Without HIV-1 in Eastern and Southern Africa. Lancet Microbe. 2025 Jun;6(6):101041. doi: 10.1016/j.lanmic.2024.101041. Epub 2025 May 16. PMID: 40388952; PMCID: PMC12134052.

- Nicola Borthwick, PhD, Natalia Fernandez, MSc, Peter J Hayes, PhD, Edmund G-T Wee, PhD, **Belkis M Akis Yildirim, MD**, Andrea Baines, BSca *et al*. Safety and immunogenicity of the ChAdOx1-MVA-vectored conserved mosaic HIVconsvX candidate T-cell vaccines in HIV-CORE 005.2, an open-label, dose-escalation, first-in-human, phase 1 trial in adults living without HIV-1 in the UK. Lancet Microbe. 2025 Mar;6(3):100956. doi: 10.1016/j.lanmic.2024.100956. Epub 2024 Nov 26. PMID: 39612921.

- Ashley C. Beavis1, Edmund G. -T. Wee, **Belkis M. Akis Yildirim**, Nicola Borthwick, Biao He, and Tomáš Hanke. Combined intranasal and intramuscular parainfluenza 5-, simian adenovirus ChAdOx1- and poxvirus MVA-vectored vaccines induce synergistically HIV-1-specific T cells in the mucosa. Front Immunol. 2023 Jul 17;14:1186478. doi: 10.3389/fimmu.2023.1186478. PMID: 37529048; PMCID: PMC10390215.

ABSTRACT

Human Immunodeficiency Virus (HIV-1) remains a global health challenge, with more than 38 million people living with the virus and over a million new infections annually. Although antiretroviral therapy has transformed HIV infection into a manageable chronic disease, lifelong treatment, high cost and drug resistance emphasize the urgent need for an effective prophylactic vaccine. The extraordinary genetic diversity of HIV-1 and its capacity to evade host immunity have hindered vaccine development for decades. This thesis aims to address these challenges by characterizing T-cell responses induced by conserved-region mosaic HIVconsvX vaccines delivered by ChAdOx1 and MVA vectors in clinical trials, and by investigating alternative PIV5 vector delivery to enhance mucosal immunity, alongside evaluating a novel VLP platform designed to elicit humoral responses, to inform next-generation HIV-1 vaccine designs.

A critical barrier to HIV vaccine success is the virus's global sequence variability. To overcome this, the HIVconsvX vaccine design focuses immune responses on functionally conserved regions of the HIV proteome using rationally engineered bivalent mosaic immunogens. In a phase I clinical trial conducted in the UK, HIVconsvX immunogens in a heterologous prime-boost regimen with ChAdOx1 and MVA vectors induced broad, high-frequency, and polyfunctional $CD8^+$ T-cell responses. Every participant mounted detectable responses, which recognized both vaccine-encoded epitopes and variant sequences beyond them.

Defining the breadth of vaccine-elicited T cell response is essential for a globally relevant HIV vaccine design. Through comprehensive epitope mapping across clinical trials in the UK and sub-Saharan Africa, this work demonstrated that HIVconsvX vaccination induced a broad epitope recognition across the vaccine immunogen in distinct cohorts. The key advantage of the HIVconsvX vaccine lies in its focus on highly conserved epitopes, therefore all have the potential to contribute to protective immunity. We also defined minimal 9-mer $CD8^+$ T-cell epitopes and their HLA restrictions to inform future vaccine designs.

Since HIV's primary gates are mucosal surfaces, effective vaccines must induce protective immunity at these sites. We evaluated an intranasal vaccine strategy using PIV5-vectored HIVconsvX immunogens. In murine models, intranasal delivery of PIV5-based vaccines, in combination with ChAdOx1 or MVA in heterologous regimens, enhanced mucosal T-cell responses. The bivalent mosaic design further expanded recognition of epitope variants beyond the vaccine immunogen.

While cellular immunity is vital for viral control, durable protection likely requires potent neutralizing antibodies. To address this, a virus-like particle-based vaccine displaying stabilized HIV Env trimers was engineered using SpyTag/SpyCatcher plug-and-display technology. Our VLP.TTT design preserved the native conformation of key broadly neutralizing antibody (bnAb) epitopes and enabled multivalent antigen display. In murine immunization studies, adjuvanted VLP.TTT induced significantly higher antibody titres after the first immunization compared with soluble Env trimers, demonstrating accelerated priming and efficient B-cell activation. These results highlight the potential of modular VLP-based systems to elicit strong humoral immunity against HIV-1.

This thesis presents a coherent, multi-arm vaccine strategy and informs future efforts toward a broadly protective HIV-1 vaccine.

CHAPTER 1: INTRODUCTION

1.1 The Global HIV/AIDS Pandemic: An Ongoing Challenge

Despite the considerable progress that has been made in prevention and treatment over the past four decades, HIV/AIDS (Human Immunodeficiency Virus/ Acquired Immune Deficiency Syndrome) pandemic remains a significant global health challenge [1]. In 2023, an estimated 39.9 million people were living with HIV worldwide, with 1.3 million new infections occurring in that year alone. Since the emergence of HIV, 88.4 million [71.3-112.8 million] people have been infected with HIV and about 42.3 million [35.7-51.1 million] people have died of AIDS-related causes; 630 000 of these deaths were in 2023 [2]. New HIV infections have been reduced by 60% since the peak with 3.3 million [2.6 million-4.2 million] people in 1995, but this fall is far short of the target of getting below 370,000 by 2025. The burden of HIV/AIDS is not evenly distributed. Sub-Saharan Africa continues to be the most severely affected region, accounting for over half of all people living with HIV globally [2, 3].

1.1.1 Historical Context and Epidemiology of HIV/AIDS

HIV/AIDS emerged in the early 1980s. The first AIDS cases were reported in men-who-have-sex with-men in 1981 [4]. The syndrome was characterized by a seriously impaired immune system. In 1983, Luc Montagnier and Françoise Barré-Sinoussi isolated the retrovirus from an AIDS case at the Pasteur Institute in Paris [5]. The virus initially referred as HTLV-3, is now named as HIV [6].

The discovery of HIV as the cause of AIDS led to rapid advancements in understanding the virus and developing diagnostic assays [7]. In 1985, the first HIV antibody test was approved by the FDA, allowing for screening of blood supplies and diagnosis of infected individuals [8].

The first anti-HIV drug zidovudine, a reverse transcriptase inhibitor was described in 1987 [9]. Subsequently, several additional targets for antiviral therapy were identified, such as HIV protease and integrase [10, 11] In the mid-1990s, treatment of HIV/AIDS was redefined by the development of HIV protease inhibitors and the introduction of combination antiretroviral therapy (cART) [10]. Thereafter, AIDS-related deaths reduced and the quality of life for people living with HIV improved [12]. The Global Fund, to Fight AIDS, Tuberculosis and Malaria, and U.S. President's Emergency Plan for AIDS Relief (PEPFAR), launched in the early 2000s. These initiatives worked closely with governments and significantly expanded access to HIV treatment and prevention services in the countries with a high HIV burden, primarily in sub-Saharan Africa, along with parts of Asia, the Caribbean, and Eastern Europe [7, 13].

Despite progress, certain populations continue to be disproportionately affected by HIV. The relative risk of acquiring HIV is 14-fold higher for people who inject drugs, 23 times higher for men who have sex with men, 9 times higher for sex workers and 20 times higher for transgender individuals than in the wider population globally. These key populations and their sexual partners accounted for 55% of new HIV infections in 2022 [2]. Young women and adolescent girls in sub-Saharan Africa remain particularly vulnerable, with AIDS-related illnesses the leading cause of death for women aged 15-59 in the region [14].

1.1.2 The Public Health and Economic Impact of HIV/AIDS

HIV/AIDS pandemic continues to pose significant public health and economic challenges globally [1]. The burden of HIV/AIDS on healthcare systems remains considerable, especially in resource-limited settings where HIV/AIDS prevalence is highest [15].

Healthcare providers in high-prevalence regions face ongoing challenges such as limited resources, lack of training, and infrastructural challenges in comprehensive HIV care, including diagnosis, treatment, and management of comorbidities [16]. The lifelong ART needs continuous engagement with health services, and creates a growing population of chronic patients requiring regular follow-up and medication straining already limited resources in many countries. This demand for care adds to the workload of health systems that are already struggling to provide basic healthcare services. For example, scaling up ART for all eligible individuals would require a substantial increase in the number of doctors [17]. Nearly two-thirds of medical admissions [18], and 20.2% to 24.5% of outpatient visits were related to HIV/AIDS care in South Africa [19], indicating a substantial burden on healthcare services contributing to overcrowding and reduced quality of care for both people living with and without HIV.

Integrating HIV services into primary healthcare services, such as tuberculosis control and maternal and child health programs demonstrates measurable improvements in health outcomes in sub-Saharan Africa [20]. Integration of ART services into maternal and child health services resulted in both improved viral suppression outcomes in postnatal, breastfeeding women who are living with HIV and initiated ART treatment during their pregnancy. 77% of women receiving integrated services were virally suppressed at 12 months postpartum compared with 56% of women who were referred to separate clinics for ART [21]. Integrated TB/HIV care was consistently cost-effective [22], and the survival can be maximized in patients co-infected with TB and HIV with $CD4^+$ cell counts <50 cells/μl by starting ART soon after TB treatment initiation [23]. Well-coordinated collaborations with host governments, private sector businesses, international partners, development financial institutions, and non-governmental organizations are necessary to maximize HIV and primary health care integration. For the program to be successful, local communities and civil society organizations must be involved [21].

The socioeconomic impact of HIV/AIDS is beyond the healthcare sector, affecting individuals, households, and entire communities. At the individual level, HIV infection can reduce the productivity, cause loss of employment, and increased health-related expenditures [24]. Average monthly household income was reportedly lower in people living with HIV than people living without HIV across Cambodia [25], China[26], India [27] and Myanmar [28] with the smallest income difference between people living with HIV and people living without HIV reported from India (US $15.41) [27] while a significant difference was reported from China[26]. The productivity loss through lost work time or caring responsibilities due to HIV/AIDS is an ongoing challenge despite advances in treatment [24]. Unemployment was 77% and 54% for people living with HIV and people living without HIV respectively; similarly, non-attendance to work per month was 2.65 and 0.67 days respectively [25]. Health service expenditure was reportedly higher in people living with HIV than people living without HIV [24]. Monthly average household HIV-related medical expenditure in people living with HIV ranged from US $14.31 (12% of household income) in Nepal [29] to US$279.91 (25% of household income) in India [27].

HIV/AIDS pandemic disproportionately affects working-age adults, leading to a reduction in the labour force and human capital in heavily affected countries. This demographic impact has long-term consequences for economic growth and development [30].

Despite these challenges, increased access to ART decreased some of the economic impacts of HIV/AIDS by allowing people living with HIV to remain productive members of society [31]. Two studies from India reported that ART led to increased employability by 47% [32] and increased income level by 25% in people living with HIV [33].

HIV's impacts on public health and economy remain substantial. Continued investment for the development of a preventive vaccine and a functional cure for HIV, treatment, and health system strengthening is crucial to mitigate these impacts and achieve global health and development goals [1].

1.2 Molecular Biology of HIV-1

1.2.1 Structure and Genome Organization of HIV-1

HIV-1 is a retrovirus with a genome consisting of two identical single-stranded positive-sense RNA molecules, each approximately 9.7 kb in length, enclosed within the core of the virus particle [34]. The mature HIV particle is approximately 100 nm in diameter, with an outer lipid bilayer derived from the host cell membrane as its envelope [35]. This envelope contains 7-14 knobs which are composed of trimers of the Env proteins [36]. The mature conical capsid (CA) structure consists of ~1500 p24, a 24 kDa structural protein, monomers assembled in a hexagonal grid that is closed by incorporating 12 pentamers [37-39]. This capsid houses the viral RNA genome along with viral enzymes Reverse Transcriptase (RT) and Integrase (IN) bound to the viral RNA [34].

HIV-1 genome contains 9 open-reading frames (ORFs) which collectively encode 15 viral proteins [40]. The *gag* ORF encodes the Gag polyprotein precursor that is later processed by viral protease (PR) into four structural proteins: matrix (MA), CA, nucleocapsid (NC), and p6 [41]. The *pol* ORF encodes the Pol protein that splits into viral three viral enzymes: PR, RT, and IN [42]. The two essential steps, the conversion of RNA genome into a double-stranded DNA and then the integration of this viral DNA genome into the chromosome of the host cell are catalysed by RT and IN respectively [43]. The *env* ORF encodes Env that is synthesized as a non-fusogenic polyprotein precursor, gp160. The Env is cleaved by furin protease into the gp120 and the gp41 subunits, which later remain non-covalently associated [44, 45]. The other six ORFs encode the accessory proteins such as virion infectivity factor (Vif), viral protein R (Vpr), viral protein U (Vpu), and negative factor (Nef), as well as the regulatory proteins like trans-activator of transcription (Tat) and regulator of expression of virion (Rev) [44] . Vif tags the potent antiviral enzymes APOBEC3G and APOBEC3F (apolipoprotein B mRNA-editing enzyme catalytic polypeptide-like 3G and 3F) to induce their proteasomal degradation in lymphocytes and monocytes [46, 47]. Vpr regulates the nuclear import of HIV-1 pre-integration complex (PIC) by interacting with karyopherin α and enhancing its affinity for viral nuclear localization signals (NLSs). This interaction facilitates the docking and transport of PIC across the nuclear pore complex (NPC). Without Vpr, the nuclear import of these complexes is significantly impaired [48]. Vpu increases the release of progeny virions from infected cells [49]. The first mechanism is counteracting the effect of

Tetherin (also known as BST-2), a host restriction factor that inhibits the release of virions from infected cells [50]. Newly synthesized CD4 molecules bind Env precursor protein with high affinity within the endoplasmic reticulum. This interaction prevents the transport and processing of Env precursor to gp41 and gp120 and reduce secretion of infectious progeny virion particles from infected cells [51, 52]. As the second mechanism, Vpu induces the rapid degradation of CD4, reducing its half-life from 6 hours to 12 minutes, through the ubiquitin-proteasomal pathway [52, 53].

Nef down-regulates the cell surface expression of CD4 [54], CD8 [55], CD28 [56], major histocompatibility complex class I (MHC I) [57] and class II (MHC II) [58] proteins, employing several strategies that linked to unique regions within the Nef protein [59]. MHC I down-regulation protects HIV-infected cells from host CTL detection, while reduced CD28 and CD4 expression likely limits the adhesion of Nef-expressing T-cell to antigen-presenting cells. These mechanisms promote the movement of HIV-infected cells in circulation and the spread of virus [60]. Additionally, Nef regulates cholesterol trafficking in HIV-infected cells by binding cholesterol via a cholesterol-recognition motif at its carboxyl-terminus, to direct newly synthesized cholesterol to the site of viral budding [60, 61]. The Tat protein binds to TAR (transactivation-responsive element), an RNA region at the 5' end of viral mRNAs, potently transactivates Long terminal repeat (LTR)-driven transcription, and increases the viral gene expression [62, 63].

HIV-1 proteome is expressed from alternatively spliced and un-spliced genomic RNAs [64]. In the early phase of infection, HIV-1 RNAs that are not fully spliced are recognized by the host cellular system as immature. They are retained in the nucleus and eventually degraded [65]. However, *rev* and the other fully spliced mRNAs are exported to the cytoplasm as they are recognized as mature transcripts [66, 67]. Once Rev protein is produced in the cytoplasm, it is imported into the nucleus through its NLS [68]. In the nucleus, Rev interacts with the Rev Response Element (RRE), which is an RNA motif in un-spliced HIV-1 transcripts, to facilitate their nuclear export to the cytoplasm, and to lead the production of the viral progeny [64, 69].

HIV-1 LTR, like its eukaryotic promoter counterparts, regulates proviral gene expression via cis-acting DNA sequences in its U3, R, and U5 regions, that include the TAR element, core promoter, enhancer, and modulatory regions [70, 71]. The LTR serves as a convergence point for host transcription factors, such as NF-κB, and Tat, Vpr viral proteins that activate the LTR to support higher levels of viral gene expression [72].

1.2.2 HIV-1 Lifecycle and Pathogenesis

The first step of HIV-1 lifecycle is the attachment of the virus to the Cluster of Differentiation 4-positive ($CD4^+$) cells, predominately $CD4^+$ T helper lymphocytes [73]. The gp120 protein interacts with the CD4 receptor on the T-cell surface, which induce a conformational change in gp120, allowing it to attach to either the C-C chemokine receptor type 5 (CCR5) or C-X-C chemokine receptor type 4 (CXCR4) co-receptors [74]. This attachment triggers structural rearrangements on gp41, which mediates the fusion of the viral and cellular membranes [74].

After the fusion, the capsid is released into the host cell cytoplasm and transported to the nucleus [73]. The RT converts the viral RNA genome into double-stranded DNA (dsDNA) [75]. The viral DNA

stably associates with IN and other proteins as PIC that is later transported to the nucleus through the nuclear pore complex (NPC) for subsequent integration into the host cell genome [76]. Prior to nuclear entry, CA is considered to be shed through uncoating. However, the recent observation showed that some CA remains associated with the PIC in the nucleus [77, 78]. In the nucleus, the PIC-associated IN inserts the viral DNA particularly into transcriptionally active chromatin regions [44]. Notably, the subset of CA molecules plays a key role in nuclear transport and preferential targeting of actively transcribed genes for HIV-1 integration [79, 80]. Viral DNA integration establishes the provirus that persists during lifetime of the host cell [81]. The provirus is transcribed by the host RNA polymerase II to generate spliced viral mRNAs and non-spliced genomic RNA [82, 83]. These viral RNA transcripts are transported from the nucleus to the cytoplasm for viral protein production and genome encapsidation [84]. The packaging of the viral RNA is a tightly regulated process. The retroviruses preferentially encapsidate their own genomic RNA over cellular RNAs through specific interactions between Gag and RNA. HIV-1 regulates genome packaging by recognizing the dimeric RNA structure, and the interaction of Gag and dimeric RNA serves as the foundation point of virus assembly [85-87]. Subsequently, the viral proteins and the viral ssRNA genome are transported to the host cell's plasma membrane, where the immature virus assembles [88]. Finally, through the late steps of budding, release, and maturation, infectious progeny virions are generated to complete the HIV-1 replication cycle [89].

HIV-1 has numerous mechanisms to evade the host immune system and establish persistent infection. The genetic variability is one of the major immune evasion strategies [90]. The HIV-1 RNA genome randomly mutates because of the error prone reverse transcriptase and lack of proofreading activity [91]. The high mutation rate contributes to escape from virus-specific antibodies and cytotoxic T lymphocytes (CTLs) [92]. Furthermore, the highly glycosylated viral envelope and its 'last-minute' conformational change at the time of viral entry make HIV-1 difficult to block with neutralizing antibodies [93]. HIV-1 also can hide from the immune system in immune-privileged sanctuaries: microglial cells of the central nervous system, and resting T-cells [93]. These mechanisms contribute to the chronic nature of HIV-1 infection and pose challenges for vaccine development.

HIV-1 infection leads to chronic immune activation, leading to B-cell hyperactivation and dysfunction. This is characterized by increased polyclonal activation, hypergammaglobulinemia, elevated production of autoantibodies, and an increased risk of B-cell malignancies [94-96]. Chronic HIV infection also results in B-cell exhaustion, marked by increased expression of inhibitory receptors, poor proliferative capacity, and impaired antibody diversification [97]. While most B-cell abnormalities are reversible with effective ART, deficits in memory B-cell numbers and function often persist despite ART, leading to impaired responses to vaccines and secondary infections [98].

HIV-1 selectively targets $CD4^+$ T-cells for infection, using their CD4 receptor surface expression and co-receptors such as CCR5 and CXCR4 for entry [73]. The progressive $CD4^+$ T-cell depletion effectively weakens the immune system, and is strongly correlated with disease progression, leading to the AIDS stage of the infection [99]. Additionally, because of the use of CCR5, infecting strains particularly infect the more differentiated effector memory subset, compromising the majority of $CD4^+$ T-cells in extra-lymphoid effector sites such as the intestinal mucosa, long before the onset of AIDS [100]. Beyond the quantitative loss, the persistent viral infection also induces functional impairments in $CD4^+$ T-cells. Functionally inactivated $CD4^+$ T-cells fail to produce effector cytokines (i.e.,

interleukin-2 and tumour necrosis factor alpha), and have reduced proliferative capacity, further compromising an efficient and effective antiviral immune response [101].

$CD4^+$ T-cells also play a role as reservoirs for latent virus. Chun *et al*. demonstrated that ART initiation in people living with HIV-1 as early as 10 days after the onset of symptoms of primary infection does not prevent the generation of latently infected $CD4^+$ T-cells carrying infectious virus [102].

HIV-1 infection causes direct and indirect pathogenic effects on both mature $CD4^+$ T-cells and their progenitor cells, mainly with apoptosis which is mediated by caspase-3 in permissive T-cells [103, 104]. Non-permissive (abortive) T-cells undergo pyroptosis which is an inflammatory cell death mediated by caspase-1, and release cytokines that cause further pyroptosis in a vicious cycle [105].

The number of apoptotic cells greatly exceeds the number of HIV-infected cells in most cases, indicative of bystander cell death [104, 106]. In non-permissive $CD4^+$ T-cells, the accumulation of incomplete reverse transcripts also activates caspase-3 and caspase-1-driven proapoptotic and proinflammatory responses [104]. Moreover, nearly every HIV protein (Env, Nef, Tat, protease, Vpr) can cause apoptosis mainly through the members of tumour necrosis factor family, or via the mitochondrial apoptotic pathway [107]. Understanding the mechanisms underlying $CD4^+$ T-cell depletion and dysfunction is critical for developing strategies to protect immune function and achieve durable HIV remission.

1.3 Host Immune Response to HIV-1

The majority of HIV-1 infections are transmitted by sexual exposure through the genital tract or rectal mucosa [108]. For sexual transmission of HIV-1 to occur, virus present in semen or vaginal secretions should cross the mucosal epithelial barrier [109]. Numerous biological factors influence the transmission rate per exposure, including virus strain and dose, epithelial damage during sexual intercourse, coexisting ulcerative anogenital infection, menstrual phase, cervical ectopy, circumcision status, use of oral contraceptives, and genetic predispositions [109-112]. Following the virus transmission, there is a ~10 days eclipse phase, before viral RNA becomes detectable in the plasma [113]. Dendritic cells (DCs) in mucosal tissues capture the virus using a surface molecule called DC-specific C-type lectin (DC-SIGN-CD209), which binds to gp120, then transport the virus to secondary

lymphoid tissues where many activated $CD4^+$ $CCR5^+$ T-cells are located [114]. Plasma virus levels increase exponentially, peaking at 21-28 days after infection [115] . Subsequently, the viral load declines over a period of 12-20 weeks and reaches a more stable level, known as the viral set point [116]. While the viral load begins to decline, the virus undergoes diversification, and multiple escape mutants are selected under the pressure of adaptive immune responses[117].

HIV-1 elicits humoral and cellular immunity but these responses are ultimately insufficient to eliminate the virus [118]. The disease progression and the eventual development of AIDS are mainly determined by the balance between viral replication and the host immune response [119]. Less than 1% of people living with HIV-1 maintain long-term control of the plasma viral load below limits of detection without antiretroviral therapy [118].

1.3.1 Innate Immunity: The First Line of Defence

The innate immune system is the body's first line of defence against viruses. It rapidly responds in the same way to invaders, which is why it is referred to as the "non-specific" immune system [120, 121]. The innate immune response to virus infection starts with the pathogen detection and innate immune signalling in the infected cell [122]. Detection of pathogen associated molecular patterns (PAMPs) in viral components by the host cell's pathogen-recognition receptors (PRRs) initiates an intrinsic innate immune response for virus restriction [120]. This response also generates cell-mediated and soluble factors, such as type I and type III interferon (IFN), proinflammatory cytokines and chemokines. These molecules recruit and activate macrophages, NK cells and DCs, to limit virus spread and to activate and modulate the adaptive immune response [123].

DCs patrol tissues, recognize antigens, participate in early immune response, and, upon antigen uptake and processing, present antigen and activate T-cells, linking innate and adaptive immunity [124]. DCs are localized in all tissues. Upon encountering an antigen, DCs mature and migrate to lymph nodes, where they engage naïve T-cells [125, 126]. However, HIV-1 exploits this process by using DCs to travel from mucosal entry sites to lymph nodes [127]. Following the virus uptake via endocytosis, DCs recognize RNA viruses via TLR7, activating a signalling cascade that results in DCs maturation. Mature DCs produces a diverse group of interleukins, including IL-2, IL-7, IL-12, IL-15, IL-18, IL 23, and IL-27, to induce or enhance maturation, activation and proliferation of Th1 cells, and cytotoxic responses [124]. DCs also secrete IFN-α, IFN-β, IL-6, and TNF α, and express CCR7 and CD40, CD80, and CD86 co-stimulatory molecules [128]. The expression of MHC-II and the co-stimulatory molecules allows DCs to present antigens to $CD4^+$ T-cells [129]. Type I IFN production limits viral replication but also activates T-cells, and leaves the lymphocytes susceptible to HIV 1 infection [124]. DCs secrete chemokines and attract $CD4^+$ $CCR5^+$ T-cells to the infection site and facilitates viral dissemination, though CCL5 can also inhibit HIV-1 entry by competing with gp120 for CCR5 binding [130]. Additionally, DCs produce the enzyme indoleamine-pyrrole 2,3-dioxygenase that shifts the Treg/Th17 balance toward immunosuppressive Tregs [131].

Monocytes and macrophages are essential components of the innate immune response, and are recruited to sites of infection and inflammation [132]. Macrophages are particularly important target cells for HIV-1, since they express CD4 and CCR5. They are involved in viral entry, transmission, and dissemination. Macrophages also contribute to viral persistence alongside latently infected $CD4^+$ T-cells [133]. They serve as viral reservoirs within various tissue compartments, including the central nervous system, lymph nodes, gut-associated lymphoid tissue, and lungs [134, 135]. Due to their long lifespan ranging from months to years and their ability to reside in nearly all tissues, macrophages play a critical role in the establishment and persistence of HIV-1 reservoir [132, 136]. Additionally, macrophages may contribute both directly, as targets of HIV-1 infection, and indirectly, as key regulators of innate immunity and inflammation, to the chronic immune activation and associated comorbidities seen in people living with HIV-1 [133]. These comorbidities such as hepatic inflammation, fibrosis, and pulmonary diseases, are observed even in the individuals receiving effective antiretroviral therapy [137, 138].

Natural killer (NK) cells eliminate virus-infected cells either by releasing lytic granules or by inducing apoptosis through death receptor pathways involving Fas ligand or TRAIL [139]. Killer immunoglobulin-like receptors (KIRs) are expressed on the surface of NK cells that regulate the

activity of NK cells after interacting with HLA-I (human leukocyte antigen class I) ligands on the target cells. The combination of KIR3DS1/L1 with HLA-Bw4-80I allele was associated with better viral control [140]. A study demonstrated that HIV-1 selectively downregulates HLA-A and HLA-B on the surface of infected cells, while sparing HLA-C and HLA-E. This selective downregulation likely enables HIV to escape from CTL and maintain the protection from NK cells [141]. NK cells also contribute to HIV-1 control through antibody-dependent cellular cytotoxicity (ADCC). They express the FcγRIIIA receptor (CD16), which binds to the Fc region of IgG antibodies. CD16 interaction activates NK cell functions and enables antigen-specific targeting of infected cells. Importantly, ADCC activity was linked to the modest efficacy observed in the RV144 trial [142].

1.3.2 Adaptive Immunity: B-Cell and T-Cell Responses

Unlike innate immunity, adaptive immunity is antigen specific and previous antigen presentation is needed for a rapid response. The adaptive immunity involves B-cells, T-cells, and antibodies, and is responsible for immunological memory [143] . The effectors of the cellular immune response, T lymphocytes, mature in the thymus, while the antibody-producing B lymphocytes arise in the bone marrow. After developing in these primary lymphoid organs, they migrate to secondary lymphoid organs, which function to capture antigens from the lymph and blood circulation [144]. Antibodies function by binding to free viral particles and preventing them from infecting host cells. T-cells primarily function by recognising and eliminating cells that have already been infected by the virus [145]. However, HIV-1 has various mechanisms to escape adaptive immunity, making it challenging to develop effective vaccines inducing broadly protective responses [115].

1.3.2.1 B-Cell Response to HIV-1 and bnAbs

The primary protective function of B cells is the production of antibodies, which carry out their roles in three main ways: neutralizing pathogens, activating macrophages and other immune cells, and activating the classical complement pathway [146]. A defining feature of humoral immunity is the generation of long-lived memory B cells and plasma cells that produce high-affinity, isotype-switched antibodies essential for host defence [147].

The protein antigens are recognized primarily by follicular B cells in lymph nodes. The activation begins upon antigen recognition by the BCR and essential helper signals from antigen-specific $CD4^+$ T-cells [148]. Once BCR binds the antigen, it internalizes the antigen and transports it to endosomal compartments, where it is degraded into peptides. These peptides are then bound to MHC-2 molecules and presented on the surface of the B lymphocyte [146]. The antigen-specific $CD4^+$ T-cells recognize these peptide-MHC-2 complexes and establish close interaction with B cells and help for their proliferation and differentiation [149]. Since the $CD4^+$ T-cell providing help is activated by the same antigen as the B cell, this interaction between these T and B cells is referred to as “cognate” or “linked” [146]. T-cell help is provided through costimulatory ligands such as CD40L and inducible co-stimulator ligand (ICOS) as well as cytokines like IL-4, IL-21, and IFN-g that stimulate B-cell proliferation and differentiation [150].

In addition to their role in humoral immunity B lymphocytes are now recognized as direct contributors to cellular immunity through at least three mechanisms. Firstly, they act as antigen-presenting cells (APCs) that enhance T-cell mediated immunity, secondly, they produce inflammatory cytokines, and finally, a subgroup of them, regulatory B cells characterized by IL-10 secretion, modulate immune responses [151].

During viral infections, only a subset of antibodies is able to directly neutralize the virus. These neutralizing antibodies typically recognize exposed structures on viral surfaces, such as envelope glycoproteins in enveloped viruses, and block the virus from binding to host receptors and entering cells [152]. Non-neutralizing antibodies can also play a role in antiviral defence by binding to Fc receptors on immune cells and mediating effector functions such as ADCC [153].

The B-cell response to HIV-1 faces many challenges due to the virus's high mutation rate and its ability to evade immune detection [154]. NAbs target gp120 and gp41, and although these proteins are exposed on the surface, they resist neutralization through occlusion of epitopes within the trimer, extensive glycosylation, variable loop extension from the surface of the complex, and steric and conformational blocking of receptor binding sites [155]. The removal of N-linked glycans near the CD4 and coreceptor binding sites increases HIV-1's sensitivity to neutralization [156].

Despite these challenges, some individuals infected with HIV-1 develop neutralizing antibodies after several years of infection [118]. Broadly neutralizing antibodies (bnAbs) have attracted significant attention in recent years, targeting highly antigenically variable viruses such as HIV, hepatitis C virus, and influenza virus [157]. They are capable of neutralizing the majority of strains of a given highly antigenically variable pathogen [158]. BnAbs exhibit high levels of somatic hypermutation and a relatively long heavy chain complementarity determining region 3 (HCDR3) [158]. Based on their epitope specificity and structural characteristics, it is possible to identify major sites of vulnerability on HIV-1 Env that are primarily targeted by bnAbs. These include the CD4 binding site (CD4bs) (targeted by VRC01, N6, and 3BNC117 bnAbs), the V3-glycan super site (targeted by PGT121, 10-1074 bnAbs), the V2-glycan site on the apex of the trimer (targeted by PGT145, PG9, PG16, CAP256-VRC26.25 bnAbs), the membrane-proximal external region (MPER) on gp41 (targeted by 2F5, 4E10, and 10E8 bnAbs), and the interface of the gp120 and gp41 subunits (targeted by PGT151 and 8ANC195 bnAbs).

1.3.2.2 $CD4^+$ T-Cells Role in HIV-1

$CD4^+$ T-Cells are the central mediators of adaptive immunity [73]. They play a critical role in orchestrating both cellular and humoral immune responses [159]. Follicular helper T-cells (Tfh) help B-cells, and are essential for germinal centre formation, affinity maturation, and the development of high-affinity antibodies and memory B cells [160]. The development of bnAbs was found positively correlated with the frequencies of $PD\text{-}1^+CXCR3^-CXCR5^+$ memory Tfh cells in people living HIV-1 [161].

Th1 cells contribute directly to antiviral defence by producing IFN-γ and TNF-α [162]. Th1 cells were shown comparatively less permissive to HIV than Th2 cells, since they express higher levels of the APOBEC3G [163] HIV controllers display a predominance of Th1-polarized, HIV-specific $CD4^+$ T-

cells [164]. Cytotoxic $CD4^+$ T-cells also contribute to the clearance of viruses [165]. A longitudinal study found that individuals with a high frequency of granzyme A^+ HIV-specific $CD4^+$ T-cells during acute infection subsequently achieved lower chronic-phase viral set points [166]. Consistently, natural controllers maintained a pool of $CD57^+$ HIV-specific $CD4^+$ T-cells with lytic granule markers over time, suggesting that cytotoxic $CD4^+$ T-cells may contribute directly to viral control [167].

1.3.2.3 $CD8^+$ T-Cells: Cytotoxic Response to HIV-1 Infected Cells

During a viral infection, naïve $CD8^+$ T-cells proliferate and differentiate into effector $CD8^+$ T-cells, which effectively target and destroy infected cells and prevent severe infection [168]. Some of the effector $CD8^+$ T-cells differentiate into memory cells, which can rapidly proliferate upon re-exposure to the antigen, to induce a rapid and robust immune response [169].

$CD8^+$ T-cells play a critical role in controlling HIV-1 infection [170]. During acute HIV-1 infection, early HIV-specific $CD8^+$ T-cells drive the sharp fall from peak viremia and help establish the viral set point, with subsequent $CD8^+$ responses contributing to its maintenance [171]. Although the majority of current vaccine strategies primarily aim to stimulate neutralizing antibodies, considerable evidence suggests that cellular immunity mediated by $CD8^+$ T-cells can sustain long- term disease-free and transmission-free HIV-1 control and can be harnessed to induce both therapeutic and preventive antiviral effects [172].

$CD8^+$ T-cells recognize viral peptides presented on MHC class I molecules on the surface of infected cells [168]. Upon activation, $CD8^+$ T-cells kill infected cells through mechanisms involving perforin-granzyme and Fas-FasL signalling [168]. Additionally, $CD8^+$ T-cells secrete antiviral cytokines such as IFN-γ and TNF-α, to inhibit viral replication and enhance the immune response [168]. IFN-γ has a critical effect on the regulation of antigen presentation by macrophages and dendritic cells, and on the induction of B cells' class switching [173, 174]. IFN-γ directly activates phagocytic cells and stimulates oxidative burst and the release of degradative enzymes, to support the host defence responses against intracellular pathogens [175, 176]. Some studies showed that, alongside the proinflammatory effects, TNF-α inhibits HIV-1 replication by inducing the production of RANTES and decreasing CCR5 expression [177]. RANTES, MIP-1α, and MIP-1β, members of the C-C chemokine family, and are natural ligands for the CCR5. By binding to CCR5, these chemokines block the receptor and prevent HIV from entering and infecting target cells, thus inhibiting viral replication [178].

Three features of HIV-specific $CD8^+$ T-cells might be involved in controlling HIV-1 viral replication: frequency, breadth of epitope recognition, and functional quality [179]. The ability of antigen-stimulated cells to secrete cytokine combinations, termed polyfunctionality, was found greater in controllers than progressors [172]. Betts *et al*. measured five different functions of HIV-specific $CD8^+$ T-cells (degranulation, IFN-γ, MIP-1β, TNF-α, and IL-2 production) in people living with HIV-1, comparing typical progressors and non-progressors (normal $CD4^+$ T-cell counts/ratios and viral load ≤ 125 RNA copies/mL). They found that non-progressors maintained a higher frequency and proportion of polyfunctional $CD8^+$ T-cells (five functions, 10-20%) compared to progressors (five functions, less than 2%). The degree of $CD8^+$ T-cell functionality was inversely correlated with viral

load, indicating that functional quality is a clinical correlate of protection from disease progression [179].

Breadth refers to the ability of $CD8^+$ T-cells to recognize multiple viral epitopes across different HIV-1 variants. Studies demonstrated that virologic control in subjects was associated with greater breadth of $CD8^+$ T-cell responses [180, 181]. Vaccine strategies aimed at inducing polyfunctional and broad $CD8^+$ T-cell responses are considered promising approaches for both therapeutic and preventive interventions against HIV-1 [182].

1.4 HLA Molecules and T-Cell Epitope Recognition

HLA molecules are cell surface glycoproteins whose primary function is to present antigens to T-cells for their recognition and response [183]. The interaction between HLA molecules, peptide antigens, and T-cell receptors (TCRs) are essential for effective T-cell responses against HIV-1. HLAs are classified into two major groups, Class I (HLA-A, -B, -C) and Class II (HLA-DR, -DQ, -DP).

1.4.1 The Role of HLA-I in Antigen Presentation

The role of HLA-I molecules in antigen presentation involves the recognition of a short peptide of intracellular origin, bound to the upper surface of the class I molecule, by $CD8^+$ T-cells. The assembly and loading of the HLA-I is a highly regulated, chaperone-mediated process. The HLA class I monomer molecule comprises a highly polymorphic heavy chain non-covalently linked to the β2-microglobulin light chain [184]. Cytosolically derived peptide antigens are transported to endoplasmic reticulum (ER) by transporter associated with antigen presentation (TAP) [185]. In the protein loading process, tapasin stabilizes the peptide loading complexes and enhances the loading of high affinity peptides into the class I binding groove [185]. Upon peptide binding to class I, the fully assembled HLA-I molecules are exported from the ER to the cell surface [186]. The closed conformation of the HLA-I antigen-binding cleft (length of ~25 Å), together with the peptide length preference of TAP-dependent peptide translocation, result in peptides of 8-10 amino acids in length (length of ~ 22 Å) being the optimum 'fit' for the HLA-I cleft [187, 188].

The HLA-I polymorphism results in significant diversity of peptide antigen presentation to T- cells [189]. HLA-B alleles mostly have better protective activity against HIV-1 than HLA-A alleles possibly because of HLA-B alleles' relative resistance to Nef-mediated down-regulation [190]. Strong correlations between the carriage of specific protective HLA alleles, notably HLA-B*57:01 and HLA-B*27:01 and slower AIDS progression are well-established. Conversely, the HLA-B*35:01 and HLA-C*04 were consistently associated with the rapid development of AIDS-defining conditions in Caucasians [191, 192].

Even small variations between closely related HLA-I molecules can lead to significant differences in peptide-binding specificity [193]. A study on the HLA alleles within the HLA-B7 supertype (HLA-B*07:02, HLA-B*39:10, HLA-B*42:01, HLA-B*42:02 and HLA-B*81:01) demonstrated that, even when an identical peptide is presented by distinct alleles, different immune selection pressure can be imposed on the virus [194].

1.4.2 The Role of HLA-II in Antigen Presentation

HLA-II molecules primarily present exogenous antigens that have been internalized by APCs [195]. HLA-II molecules present peptides to the TCR of $CD4^+$ T-cells [196]. The binding groove of HLA-II molecules is open at both ends, which means that although there is some restriction on the length of peptides accommodated within it, the N- and C-terminal ends of the peptide can extend beyond the groove. This structural feature enables HLA-II molecules to bind a broad spectrum of peptides, typically 12-26 amino acids in length [197].

Ferre *et al*. demonstrated that HIV controllers with both HLA-DRB1*13 and HLA-DQB1*06 had highly polyfunctional mucosal $CD4^+$ T-cells compared to individuals with HLA-DQB1*06 alone or other class II alleles [198].

1.4.3 Epitope Selection and Immune Control of HIV-1

The protective HLA alleles are known for their ability to present the most conserved viral epitopes to the HIV-specific T-cells [199]. This immune recognition drives selective pressure on the virus and leads to development of escape mutations in the targeted viral epitopes. In a study, a robust correlation between the immune response frequencies to epitopes and escape mutation rates in Gag and Pol was observed [200]. However, when these mutations arise in the highly conserved regions of the HIV-1 genome, they often result in considerable fitness cost for the virus [201].

In some cases, the dominance of specific $CD8^+$ T-cell responses may actually limit the development of potentially more effective responses to conserved epitopes which are often subdominant [202]. One study conducted in Denmark showed that immune responses can be redirected toward these conserved epitopes during untreated chronic HIV-1 infection [203]. Frahm *et al*. also suggested that $CD8^+$ T-cells targeting subdominant epitopes may contribute to *in vivo* viral control [204]. Similar protective roles of subdominant responses were observed in the immune control of lymphocytic choriomeningitis virus [205], CMV [206], and pathogenic SIV [207]. A promising HIV-1 vaccine strategy would be to redirect the $CD8^+$ and $CD4^+$ T-cell immunity to target conserved, therefore subdominant epitopes [203, 208].

1.4.4 Epitope Mapping and Validation

Understanding the characteristics of vaccine-induced immune responses is necessary for rational vaccine design. The known sequence of the vaccine immunogen simplifies the identification of vaccine-induced T-cell epitopes and narrows down the number of potential antigens that need to be tested in epitope mapping assays [209].

After *in vitro* stimulation through peptide pulsing, a range of methods can be used to identify T-cell epitopes, including enzyme-linked immune absorbent spot (ELISpot), intracellular cytokine staining (ICS), activation-induced markers, and multimer staining [210]. The ELISpot assay quantifies antigen-specific T-cells based on their secretion of IFN-γ following brief ex vivo stimulation with individual

or multiple peptide antigens [211]. The results are expressed as the frequency of cytokine-producing cells [209].

To enhance efficiency and minimize costs, pooled-peptide mapping strategies have been developed. Assays using small peptide pools (7-30 peptides per pool) demonstrate high sensitivity, effectively detecting responses to individual positive peptides as well as capturing combined responses to multiple peptides. Once reactive pools are identified, deconvolution steps are performed to determine the specific stimulatory peptides [209].

Since experimental mapping of optimal $CD8^+$ T-cell epitopes is time-consuming procedure, computational tools have been created to predict HLA-epitope binding interactions. The Immune Epitope Database (IEDB) is widely employed to predict which peptides are likely to bind specific HLA alleles using established binding motifs and structural information. These predictions inform experimental validation and aid in prioritizing peptide candidates for synthesis and testing [212].

Experimental validation can be conducted using APCs engineered to express single HLA alleles, tetramer staining combined with ICS, or assays involving anti-HLA antibodies [213-215]. HLA restriction is confirmed when T-cell activation is observed only in the presence of the appropriate HLA-epitope combination. Newly identified epitopes and their associated HLA restrictions are cross-referenced with the existing database to determine their novelty and significance [216].

1.5 Antiretroviral Therapies

1.5.1 Combined Antiretroviral Therapy and Emerging Long-Acting Agents

Combined antiretroviral therapy has revolutionized HIV/AIDS treatment, transforming the fatal disease into a manageable chronic condition for those who are motivated to take therapy and who have access to lifelong treatment [217]. CART regimens consist of a combination of three or more antiretroviral drugs that target different stages of the HIV life cycle, suppress HIV viremia, restore the immune system, improve the quality of life of people living with HIV, and are associated with a reduction in new infections [218, 219].

Current HIV treatment includes five different classes of antiretrovirals targeting multiple stages of the HIV replication cycle. Entry inhibitors block the attachment of HIV envelope glycoprotein gp120 to CCR5 co-receptors (Maraviroc) or the cell fusion mediated by HIV gp41 (Enfuvirtide). Nucleoside reverse transcriptase inhibitors and non-nucleoside reverse transcriptase inhibitors block the reverse transcription of viral RNA to cDNA. Integrase strand transfer inhibitors (INSTI) inhibit the integration of pro-viral DNA into host genome, and protease inhibitors inhibit the protease-mediated cleavage of gag and gag-pol precursors, resulting in the production of non-infectious virus particles [220] According to the guidelines for the use of cART in adults and adolescents with HIV, for most people, INSTI-containing regimens is recommended as the first-line treatment since they are highly effective, better tolerated and cause fewer treatment discontinuations [221].

In the recent years, novel types of antiretrovirals with new mechanisms of action and long-acting formulations have been developed, offering a better treatment adherence and additional therapeutic

options for patients with multiclass drug-resistant HIV infection. Ibalizumab is the first monoclonal antibody approved for the treatment of HIV-1 infection. This long-acting post attachment inhibitor binds to the extracellular CD4 domain, leading to conformational changes of the $CD4^+$ T-cell receptor-gp120 complex and blocking HIV entry. Ibalizumab is designed for twice-monthly intravenous administration in combination with other antiretrovirals. In clinical trials, Ibalizumab-based combinations decreased the viral load and increased the $CD4^+$ T-cell count in patients with multidrug-resistant HIV-1 infection (Figure 1.1) [222, 223].

Long-acting injectable formulations, cabotegravir and rilpivirine, have also emerged as promising options. SOLAR and ATLAS-2M studies showed that bimonthly cabotegravir/rilpivirine injections have similar efficacy to a commonly used INSTI-based first-line regimen. The cabotegravir/rilpivirine regimen is generally well tolerated, with injection site reactions being the most frequent side effect [224, 225].

Lenacapavir (LEN), is a long-acting HIV-1 capsid inhibitor, was approved in the United States for multidrug-resistant HIV treatment in December 2022 and designated as Science's 2024 Breakthrough of the year [226] [227]. Recently completed studies also support its use in pre-exposure prophylaxis [228, 229]. Its approval for prevention is currently under review by the U.S. Food and Drug Administration (FDA) [226]. LEN disrupts key viral replication processes, including nuclear import of pre-integration complexes, virion production, and capsid assembly. Current clinical use is twice-yearly subcutaneous injection [226].

In a Phase 2/3 study, CAPELLA, LEN was tested in individuals with multidrug-resistant HIV-1. LEN was added to participants' optimized baseline regimen. Among 72 participants, 66% decrease in viral load was achieved in 88% of LEN recipients versus 17% of placebo recipients by day 15. At week 52, 78% of participants had an HIV viral load less than 50 copies/ml (ClinicalTrials.gov number, NCT04150068) [230, 231].

In a Phase 2 study, CALIBRATE, LEN was assessed in treatment-naive adults, compared to a control group receiving bictegravir/emtricitabine/tenofovir alafenamide [232]. At week 54, virological suppression rates ranged from 85 to 92%, comparable to standard treatment (ClinicalTrials.gov number, NCT04143594) [232]. In both clinical trials the most frequent adverse events were mild-to moderate injection site reactions, headache, and nausea [231, 232].

In PURPOSE1 and PURPOSE2 studies, LEN was evaluated in pre-exposure prophylaxis [228]. PURPOSE1 was conducted in South Africa and Uganda, enrolled over 5300 healthy cisgender women and adolescent girls aged 16-25 years. Three groups of participants received either twice-yearly subcutaneous LEN, daily oral emtricitabine/tenofovir alafenamide (F/TAF), or daily oral emtricitabine/ tenofovir disoproxil fumarate (F/TDF). LEN achieved 100% efficacy, with zero infections. The background HIV incidence rate was 2.41 per 100 people years, and was 2.02 and 1.69 per 100 people years in the F/TAF and F/ TDF groups, respectively (ClinicalTrials.gov number, NCT04994509) [228]. PURPOSE2 study enrolled healthy 3,273 cisgender and transgender men and women, and gender nonbinary individuals who have sex with male partners [229]. In the LEN receiving group, only two new infections occurred in 2180 participants. Nine new infections occurred in 1087 participants in the oral PrEP group receiving F/TDF (ClinicalTrials. Gov number,

NCT04925752) [229]. Future research and policy efforts should prioritize optimizing the clinical use and improving global accessibility to help HIV elimination targets [226].

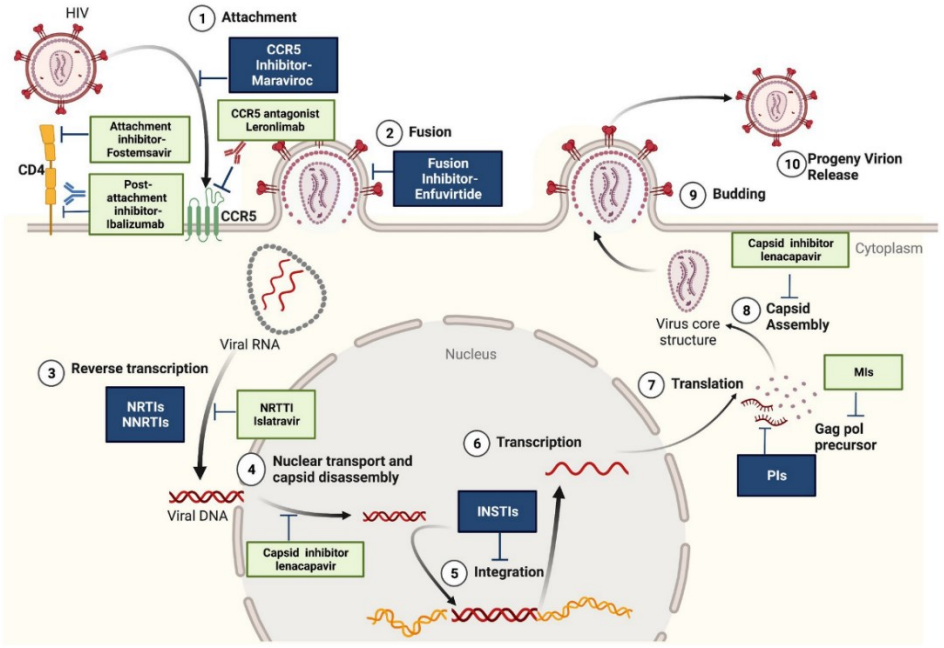

Figure 1.1 Classes of antiretroviral agents for HIV treatment. Dark colours indicate conventional therapies (entry inhibitors, NRTIs, NNRTIs, INSTIs, PIs) while light colours show newly approved drugs (fostemsavir, ibalizumab, lenacapavir) and agents in advanced clinical trials (leronlimab, islatravir, maturation inhibitors (MI)). This figure is adapted from Temereanca A, Ruta S. Strategies to overcome HIV drug resistance-current and future perspectives. Frontiers in Microbiology. 2023. Licensed under CC-BY[233].

Although cART has prolonged life, the treatment also pose a challenge for the quality of life as it can cause significant side effects in addition to the potential for drug toxicity and interaction [234]. The most common short-term adverse effects of cART are gastrointestinal (nausea, vomiting, diarrhea), central nervous system (headache, dizziness), and skin rash, while longer-term complications may involve lipid abnormalities, renal and bone toxicity [235, 236]. Some antiretroviral drugs have been associated with specific adverse effects; for instance, Indinavir (PI) is poorly water-soluble and can crystallise in urine, and may cause obstruction in the renal tubules and urethra. The obstruction can present as renal colic, abdominal pain, and haematuria. NRTIs can cause hepatic steatosis after more than 6 months of therapy, possibly by mitochondrial toxicity [235]. Cardiovascular mortality increased from 1.95% to 4.62% in people living with HIV between 1999 and 2013 [237]. Even though traditional risk factors and persistent inflammation may contribute to this increase, early screening and management of dyslipidaemia are important to reduce cardiovascular risk in people receiving cART [236].

Despite the success of ART, it does not eliminate the latent HIV reservoir, necessitating lifelong treatment [238]. For many individuals in resource-limited settings, consistent access to ART can be difficult [239]. Adherence to treatment is essential to effectively suppress viral replication, and reduce transmission [240]. The potential side effects, cumulative toxicity, and the economic burden of lifelong

ART underscore the need for preventive measures [217, 241]. A safe and effective vaccine, together with the implementation of non-vaccine prevention tools, is essential for the sustained end of HIV/AIDS pandemic [241].

1.5.2 Antibody Mediated Prevention trials

The Antibody Mediated Prevention (AMP) trials tested passive immunization with bnAbs, specifically VRC01 which targets the CD4 binding site of HIV-1 envelope glycoprotein, for HIV prevention. The AMP trials consisted of two parallel phase 2b HIV-1 prevention efficacy studies conducted simultaneously across multiple continents. HVTN 704/HPTN 085 (NCT02716675) was conducted among men and transgender persons who have sex with men in the United States, Peru, Brazil, and Switzerland, enrolling 2,700 participants. In parallel, HVTN 703/HPTN 081 (NCT02568215) was conducted among sexually active women in seven sub-Saharan African countries including Botswana, Kenya, Malawi, Mozambique, South Africa, Tanzania, and Zimbabwe, enrolling 1,500 participants. Both trials employed a randomized, double-blind, placebo-controlled design with participants receiving either 10 mg/kg VRC01, 30 mg/kg VRC01, or a control preparation administered intravenously every 8 weeks for a total of 10 infusions over approximately 20 months [242].

In the HVTN 704/HPTN 085 trial, HIV-1 infection rates were 2.35 per 100 person-years among participants receiving VRC01 (combined dosage groups) compared to 2.98 per 100 person-years in the placebo group, resulting in an estimated prevention efficacy of 26.6% (95% CI, −11.7 to 51.8; P=0.15). Similarly, in the HVTN 703/HPTN 081 trial, infection rates were 2.49 per 100 person-years in the combined VRC01 groups versus 3.10 per 100 person-years in the placebo group, yielding an estimated prevention efficacy of 8.8% (95% CI, −45.1 to 42.6; P=0.70). While VRC01 did not demonstrate statistically significant superiority over placebo in preventing overall HIV-1 acquisition, subsequent analyses focusing on HIV-1 strains that were sensitive to VRC01 neutralization showed proof-of-concept that bnAb prophylaxis can achieve protective efficacy [242].

1.6 Challenges in Developing an Effective HIV-1 Vaccine

The development of a safe and effective HIV-1 vaccine would be the best solution for the ultimate control of the AIDS pandemic, but despite decades of research and advances in our understanding of HIV-1 pathogenesis and immunology, no vaccine is licenced [243]. HIV-1's extraordinary diversity, its ability to evade adaptive immune responses, immune system's inability to produce broadly neutralising antibodies, the early establishment of latent viral reservoirs, and the lack of clear immune correlates of protection remain as remarkable challenges for the vaccine development [244].

1.6.1 Limitations in Animal Models

Animal models play a critical role in evaluating antiretroviral therapies for HIV-1 treatment and in advancing vaccine development [245]. However, HIV's highly restricted species tropism limits the use of most standard small animal models in AIDS research [246]. While humanized mouse models make it possible to model HIV-1 infection of human cells *in vivo* and to design studies using

genetically identical animals, they are limited in replicating HIV-1's impact on non-hematopoietic tissues and do not fully mimic basic features of the disease as it occurs in humans. Additionally, these models remain technically challenging and time-consuming [247]. The infection of macaques with SIV or SHIV represents a widely accepted system for AIDS research [248]. The development of minimally modified simian-tropic strains of HIV-1 that can consistently cause disease in macaques may eventually make it possible to directly test the effectiveness of vaccines and antiretroviral drugs in non-human primate models [245].

1.6.2 The Genetic Diversity of HIV-1

Similar to other human RNA viruses, HIV-1 has a high genetic diversity, primarily because of its high mutation rate [249], retroviral recombination, and rapid viral replication and turnover [250, 251]. HIV-1 is classified into four major genetic groups: M, O, N, and P. The vast majority of infections worldwide are caused by group M which was further diversified into 10 distinct subtypes: A, B, C, D, F, G, H, J, K, and L [34, 252]. Within group M, the average genetic difference between subtypes is approximately 15% in the gag gene and around 25% in the env gene [253]. Subtype C is the most widespread, accounting for more than half of all global HIV-1 cases, especially prevalent in southern Africa and India. Subtype B is the main form in America, Western Europe, and Australia, while subtype A is commonly found in eastern Africa and parts of eastern Europe [253, 254]. Recombination between group M subtypes have led to circulating recombinant forms (CRFs) [251, 255]. CRF01_AE and CRF02_AG recombinant forms are highly prevalent in Southeast Asia and West Africa, respectively [253]. To date, 118 distinct CRFs have been documented worldwide, and these CRFs responsible for approximately 17% of all global HIV infections [251, 252]. This extensive global diversity in HIV-1 remains a major barrier to the development of a universally effective HIV/AIDS vaccine [251, 256].

1.6.3 The Lack of Immune Correlates

A correlate of protection is an immune marker that reflects a response to vaccination and predicts vaccine efficacy [257]. One of the major ongoing challenges is the absence of a well-established immune correlate that can reliably predict protection against HIV-1 infection, because of the inability of people living with HIV-1 to fully clear the virus [244].

In the RV144 clinical trial, which evaluated the canarypox vector vaccine (ALVAC-HIV [vCP1521]) in combination with the gp120 AIDSVAX B/E vaccine, a vaccine efficacy of 31.2% was observed for HIV-1 infection prevention over the 42 months period [258]. This modest efficacy enabled detailed investigations into potential immune correlates that might be predictive of protection. Antibodies of the IgG class targeting the V1/V2 regions of the HIV-1 envelope glycoprotein were associated with a reduced risk of infection, whereas higher levels of plasma Env-specific IgA antibodies correlated with reduced vaccine efficacy [142].

Furthermore, envelope-specific IgG3 responses were correlated with the reduced HIV-1 acquisition risk and were associated with enhanced antibody Fc-mediated functions [259].

A follow-up immune correlates analysis identified that polyfunctional $CD4^+$ T-cell responses were associated with reduced infection risk [260]. Two distinct subsets of polyfunctional antigen-specific T-cells showed a significant correlation with reduced HIV-1 risk: one subset expressed CD40L, IL-2, IL-4, IFN-γ, and TNF-α, and the other expressed CD40L, IL-2, and IL-4. Notably, IL-2, IL-4 and CD40L were part of both subsets that correlated with reduced infection risk [260]. These findings suggest that the polyfunctionality of T-cell responses could be crucial for achieving protective immunity against HIV-1 [261].

1.6.4 Integration into host chromosomes

The early and irreversible integration of HIV-1 DNA causes the lifelong infection and evasion from both immune responses and ARTs. These latent proviruses can periodically reactivate, leading to renewed viral replication and rebound viremia [262]. The initiation of cART as early as 10 days after the onset of symptoms of primary HIV-1 infection cannot prevent latent reservoir formation [102]. Since existing integrated proviruses are not cleared by current immune or therapeutic strategies, effective vaccines must act at the very earliest stages of infection or elicit potent immune responses capable of recognizing and clearing cells with integrated proviruses [244].

Novel vaccine approaches are being investigated that focus on targeting the viral latency. The "Kick and kill" strategy aims to reactivate and eliminate latently infected cells. The RIVER trial, a phase 2 randomized study, aimed to "kick" latent HIV-1 using Vorinostat (a histone deacetylation inhibitor), then "kill" exposed infected cells through vaccine induced T-cell responses. The vaccine regimen was the HIV-1 conserved region immunogen (HIVconsv), administered in a ChAdV63.HIVconsv prime, MVA.HIVconsv boost protocol. The trial enrolled individuals with recent HIV infection who initiated ART rapidly after diagnosis, then randomized them to continue ART alone or to receive additional kick and kill interventions. Despite successful immune activation and the safe administration, results showed no significant difference in the reduction of HIV reservoir size between the two groups [263].

1.7 HIV-1 Vaccine Strategies

A safe and highly effective HIV-1 vaccine, together with practical administration and long-term protection, is considered the best strategy for ultimately stopping HIV/AIDS pandemic [264]. Modelling data suggest that a 70% efficacious vaccine introduced in 2027 with strong uptake and five years of protection could reduce annual new infections by 44% over the first decade, and by 78% in 2070 [265].

Traditional vaccine platforms such as live attenuated viruses, inactivated whole viruses and protein subunits have been highly effective against many viral pathogens. However, their applicability to HIV-1 remains limited [244]. Live attenuated viruses have afforded substantial protective efficacy against SIV challenges in rhesus monkeys, but they are unlikely to be used in humans due to potential safety risks [244, 266, 267]. On the other hand, inactivated whole viruses and protein subunits are limited by their inability to induce broadly reactive neutralizing antibody responses as well as by their inability to elicit $CD8^+$ T lymphocyte responses [268, 269].

In the four decades since HIV-1 was first identified, nine vaccine efficacy trials and two passive immunization trials that aim to evaluate protection from HIV-1 acquisition (Table 1.1) [270]. Seven of the nine vaccine trials employed canarypox or adenovirus serotypes replication-deficient viral vectors. These large-scale studies enrolled thousands of participants and required several years of follow-up to analyse of immune correlates associated with either vaccine-induced protection or failure to prevent infection [271].

Study	Start-Completion		Vaccine/Approach	Location	Outcome/Comments
VAX004 (NCT00002441)	1999	January 2000	Bivalent clade B gp120 in aluminium-based adjuvant	USA, Europe	No efficacy
VAX003 (NCT00006327)	March 1999	August 2000	Bivalent CRF_01AE/B gp120 in aluminium-based adjuvant	Thailand	No efficacy
HVTN 502 (Step Study) (NCT00095576)	November 2004	September 2009	Adenovirus type 5 clade B Gag/Pol/Nef	USA	No efficacy
HVTN 503 (Phambili study) (NCT00413725)	December 2006	July 2015	Adenovirus type 5 clade B Gag/Pol/Nef	South Africa	No efficacy
RV144 (NCT00223080)	September 2005	April 2009	Attenuated recombinant canarypox virus with Gag/Pol/Env; bivalent CRF_01AE/B gp120 in aluminum-based adjuvant	Thailand	Estimated 31.2% vaccine efficacy at 42 months; 12-month efficacy, 60%
HVTN 505 (NCT00865566)	May 2009	October 2017	Plasmid DNA vaccine (expressing clade B Gag, Pol, and Nef and Env proteins from clades A, B, and C) + rAd5 vector boost (expressing clade B Gag-Pol fusion protein)	USA	No efficacy
HVTN 703/HPTN 081 (NCT02568215)	May 2016	March 2021	AMP trial of VRC01 neutralizing antibody infusion IV	Sub-Saharan Africa	Did not prevent overall HIV-1 acquisition, but showed that bNAB prophylaxis can be effective.
HVTN 704/HPTN085 (NCT02716675);	April 2016	December 2020	Antibody Mediated Protection (AMP) trial of VRC01 NAb infusion IV	North America, South America, Switzerland	Did not prevent overall HIV-1 acquisition, but showed that bNAB prophylaxis can be effective.
HVTN 702 Uhambo (NCT02968849)	October 2016	September 2021	Attenuated recombinant canarypox virus with Gag/Pol/Env; bivalent gp120s in MF59	South Africa	No efficacy
HVTN 705 Imbokodo (NCT03060629)	November 2017	August 2021	Ad26, 4 valent T-cell mosaic genes, boost with clade C gp140 Env in aluminum-based adjuvant	Sub-Saharan Africa	No efficacy
HVTN 706 Mosaico (NCT03964415)	October 2019	January 18, 2023	Ad26.Mos4.HIV + boost with clade C gp140 Env in aluminum-based adjuvant	USA, Spain, Central/South America	No efficacy

Table 1.1 The summary of HIV-1 vaccine efficacy trials. [270]

Current vaccine strategies can be categorized into antibody-based and T-cell-based approaches. Antibody-based strategies have explored a range of immunogen formats, including monomeric and trimeric envelope glycoproteins, virus-like particles (VLPs), and engineered platforms that mimic the native structure of the HIV-1 envelope.

1.7.1 Antibody-Based Vaccine Strategies

The most effective non-HIV-1 vaccines used in clinical settings primarily protect by inducing neutralizing antibodies [272]. Thus, the induction of bnAbs is a prime goal of HIV-1 vaccine development [273]. The first generation of HIV-1 vaccines tested in clinical trials using gp120 as an antigen [273]. The only trial that showed a modest efficacy in reducing HIV-1 transmission (31.2%) was the RV144 (NCT00223080) trial of the CRFAE_01 canarypox/gp120 vaccine in Thailand [258]. However, the phase IIb/III clinical trial designed to improve the RV144 trial, HVTN 702 (NCT02968849) did not show a significant efficacy [274]. The HVTN 705 Imbokodo (NCT03060629) and HVTN 706 Mosaico (NCT03964415) clinical trials used an Ad26 vector encoding tetravalent T-cell mosaic antigens and a clade C gp140 Env protein boost. No safety concerns were observed but these vaccine regimens did not provide a significant protection against HIV-1 infection [275, 276].

HVTN 135 (NCT04607408) phase I randomized, placebo-controlled trial evaluated the safety and feasibility of a novel HIV-1 vaccine in new-borns exposed to HIV-1 in South Africa, using the CH505 transmitter-founder (CH505TF) gp120 immunogen adjuvanted with GLA-SE—a synthetic TLR4 agonist formulated in stable emulsion. Thirty-eight healthy infants born to mothers living with HIV-1 were vaccinated. They were negative for HIV-1 nucleic acid at birth. They received five doses of either the vaccine or placebo from within five days of birth up to 54 weeks, with two years of follow-up. All infants received antiretroviral prophylaxis during the trial period. The vaccine was well-tolerated and no serious vaccine-related adverse events observed. No HIV-1 infection occurred during follow-up. These results demonstrate the safety and operational practicality of conducting early-phase HIV-1 vaccine trials in neonates [277].

Current vaccine strategies now focus on germ-line targeting to activate precursor B cells and guide their maturation toward bNAb production [158]. For example, the eOD-GT8 molecule has been engineered to bind germline versions of VRC01-like CD4bs bnAbs [278]. In clinical trials, this vaccine showed a favourable safety profile and induced VRC01-class broadly neutralizing antibody precursors in 97% of recipients. These bnAb precursors shared key features with mature bnAbs and showed somatic hypermutation and increased affinity after boosting, although no neutralizing antibodies were detected which was consistent with the immunogen's design to prime precursor B cells rather than induce mature neutralization [278]. This trial provided clinical proof of concept for germline-targeting vaccine priming, supporting further development of boosting regimens to induce bnAbs and encouraging broader application of this strategy to HIV and other pathogens [158].

In addition to soluble trimers, the presentation of multiple immunogens on the surface of nanoparticles have also been proposed to further improve the elicited antibody responses [279]. For example, a study demonstrated that displaying HIV-1 Env trimers on SOSIP-I53-50NPs self-assembling protein

nanoparticles induced 60-fold higher autologous Tier-2 neutralizing antibody titres in rabbits compared to soluble trimers [280].

1.7.1.1 Trimers and Stabilized Trimers

The host immune system can sometimes respond to HIV- 1 infection by producing bnAbs that recognize relatively conserved epitopes on the Env glycoprotein. Thus, Env- mimetic immunogens were developed by using recombinant protein technologies [281]. These immunogens, such as the SOSIP.664, incorporate modifications like disulphide bonds and cleavage site alterations to enhance structural stability. MPER at the C- terminus of gp41 was truncated as it causes aggregation, which makes protein purification challenging [281]. Designing the native-like stabilized Env trimer immunogens aims to minimize the induction of non-Nabs to monomers, dimers and malformed trimers and focus the response on NAb epitopes [281]. The BG505 clade- A sequence was utilized in the SOSIP.664 construct. The sequence was derived from a 6- week- old Kenyan infant who developed a bNAb response after become HIV- 1 infected at birth [282]. These trimers have shown the ability to induce autologous tier 2 neutralizing responses in animal models [281]. The triple tandem trimer (TTT) design was designed by Del Moral-Sánchez *et al*., by genetically linking three Env protomers in a single open reading frame and expressing as native-like trimers. Viral vectored Env TTT induced higher proportion of trimer-specific responses than SOSIP.664 trimers while inducing similar neutralization titres [283].

1.7.1.2 Virus-Like Particles (VLPs)

VLPs are non-infectious nanostructures that mimic the organization and conformation of native viruses but lack viral genetic material, making them safe vaccine platforms [284]. VLPs can induce strong humoral and cellular immune responses because of their dense repetitive structure [285]. The structural proteins from viruses such as human papillomavirus (HPV), HBV and HIV-1 are utilized for the VLP production [286]. Gag polyprotein can self-assemble into VLPs without requiring any other viral protein [287]. Two types of HIV-1 VLPs can be produced: Gag-VLPs are produced when only the gag gene is expressed in host cells and resemble immature HIV virions, while Gag-Env VLPs are formed when both gag and env genes are co-expressed, resulting in VLPs that display envelope proteins on their surface [288, 289]. The only VLP-based HIV-1 candidate in phase I/II trials was the yeast-derived p24 VLPs [290, 291]. This vaccine candidate did not induce significant humoral and cellular immune responses [290, 291]. A recent study demonstrated that, a mRNA vaccine co-expressing multiclade HIV-1 Env and SIV Gag proteins to generate VLPs induced antibodies capable of broad neutralization and reduced the risk of infection in rhesus macaques. Upon repeated mucosal challenge with a heterologous tier-2 SHIV, vaccinated macaques showed a 79% reduction in per-exposure risk of infection compared to controls [289].

1.7.1.3 Adjuvants for HIV-1 Vaccines: Focus on MF59™

Adjuvants may enhance the magnitude, breadth, and longevity of antigen-specific immune responses, and have minimal toxicity or long-term immune effects on their own [292, 293]. Addition of adjuvants into HIV-1 vaccines has potential to lower the amount of antigen dose and/or reduce the number of immunizations needed for protection, as well as improve the efficacy of vaccines by enhancing neutralizing antibodies or extending the duration of the protective response [294, 295]

Oil in water (O/W) emulsions are among the most widely used adjuvants [295]. MF59™ consists of an oil (squalene)-in-water nano-emulsion composed of droplets under 250 nanometres in diameter [295, 296]. It is licensed for use in influenza vaccines in Europe [296]. It has also been tested in vaccine candidates for herpes simplex virus (HSV), hepatitis B virus (HBV) and HIV, including a recent study demonstrating protection of macaques against SHIV challenge using a prime-boost approach [297]. In this study, an alphavirus replicon particle prime was boosted by an env protein in MF59™ and resulted a complete protection against mucosal challenge [297]. MF59™ has a favourable safety profile and has been shown to significantly enhance antibody titres across multiple antigens with a reportedly more balanced Th1/ Th2 response than that obtained with alum alone [295].

1.7.1.4 A Novel Approach: HBsAg-Based VLPs Displaying HIV-1 Envelope Proteins

Our innovative HIV-1 vaccine candidate utilizes VLPs derived from the hepatitis B surface antigen (HBsAg). These VLPs are decorated with TTT native-like HIV-1 Env single-chain trimers. HIV-1 envelope proteins are covalently attached to the VLP surface employing SpyTag/SpyCatcher system.

1.7.1.4.1 HBsAg VLPs in Vaccine Development

HBsAg was among the first viral proteins used to form VLPs [298]. This platform led to the development of the first recombinant VLP-based vaccine in the yeast expression system in early 1980s [299]. HBsAg is the most abundant 25 KDa highly hydrophobic envelope lipoprotein that mimics mature virus appearance and self-assembles into 22 nm spherical particles that can induce an immune response against Hepatitis B infection [300]. HBsAg has been recombinantly produced using yeast or mammalian cell expression systems [301]. The first recombinant human vaccine against HBV utilising surface antigens was approved in 1986 and has been safely used in humans for decades as an effective HBV vaccine worldwide [302, 303]. Moreover, HBsAg VLP was demonstrated to be safe and immunogenic in humans as carrier for heterologous malaria antigens. RTS,S/AS01 Mosquirix™, a pre-erythrocytic vaccine, consisting of the co-expression of the central-repeat and C-terminal regions of the Plasmodium falciparum circumsporozoite protein (CSP) fused to HBsAg, along with a fourfold excess of unfused HBsAg [304]. Among children aged 5-17 months who received four doses of RTS,S, the vaccine reduced malaria by 39% [305]. R21/Matrix-M is a next-generation malaria vaccine that consists of a 1:1 fusion protein of CSP and HBsAg, without the excess unfused HBsAg [306]. R21/Matrix-M contains ~25 μg of CSP in a 50 μg R21 dose, compared to 10 μg in RTS,S [306].

R21/Matrix-M had over 75% efficacy against clinical malaria with seasonal administration in a phase 3 trial enrolling over 4800 children across four countries [307]. The regular, highly structured surface of HBsAg VLPs allows for the insertion or display of heterologous epitopes, making them a flexible platform for multivalent or chimeric vaccines [1][6].

Because of their particulate nature, molecular stability, high density and repetitive display of epitopes, HBsAg VLPs are broadly applicable for the delivery of small molecules, including bacterial epitopes [308, 309].

1.7.1.4.2 Covalent Protein Coupling with SpyTag/SpyCatcher System

The SpyTag/SpyCatcher system is a protein ligation technology derived from the CnaB2 domain of the fibronectin-binding protein FbaB from Streptococcus pyogenes [310]. The system enables the covalent and irreversible conjugation of two proteins via spontaneous formation of an isopeptide bond between the SpyTag peptide and the SpyCatcher protein partner [311]. The decoration of VLPs using SpyTag technology has been used for the display of diverse antigens, including those from SARS-CoV-2, plasmodium spp., influenza A virus, cancer cells (PD-L1) and HIV-1 [312, 313].

SpyTag/SpyCatcher-mediated antigen display markedly increased antibody titre, affinity, and functional efficacy compared to monomeric protein vaccines [314].

1.7.2 T-Cell-Based Vaccine Strategies

Two HIV prevention vaccine trials, despite showing no efficacy in preventing infection, revealed interesting associations with T-cell responses in follow-up subset analyses [315]. In the HIV Vaccine Trials Network 505 (HVTN 505) trial, participants who were at increased risk for HIV-1 infection received a DNA prime followed by a recombinant adenovirus serotype 5 (rAd5) vector boost vaccine [316]. The vaccine encoded clade B Gag, Pol, and Nef, along with Env proteins from clades A, B, and C, and was administered at weeks 0, 4, and 8. The rAd5 boost, given at week 24, expressed a clade B Gag-Pol fusion protein and Env glycoproteins from clades A, B, and C [316]. Although the vaccine group showed no reduction in HIV-1 acquisition or viral load after infection, subset analysis revealed a strong inverse correlation between HIV-1 infection risk and Env-specific $CD8^+$ T-cell response and Env-specific $CD8^+$ T-cell polyfunctionality [317].

The Step vaccine trial evaluated the Merck rAd5 HIV-1 vector, which carried genes encoding the natural clade B Gag, Pol, and Nef proteins [318]. Although the vaccine elicited interferon-γ ELISPOT responses, did not reduce the risk of HIV-1 infection. Instead, an unexpected increase in HIV-1 acquisition was observed among vaccinated men who were uncircumcised and/or Ad5-seropositive [318]. Similar results were reported in a second study, HVTN 503/Phambili, conducted in South Africa [319].

1.7.2.1 T-cell immunogen design

T-cell responses are not equally effective in HIV-1 control; some epitope-specific responses are linked to better control of the infection. This fact has led to diverse immunogen designs [320].

1.7.2.1.1 HTI, Conserved Elements, and Network Topology Approaches

The HTI (HIVACAT T-cell Immunogen) represents a design guided by functional T-cell response data, which has recently demonstrated a clinical efficacy signal in the therapeutic vaccine context among early-treated individuals who are living with HIV-1 [321]. The HTI approach is founded on identifying T-cell responses and specificities that are primarily observed in individuals with low HIV viral loads and distinguishing these from responses that predominate in viral immunity among individuals with high viremia [322]. These investigations were performed across more than 1000 individuals from different ethnic backgrounds and viral clades, and identified beneficial regions in Gag, Pol and Vif regions [322]. In its final configuration, the HTI immunogen comprises approximately 500 amino acids and incorporates more than 50 well-characterized, optimal T-cell epitopes [322]. The recently published findings from the AELIX-002 clinical trial demonstrated extended viral control in vaccinated participants compared to placebo recipients, representing the most robust clinical efficacy signal documented to date [321].

Mullins *et al*. proposed the conserved elements (CE) design that deliberately includes viral segments conserved across the group M HIV-1 strains and excludes variable segments [323]. A non-human primate study demonstrated that macaques immunized with a DNA vaccine containing CE from SIV p27 Gag and HIV-1 Env developed extensive, robust and long-lasting cytotoxic T-cell responses directed against conserved protein regions of SIV Gag and HIV Env. While the vaccine did not achieve complete infection control, an inverse relationship between Gag CE-specific $CD8^+$ T-cell responses and peak viral loads was observed [324].

Gaiha *et al*. proposed that assessing the topological network score of an epitope can provide valuable insights for the T-cell vaccine design. In their work, they explain differences in HIV-1 immune escape by considering epitopes within the structural framework of HIV-1 proteins, applying principles of network theory. Their findings suggest that epitopes composed of amino acids with extensive structural interactions within the three-dimensional protein are less able to mutate without significant functional cost, and these conserved epitopes are often associated with protective HLA types. Using crystallographic data from several HIV-1 proteins, the researchers examined the interactions of each amino acid within peptide epitopes. These interactions included hydrogen bonds, van der Waals forces, salt bridges, di-sulphide bonds, cation-π interactions, metal coordination, and hydrophobic packing. By mapping these interactions, they calculated network metrics that quantified the structural importance of each residue. They demonstrated a correlation between high network scores, stronger T-cell responses, and enhanced viral control [325, 326].

1.7.2.1.2 Design and Development of a Conserved Mosaic Vaccine Immunogen (HIVconsv)

The HIVconsv vaccine was developed to broadly cover the major HIV-1 clades A, B, C, and D. This design directs T-cell responses toward the virus's most conserved regions, and limits the virus's ability to mutate without a significant cost to its fitness [327]. Another benefit of this strategy is its simplicity, as it uses only a single immunogen for both design and delivery [327]. The HIVconsv immunogen was constructed from 14 regions, each range from 27 to 128 amino acids in length, totalling 778 amino acid residues, chosen based on their sequence conservation [327].

Preclinical toxicity studies in BALB/c mice showed that the MVA.HIVconsv, pSG2.HIVconsv, and ChAdV63.HIVconsv vaccines were well tolerated [328]. HIVconsv vaccines were tested in HIV-CORE (HIV COnserved REgions) clinical trials and demonstrated an excellent safety and tolerability profile [329]. The initial phase I HIV-CORE 002 trial conducted in Oxford, UK, evaluated the pSG2.HIVconsv (D), ChAdV63.HIVconsv (C), and MVA.HIVconsv (M) vaccines in healthy, HIV-1/2-uninfected adults [330]. The study demonstrated strong induction of HIV-1-specific T-cell responses, and $CD8^+$ T-cell effectors were able to inhibit replication of various HIV-1 strains in autologous $CD4^+$ T-cells *in vitro*. The CM and DDDCM regimens were found to be the most effective [331].

1.7.2.2 The Bi-Valent Mosaic Vaccine Immunogen (HIVconsvX)

The second-generation conserved mosaic vaccine, HIVconsvX, is 872 aa in length, and composed of six fragments, ranging in length from 29 to 333 aa [332]. To enhance coverage of global HIV-1 diversity, the HIVconsvX design consists of two complementary mosaic sequences. The amino acid sequences of mosaic 1 and mosaic 2 differ by approximately 10% [332, 333]. The two mosaic sequences provide a perfect 9/9-aa match to at least 80% of potential T-cell epitope (PTE) variants present across the diverse HIV-1 strains in the LANL-HSD alignments [332].

Beneficial epitopes were defined by Mothe *et al*., based on their association with lower viral loads in approximately 1,000 individuals living with HIV-1 clade B or C [334]. The HIVconsvX design includes 33 of the 48 beneficial epitopes. Notably, Env was intentionally excluded from this design; despite containing a short-conserved region, it lacks any of the defined beneficial epitopes [332]. The human tissue plasminogen activator leader sequence was added to the start of the immunogens, which was shown to improve T-cell induction following intramuscular delivery of plasmid DNA vectored HIVconsv vaccines [335].

PBMCs from 120 treatment-naive Japanese people living with HIV-1 clade B were tested for responses to HIVconsvX. The magnitude of $CD8^+$ T-cell responses showed a significant inverse correlation with plasma viral load ($P = 0.0201$) and a strong positive correlation with $CD4^+$ T-cell counts ($P = 1.22 \times 10^{-5}$) [332].

In this thesis, we comprehensively characterized the T-cell responses induced by HIVconsvX vaccine in two clinical studies, HIV-CORE 005.2 and HIV-CORE 006 [336, 337].

1.7.3 Vaccine Vector Platforms

Delivery vectors are essential elements of an effective vaccine, as they modulate both innate and adaptive immunity [338]. Vaccine vectors can significantly impact the magnitude and breadth, as well as the phenotypic and functional characteristics of vaccine-induced immune responses [339]. Viral vectors possess natural adjuvant characteristics because they exhibit various PAMPs that stimulate the innate immune system [340]. In addition to their ability to stimulate strong and long-lasting immune responses, their safety, transgene insertion capacity, manufacturing scalability and stability, as well as the potential impact of pre-existing immunity impact the vector choice [338]. It is known that pre-existing anti-vector immunity can reduce vaccine specific immune response due to the neutralization by pre-existing anti-vector antibodies in humans [341]. Therefore, strategies that enhance vaccine immunogenicity while reducing safety risks continue to be an urgent priority in the development of a safe and effective vaccine for HIV/AIDS [338].

1.7.3.1 Chimpanzee Adenovirus (ChAdOx1) Vector

Adenovirus vectors are among the most effective tools for inducing both antibody and cellular immune responses to inserted transgenes, and induce stronger T-cell responses compared to naked DNA or MVA vaccine platforms [338, 342]. Recently, the development of new vectors has focused on serotypes to which the human population is less exposed in order to circumvent pre-existing anti vector immunity. Chimpanzee adenovirus (ChAd) Y25-based vectors have been engineered and evaluated as vaccine platforms targeting a range of infectious agents, including rabies, MERS, and, more recently, SARS-CoV-2 [343-345]. These vectors are characterized by deletions in the E1 gene, which is necessary for viral replication, and the E3 gene, which encodes proteins involved in immune modulation [346]. The removal of the E1 gene makes the vector replication-deficient, while additional modifications to the E3 and E4 regions enhance its capacity for transgene insertion and improve the efficiency of vaccine production [347].

Research demonstrated that oral/intranasal administration of ChAd-vector based anti-rabies vaccine (AdC68rab.gp) induced durable mucosal antibody response and protected against intranasal virus challenge [344]. ChAd has emerged as a prominent viral vector platform, with the ChAdOx1 nCoV-19 vaccine for SARS-CoV-2 advancing to phase III clinical trials in 2020 and receiving emergency use authorization in multiple countries [343, 348]. The vaccine induced strong Th1-polarized immunity, with $CD4^+$ T-cells releasing interferon-γ and tumor necrosis factor-α, and the production of antibodies predominantly within the IgG1 and IgG3 subclasses. The vaccine also stimulated $CD8^+$ T-cells with diverse effector functions, including cytotoxicity and polyfunctionality [349].

While rare adverse events such as vaccine-induced immune thrombotic thrombocytopenia ,capillary leak syndrome, and Guillain-Barre syndrome have been documented during widespread use of ChAdOx1, this platform continue to be prominent due to its robust safety profiles, capacity to elicit potent immune responses, and suitability for large-scale production [347].

1.7.3.2 Modified Vaccinia Virus Ankara (MVA) Vector

Poxviruses engineered to express foreign genes have become well-established tools in biomedical research for developing new vaccines. The high capacity for heterologous DNA insertion, absence of long-term persistence in the host, wide range of target cells, strong immunogenicity and vaccine efficacy, and the relative simplicity of production are important contributors to their success [350]. MVA does not replicate in humans as a result of extensive serial passaging in chick embryo fibroblasts, which led to the loss of over 10% of its genome. Its safety profile was thoroughly established during the smallpox eradication campaign [351-353]. MVA vectors are especially important for eliciting robust T-cell responses against intracellular pathogens and cancers, but they have also been shown to generate strong, high-titre antibody responses in various disease models, such as SIV and malaria [354, 355]. In both pre-clinical and clinical malaria studies, recombinant MVA was highly immunogenic by inducing strong and protective cellular and antibody responses to malaria antigens, either alone or as a booster following priming with vectors like DNA, fowlpox, or ChAd63 [356-358].Recombinant MVA85A, which expresses the mycobacterial antigen Ag85A, also elicited robust and long-lasting T-cell responses in multiple clinical studies [359, 360].

Phase I and II trials involving MVA expressing HIV antigens, either as a standalone vaccine or in various prime-boost regimens, demonstrated moderate to strong immunogenicity [361-364]. The MVA-B candidate HIV vaccine, which encodes the monomeric gp120 along with a Gag-Pol-Nef polyprotein from clade B, was administered without prior priming and, in Phase I/II studies, elicited durable, robust, and polyfunctional effector memory T-cell and antibody responses [362, 363].

1.7.3.3 Parainfluenza Virus 5 (PIV5) Vector: A Novel Approach

Parainfluenza virus 5 (PIV5), formerly known as simian virus 5 (SV5), is an enveloped virus from the Paramyxoviridae family, characterized by a non-segmented, negative-sense single-stranded RNA genome in 15,246 nucleotides length, which encodes eight proteins [365]. PIV5 is believed to infect humans as well as a wide range of animal species, such as dogs, cats, hamsters, guinea pigs, and cattle. In these reservoir hosts, the infection is typically asymptomatic, with the exception of kennel cough observed in dogs [366, 367]. PIV5 possesses several key characteristics that make it a promising platform for vaccine development, such as a strong safety profile, easy genetic modification, broad tissue tropism, and strong immunogenicity [368, 369]. Numerous studies to date have identified PIV5 vectors as effective platforms for vaccine development, demonstrating their ability to protect against both viral and bacterial infections in multiple animal models [365]. In addition, PIV5 replication within the respiratory tract provides a promising method to administer vaccines, where mucosal immunity is important for protection against pathogen infection [370].

PIV5 is capable of efficiently transporting genes derived from various viruses, including influenza, rabies, respiratory syncytial virus (RSV), and severe acute respiratory syndrome coronavirus 2 (SARS-CoV-2) [371-374]. The rPIV5-H5, which expresses the hemagglutinin (HA) protein of the H5N1 influenza virus, was evaluated for protection against a highly pathogenic avian influenza H5N1

challenge in mice. A single intranasal dose of rPIV5-H5 effectively protected the mice from the H5N1 infection [371]. PIV5-G, encoding the G gene of rabies virus, demonstrated comparable efficacy to LBNSE-GM-CSF, which is considered the most successful post-infection rabies treatment for animals, when used in treating mice following rabies infection [372]. Several preclinical successes have resulted in early positive clinical trial outcomes for the COVID-19 and RSV vaccines. The intranasal PIV5-vectored RSV vaccine, BLB201, was shown to be safe and capable of inducing an immune response in healthy adults in a phase 1 clinical trial [373]. CVXGA1, an intranasal COVID-19 vaccine based on PIV5 that expresses the SARS-CoV-2 Spike protein, was assessed in a phase 1 study involving adults and teenagers. The vaccine was well tolerated with no serious adverse events reported and induced Spike-specific antibodies in the blood and mucosa, as well as $CD8^+$ cytotoxic T-cell responses [374]. Due to its strong efficacy, versatile administration, and safety profile, PIV5 is a promising vaccine vector.

1.7.3.4 Synergistic Effects of Prime-Boost Combinations

Prime-boost strategies have been used in the development of vaccines targeting various infectious diseases to improve both cellular and humoral immune responses [375]. Studies demonstrated that prime-boost immunizations can be administered using different vaccine delivery methods while employing the same antigen, known as a "heterologous" prime-boost strategy. In many cases, the heterologous approach was found to be more effective than the homologous prime-boost regimen [376]. In a recent clinical study, a heterologous regimen, administering the BBIBP-CorV vaccine as the initial dose followed by the Ad26.COV2.S vaccine as a booster, elicited a strong humoral immune response, compared to homologous vaccination group [377].

The heterologous prime-boost regimen using chimpanzee adenoviruses as the prime vector followed by MVA as the booster is a well-characterized and clinically validated approach. In a preclinical study, prime-boost regimens chimpanzee adenoviruses AdCh63 and AdC9 followed by MVA (A-M) elicited sustained strong $CD8^+$ T-cell responses that surpass those achieved by a single prime. Boosting with MVA enhanced the polyfunctional capacity of $CD8^+$ T-cell responses [378].

Multiple variables, including which antigen is chosen, the type of vector used, method of delivery, dosage, adjuvant selection, the boosting schedule, the sequence of vector administration, and the timing between vaccinations, play a role in determining the effectiveness of prime-boost immunization strategies [375]. In a clinical study, researchers evaluated prime-boost regimens using ChAdOx1 and MVA viral vectors expressing conserved influenza A antigens. These vaccinations were given at two different intervals: 8 weeks and one year apart. The study demonstrated that the vaccination protocols were safe and induced the T-cell responses to influenza antigens in participants, with an additional boost observed after the second dose. Importantly, researchers did not observe a difference in the generation or persistence of immune responses between the groups receiving the vaccines 8 weeks apart versus a year apart [379].

1.8 Clinical Development of The HIVconsvx Vaccines

The clinical development of HIVconsvX vaccines includes both completed and ongoing trials, conducted across diverse populations and geographic locations. The studies summarized in the Table 1.2 below involve approaches ranging from monovalent and polyvalent vaccine regimens (such as C1-M3M4/P-P or M3/M4/M4/P) to more complex multi-component and combination strategies, tested in sites across the UK, Africa, the USA, Italy, Brazil, and Thailand. The trials are Phase 1 or Phase 2, primarily assessing safety and immunogenicity in people living with or without HIV-1.

Completed trials HIV-CORE 005.2 and HIV-CORE 006 have shown the vaccine regimens to be well tolerated, with broad and polyfunctional T-cell responses in UK and Africa [336, 337]. Other studies, such as DC-HIV04 and the M&M Study, focus on therapeutic vaccination strategies. The M&M Study confirmed safety and immunogenicity, while older age was associated with reduced T-cell response [380]. Recent and ongoing studies (e.g., IMPAACT 2039A-B, AbVax, RV630) expand the pipeline, investigating the effects of these vaccine strategies in children, adolescents, and adults with innovative combinations involving antibodies.

The clinical evaluation of HIVconsvX vaccines demonstrates promising immunogenicity and safety profiles, with ongoing research expected to further clarify their role in cure and prevention strategies for HIV-1.

Study	Population	Intervention	Site	Phase/ Identifier	n	Status	Summary Findings	Publication/Citation
EAVI2020 HIV-CORE 005.2	18-65y	C1-M3M4/P-P	Oxford, UK	Phase 1 NCT04586673	13	Jul21-Aug22 Completed	Vaccine regimen well tolerated with broad, polyfunctional T-cell responses against HIVconsvX in all recipients. No serious adverse events.	[336]
EDCTP GREAT HIV-CORE 006	18-50y	C1-M3M4/P-P	Masaka, Uganda; Kilifi & Nairobi, Kenya; Lusaka, Zambia	Phase 1 NCT04553016	88	Aug21-Nov22 Completed	Vaccine regimen well tolerated; 99% vaccinees developed broad HIVconsvX-specific T-cell responses in African populations. Responses comparable to UK findings, encouraging for cure/prevention strategies.	[337]
DC-HIV04	18-65y, PLWH	HIVconsvX peptide-pulsed DC Autologous DC loaded with Autologous inactivated virus	Pittsburgh, PA & Columbus, OH, USA	Phase 1 NCT03758625	40	Nov18-Feb25 Completed	Safety, tolerability and immunogenicity of a therapeutic HIV Vaccine composed of autologous DCs loaded with autologous inactivated whole virus or conserved peptides in ART-treated PLWH; results pending.	-
The M&M Study	18-65y PLWH	M3/M4/M3/M4/P	Chapel Hill, NC, USA	Phase 1 NCT03844386	24	Feb19-Apr22 Completed	MVA.HIVconsvX vaccine is safe and induces T-cell responses in PLWH on ART. Older age associated with reduced T-cell response; ART duration may help. No virological change observed.	[380]
The CM Study HIV-CORE 008	18-70y PLWH	C62-M4/P-P, C1C62-M3M4/P-P	Chapel Hill & Durham, NC, USA	Phase 1 NCT05604209	18	Oct22-Jan25 Completed	First trial of C62 and C1 vaccines in PLWH on ART. Study examined safety and immunogenicity, with regimen under evaluation; results pending.	-
EAVI2020 HIV-CORE 007	18-60y PLWH	C1-M3M4/P-P ATI	Milan, Italy	Phase 1/2b CITIS 2024-514581-39-00	33	Started Nov23 Recruiting	Safety and efficacy of vaccine candidates with ART interruption under study; results pending.	-
ACTG A5374 HIV-CORE 009	≥18y PLWH	C1C62-M3M4-M4+2 bnAbs+Vesatolimod/P-P/P-P ATI	Multisite USA & Brazil	Phase 1/2a NCT06071767	45	Started Oct23 Recruiting	Evaluates the safety and immunogenicity of triple immune strategy (vaccines + bnAbs + booster) for HIV cure; results pending.	-
IMPAACT 2039A **IMPAACT 2039B HIV-CORE 010**	5-11y PLWH	2 bnAbs individually, C1C62-M4 C162-M4+3 bnAb ATI	Multisite Africa, Brazil & USA	Phase 1 Phase 2b	110	In development Aim for Jan26	Early-stage therapeutic and prevention study in children; results pending.	-
AbVax Vaccinal Effect HIV-CORE 011	18-65y PLWH	TIIv+2 mAbs ATI, C1C62-M4+TIIv+2 mAbs ATI	Oxford & London, UK	Phase 2b	48	In development Aim for Jun25	Early-stage study combining vaccines and antibody therapy; results pending.	-
RV630 VaccEff+gp120 HIV-CORE 012	18-60y PLWH	2 mAbs+C1C62-M4+gp120/ALFQ ATI	Thailand	Phase 1 NCT06484335	48	Started Apr25 Recruiting	Early-phase combination antibody + vaccine approach; results pending.	-

Table 1.2 The Summary of HIV Vaccine Clinical Trials. This table is adapted from a table provided by Prof. Tomáš Hanke, and used with permission.

1.9 Thesis Objectives

This thesis's main objective is to develop novel vaccine approaches that target HIV-1 to induce protective adaptive immune responses. The thesis specifically aims to investigate T-cell and B-cell based approaches, utilising mosaic immunogens, innovative delivery vectors, and a next-generation VLP platform in order to provide novel contributions to the rational design of an HIV-1 vaccine.

The specific objectives of the thesis are:

1. To characterize the immunogenicity and breadth of T-cell responses induced by conserved-region mosaic HIV-1 vaccines in humans.

- Evaluate the frequency, magnitude, and functional quality of T-cell responses following immunization with mosaic HIVconsvX immunogens delivered via ChAdOx1/MVA.
- Map specific epitope targets of vaccine-induced T-cells, including known and novel epitopes, and assess HLA restriction.
- Assess cross-recognition of epitope variants to determine the potential breadth of immune coverage against global HIV-1 diversity.

2. To develop and optimize alternative delivery platforms, with a focus on the PIV5-vectored system, for improved induction of mucosal and systemic immunity against HIV-1.

- Evaluate the efficiency of the bi-valent mosaic design of HIVconsvX for inducing mucosal T-cell responses that are capable of recognizing epitope variants beyond these present in the vaccines.
- Investigate the elicitation of immune responses following PIV5-vectored HIVconsvX administration, within a prime-boost regimen alongside ChAdOx1 or MVA vectored HIVconsvX vaccines.

3. To design and engineer a novel VLP vaccine platform displaying stabilized, native-like HIV-1 envelope trimers for the induction of broadly neutralizing antibody responses.

- Design, clone, and express VLPs consist of HBsAg decorated with Env single-chain trimers using SpyTag/SpyCatcher technology.
- Purify, characterize, and validate structural integrity and antigenicity of VLPs.
- Evaluate the immunogenicity of these VLPs in mice, with quantitative assessment of antibody titres.

By achieving these objectives, this thesis aims to contribute to innovations towards the ultimate goal of safe and globally effective vaccines against HIV-1.

CHAPTER 2: MATERIALS AND METHODS

2.1 Characterization of T-Cell Responses to Conserved Mosaic HIV-1 Vaccines in People living without HIV-1 in Oxford-Chapter 3

2.1.1 HIV-CORE 005.2 Clinical Trial Design and Authorization

HIV-CORE 005.2 (NCT04586673) was a phase 1, first-in-human, single-centre, open-label, dose-escalation clinical trial aimed at evaluating the safety and immune response of the experimental HIVconsvX HIV-1 vaccines. The research was conducted at the Centre for Clinical Vaccinology and Tropical Medicine, University of Oxford, in Oxford, UK. Sponsored by the University of Oxford, the study received a favourable opinion from the East of England–Cambridge Central Research Ethics Committee (20/EE/0036) and was approved by the UK Medicines and Healthcare Products Regulatory Agency (CTA21584/0425/001-0001; EudraCT 2019-003973-25; IRAS263882). The trial adhered to the ethical standards set by the Declaration of Helsinki (2008) and followed international Good Clinical Practice guidelines established by the International Council on Harmonisation.

2.1.2 HIV-CORE 005.2 Trial Participants and Enrolment Criteria

Healthy adult men and non-pregnant women were eligible for recruitment. They were living without HIV-1 and HIV-2, considered to have a low risk of contracting HIV-1, between the ages of 18 and 65, fully understood the study's aims and procedures as outlined in the participant information sheet, and were able to give written informed consent. Eligibility was determined by laboratory results, review of medical history, physical examination findings, and responses to questions about any behaviours that might increase the risk of HIV-1 acquisition. Regarding COVID-19 vaccinations, participants could not have previously received a simian adenovirus-based COVID-19 or experimental vaccine before or during the trial, or, if they received the UK National Health Service COVID-19 vaccine, it had to be administered at least three months after the C1 vaccination. All participants underwent tissue typing for HLA class I and class II alleles.

2.1.3 Vaccine Details

The tHIVconsvX represents the second generation of conserved T-cell immunogens, comprising two regions from Gag, including the entire p24 protein, and four regions from Pol, all chosen for their high sequence conservation. The Env protein was deliberately omitted due to a lack of beneficial epitopes [334]. The amino acid sequences for full-length Gag and Pol were designed as a bivalent mosaic, differing by roughly 10% in amino acids, which together provided a perfect match to 80% of group M HIV-1 potential T-cell epitope (PTE) variants. These conserved regions were arranged specifically to reduce the likelihood of inducing T cells targeting irrelevant junctional epitopes. Genes encoding the HIVconsv1, HIVconsv3, and HIVconsv4 immunogens were inserted into replication-deficient vaccine vectors, ChAdOx1 and MVA, and administered using a prime-boost strategy. This regimen involves priming with ChAdOx1.tHIVconsv1 (C1) followed by boosting with MVA.tHIVconsv3 (M3) plus MVA.tHIVconsv4 (M4), collectively referred to as C1-M3M4.

The ChAdOx1.HIVconsv1 (C1) ($5x10^{10}$ virus particles/mL) vaccine, as described in the study by Ondondo *et al*. [332], was produced, formulated, and vialled in accordance with Good Manufacturing

Practice (GMP) standards, at Advaxia Biologics, Pomezia, Italy. MVA.HIVconsv3 (M3) ($1x10^8$ plaque-forming units (PFU)) and MVA.HIVconsv4 (M4) ($0.9x10^8$ PFU/mL) vaccines were produced, formulated, and vialled under GMP conditions by IDT Biologika GmbH in Dessau-Roßlau, Germany.

2.1.4 Peptides

The HIVconsvX peptides (C001-C401) (GenScript Biotech). These peptides were initially reconstituted to a concentration of 40 mg/mL using dimethyl sulfoxide (DMSO), then further diluted to stock of 4 mg/ml in phosphate-buffered saline (PBS) (Sigma Aldrich).

For ELISpot and ICS assays, the peptides were combined into ten distinct pools, designated as P1 through P10. Each pool was composed of a collection of 34 to 47 paired peptides, including both mosaic 1 and mosaic 2 variations. Each peptide was reconstituted as a 3 µg/mL, 2x of the final concentration in R10 medium (RPMI 1460 supplemented with 10% foetal bovine serum (FBS), 5 mL L-glutamine, 5 mL sodium pyruvate, 5 mL HEPES, and penicillin-streptomycin antibiotics (Sigma Aldrich).

2.1.5 Isolation and Cryopreservation of PBMCs

Blood samples were collected using heparinized vacutainers (Becton Dickinson). Peripheral blood mononuclear cells (PBMCs) were isolated within 6 hours (h). The PBMCs were used for the *ex vivo* fresh ELISpot assay or cryopreserved for subsequent evaluations.

2.1.6 IFN-γ ELISpot Assay

2.1.6.1 Plate Preparation

96-well sterile filtration ELISpot plates (S5EJ044I10; Merck Millipore) were pre-wetted with 15 µL of 35% ethanol for 1 minute. Then washed 4 times with sterile PBS. Plates were coated overnight at 4 °C with anti-IFN-γ antibody (10 µg/mL in PBS; clone 1-D1K; Mabtech). Prior to use, the plates were washed with PBS and blocked with R10 medium for at least 1 h at 37 °C.

2.1.6.2 PBMC Separation

10 mL of blood was poured into labelled leucosep tubes, centrifuged at room temperature (RT) for 10 minutes at 1000g without brake. 4 mL of the plasma layer was removed and stored at -80 °C in labelled 2 mL vials. The PBMC layer was processed for the ELISpot assay and leftover PBMCs were frozen by using 10% DMSO in FBS. PBMCs were plated at $2x10^5$ cells/well in 50 µL.

2.1.6.3 Assay Design

The design included 3 experimental wells for each HIVconsvX pool (P1-P10), 6 negative no-peptide control wells, 3 wells with 10 µg/mL PHA (Sigma Aldrich) as a positive control, and 2 wells with

NKL cell line cultured with PMA (4 µg/mL) and ionomycin (1 µg/mL; both from Sigma Aldrich) for quality control (aiming for 200 spot-forming units, SFU). The NK cells were adjusted to 1 x 10^4 cells/mL in R10 and 50µL added per well.

Plates were incubated overnight at 37° C in 5% CO_2.

2.1.6.4 Spot Visualization

Spots were visualized using biotin anti-IFN-γ antibody (1 in 1000) combined with streptavidin/alkaline phosphatase (1 in 1000) (Mabtech). Colour development was achieved using BCIP/NBTPlus substrate (Mabtech). The reaction was stopped after 5 minutes by washing with tap water. The plates were air-dried overnight. Spots were counted using an AID ELISpot Reader and version 5.0 software (AID GmbH). The median number of SFU in no-peptide wells was subtracted from test wells. The working principle of IFN-γ ELISpot assay was summarized in Figure 2.1.

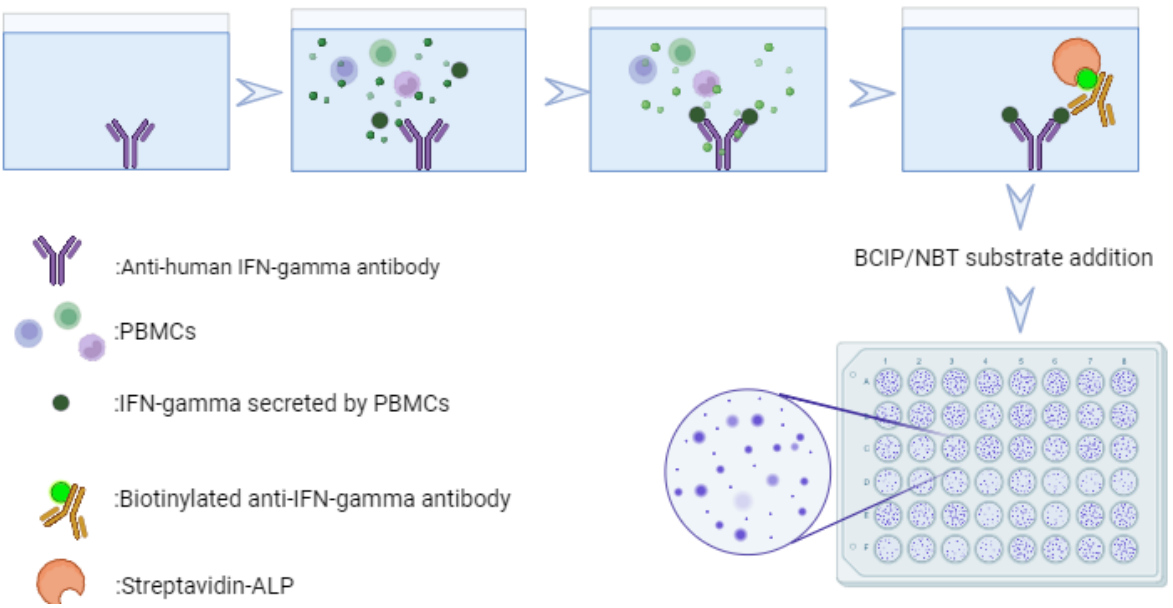

Figure 2.1 The Working Principle of the ELISpot Assay. Designed by using BioRender.com.

2.1.6.5 Variant Peptides IFN-γ ELISpot Assay

Following the initial 15-mer peptide mapping, the two most immunogenic 15-mer peptides were identified for each participant. For each of these, reported HIV-1 epitopes contained within the 15-mer sequences were identified using the Los Alamos National Laboratory (LANL) HIV sequence database, according to the corresponding participant's HLA type. Variant peptides, 8, 9, or 10 amino acids in length and differing by a single amino acid from these reported epitopes, were then selected for further analysis. These variant peptides were not present in either the mosaic 1 or mosaic 2 immunogen sequence and had a population frequency greater than 1% according to LANL database. These variant peptides were ordered from GenScript Biotech, Oxford, UK with ≥80% purity, and subsequently tested

for their ability to induce T cell responses, using the same 14-day culture and IFN-γ ELISpot assay protocol used in the initial epitope mapping.

2.1.6.6 Junctional Peptides IFN-γ ELISpot Assay

Unexpanded PBMCs from each HIVCORE-005.2 clinical trial participant were used to assess the response to junctional epitopes. Cryopreserved PBMCs were thawed, then an equal volume of pre-warmed R10 medium (1mL) supplemented with 50 U/mL benzonase nuclease (MilliporeSigma Novagen, cat. no. 70.664.3) at 37 °C was added dropwise to minimize cell aggregation. Cells were washed, counted, and stimulated with a pool of junctional epitopes (J1–J31) (GenScript Biotech). The immunogenicity of these peptides was assessed by IFN-γ ELISpot assay following the previously described protocol.

2.1.7 Intracellular Cytokine Staining (ICS) Assay

ICS assays was performed according the Jenner Laboratory protocol (THP 048, Version 1.0).

2.1.7.1 Sample Preparation

Cryopreserved PBMCs were thawed and resuspended in R10 medium. Short term cell lines (STCL) (TH A030, Version 4.0, described in details elsewhere) were set up, by stimulating the cells with individual peptide polls. After 10-days culture, PBMCs were resuspended in R10 at a concentration of $1x10^6$ cells/mL. PBMCs were stimulated with personalized ten strongest peptide pairs identified in the mapping (1.5 µg/mL of each peptide), or with 1 µg/mL SEB (positive control), or with R10 (negative control).

Master mix 1 was prepared, including anti-CD28 and anti-CD49d (2 µL/mL), anti-CD107a FITC (20 µL/mL) (Biolegend), Brefeldin A (2 µL/mL from a 5 mg/mL stock) (Biolegend), and Golgi stop (BD Biosciences) (1.4 µL/mL). Master mix 1 (100 µL) was added to each well of the plate.

The plate was incubated for 6 h at 37 °C with 5% CO_2. After incubation, the plate was transferred to 4° C and left overnight.

The following day, the plate was centrifuged at 1800 RPM for 5 minutes, and the supernatant was discarded. PBSA (PBS + 0.2% BSA + 0.02% sodium azide) 150 µL was added to each well, mixed, and cells were resuspended by pipetting. The plate was spun down again, supernatant was discarded, and cells were washed twice with PBSA by centrifugation.

2.1.7.2 Membrane Staining

Membrane master mix was prepared using AQUA Live/dead (4 µL/mL) (Invitrogen), anti-CD8 PE-Dazzle (4 µL/mL) (BioLegend), anti-CD4 PE-Cy7 (20 µL/mL) (BioLegend) , and FACS Buffer (972 µL/mL). Then 50 µL of master mix was added to each well, and the plate was incubated for 30 minutes at 4° C.

After the incubation, the plate was washed twice with PBSA by centrifugation. 100 µL of neat Fix/Perm (BD Biosciences) was added to each well, mixed, and incubated for 15 minutes at 4° C.

The plate was washed three times with perm wash buffer (10X, BD Biosciences, diluted in PBSA) by centrifugation.

2.1.7.3 Intracellular Staining

Intracellular master mix was prepared including anti-CD3 PE-Cy5 (4 µL/mL) (Biolegend), anti-IFN-γ V450 (80 µL/mL) (Biolegend), anti-TNF-α APC-Cy7 (20 µL/mL) (Biolegend), anti-IL-2 PE (200 µL/mL) (BD Biosciences), and anti-CCL3 APC (40 µL/mL) (Miltenyi Biotec) in perm wash buffer (656 µL/mL). Then 50 µl of master mix was added to each well, and the plate was incubated at 4 °C for 30 minutes (Table 2.1).

The plate was washed three times with perm wash buffer by centrifugation. Then 100 µL of 1% paraformaldehyde in PBS was added to fix cells in each well. The plate was stored at 4 °C until acquisition.

2.1.7.4 Data Acquisition and Analysis

BD Fortessa flow cytometer (BD Biosciences) was used for data acquisition, adjusting 100,000 events for displaying and recording. Flowjo software (Tree Star) and SPICE (NIAID) software were used for data analysis.

Epitope mapping ICS				
Antigen	**Fluorochrome**	**Channel**	**Cat. No.**	**Company**
Live/Dead	Aqua	V525	L34957	Life Technologies
CD3	PE-Cy5	YG670	300410	Biolegend
CD4	PE-Cy7	YG780	317414	Biolegend
CD8	PE-Dazzle	YG610	344744	Biolegend
IFN-γ	V450	V450	560371	Biolegend
IL-2	PE	YG586	559334	BD
MIP-1α/CCL3	APC	R660	130-103-630	Miltenyi Biotec
CD107a	FITC	B530	328606	Biolegend
TNFα	APC-Cy7	R780	562084	BD

Table 2.1 The antibody panel used for ICS.

2.2 Epitope Mapping of HIVconsvX-Induced T-Cell Responses in UK and African Clinical Trials-Chapter 4

The epitope mapping experiments described in this chapter were conducted using cryopreserved PBMCs derived from participants in the HIV-CORE 005.2 and HIV-CORE 006 clinical trials.

2.2.1 HIV-CORE 005.2 Clinical Trial Design and Authorization

The details of the clinical trial design, participant recruitment, and ethical authorization are provided on the first page of the Materials and Methods chapter.

2.2.2 HIV-CORE 006 Clinical Trial Design and Authorization

HIV-CORE 006 was a phase 1, double-blind, randomized, placebo-controlled clinical trial conducted across four Clinical Research Centres in Uganda, Kenya (two sites), and Zambia. The participating centres were: the Medical Research Council/Uganda Virus Research Institute and London School of Hygiene & Tropical Medicine Uganda Research Unit (MUL) in Masaka, Uganda; the KEMRI-Wellcome Trust Research Programme (KWTRP) in Kilifi, Kenya; the KAVI-Institute for Clinical Research, University of Nairobi (KAVI-ICR) in Nairobi, Kenya; and the Center for Family Health Research Zambia (CFHRZ) in Lusaka, Zambia.

Ethics approvals for HIV-CORE 006 were obtained as follows: for MUL, from the Uganda Virus Research Institute Research and Ethics Committee (GC/127/20/06/761), Uganda National Council for Science and Technology (HS844ES), and National Drug Authority (CTC 0171/2021); for KWTRP, approvals came from the Clinical Science Committee (CSC 180), KEMRI Scientific and Ethics Review Unit (KEMRI/SERU/CGMR-C/180-2020/4025), the National Commission for Science, Technology, and Innovation (286477; licence NACOSTI/P/20/6699), and the Pharmacy and Poisons Board (PPB/ECCT/20/10/01/2021); for KAVI-ICR, from the Kenyatta National Hospital Ethics Research Committee (P863/10/2019) and the Pharmacy and Poisons Board (PPB/ECCT/20/06/09/2020); and for CFHRZ, from the University of Zambia Biomedical Research Ethics Committee (495-2019), the Zambia Medicines Regulatory Authority (CT-098), the National Biosafety Authority (NBA/101/16/1), National Health Research Authority, and the Oxford Tropical Research Ethics Committee (OxTREC 56-19). The trial followed the ethical principles of the 2008 Declaration of Helsinki, and was conducted in line with International Conference on Harmonization Good Clinical Practice as well as Good Participatory Practices.

The vaccine formulations and administration procedures were identical to those used in the HIV-CORE 005.2 clinical trial. The criteria for participant selection were the same as in the HIV-CORE 005.2 trial and have been detailed previously.

2.2.3 Short-Term Cell Lines and Peptide Mapping

Short-Term Cell Lines and Peptide Mapping was performed according the Jenner Laboratory protocol (TH A030, Version 4.0).

2.2.3.1 Thawing and Preparation

Cryopreserved PBMCs were thawed. Nine-fold volume of R10 medium was warmed to 37° C, then was added dropwise to the thawed PBMCs.

2.2.3.2 Cell Setup and Expansion

Cells were set up at a concentration of 1-3x10^6 cells/mL in R10 medium. R10 was further supplemented with 25 ng/mL IL-7 (PeproTech). The same peptide pools were used as the fresh ELISPOT assay. Cells were expanded in this medium for a duration of 10 days to establish short-term cultured lines (STCL).

On day 3, cultures were supplemented with 100 IU/mL IL-2 (PeproTech). On day 7, cultures received both IL-2 and fresh culture medium.

On day 10, the cells were washed three times with culture medium. They were re-suspended in 1 mL of medium. Cells were placed with loose lids in an incubator at 37 °C and 5% CO_2 for 48 h rest.

2.2.3.3 Peptide Plate Preparation

High-purity (≥90%) 15-mer peptides overlapping by 11 amino acids (C001–C401, GenScript Biotech, Oxford, UK), corresponding to mosaic 1 and mosaic 2 HIVconsvX immunogens, were reconstituted to 40 mg/mL in DMSO and subsequently diluted to 4 mg/mL working stocks in PBS. Peptides were organized into ten pools (P1–P10), each containing 34 to 47 peptides, with both mosaic 1 and mosaic 2 peptide pairs present within the same pool. Peptide pools were prepared in R10 medium and used at a final concentration of 1.5 µg/mL per peptide. For peptide mapping experiments, 2x concentrated stocks of individual peptide pairs or peptides were prepared in peptide plates. Wells containing only R10 medium were used as negative controls, whereas wells supplemented with PMA (8 µg/mL) and ionomycin (2 µg/mL) served as positive controls (Figure 2.2).

Pool 1						Pool 6					
001/002	001/002	019/020	019/020	037/038	037/038	220/221	220/221	238/239	238/239	256/257	256/257
003/004	003/004	021/022	021/022	039/040	039/040	222	222	240/241	240/241	258/259	258/259
005/006	005/006	023/024	023/024	041/042	041/042	224/225	224/225	242/243	242/243	260/261	260/261
007/008	007/008	025/026	025/026	043/044	043/044	226/227	226/227	244/245	244/245	Pos	Pos
009/010	009/010	027/028	027/028	Pos	Pos	228/229	228/229	246/247	246/247		
011/012	011/012	029/030	029/030			230/231	230/231	248/249	248/249		
013/014	013/014	031/032	031/032			232/233	232/233	250/251	250/251		
015/016	015/016	033/034	033/034	Mock	Mock	234/235	234/235	252/253	252/253	Mock	Mock
017/018	017/018	035/036	035/036	Mock	Mock	236/237	236/237	254/255	254/255	Mock	Mock

Figure 2.2 An example plate layout for 15-mer epitope mapping IFN-γ ELISpot assays. Each number corresponds to the code of an individual peptide. Each well contains a combination of two consecutive peptides.

For fine epitope mapping, 9-mer peptides overlapping by 8 amino acids (Synpeptide, China) were used. Based on the initial 15-mer mapping data, all 9-mer peptides within 15-mer peptides that elicited responses greater than 1,000 SFU per million PBMCs were further tested. PBMCs from the responding individuals were restimulated with these selected 9-mer peptides, following the same IFN-γ ELISpot assay protocols used for the original 15-mer epitope mapping.

2.2.3.4 Epitope prediction and HLA restriction

Peptides identified through ICS analysis, along with each participant's HLA information, were analysed using the ELF (Epitope Location Finder) tool (www.hiv.lanl.gov). These results were then compared to previously documented epitopes obtained from CTL databases.

2.2.4 HLA Restriction Analysis by ICS

The HLA restriction of previously mapped $CD8^+$ T cell epitopes was determined using an ICS protocol with .221 cell lines transfected with single HLA alleles, complying with the Jenner Laboratory protocol (J390, Version 1.0).

2.2.4.1 Cell Lines and Culture Media

721.221 cell lines transfected with single HLA alleles were used as antigen-presenting target cells. Cells were maintained in R20 complete media, consisting of RPMI 1640 supplemented with 20% heat-inactivated FBS, 200 μM L-glutamine, 1 mM sodium pyruvate, penicillin-streptomycin (final concentration 100 U/mL), and puromycin (final concentration 4 μg/mL). Effector cells were short-term cell lines (STCLs) generated from previously vaccinated donors and expanded in R10 media.

2.2.4.2 Thawing and Maintenance of .221 Target Cells

Cryopreserved 721.221 cell lines were rapidly thawed into R20 medium, washed, and resuspended at 0.5×10^6 cells per well in 2 mL R20 in 12-well plates. Cultures were incubated at 37 °C in a humidified 5% CO_2 incubator. Cells were fed every 2-3 days by replacing half of the media with fresh R20. Cells were split 1:1 twice weekly and maintained at a relatively high density to support growth.

2.2.4.3 Preparation of Peptide-Pulsed Target Cells

Peptides (GenScript) were prepared at 200 μg/mL in R10. For each condition, 721.221 target cells were counted and 0.6×10^6 cells were incubated with 25 μL peptide solution (or R10 for un-pulsed controls) for 1 h at 37 °C, 5% CO_2. Cells were then washed three times with R10 to remove excess peptide.

2.2.4.4 HLA Restriction Assay Setup

STCL effector cells were washed and rested for at least 24-36 h before use. For each assay, target and effector cells (0.2×10^6 each) were co-cultured at a 1:1 effector:target (E:T) ratio in 96-well round-bottom plates in a final volume of 100 μL R10. Negative controls included unpulsed targets plus effectors; positive controls included effector cells plus soluble peptide at 5 μg/mL final concentration.

CD28 and CD49d co-stimulatory antibodies (each to 1 μg/mL final concentration) were added to all wells. Cultures were incubated for 1 h at 37 °C, followed by the addition of Brefeldin A (final

concentration 10 µg/mL) to block cytokine secretion. Cells were incubated for an additional 4-5 h and then stored overnight at 4 °C prior to ICS staining.

2.2.4.5 ICS

The next day, cells were stained according to standard ICS protocols to assess cytokine production in specific T cell populations. Data acquisition was performed by flow cytometry.

All procedures were performed using sterile technique in a class II safety cabinet, and all media were stored at 4 °C for a maximum of one month after preparation.

Antigen	Fluorochrome	Channel	Cat. No.	Company
Live/Dead	Aqua	V525	L34957	Life Technologies
CD3	PE-Cy5	YG670	300410	Biolegend
CD4	PE-Cy7	YG780	317414	Biolegend
CD8	PE-Dazzle	YG610	344744	Biolegend
IFN-γ	V450	V450	560371	Biolegend
TNFα	APC-Cy7	R780	562084	BD

Table 2.2 The antibody panel used for ICS during HLA restriction assay.

2.2.5 Statistical Analysis

Analyses were conducted using GraphPad Prism version 9.5.0. The Shapiro-Wilk test was employed for analysing the normality of the data. For nonparametric data, comparisons were conducted using the Kruskal-Wallis test. Dunn's multiple comparison post-test was applied as a follow-up analysis. Two-tailed P values were utilized in the analysis. The significance threshold was accepted as less than 0.05 to determine statistical significance.

2.3 Mucosal Delivery of the HIVconsvX immunogens Using Parainfluenza Virus in a Murine Model-Chapter 5

2.3.1 Animals and Immunizations

Six weeks old female inbred BALB/c mice from Envigo were immunized intranasally and intramuscularly under general anaesthesia. All animals and procedures were used in accordance with the terms of the UK Home Office Animals Act with Project License number PP1892852 (PIL number: I46427560). Procedures were approved by the University of Oxford Animal Care and Ethical Review Committee.

Mice were allocated into experimental groups and immunized with PIV5.HIVconsv5 (P1), PIV5.HIVconsv2 (P2), ChAdOx1.tHIVconsv1 (C1), ChAdOx1.HIVconsv62 (C62), MVA.tHIVconsv3 (M3) and MVA.tHIVconsv4 (M4). Each group was immunized intranasally with 1.59 x 10^6 pfu of P5, or 5.3 x 10^6 pfu of P2, or a combination of half doses of P2 and P5, respectively. Booster immunizations were administered with two-week intervals. Either nine days, or two weeks following the final immunization, the animals were euthanized for tissue collection.

2.3.2 Construction and Production of PIV5.HIVconsv2 and PIV5.HIVconsv5 Vaccines

The PIV5.HIVconsv2 and PIV5.HIVconsv5 vaccines were constructed and provided by our collaborators, Ashley C. Beavis and Biao He, from the Department of Infectious Diseases, College of Veterinary Medicine, University of Georgia, USA. The information in this section was adapted from our joint publication [381].

PIV5 served as the parental backbone for the generation of recombinant viruses P2 and P5. DNA fragments encoding HIVconsv2 or HIVconsv5 antigens (synthesized by Genscript, Piscataway, NJ, USA) were inserted as additional open reading frames (ORFs) between the SH and HN ORFs of PIV5, following protocols previously described [368]. To construct the recombinant P2 and P5 vaccine viruses, plasmids carrying the full-length genome cDNA for either P2 or P5, along with helper plasmids (pT7 polymerase, pPIV5-NP, pPIV5-P, and pPIV5-L), were co-transfected into HEK293T cells at 60-80% confluency in 6-cm² plates. Twenty-four hours post-transfection, cells were detached using trypsin and combined with 1×10^6 Vero cells in a 10-cm² dish. The cultures were maintained at 37 °C with 5% CO_2 for seven days, after which the supernatant was harvested. Recombinant viruses were isolated by plaque purification in Vero cells: the supernatant was serially diluted and applied to Vero cells overlaid with 2% low melting point (LMP) agarose in DMEM5. After 7-14 days, individual plaques were picked and expanded further in Vero cells. Following 5-7 days of expansion, the medium was collected and clarified by centrifugation at 1000 rpm for 5 minutes. The supernatant was then mixed with one-tenth volume of 10× sucrose-phosphate-glutamate (SPG) buffer and stored at -80 °C.

Plaque assays were performed to determine the titers of P2 and P5. Vero cells were infected with serially diluted virus, overlaid with 2% LMP agarose in DMEM5, and incubated for 10-14 days. The overlay was removed, cells were fixed in 2% paraformaldehyde, and plaques were visualized by staining with 0.5% crystal violet in 25% methanol. The sequences of full-length recombinant PIV5 genomes were verified by Sanger sequencing, and expression of the inserted HIVconsv2 and HIVconsv5 antigen genes by P2 and P5 viruses was confirmed.

2.3.3 Murine IFN-γ ELISpot Assay

2.3.3.1 Peptide Preparation

H-2d class I-restricted epitopes and their variants were previously identified in BALB/c mice by Wee *et al*. [382]. The peptides used were of at least 90% purity (Synpeptide, Shanghai, China). These peptides were dissolved in DMSO (Sigma-Aldrich) to make a stock concentration of 10 mg/mL, and they were stored at -80 °C until utilized. Peptides were prepared at a stock concentration of 4 µg/mL (2x of final concentration) each.

2.3.3.2 Isolation of Immune Cells from Spleen

Spleen tissue was harvested and pressed through a 70-µm sterile nylon-mesh cell strainer (Fisher Scientific) using a 5-mL syringe rubber plunger. Red blood cells were removed using ACK lysis buffer (0.14 M NH_4Cl, 10 mM $KHCO_3$, and 100 mM Na_2EDTA). Cells were washed and resuspended in R10 medium (RPMI 1640 supplemented with 1% Pen/Strep, 10% FBS, and β-mercaptoethanol). Cell count was performed using a CASY cell counter.

2.3.3.3 Isolation of Immune Cells from Lungs

Dissected lung organs were cut into 1-mm^2 segments. Segments were digested in a 1.8 mL volume of R0 medium supplemented with β-mercaptoethanol, containing 1.4 mg/ml Collagenase (Sigma Aldrich) and 60 µg/ml DNase Type IV (Sigma Aldrich) for 60 min in the shaking incubator at 37 ^oC. The reaction was terminated by adding 200 µL of FCS. Cells from lungs were processed similarly to those isolated from the spleen.

2.3.3.4 Plate Setup

Plates (96-well) from Millipore (MAIPS4510) were precoated with 5 µg/mL anti-IFN-γ monoclonal antibody (mAb) from Mabtech. Plates were incubated at 37 °C in a 5% CO_2 environment for 18 h.

Each sample was tested in triplicate or duplicate wells. Splenocytes were plated at a concentration of 50,000 cells/well. Lung cells were plated at a concentration of 10,000 cells/well. Peptide were added to relevant well as 50 µL at a final concentration of 2 µg/mL. The plates were incubated at 37 °C in a 5% CO_2 environment for 18 h. Then they were washed with 6x with PBS after incubation. Biotinylated anti-IFN-γ mAb (1:1000) from Mabtech was added to each well and incubated at RT for 2 hours.

After washing with PBS, plates were incubated with streptavidin-conjugated alkaline phosphatase (1:1000) from Mabtech at RT for 1 hour. The plates were washed again with PBS.

Individual spot-forming units (SFU) appeared as dark spots after a 10-minute reaction with a substrate comprising BCIP/NBT (5-bromo-4-chloro-3-indolyl phosphate and nitro blue tetrazolium), (BioRad AP Conjugate sub kit 170-6432). SFUs were quantified using the AID ELISpot Reader System (Germany). The frequencies of responding wells were calculated as SFU/10^6 splenocytes and lung cells. Background frequencies from no-peptide assay wells were subtracted from the calculated values.

2.4 Development of Triple Tandem Trimer SpyTag/SpyCatcher Virus-like Particles-Chapter 6

2.4.1 TTT Gene Sequence Design

In this study, we used the Triple Tandem Trimer (TTT) gene design, as originally developed and published by del Moral-Sánchez *et al*. (2024) [283]. The research group kindly shared the TTT gene sequence with us, and granted permission for its use. The TTT construct is based on single-chain versions of the BG505 SOSIP.v8.4 trimer, which was derived from the BG505 SOSIP.v4.1 sequence by the addition of several MD39 trimer-stabilizing mutations (106E, 271I, 288L, 304V, 319Y, 519S, 568D, 570H, and 585H) [383]. In the single-chain (SC) SOSIP.v8 format, the conventional R6 furin cleavage site is substituted with a flexible 15-amino acid linker (GGSGGGGSGGGGSGG). To generate the TTT construct, three SC SOSIP.v8 protomers were genetically fused via flexible 11-amino acid Gly-Ser linkers (GSGGSGGSGSG), in a single open reading frame encoding the trimeric structure. The construct begins with a synthetic leader peptide sequence (MDRAKLLLLLLLLLPQAQA). We added Pk tag (IPNPLLGLD) to the C-terminus, connected by an additional GGSGGSGGSG linker, after residue 664 to facilitate detection by Western Blotting. All gene sequences were codon-optimized for mammalian expression and synthesized commercially (Genscript).

2.4.2 Addition of SpyTag to the TTT Gene Construct

SpyTag and SpyTag002 sequences were incorporated at the C-terminus of the TTT.Pk gene sequence using Polymerase Chain Reaction (PCR). Both SpyTag (AHIVMVDAYKPTK; 13 amino acids) and SpyTag002 (VPTIVMVDAYKRYK; 14 amino acids) sequences were reverse-translated and optimized for human codon usage to enable efficient mammalian expression [384].

To add the tag sequence, gene-specific reverse primers were designed, encoding the C-terminal Pk tag, a flexible Gly-Ser-Gly (GSG) linker, the selected humanized SpyTag or SpyTag002 coding sequence, a stop codon, and a NotI restriction site for downstream cloning (custom synthesized by Merck, Sigma-Aldrich). PCR amplification was performed using the GSC1-FOR forward primer and either the SpyTag-REV or SpyTag002-REV primer on the TTT.Pk plasmid template.

PCR reactions were prepared in a final volume of 50 µL. Each reaction contained 1 µL of template DNA (p5848, 50 ng/µL), 5 µl of forward primer (10 µM stock), 5 µL of reverse primer (10 µM stock), 1 µL of DMSO, 13 µL of nuclease-free water, and 25 µL of Phusion HF Mastermix (New England Biolabs). The reaction mixtures were thoroughly mixed and briefly centrifuged before being placed in the thermal cycler. Two replicate tubes were set up for each reaction.

Thermal cycling was performed as follows: an initial denaturation at 98 °C for 2 minutes, followed by 35 cycles of 98 °C for 15 seconds (denaturation), 62 °C for 30 seconds (annealing), and 72 °C for 6 minutes (extension). The program concluded with a final extension step at 72 °C for 10 minutes, then samples were held at 4 °C until further use.

Following PCR amplification, the 6 kbp product was separated by agarose gel electrophoresis. The corresponding DNA band was excised under UV illumination and purified using the QIAquick Gel Extraction Kit (Qiagen) according to the manufacturer's instructions. Briefly, the excised gel slice was weighed and incubated with three volumes of Buffer QG (5.5 M guanidine thiocyanate, 20 mM Tris-

HCl, pH 6.6) at 50 °C until completely dissolved. After verifying full dissolution, one gel volume of isopropanol was added, and the mixture was transferred to a QIAquick spin column placed in a 1.5 mL collection tube (Sarstedt, cat. no. 72.706.400). The column was centrifuged at 13,000*g* for 1 minute, and the flow-through was discarded. The column was then washed with 500 µL of Buffer QG, followed by 750 µL of Buffer PE, each with centrifugation. To remove residual wash buffer, the column was centrifuged for an additional minute at maximum speed. DNA was eluted by adding 30 µL of nuclease-free water directly to the centre of the membrane, incubating for 1 minute at room temperature, and spinning at 13,000*g* for 1 minute. The concentration of the purified DNA was measured by NanoDrop One Spectrophotometer (Thermo Scientific).

For restriction digestion, 40 µL of PCR-amplified TTT.PkSpyTag and TTT.PkSpyTag002 inserts were incubated with 2.5 µL KpnI-HF, 2.5 µL NotI-HF, and 5 µL CutSmart buffer (all from New England Biolabs) in a final reaction volume of 50 µL. In parallel, 4 µL of pTH (p71) vector DNA was digested in a 50 µL reaction containing 2.5 µL KpnI-HF, 2.5 µL NotI-HF, 5 µL CutSmart buffer, and 36 µL nuclease-free water. All digestion reactions were incubated at 37 °C for 1 h.

Following the initial digestion, 1 µL of calf intestinal alkaline phosphatase (Quick CIP; New England Biolabs) was added to the vector digestion mixture, which was then incubated for an additional hour at 37 °C to dephosphorylate the vector DNA and prevent self-ligation. Digested products were purified using the QIAquick PCR Purification Kit (Qiagen) prior to ligation.

To confirm their relative size 1 µL of each sample was run on an agarose gel alongside a DNA mass ladder. The purified inserts (6029 bp or 6032 bp) and vector backbone (4846 bp) were then used for ligation.

Ligation reactions were set up in a final volume of 20 µL. For each reaction, 1 µL of pTH vector was combined with 16 µL of insert DNA. To this mixture, 2 µL of ligation reaction buffer and 1 µL of T4 DNA ligase (both from New England Biolabs) were added. The reaction was mixed and incubated at 16 °C overnight. The ligated plasmid lengths were 10.875 kbp for pTH.TTTPkSpytag and 10.878 kbp for pTH.TTTPkSpyTag002 (Figure 2.3). Following ligation, 5 µL of the reaction mixture was used for transformation into competent bacterial cells.

2.4.3 Transformation into *E. coli*

Competent Stellar *E. coli* cells (HST08 strain, Takara Bio) were transformed with the plasmid and incubated at 42 °C for 40 seconds and then on ice for 2 minutes. Then 1 mL of SOC (Super Optimal Medium with Catabolic Repressor) medium was added, and the mix was incubated at 37 °C for 30 minutes. The culture was spread onto LB (Luria-Bertani) agar plates containing the Ampicillin antibiotic for overnight incubation at 37° C. Ten colonies were picked, and was inoculated into 5 mL of LB broth media (Tryptone (10 g/L), Yeast Extract (5 g/L), Sodium Chloride (NaCl, 10g/L), Distilled Water) with Ampicillin, and incubated overnight in the shaking incubator at 37 °C, 250 RPM.

2.4.4 Plasmid DNA Extraction

Plasmid DNA was isolated from cultures using the QIAprep Spin Miniprep Kit (Qiagen), in accordance with the manufacturer's instructions. The overnight culture was harvested by centrifugation at 12,000*g* for 1 minute at room temperature. The supernatant was discarded, and the bacterial pellet was thoroughly resuspended in 250 µL of P1 buffer (50mM Tris-HCl pH 8.0, 10mM EDTA, RNase A) by vortex. Subsequently, 250 µL of P2 buffer (lysis buffer, 200 mM NaOH, 1% SDS) was added, and the tube was gently inverted 4-6 times to ensure complete cell lysis. This step was followed by the addition of 350 µL of N3 buffer (neutralization buffer, 3.0 M potassium acetate, pH 5.5, with guanidine hydrochloride). The mixture was inverted again several times until a homogeneous suspension was achieved and a white precipitate formed.

The sample was centrifuged at 12,000*g* for 10 minutes at room temperature to pellet cellular debris and precipitated proteins. The resulting clear supernatant, containing plasmid DNA, was transferred to a QIAprep spin column over a 2 mL collection tube. The column was centrifuged at 12,000*g* for 1 minute and the flow-through discarded.

To wash the DNA, 500 µL of Buffer PB (5M guanidine hydrochloride, 30% isopropanol, pH ~6.6) was applied to the column and centrifuged for 1 minute, followed by disposal of the flow-through. Next, 750 µL of Buffer PE (10mM Tris-HCl, 80% ethanol, pH 7.5) was added to the column, which was then centrifuged for another minute. After discarding the flow-through, the column was centrifuged once more for 1-2 minutes to remove any residual wash buffer.

The QIAprep column was then placed in a clean 1.5 mL microcentrifuge tube. To elute the plasmid DNA, 100 µL of nuclease-free water was applied directly to the centre of the membrane. Following a 1-minute incubation at room temperature, the column was centrifuged for 1 minute at 12,000*g* to recover the DNA.

The presence and correct size of the insert were verified by restriction enzyme digestion with SalI-HF (New England Biolabs). For each sample, 500 ng of plasmid DNA was mixed with 1 µL SalI-HF (20 U/µL), 2 µL of 10X CutSmart Buffer (NEB), and nuclease-free water in a final reaction volume of 20 µL. The digestion reaction mixtures were incubated at 37 °C for 2 h.

After digestion, 4 µL of 6X loading dye was added to each reaction. Samples were loaded onto a 1% agarose gel in 1X Tris-acetate-EDTA (TAE) buffer with SYBR™ Safe DNA Gel Stain (Invitrogen) for band visualization, and run at 120 V for ~30 minutes. A molecular weight DNA ladder (GeneRuler 1 kbp, Thermo Scientific) was included as a size standard. DNA fragments were visualized and imaged under UV illumination using Bio-Rad gel imaging system. The correct linear DNA fragments size (9 kbp and 2 kbp) were confirmed. Positive clones were selected and sent for Sanger sequencing (Source Bioscience) to confirm the presence of SpyTag and SpyTag002.

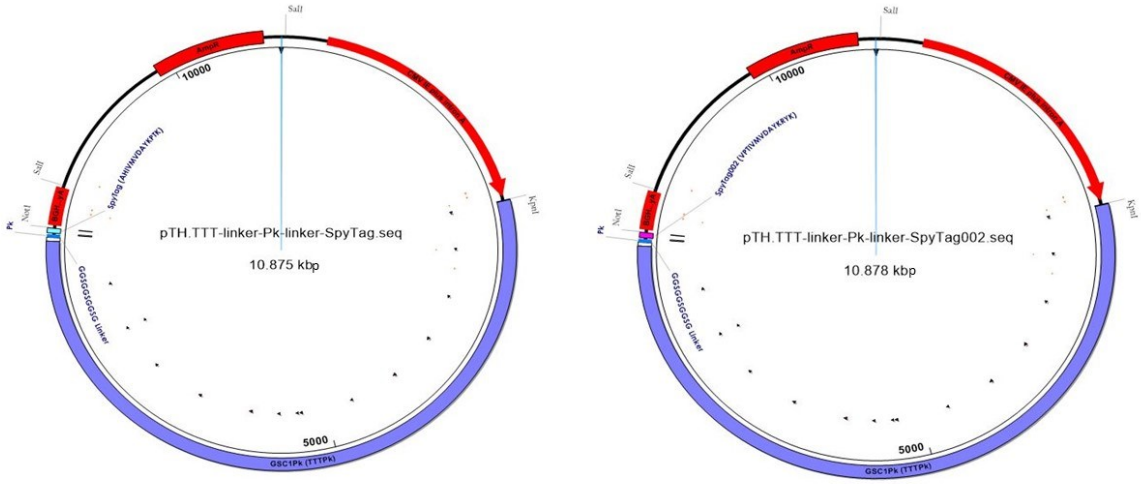

Figure 2.3 The Map of pTH.TTTPkSpytag and pTH.TTTPkSpyTag002.

2.4.5 Expi293 Cell Transfection

Expi293F cells were kindly provided by the Sandy Douglas group (The Jenner Institute, University of Oxford). Expi293F cells were maintained in Expi293 Expression Medium (Gibco) at 37°C, with ≥80% relative humidity and 8% CO_2, in vented Erlenmeyer shaker flasks on a shaker (125 RPM). The cells were passaged at least three times post-thaw prior to transfection to ensure viability above 90%.

For transfection, Expi293F cultures were adjusted to a density of 3×10^6 viable cells/mL in pre-warmed Expi293 Expression Medium. Plasmid DNA (pTH.TTTPkSpyTag or pTH.TTTPkSpyTag002) was prepared to a final concentration of 1 µg DNA per mL of culture and diluted in Opti-MEM I Reduced Serum Medium (Thermo Fisher Scientific). Separately, ExpiFectamine 293 Transfection Reagent (Gibco) was diluted in Opti-MEM I as per the manufacturer's protocol (162 µL ExpiFectamine reagent for 60 mL of culture). The diluted ExpiFectamine and plasmid DNA were incubated for 5 minutes at room temperature, then combined and incubated for an additional 15 minutes to allow complex formation.

The DNA-ExpiFectamine complexes were added dropwise to the cell culture. The cultures were returned to the incubator and shaken at 37 °C, 8% CO_2. ExpiFectamine 293 Transfection 360 µL Enhancer 1 mL and 3.6 mL Enhancer 2 (Gibco) were added to the cultures 18-22 h post-transfection.

Cells were harvested 5 days post-transfection, by centrifuge the culture at 3,000*g* for 15 minutes at RT.

2.4.6 GNL Purification

The harvested cell culture supernatants were filtered through a 0.22 µm pore-size filter to remove residual cell debris. The filtered supernatants were purified by using Galanthus nivalis lectin (GNL) affinity chromatography. Before the first use, agarose-bound GNL (Vector Laboratories, cat. no. AL-1243) was washed three times with cold PBS. The harvested and filtered culture supernatant was mixed with 5 mL agarose-bound GNL and incubated for 1 h at 4 °C with gentle shaking. Following incubation, the mixture was loaded onto a column and allowed to pass through the filter. After washing the column with five column volumes of cold PBS, the bound proteins were eluted with 5 mL of 1 M α-methyl-D-mannopyranoside (pH 8.0) (Sigma Aldrich).

2.4.7 Expression Analysis - Coomassie Staining and Western Blotting

The expression of the protein was confirmed through western blot analysis using anti-PkTag and anti-Env antibodies and Coomassie staining. The sample (39 µL) was mixed with 6 µL NuPAGE™ Sample Reducing Agent (10X) (Invitrogen™) and 15 µL NuPAGE™ LDS Sample Buffer (4X) (Invitrogen™) to make up a total of 60 µL, then incubated at 90 °C for 5 minutes.

The samples along with the TTT-Pk positive control and were loaded (10 µL per well) on an NuPAGE™ Tris-Acetate Mini Protein Gels, 3 to 8% (Invitrogen) alongside the 5 µL of HiMark Pre-Stained Protein Standard (Invitrogen). One of the gels was directly transferred to Quick Coomassie Staining solution (Generon) and incubated at RT overnight.

The transfer of proteins from gels to membranes was performed using the Trans-Blot Turbo transfer system (Bio-Rad) onto 0.2 µm nitrocellulose membranes (Bio-Rad). The High Molecular Weight setting was selected, and transfer was carried out for 10 minutes.

Western blotting was performed using the iBind™ Automated Western System (Thermo Fisher Scientific, Cat. No. SLF1020). After electrophoretic protein transfer, each membrane was incubated in 1X iBind™ Solution (prepared freshly by diluting 6 mL iBind™ FD 5X Buffer and 75 µL iBind™ 100X Additive with distilled water to a final volume of 30 mL) for 5 minutes.

The iBind™ Card was placed in the iBind™ device and pre-wetted evenly with 5 mL 1X iBind™ Solution across the Flow Region, and 1 mL solution was added to the central membrane area. The pre-wetted membrane was placed protein-side down onto the card, and rolled with the blotting roller to remove air bubbles. The device lid was closed and the designated wells were loaded sequentially as follows, well 1: 2 mL primary antibodies (anti-Pk tag, anti-Env) diluted 1:1000 in 1X iBind™ Solution, well 2: 2 mL 1X iBind™ Solution (wash), well 3: 2 mL secondary antibody (Alkaline Phosphatase AffiniPure® Goat Anti-Mouse IgG (H+L) (Jackson ImmunoResearch) for anti-Pk tag and anti-Env 1:1000, well 4: 6 mL 1X iBind™ Solution. After the 3 hours run, membranes were rinsed in distilled water and BCIP®/NBT tablets (Sigma-Aldrich), dissolved in 10 mL distilled water, was used for membrane development. The membranes were washed by water after the band development to stop reaction.

2.4.8 Protein Quantification

Protein concentration was measured using the Pierce BCA Protein Assay Kit (Thermo Scientific, catalogue no. 23227). A series of bovine serum albumin (BSA) standards were prepared alongside the experimental samples. Working Reagent (WR) was prepared by mixing BCA Reagent A with BCA Reagent B at a 50:1 ratio just prior to use. For the microplate protocol, 25 µL of each protein sample or BSA standard was pipetted into appropriately labelled wells of a microplate, followed by the addition of 200 µL of the freshly prepared WR to each well. The plate was incubated at 37 °C for 30 minutes. After incubation, the absorbance at 562 nm was measured using a microplate reader (BMG LabTech CLARIOstar). The protein concentration of each sample was calculated by plotting the absorbance values against the BSA standard curve and interpolating the unknown sample concentrations.

2.4.9 Production of SpyCatcher.HBsAg VLPs by SpyBiotech

SpyCatcher.HBsAg VLPs used in this study were produced by our collaborator, following this method adapted from their published protocol [304]. The yeast *Pichia pastoris* (PichiaPink Expression System, Invitrogen) was transformed with the pPink-HC vector containing a single copy of the SpyCatcher.HBsAg gene sequence (N1SpyCatcher-GSG3 spacer-PVTN spacer-HBsAg S protein EPEA). Production was conducted in a 10 L scale BIOSTAT B benchtop bioreactor (Sartorius Stedim Biotech, Germany) using a high cell density, fed-batch fermentation procedure under the control of the AOX1 promoter according to Invitrogen's guidelines. Fermentation started with 4 L basal salts medium and 4% glycerol, inoculated with 400 mL of seed culture at OD600 = 2.0 to initiate batch phase growth, followed by an 8 h glycerol fed-batch to boost biomass. After the initial glycerol was consumed, expression was induced for 72 h by switching the feed to methanol. Following fermentation, 100 g of wet cell pellet was resuspended in 200 mL ice-cold lysis buffer (20mM Tris-HCl pH 8.0, 5mM EDTA) and lysed by high pressure homogenization at 1,000 bar (APV 2000, SPX Flow Technology, Germany). The cell pellet was collected by centrifugation at 12,000*g* at 4° C for 30min and washed twice with ice-cold lysis buffer. SpyCatcher.HBsAg was released by mixing the pellet with 500 mM NaCl and 0.5% Tween 20, followed by centrifugation at 12,000*g* at 4 °C to recover the supernatant. Protein adsorption was performed by incubating the SpyCatcher.HBsAg-containing supernatant with Aerosil-380 pre-equilibrated with binding buffer (20mM Tris pH 8.0, 500mM NaCl) for 15 h at 4 °C. Aerosil-380 was collected by centrifugation at 3,200*g* at 4 °C for 10min, washed twice with binding buffer, and eluted in 80 mL of 50 mM sodium bicarbonate pH 10.5, 1.2 M urea at 37 °C for 2 h. The eluate was clarified using 0.22 µm vacuum filtration. Further purification utilized CaptureSelect C tag XL Affinity Matrix (Life Technologies) per manufacturer's instructions, followed by size-exclusion chromatography on an XK column with Superose 6 Prep Grade resin (GE Healthcare). SpyCatcher.HBsAg fractions were treated overnight with 3 M KSCN at 4 °C, and KSCN was removed by extensive dialysis against TBS. The product was incubated at 37 °C for 5 days before use. SpyCatcher.HBsAg VLPs were stored at -80 °C until use.

2.4.10 HPLC Analysis of TTT.PkSpyTag002 protein and SpyCatcher.HBsAg VLP conjugate

To optimize the conjugation of the TTT.PkSpyTag002 protein with SpyCatcher.HBsAg VLPs, High-Performance Liquid Chromatography (HPLC) was performed using an Agilent 1260 Infinity HPLC system with a Multi-Detector Suite (including UV, refractive index, and light scattering detectors). The analysis used a 200 nm column, 0.5 mL/min flow rate at room temperature, in accordance with Douglas group protocol D60, version 3.0. The HPLC analysis was carried out with guidance and direction of Catherine Cherry, Rameswara Segireddy, and Shawkat Hussain.

Samples were prepared by diluting the purified TTT.PkSpyTag002 protein in PBS, then centrifuged to remove particulates. The injection volume was set to 100 µL. For the analysis, samples were prepared to include a constant amount of HBsAg VLP (30 µg per sample; 1 µg/µL stock), except for the TTT.PkSpyTag002 alone control. Various molar VLP/TTT.PkSpyTag002 protein ratios were tested, specifically 0.08, 0.15, 0.3, 0.5, and 0.8, using a TTT.PkSpyTag002 protein stock concentration of 0.6 µg/µL. These mixtures were incubated for 3 h at room temperature before injection. Additional experimental conditions were examined, including overnight incubation, acidic (pH:5), and shaking at 300 RPM (Table 2.3).

Molar ratio			ug/uL	ug in reaction	mw	moles	uL of stock	ug total	Buffer to add	conc ug/mL	total volume		
Sample 1	0.08	VLP	1	30.00	36000	8.3333E-10	30.00				3 h incubation		
		TTT	0.6	14.80	2E+05	6.6667E-11	24.67	44.80	220.00	163.11	274.67		
Sample 2	0.15	VLP	1	30.00	36000	8.3333E-10	30.00				3 h incubation		
		TTT	0.6	27.75	2E+05	1.25E-10	46.25	57.75	200.00	209.05	276.25		
Sample 3	0.3	VLP	1	30.00	36000	8.3333E-10	30.00				3 h incubation		
		TTT	0.6	55.50	2E+05	2.5E-10	92.50	85.50	150.00	313.76	272.50		
Sample 4	0.5	VLP	1	30.00	36000	8.3333E-10	30.00				3 h incubation		
		TTT	0.2	92.50	2E+05	4.1667E-10	462.50	122.50	90.00	210.30	582.50		
Sample 5	0.8	VLP	1	30.00	36000	8.3333E-10	30.00				3 h incubation		
		TTT	0.6	148.00	2E+05	6.6667E-10	246.67	178.00	0.00	643.37	276.67		
Sample 6	0.5	VLP	1	30.00	36000	8.3333E-10	30.00				Overnight incubation		
		TTT	0.6	92.50	2E+05	4.1667E-10	154.17	122.50	90.00	446.81	274.17		
Sample 7	0.5	VLP	1	30.00	36000	8.3333E-10	30.00				3 h incubation		
		TTT	0.6	92.50	2E+05	4.1667E-10	154.17	122.50	90.00	446.81	274.17	Addition buffer Ph:4.8	
Sample 8	0.8	VLP	1	30.00	36000	8.3333E-10	30.00				VLP Alone		
		TTT	0.6	0.00	2E+05	6.6667E-10	0.00	30.00	244.17	109.42	274.17		
Sample 9	0.8	VLP	1	0.00	36000	0	0.00				Antigen Alone		
		TTT	0.6	92.50	2E+05	0	154.17	92.50	120.00	337.39	274.17		
Sample 10	0.5	VLP	1	30.00	36000	8.3333E-10	30.00				3 hrs incubation		
		TTT	0.6	92.50	2E+05	4.1667E-10	154.17	122.50	90.00	446.81	274.17	Shaking Incubation 300 RPM	

Table 2.3 Experimental Setup for HPLC Analysis. HBsAg VLP and TTT.PkSpyTag002 Mixture Conditions.

2.4.11 Confirmation of Particle Formation

Particle formation was confirmed by Negative Staining Electron Microscopy conducted at the Dunn School of Pathology facilities by Charlotte Melia and Raman Dhaliwal.

2.4.12 Western Blot Analysis for Conjugation Verification

Conjugation was also confirmed by Western blot using CaptureSelect™ Biotin Anti-C tag Conjugate as the primary antibody (Thermo Scientific, 7103252100). Streptavidin-alkaline phosphatase (R&D Systems) was used as the secondary detection reagent, and blots were visualized using the iBind™ Western System (Invitrogen), as explained previously.

2.4.13 GNL Capture ELISA for BnAb Binding

The 96-well Nunc™ MaxiSorp™ ELISA Plates (Biolegend) was coated with GNL (Vector Laboratories, cat. no. L-1240) at a concentration of 20 µg/mL in 0.1 M $NaHCO_3$, pH 8.6, and incubated overnight at 4 °C. After coating, the plates were blocked with Casein Blocker in PBS (Thermo Fisher Scientific, cat. no. 37528). Subsequently, 100 µL of purified protein (TTT.PkSpyTag) and conjugated proteins (TTT.PkSpyTag with SpyCatcher.HBsAg VLP) samples in PBS (1 µg/mL) were added to the wells and incubated for 2 hours at room temperature.

After a double wash step with PBS to remove unbound proteins, 3-fold serial dilutions of test primary antibodies (bNAbs) prepared in Casein Blocker were added and incubated for 2 h at RT. Starting antibody concentrations were 1 µg/mL for antibodies, 2G12, VRC01, PGT145, and PGT121 (the antibodies were kindly provided by Lachlan Deimel and Quentin Sattentau).

Following three washes with PBS, HRP-labeled goat anti-human IgG (Jackson ImmunoResearch, cat. no. 109-035-003) diluted 1:3000 in Casein Blocker was added and incubated for 1 h. Plates were washed five times with PBS/0.05% Tween-20. The 50 µL of TMB High Sensitivity Substrate Solution (Biolegend, cat. no. 421501) was added to each well. After 10 minutes, the colorimetric reaction was stopped by adding 50 µL of Stop Solution for TMB Substrate (Biolegend, cat. no. 423001) to wells. The optical density (OD) at 450 nm was measured to generate binding curves for the analysis of bnAb binding to the captured proteins (BMG LabTech CLARIOstar).

2.4.14 SMAA.TTT Complexes Preparation

TTT.Pk proteins were harvested according to Expi293 cell transfection manual and and purified using GNL chromatography. Staphylococcus aureus (StaphA) cells (200 µL) were washed three times with 1 mL of cold phosphate-buffered saline (PBS). Each wash was followed by centrifugation at 10,000 RPM for 5 minutes. The final bacterial pellet was resuspended in 40 µL cold PBS. Subsequently, 40 µL of Pk336 antibody (2 mg/mL) was added to the StaphA suspension. The mixture was incubated on ice for 1.5 h and gently mixed every 15 minutes to promote conjugation. The conjugated cells were washed three additional times in 1 mL cold PBS to remove unbound antibodies. The bacterial pellet was resuspended in 231 µL PBS, and 200 µg of purified TTT.Pk protein was added, bringing the total reaction volume to 1 mL. The complex was incubated for 2 h on a roller shaker to facilitate conjugation.

The mixture was then washed three times with 1 mL cold PBS. The first supernatant from these washes was retained quantify unconjugated antigen.

2.4.15 Mouse Immunization

Six weeks old female inbred BALB/c mice from Envigo were immunized. All animals and procedures were used in accordance with the terms of the UK Home Office Animals Act with Project License number PP1892852 and PP0984913 (PIL number: I46427560). Procedures were approved by the University of Oxford Animal Care and Ethical Review Committee.

Each mouse received 10 µg of TTT.Pk (or respective conjugated protein, VLP.TTT or SMAA.TTT) per immunization dose. The antigen was diluted to the appropriate volume in PBS and mixed 1:1 with Addavax adjuvant (InvivoGen) to a final volume of 100 µL per mouse (50 µL antigen solution + 50 µL Addavax). Prior to immunization, vaccines were prepared by combining the protein and adjuvant, followed by thorough mixing to ensure emulsion formation.

For the preparation of VLP.TTT vaccines, HBsAg VLPs were used at 3.24 µg per mouse dose, mixed with 10 µg of TTT.PkSpyTag002 protein in a total volume of 19.89 µL. The proteins were combined and first incubated with shaking at 300 RPM for 3 h at RT, followed by an additional overnight incubation at 4 °C without shaking to facilitate efficient conjugation and complex formation. Prior to administration, the antigen mixture was brought to 50 µL with PBS and mixed 1:1 with Addavax adjuvant.

All mice were immunized by intramuscular injection (50 µL per leg). Immunizations were carried out under general isoflurane anaesthesia. The immunization schedule (including the number of doses and intervals) followed the approved study design for the specific experiment. Following each immunization, mice were monitored for general well-being and any signs of adverse reactions. Blood samples were collected using Sarstedt Microvette 300 K2E at defined time points. The serum was separated by centrifugation at 10,000 RPM for 10 minutes.

2.4.16 Endpoint ELISA

Nunc™ MaxiSorp™ ELISA Plates (Biolegend) were coated directly with TTT.Pk antigen at a concentration of 2 µg/mL in bicarbonate coating buffer (0.1 M $NaHCO_3$, pH 8.6), 100 µL per well, and incubated overnight at 4 °C in a humidified box. Plates were washed three times with PBS containing 0.05% Tween 20 (PBS-T), then blocked with 200 µL per well of Casein Blocker in PBS (Thermo Fisher Scientific, cat. no. 37528) for 1 h at room temperature.

Serum samples were prepared as 3-fold serial dilutions in Casein Blocker in PBS, starting at 1:100, and added in duplicate to the plate, along with background, negative, and positive controls. The plate was incubated for 2 h at RT and then washed five times with PBS-T. Goat Anti-Mouse IgG Antibody, HRP conjugate (Sigma-Aldrich) was diluted 1:15,000 in Casein Blocker in PBS and 50 µL was added to each well, followed by an incubation at RT for 1 h. Plates were again washed three times with PBS-T.

For development, 50 µL of TMB Substrate (Biolegend, cat. no. 423001) was added to each well and the plate was incubated for 10 minutes to allow color development. The reaction was stopped by adding 50 µL of Stop Solution for TMB Substrate (Biolegend, cat. no. 423001) to each well, which changed

the colour from blue to yellow. Plates were read immediately at 450 nm using BMG LabTech CLARIOstar plate reader. Data analysis was carried out by subtracting background, determining control means, and calculating the endpoint titre, using a cut-off of the mean negative control optical density plus three standard deviations.

CHAPTER 3: CHARACTERIZATION OF T-CELL RESPONSES TO CONSERVED MOSAIC HIV-1 VACCINES IN PEOPLE LIVING WITHOUT HIV-1

3.1 Introduction

3.1.1 Rationale for Targeting Conserved HIV-1 Regions

The extraordinary genetic diversity and rapid mutation rate of HIV-1 present significant challenges to vaccine design, and often cause viral escape from immune responses targeted at variable regions [90, 92, 251]. Targeting the most conserved regions of the HIV-1 proteome offers a promising strategy to overcome this challenge [327]. The HIVconsvX mosaic vaccines are engineered to present highly conserved viral epitopes that are common to most circulating HIV-1 variants, thereby maximizing the likelihood of effective immune recognition across diverse global strains [332]. By focusing immune responses on these conserved regions, the aim is to reduce the risk of ineffective responses and immune escape, and achieve more robust control of infection [332].

3.1.2 Characterization of Vaccine-Induced T-Cell Responses

Understanding the quality and breadth of T-cell responses elicited by vaccination is crucial for evaluating immunogenicity and predicting efficacy [179]. This chapter examines the T-cell responses induced in participants of the vaccine trial, HIV-CORE 005.2 (NCT04586673). In this trial, the conserved mosaic vaccine HIVconsvX was delivered by the vectors ChAdOx1.HIVconsv1 (C1) and MVA.tHIVconsv3 & MVA.tHIVconsv4 (M3&M4) vaccines in the C1-M3M4 regimen in healthy people living without HIV-1 in Oxford, UK. Immune responses were analysed using IFN-γ ELISpot assay and multi-parameter flow cytometry, and the responses to both vaccine-encoded epitopes and epitope variants beyond the vaccine immunogen were quantified. The breadth of recognition, and the polyfunctionality of CD8+ T cells, multiple cytokine productions and degranulation phenotypes, were evaluated. This study also addresses the specificity of responses, by the detection of responses to unnatural junctions arising from mosaic immunogen design.

3.1.3 HIVconsvX vaccine design

The HIVconsvX immunogen (Figure 3.1) was developed by Prof. Tomáš Hanke and his team. It comprises two highly conserved regions from Gag, including the full-length p24, and four from Pol, selected on the basis of sequence conservation, without consideration of the number of known epitopes or HLA coverage [332]. To identify these regions, alignments of global HIV-1 protein sequences from the Los Alamos National Laboratory HIV Sequence Database (as of September 2013) were used to generate bivalent mosaic sequences of the full Gag and Pol proteins. These mosaics differed by approximately 10% of amino acids and, together, achieved a perfect match to 80% of all potential T-cell epitope (PTE) variants within group M HIV-1 [332].

The HIVconsvX immunogens uses three distinct strategies to effectively stimulate CD8+ T cells. First, they use six regions of HIV-1 proteins that are functionally conserved across HIV-1 M group clades, making it difficult for HIV-1 to escape without the fitness cost [327, 332]. Second, they include bivalent complementary mosaic immunogens, which optimize global epitope matching and the breadth of responses, as well as block common escape paths [332]. Third, they contain epitopes associated with low viral load in infected untreated individuals, which have been demonstrated to induce protective responses. The vaccine contained 33 of the 48 beneficial epitopes defined by Mothe *et al*.

[332, 334]. Env was intentionally left out because it has only a short, conserved segment and it doesn't contain any beneficial epitope [332].

The six regions were reordered to minimise immune responses to irrelevant junctional neo-epitopes, thereby preventing any junction from being immunised more than once (Figure 3.2). Region boundaries were further refined to maximise the inclusion of protective epitopes [334]. Genes encoding HIVconsv1, HIVconsv3, and HIVconsv4 were inserted into replication-deficient ChAdOx1 and MVA vectors and administered in heterologous prime-boost regimens, which have been shown to be safe and highly immunogenic in humans [385].

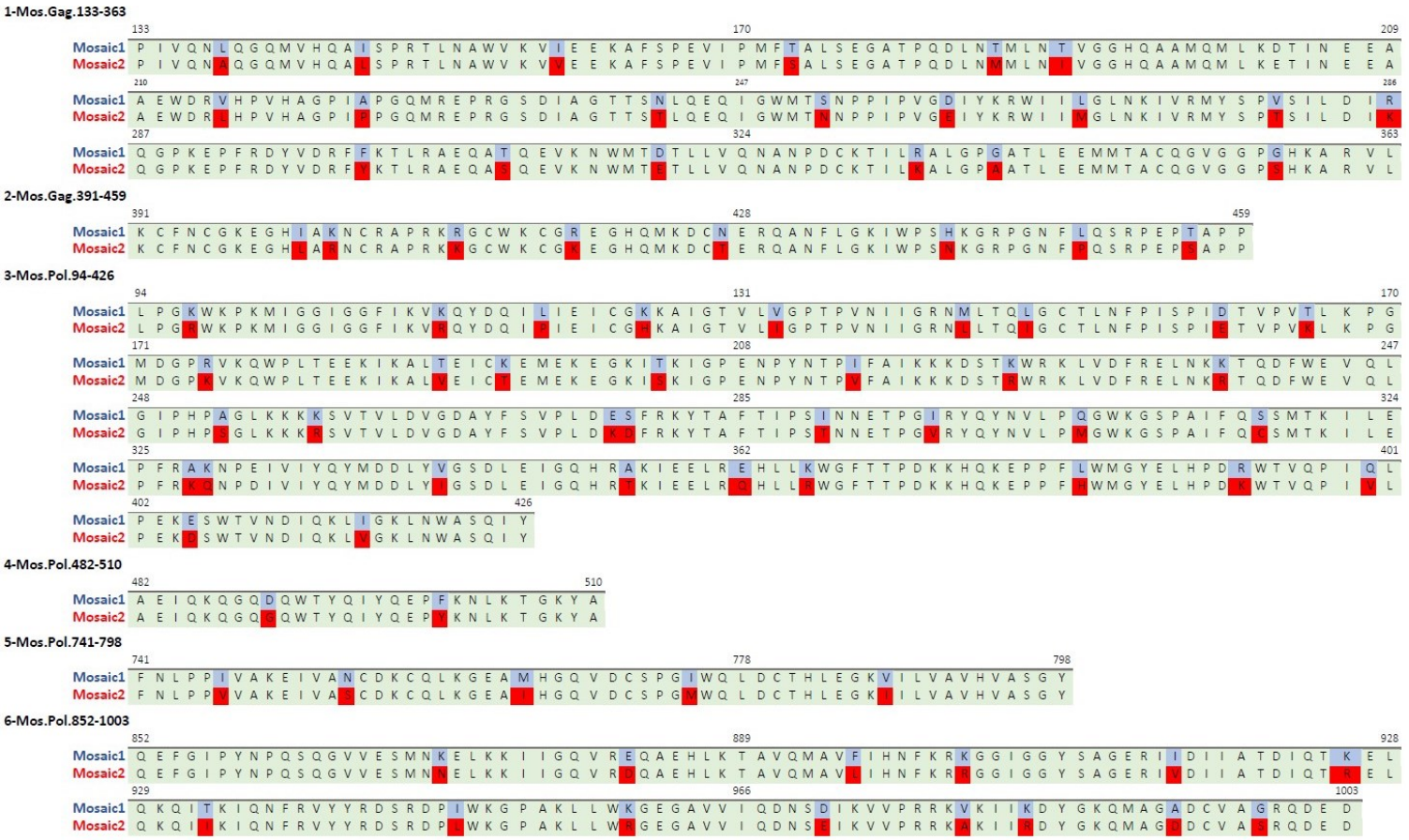

Figure 3.1 The six regions of the HIVconsvX vaccine mosaic 1 and 2.

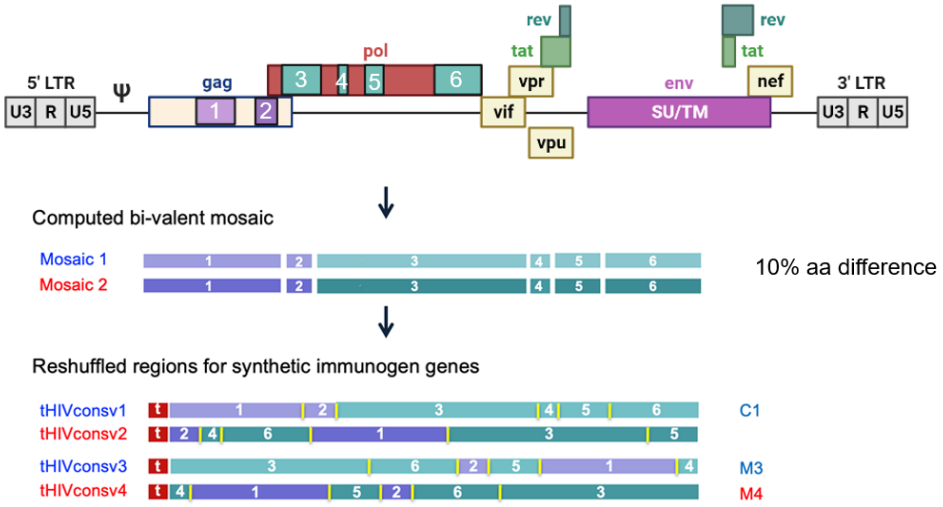

Figure 3.2 HIVconsvX bivalent conserved mosaic vaccine design. The six most conserved regions of the HIV-1 proteome were reconstructed into two immunogens, Mosaic 1-blue and Mosaic 2-red. Bi-valent mosaics were computed using the Gag (regions 1 and 2) and Pol (regions 3-6) proteins of the HIV-1 group M proteomes from Los Alamos National Laboratory (LANL) HIV Sequence database. To avoid immunizing with any junction more than once, the six regions of Mosaic 1 and Mosaic 2 were rearranged into six distinct orders. In the immunogen name, 't' represents the human tissue plasminogen activator leader sequence, whereas 'Pk' refers to the C-terminal Pk tag, which is recognised by specific monoclonal antibodies.

3.1.4 The HIV-CORE 005.2 Clinical Trial

A Phase 1 clinical trial was conducted to test the safety and immunogenicity of the HIVconsvX vaccine. The study involved two groups of healthy volunteers who were living without HIV-1/2 (Figure 3.3). Group 1 (n = 3) received one-tenth of the standard adult dose of C1 and were closely monitored for local and systemic reactogenicity. Upon confirmation of safety, Group 2 (n = 10) received the full adult doses of the C1-M3M4 regimen. The primary objective of the trial was to assess the safety and tolerability of the vaccine. The secondary objectives were to determine the percentage of vaccine recipients who developed HIVconsvX-specific T-cell responses after being given the C1-M3M4 vaccine regimen, and to evaluate the frequency, breadth, and duration of HIVconsvX-specific T-cell responses in vaccine responders. Additionally, the study aimed to evaluate the ability of the HIVconsvX-specific T-cell responses to inhibit replication *in vitro* of viruses from four major HIV-1 clades A, B, C, and D. The exploratory objective was to assess the polyfunctionality of the HIVconsvX-specific T-cells in the vaccine responders. Blood samples were collected from the volunteers on days 0, 35, 42, and 140 (Figure 3.4).

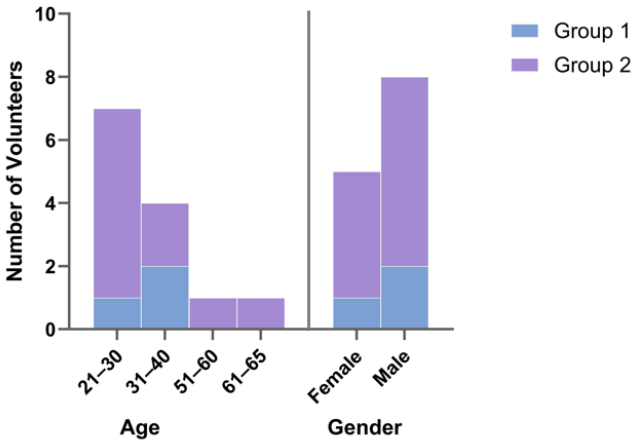

Figure 3.3 Demographics.

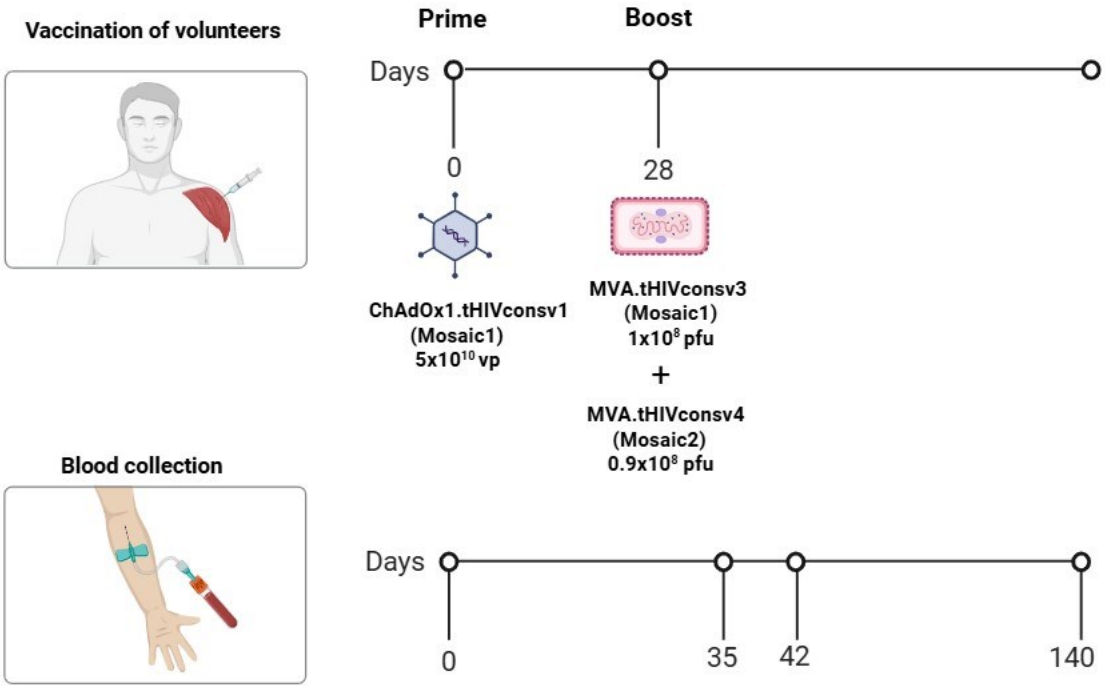

Figure 3.4 HIVCORE-005.2 vaccination regimen, doses and blood sampling. The heterologous prime-boost vaccination regimen using three vaccines: ChAdOx1.tHIVconsv1 (mosaic 1), MVA.tHIVconsv3 (mosaic1), and MVA.tHIVconsv4 (mosaic2)**.**

3.2 Aims:

- To characterize the frequency and breadth of the HIVconsvX-specific T-cell responses in vaccine recipients.
- To assess the polyfunctionality of vaccine-induced T-cells by Intracellular Cytokine Staining assays.
- To evaluate the immune response to epitope variants not included in the vaccine bi-valent immunogens.
- To assess the specific T-cell responses to junctional epitopes which arise from the lining the six regions into one ORF.

3.3 Results:

3.3.1 The HIVconsvX vaccines induced high frequencies of HIV-1-specific T cells

The IFN-γ ELISpot assay was used to quantify HIVconsvX-specific T-cells as the primary immunological readout. Freshly isolated peripheral blood mononuclear cells (PBMC) were re-stimulated with 399 15-mer peptides overlapping by 11 aa (15/11) representing the entire HIVconsvX immunogen. The peptides were divided into 10 pools of 34–47 peptides. All (100%) vaccine recipients responded to the C1-M3M4 regimen; median (IQR) = 4432.5 (2750–5820) spot-forming units (SFU)/10^6 PBMC at peak time point (D35). Compared to pre-vaccination, on day 35 and day 42, vaccine-induced responses were statistically significantly different ($p<0.0001$ and $p=0.0030$ respectively). At the end of the monitoring period, on day 140, the vaccine-induced response was still detectable although lower than earlier time points, with a total net frequency of median (IQR) = 595 (320-1495) SFU/10^6 PBMC ($p=0.1130$) (Figure 3.5).

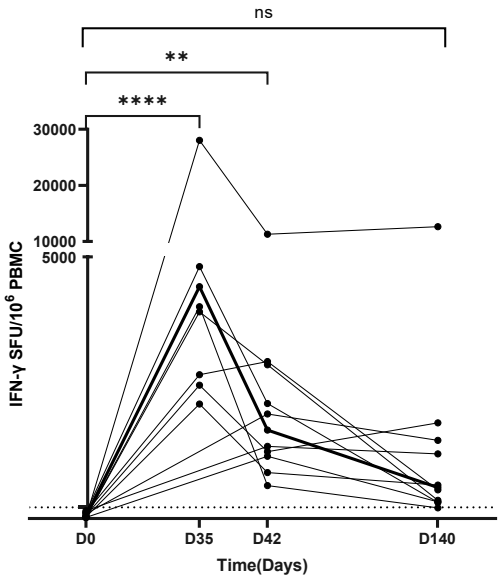

Figure 3.5 The totals (sum of all pools) of net T-cell frequencies as SFU per million of PBMCs. Freshly isolated, unexpanded PBMCs were stimulated with Pools 1-10 of overlapping 15/11 peptides spanning the entire HIVconsvX immunogen, and the IFN-γ release measured in an ELISpot assay. Individual participant responses are displayed as separate lines. The solid line shows the group median. The horizontal dotted line indicates pre-vaccination total HIVconsvX-specific frequencies of T-cells plus three SDs. The T-cell responses reached their peak on day 35 (D35). HIVconsvX vaccination induced statistically significant responses on day 35 and day 42 (D42) compared to pre-vaccination levels ($p<0.0001$ and $p=0.0030$ respectively). On the day 140 this difference was not statistically significant ($p=0.1130$) (Shapiro-Wilk test, Dunn's multiple comparisons test).

3.3.2 HIVconsvX vaccination expands the breadth of HIV-1–specific T-cell responses

HIVconsvX vaccination elicited robust and broad T-cell responses in the C1–M3M4 regimen. The participants recognised a median (IQR) = 9 (8-10) out of 10 peptide pools on day 35. Positive pools were defined as those with IFN-γ responses exceeding the pre-vaccination frequency plus three standard deviations for each pool, corresponding to a cut-off of 50 SFU per million PBMCs. The number of positive peptide pools increased significantly at all post-vaccination time points compared to baseline (****: $p<0.0001$ **: $p=0.0041$ *: $p=0.0459$) (Figure 3.6 A). This expansion in breadth indicates the induction of responses targeting multiple functionally conserved regions of HIV-1. At the peak time point (D35), analysis of net frequencies showed clear differences in immunogenicity among the HIVconsvX peptide pools. While all pools contributed to the overall breadth of the T-cell response, and elicited responses were above the positivity cut-off, certain pools stimulated particularly strong IFN-γ production, with SFU counts reaching or exceeding 1,000 SFU per 10^6 PBMCs. In particular, pools 2 and 6 elicited the most robust responses (***: $p = 0.0003$, **: $p = 0.0016$, *: $p = 0.0153$) (Figure 3.6 B)

A.

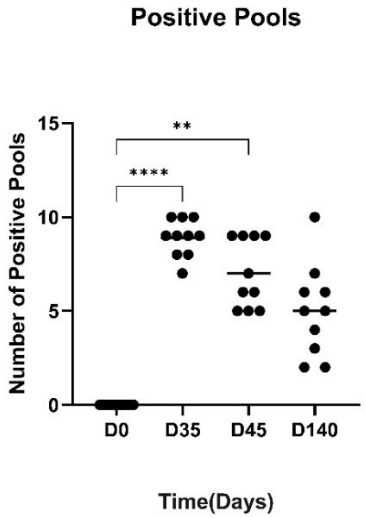

B.

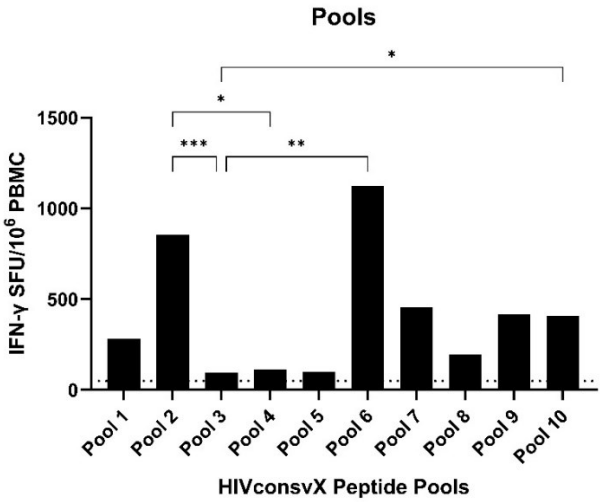

C.

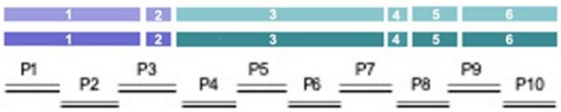

Figure 3.6 The breadth of vaccine-induced IFN-γ ELISpot responses. A) The number of positive pools for all individuals at each time point was shown. A pool was positive if the SFU exceeded the cut-off threshold of 50 SFU per million PBMCs. Friedman Test; ****: p<0.0001 **: p=0.0041 *: p=0.0459. B) The net frequencies of T cells recognizing individual peptide pools on day 35. Friedman Test; ***: p=0.0003, *: p=0.0153, **: p=0.0016. C) HIVconsvX peptide pools.

3.3.3 Minimum junction-specific responses were detected

Chimeric immunogens inevitably contain junctional epitopes at the interfaces between regions, and minimizing these potentially misleading, junction-specific responses is essential for accurate immunogenicity assessment. To evaluate T-cell recognition of these non-HIV junctional epitopes, we performed IFN-γ ELISpot assays using frozen, unexpanded PBMCs collected on day 42. The assay employed a single peptide pool of 31 junctional peptides, each spanning seven amino acids from the end of one region and the start of the next. Responses are shown as net SFU values (Figure 3.7). Although some junction-specific responses were detected (Median (IQR) = 76.25 (30–105)), they were markedly lower than responses to epitopes within the vaccine immunogen.

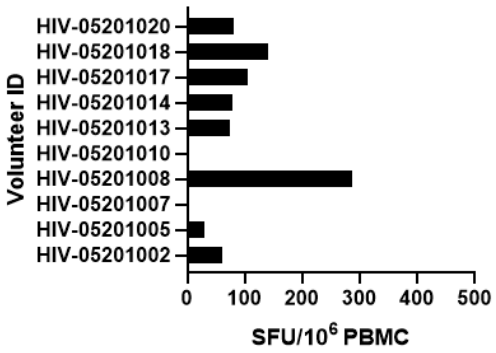

Figure 3.7 The junction-specific response induced by vaccination. Volunteer IDs were plotted on the y-axis, while the x-axis represents the frequency of T-cell responses. All data were collected using the IFN-γ ELISpot assay, and frozen unexpanded PBMCs were used.

3.3.4 HIVconsvX vaccine-elicited CD8$^+$ T-cells were polyfunctional

To evaluate the functionality of vaccine-induced T-cells, a multi-colour flow cytometry analysis was conducted to measure their ability to produce the cytokines IFN-γ, TNF-α, IL-2, and MIP-1α (CCL3), and degranulation (measured by CD107a surface expression). Samples from the day 35 were used, and the 10 peptide pairs inducing the highest ELISpot responses were selected for each individual based on the 15-mer epitope mapping assays (described in detail in Chapter 3). Each participant's peptide-specific responses for all measured functions are detailed in the supplementary material. Across the 20 peptides evaluated for each participant, those inducing maximal IFN-γ production were selected to quantify polyfunctional capacity by Boolean gating strategy. The frequency of CD8$^+$ T-cells expressing five, four, three, two, or one simultaneous effector functions was determined, with median (IQR) values of 0.28% (0.089-0.62), 5.39% (2.01-8.18), 2.38% (1.15-4.82), 2.34% (1.69-2.76), and 5.25% (4.82-6.19) of total CD8$^+$ T-cells, respectively. Notably, the most prevalent subset of polyfunctional CD8$^+$ T-cells was those exhibiting four effector functions. Within these quadruple-positive CD8$^+$ T-cell populations, the combination of IFN-γ, TNF-α, MIP-1α, and CD107a was the most prevalent, observed in eight out of ten participants (Figure 3.8).

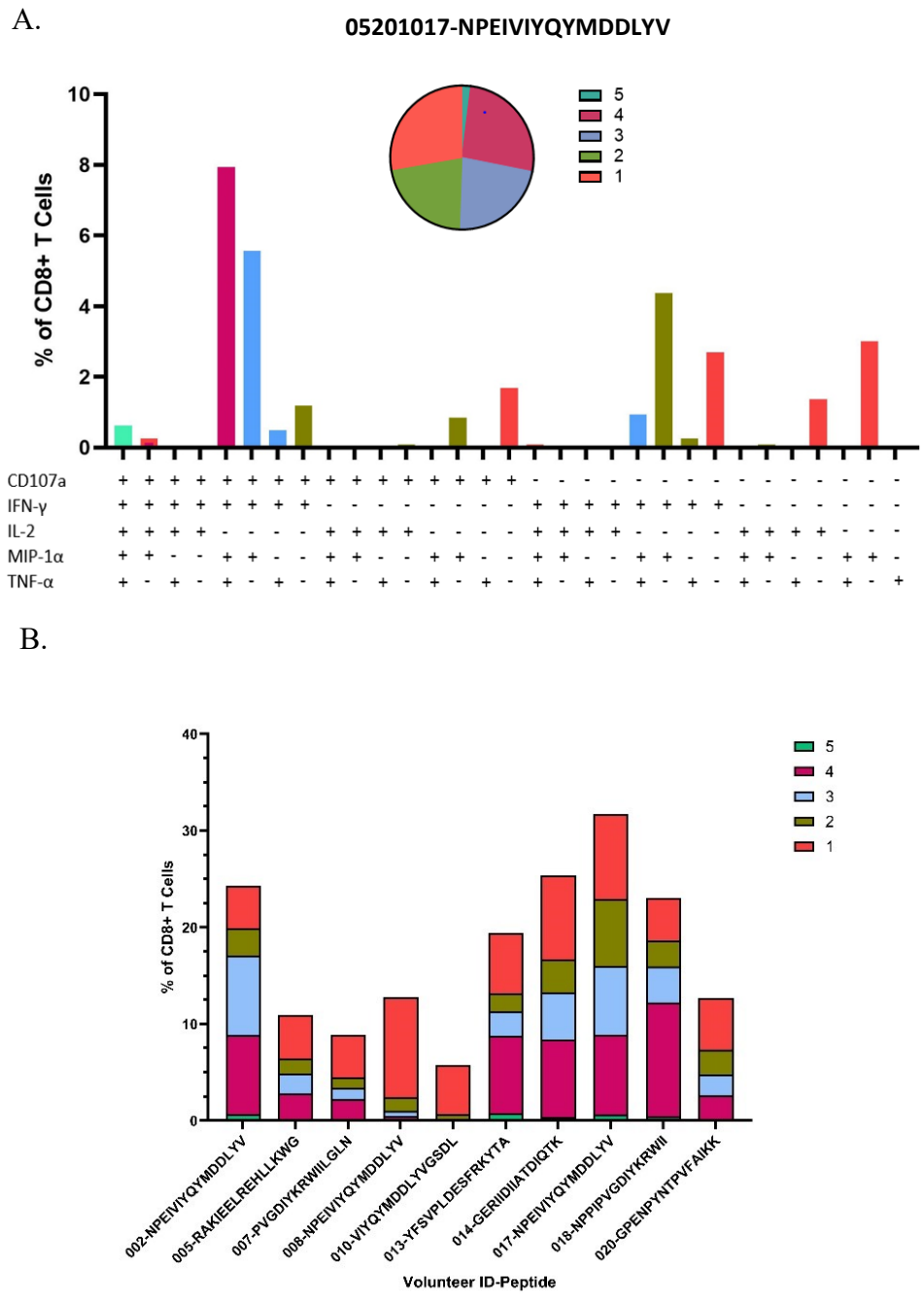

Figure 3.8 Functionality structure of vaccine-elicited CD8$^+$ T-cells. A) Flow cytometric analysis of participant 05201017's PBMCs, restimulated with peptide C256 (NPEIVIYQYMDDLYV), demonstrated the distribution of CD8+ T-cells expressing combinations of five effector functions: IFN-γ, TNF-α, IL-2, MIP-1α, and CD107a. The percentage of CD8+ T-cells exhibiting each functional combination is illustrated. Peptide C256 was selected for detailed figure because it elicited responses in the highest number of participants by 15-mer epitope mapping assay, indicating broad immunogenicity across the cohort. **B)** The summary bar chart illustrating the proportions of CD8$^+$ T-cells, across all participants, simultaneously expressing five, four, three, two, or one effector functions. Each stacked bar represents the distribution of polyfunctionality from highest (five functions) to lowest (single function).

C.

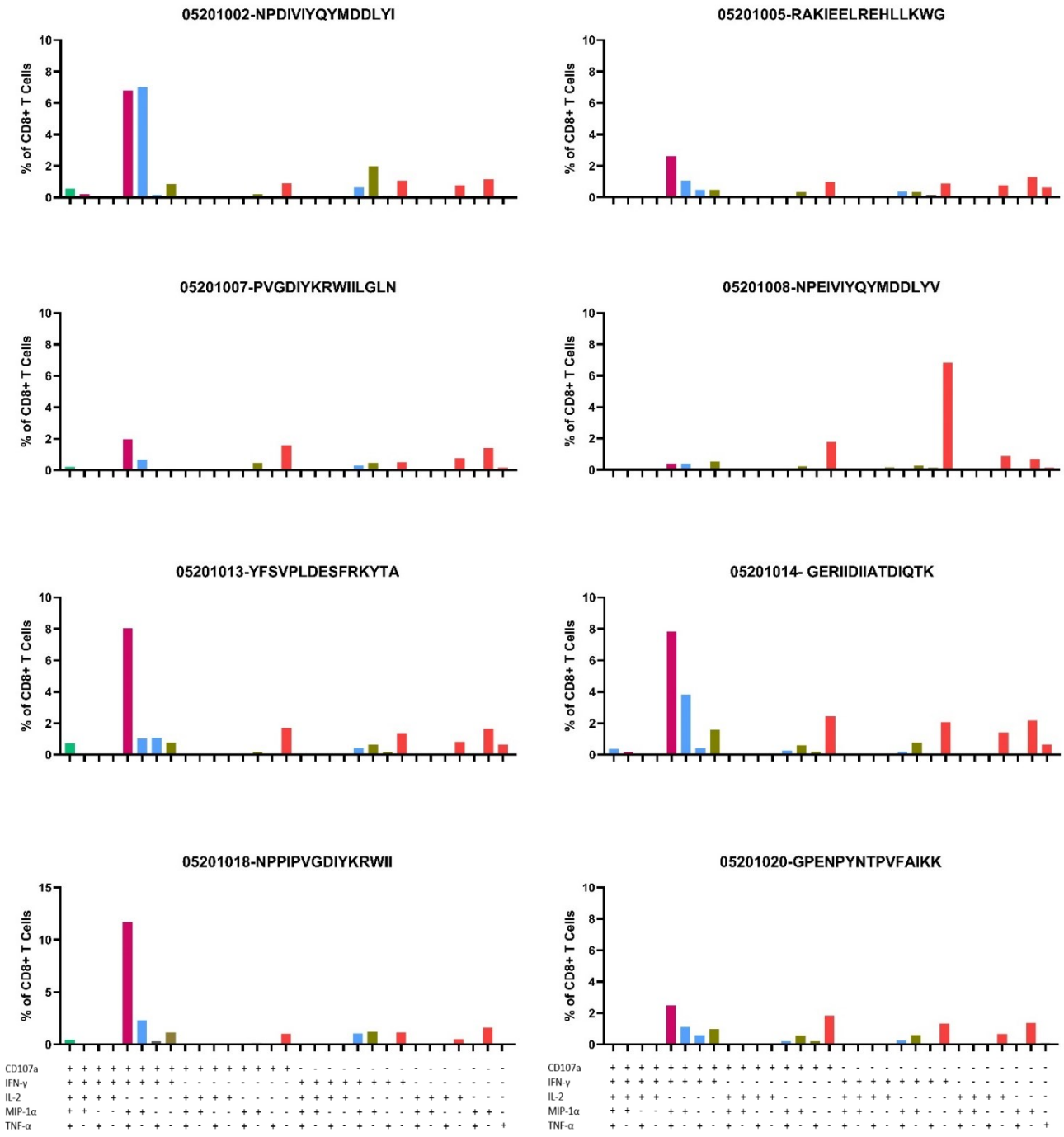

Figure 3.9 Functional profiles of vaccine-induced CD8$^+$ T-cell responses for each participant. The functional combinations of CD8$^+$ T-cells responding to the peptide that induced volunteers' highest IFN-γ production are shown.

3.3.5 HIVconsvX vaccines induces variant recognition

To address the genetic diversity of HIV-1, it is essential to evaluate the depth of variant recognition elicited by vaccination. In this study, for each participant, the 15-mer peptide pair that induced the strongest response in the epitope mapping assay was selected. Within these 15-mer peptides, all reported epitopes were identified using the LANL-HIV Sequence Database. For every epitope, all variant sequences with a global prevalence greater than 1% were determined based on database records (Table 3.1). These prevalent variants, along with the reference sequences from mosaic 1 and mosaic 2 immunogens, were tested. Frozen, unexpanded PBMCs collected at Day 35 were assayed ex vivo by IFN-γ ELISpot. In multiple cases, robust T cell recognition of epitope variants was observed, demonstrating the capacity of HIVconsvX vaccination to elicit responses beyond those encoded within the mosaic immunogens (Figure 3.9).

15 mer Peptide ID	Sequence	Variants	Frequency
C017	SPEVIPMFTALSEGA	EVIPMFSAL	60.59
C018	SPEVIPMFSALSEGA	EVIPMFTAL	31.69
		EIIPMFSAL	2.02
		EVIPMFAAL	1.66
C060	NPPIPVGDIYKRWII	GEIYKRWII	47.9
C061	NPPIPVGEIYKRWII	GDIYKRWII	41.5
		GEIYKRWIV	3.18
		GEIYKKWII	1.72
		EIYKRWII	47.93
		DIYKRWII	41.51
		EIYKRWIV	3.18
		EIYKKWII	1.72
C082	VDRFFKTLRAEQATQ	DRFFKTLRA	37.51
C083	VDRFYKTLRAEQASQ	DRFYKTLRA	50.58
		DRFFKVLRA	2.8
		DRFFKALRA	1.84
		DRFYKVLRA	1.67
		DRFFKCLRA	1.63
		DRFYRTLRA	1.13
C182/C183	TEEKIKALTEICKEM	ALVEICTEM	24.78
	TEEKIKALVEICTEM	ALTEICKEM	12.68
		ALTEICTEM	10.57
		ALTAICEEM	9.33
		ALIEICTEM	5.26
		ALTAICDEM	5.02
		ALTEICEEM	3.64
C194	GPENPYNTPIFAIKK	NTPVFAIKK	62.47
C195	GPENPYNTPVFAIKK	NTPIFAIKK	33.75
		NTPVFAIRK	1.24
C220	KKSVTVLDVGDAYFS	TVLDVGDAY	96.29
C221	KRSVTVLDVGDAYFS	SVLDVGDAY	0.95
		TILDVGDAY	0.82
C226	YFSVPLDESFRKYTA	VPLDKDFRKY	20.15
C227	YFSVPLDKDFRKYTA	VPLDESFRKY	17.38
		VPLDEDFRKY	12.51
		VPLDKEFRKY	10.13
		VPLDENFRKY	8.39
		VPLYEDFRKY	6.35
		VPLDEGFRKY	5.87
		VPLHEDFRKY	3.49
		VPLDEEFRKY	1.38
C254	FRAKNPEIVIYQYMD	NPEIVIYQY	30.91
C255	FRKQNPDIVIYQYMD	NPDIVIYQY	29.65
		NPEMVIYQY	9.6
		NPEIIIYQY	5.75
		NPELVIYQY	2.98
		NPDMVIYQY	2.52
		NPDLVIYQY	2.13
		NPEVVIYQY	1.94
		NPDIIIYQY	1.79
		NPEMIIYQY	1.53
C256	NPEIVIYQYMDDLYV	YQYMDDLYV	93.3
C257	NPDIVIYQYMDDLYI	YQYVDDLYV	2.4
		CQYMDDLYV	1.26
		YQYMDDLYI	0.97
		QYMDDLYV	94.59
		QYVDDLYV	2.84
		QYMDDLYI	0.99
		QYIDDLYV	0.27

15 mer Peptide ID	Sequence	Variants	Frequency
C268	RAKIEELREHLLKWG	EELREHLLKW	18.21
		EELRAHLLSW	14.06
		EELRQHLLRW	13.26
		EELRQHLLKW	11.56
		EELREHLLRW	9.41
		EELRAHLLKW	3.32
		EELRGHLLKW	2.11
		EELRDHLLKW	1.79
		EELRAHLLRW	1.45
		EELRQHLLGW	1.31
C269	RTKIEELRQHLLRWG	ELRQHLLRW	13.67
		ELREHLLKW	18.52
		ELRAHLLSW	14.55
		ELRQHLLKW	11.76
		ELREHLLRW	9.6
		ELRAHLLKW	3.44
		ELRGHLLKW	2.11
		ELRDHLLKW	1.94
		ELRAHLLRW	1.5
		ELRQHLLGW	1.31
C270	EELREHLLKWGFTTP	EELREHLLKW	18.21
		EELRAHLLSW	14.06
		EELRQHLLRW	13.26
		EELRQHLLKW	11.56
		EELREHLLRW	9.41
		EELRAHLLKW	3.32
		EELRGHLLKW	2.11
		EELRDHLLKW	1.79
		EELRAHLLRW	1.45
		EELRQHLLGW	1.31
C271	EELRQHLLRWGFTTP	ELRQHLLRW	13.67
		ELREHLLKW	18.52
		ELRAHLLSW	14.55
		ELRQHLLKW	11.76
		ELREHLLRW	9.6
		ELRAHLLKW	3.44
		ELRGHLLKW	2.11
		ELRDHLLKW	1.94
		ELRAHLLRW	1.5
		ELRQHLLGW	1.31
C304	DQWTYQIYQEPFKNL	IYQEPFKNL	76.44
C305	GQWTYQIYQEPYKNL	IYQEPYKNL	5.41
C306	YQIYQEPFKNLKTGK	IYQEQYKNL	4.15
C307	YQIYQEPYKNLKTGK	IYQEQFKNL	1.82
		IYQEPHKNL	1.58
		IFQEPFKNL	1.45
C310/C311	FNLPPIVAKEIVANC	LPPIVAKEI	48.32
	FNLPPVVAKEIVASC	LPPVVAKEI	36.44
		IPPVVAKEI	4.03
		LPPVIAKEI	3.35
		LPPIIAKEI	2.59
		LPPVVAREI	1.12
C370/C371	LQKQITKIQNFRVYY	KIQNFRVYY	83.47
	LQKQIIKIQNFRVYY	KVQNFRVYY	2.3
		KIQNFRVYF	2.25
		NIQKFRVYY	1.84
		KIQKFRVYY	1.53
		QIQNFRVYY	1.48
		KLQNFRVYY	1.33

Table 3.1 Variants that had a prevalence of over 1% according to the LANL database.

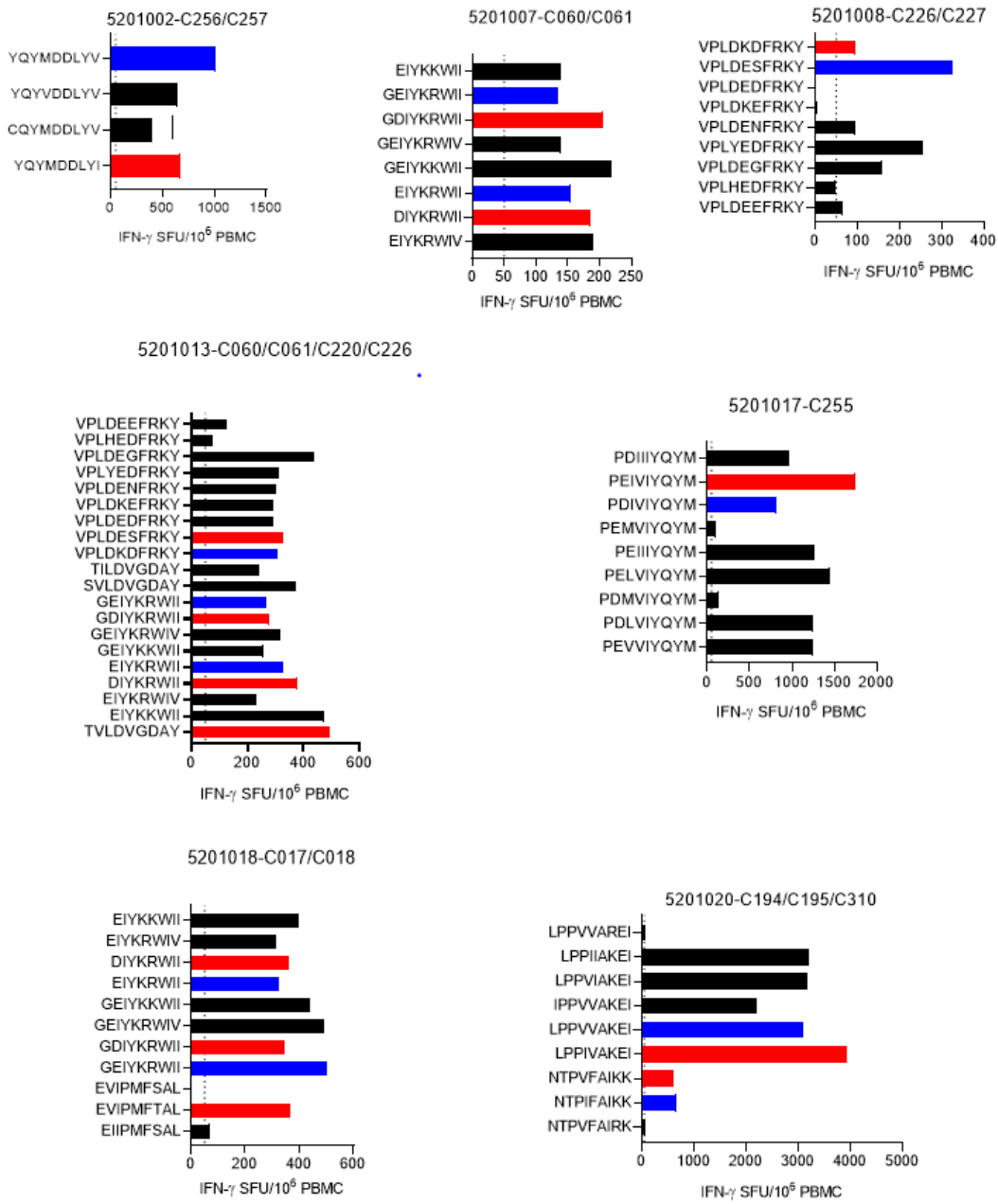

Figure 3.9 The recognition of epitope variants by vaccine-induced T cells. The epitopes found in mosaic 1 and 2 are indicated by blue and red-framed bars, respectively. The variants that were beyond the vaccine immunogens are denoted by black-framed bars. Volunteer IDs and parental epitope ID's are indicated on the top of each graph. Epitope sequences were plotted on the y-axis, while the x-axis represents the frequency of T-cell responses. All data were collected using the IFN-γ ELISpot assay on frozen unexpanded PBMCs.

3.4 Discussion

The extraordinary global diversity of HIV-1 is a significant obstacle to the development of an effective vaccine [244]. Traditional vaccine antigens, derived from natural HIV-1 sequences, have thus far demonstrated only limited ability to induce broad cellular immune responses in both nonhuman primate models and human clinical trials [386]. By contrast, polyvalent mosaic antigens have been rationally engineered to enhance cellular immune coverage against the vast heterogeneity in circulating HIV-1 strains [333]. In this context, the HIVconsvX vaccines, comprised of functionally conserved mosaic immunogens, were evaluated for their safety and immunogenicity in a Phase I clinical trial involving volunteers living without HIV-1/2 in the United Kingdom. The vaccine regimen used recombinant, replication-deficient ChAdOx1 vector for priming and MVA vectors for boosting, in a heterologous prime-boost strategy to maximize immunogenicity.

Results from the clinical trial show that the HIVconsvX immunogens administered in the C1-M3M4 regimen stimulated strong HIV-1-specific T-cell responses in all participants. Every recipient developed detectable immune responses after vaccination, and all vaccine components were well tolerated. At the peak time point, the vaccines induced the production of IFN-γ–producing T-cells, with a median exceeding 4,000 SFU per one million PBMCs. Importantly, the induced T-cells were broadly specific, they recognized HIV-1 epitope variants that were not only found within the vaccine but also beyond those encoded in the immunogens. These results support earlier studies showing that mosaic vaccines can generate greater breadth and depth of cellular immune responses compared to consensus or clade-specific approaches [386].

The ability of antigen-stimulated CD8+ T-cells to simultaneously perform multiple functions, known as polyfunctionality, has been associated with better viral control in multiple studies [179, 387]. For example, Betts *et al*. showed that non-progressors with stable CD4+ counts and low viral load maintain a higher proportion of polyfunctional CD8+ T cells (exhibiting five functions such as degranulation, IFN-γ, TNF-α, IL-2, and MIP-1β production) compared to typical progressors, and that the degree of polyfunctionality is inversely correlated with viral load [179]. In line with these findings, flow cytometric analyses in the HIVconsvX vaccine trial revealed that vaccine-induced CD8+ T cells were largely polyfunctional, with quadruple-positive subsets most commonly observed.

The mosaic vaccine designs contain junctional neo-epitopes at region interfaces. Our study showed that junction-specific responses were minimal and the magnitude lower than responses directed at internally encoded epitopes, validating the reshuffling strategy to reduce irrelevant immune activation.

Previous vaccine studies, including RV144 and HVTN 702, aimed to induce both antibody and cellular responses, but the protection observed was modest and often not confirmed in subsequent studies [258, 259, 274]. While RV144 provided marginal protective efficacy (~31%), later trials struggled to replicate these results. Cellular responses, particularly CD8+ T-cell functionality and breadth, remained limited in these earlier studies. In contrast, the HIVconsvX immunogens, in both UK and African trials, elicited high frequencies of IFN-γ-producing T cells with broad epitope recognition [336, 337]. All participants responded to the vaccine, and the median magnitude and breadth of the T-cell response compared favourably to those induced by previous candidates. Earlier mosaic approaches, such as Ad26.Mos.HIV, and previous HIVconsv vaccine designs also demonstrated good breadth and magnitude of responses, and showed promise in eliciting polyfunctional CD8+ T-cell responses in preclinical and early-phase clinical studies. The second generation HIVconsvX immunogen design, delivered by C1-M3M4 regimen consistently achieved strong immunogenicity across diverse populations.

HIVconsvX vaccines are designed to include only functionally conserved regions of HIV, thereby avoiding immune responses that would be directed at highly variable parts of the full-length viral proteins. By employing a bivalent mosaic immunogen approach, HIVconsvX achieves broader and more efficient coverage of viral diversity. Additionally, the use of potent heterologous vector delivery systems in HIVconsvX is expected to outperform the vaccine strategies used in the STEP (HVTN 502) and Mosaico studies [276, 318]. Employing ChAdOx1 and MVA vectors helps to overcome the anti-vector immunity challenges that limited the effectiveness of Ad5-based vaccines in the STEP study.

To conclude, the HIVconsvX mosaic vaccine regimen represents a significant advance in HIV vaccine immunology, delivering broad, high-frequency, and polyfunctional T-cell responses targeting conserved viral regions. As supported by both trial data and contemporary literature, such approaches offer robust, cross-clade immune protection and may pave the way for a new generation of efficacious HIV vaccines.

3.5 Limitations

As this was a phase 1 trial the study was conducted on a relatively small group of healthy people living without HIV-1/2. A larger sample size could potentially provide more robust and verifiable results.

The study's follow-up duration was 140 days. Longer-term follow-up could provide insights into the durability and persistence of the vaccine-induced T-cell responses and T-cell memory.

The study was conducted in a single location (UK). Differences in environmental factors or genetic backgrounds across various regions can influence the effectiveness of the vaccine.

The assessment heavily depended on laboratory techniques like ELISpot and flow cytometry, which can introduce variability in the outcomes. Additionally, certain assays involved the use of frozen cells, and the freezing process itself can impact the results.

A notable limitation of our study is that it focuses only on PBMCs, while the most critical immune response and elimination of HIV-1-infected cells actually takes place within lymphoid organs and tissues [388].

CHAPTER 4: EPITOPE MAPPING OF HIVCONSVX-INDUCED T-CELL RESPONSES IN UK AND AFRICAN CLINICAL TRIALS

4.1 Introduction

This chapter presents a comprehensive mapping of T-cell responses induced by the HIVconsvX vaccine in participants from two clinical trials conducted in the UK and Africa. Using overlapping peptides spanning the HIVconsvX immunogen, cultured ELISpot assays were performed on PBMCs from vaccinated and placebo recipients to evaluate the breadth of vaccine-elicited T-cell recognition. Mapping included initial screening of 399 overlapping 15-mer peptides to identify responsive peptide pairs, followed by fine mapping of selected peptides to predict minimal 9-mer epitopes and their HLA restriction.

4.1.1 Importance of Broad, Multi-Epitope T-cell Responses Targeting Conserved Regions in HIV Control

HIV-1 has an extensive viral diversity, and in people living with HIV-1, the immune system tends to target immunodominant regions of the viral genome that are highly variable [315]. In contrast, HIV-1 elite controllers and long-term non-progressors mount strong CTL responses to subdominant epitopes that are rarely targeted in typical infection [389]. These epitopes are structurally conserved and display few mutations at HLA anchor residues and T-cell receptor interaction sites [172]. Multiple studies indicate that redirecting host immunity toward conserved regions of the HIV-1 proteome can improve both the breadth and specificity of the response while limiting viral escape [322, 390].

Traditional vaccines containing full-length immunogens tend to elicit responses against immunodominant, therefore variable sites [391]. Conversely, new immunogens that incorporate multiple conserved sites may help safeguard host immunity against viral escape and prevent rebound after ART interruption [392].

Eliciting a broad and multi-epitope T-cell response is essential for the effective control of HIV [387, 393]. Individuals mounting responses to multiple Gag epitopes demonstrate improved control of plasma virus loads compared to those with narrower responses [1]. Therefore, designing vaccines that induce robust, broadly directed T-cell immunity against conserved HIV regions is desirable, and more likely to protect against diverse HIV strains.

4.1.2 Minimal Epitope Length and the Importance of HLA Restriction

Peptide presentation to $CD8^+$ T-cells is structurally constrained by the closed-ended HLA-I binding groove, which typically presents peptides of 8-10 amino acids, with 9-mers being the most prevalent length [188, 394]. Accurate mapping of minimal 9-mer epitopes and their HLA-I restrictions is critical to characterizing vaccine-elicited T-cell specificity and predicting immunogenicity across populations with diverse HLA frequencies. Defining the optimal epitopes presented by each HLA allele informs future epitope-centric immunogen designs, guides computational prediction of immunogenicity, and informs the selection of conserved regions for inclusion in next-generation HIV vaccines.

4.1.3 The LANL HIV Immunology Database

The Los Alamos National Laboratory (LANL) HIV Database is a widely used open-access source for HIV sequence and immunology data [395]. To support vaccine design and immunological research, the database integrates experimental findings, genetic sequence information, and analytical tools tailored to the unique challenges posed by HIV diversity.

Within the Immunology Database, a global collection of experimentally verified T-cell and B-cell epitopes is accessible with their HLA restrictions, protein location, and associated publications. $CD8^+$ T-cell epitopes are further classified as "A-list" and "B-list" epitopes according to the strength and clarity of supporting evidence [396]. The "A list" consists of best-defined T-cell epitopes that meet criteria for HLA restriction, minimal optimal sequence, and validation across multiple studies. The "B list" includes all published and unique HIV epitopes, regardless of whether the minimal optimal sequence or HLA restriction have been validated. LANL also provides tools for sequence alignment, epitope mapping, conservation analysis, HLA-binding predictions, and population coverage modelling resources that are essential for rational vaccine design.

In this chapter, after mapping vaccine-induced responses to minimal epitopes, we utilized the LANL HIV Immunology Database epitope search and prediction tools to determine whether our high-magnitude 9-mer epitopes had been reported previously and to predict their likely restricting HLA alleles. This integration of experimental mapping with LANL computational resources enabled us to distinguish unreported epitopes from those already described in the literature, both validating our findings and expanding the existing knowledge base of HIV-specific $CD8^+$ T-cell responses.

4.1.4 The HIV-CORE 005.2 and HIV-CORE 006 clinical trials

The HIVconsvX T-cell vaccine strategy was first evaluated in humans in the HIV-CORE 005.2 trial, an open-label, dose-escalation, phase 1 study conducted at the University of Oxford, UK. Thirteen healthy HIV-negative adults (aged 18-65) were enrolled between July 2021 and August 2022. Participants were allocated into two groups: three volunteers in group 1 received a low priming dose of ChAdOx1.tHIVconsv1 (C1), while ten participants in group 2 received a full standard dose of C1, followed four weeks later by a heterologous boost with MVA.tHIVconsv3 (M3) and MVA.tHIVconsv4 (M4) (the C1–M3M4 regimen). Volunteers were followed up for 140 days. The regimen was safe and well tolerated, with no serious adverse events reported. All vaccine recipients mounted robust T-cell responses, peaking at a median of 4,433 IFN-γ spot-forming units (SFU) per 10^6 PBMCs and recognising a median of 9 out of 10 peptide pools spanning the HIVconsvX immunogen. Vaccine-elicited T-cells were broadly reactive, polyfunctional, cross-clade, and capable of inhibiting HIV-1 from clades A, B, C, and D [336].

The HIV-CORE 006 trial extended the evaluation of HIVconsvX into African populations with diverse circulating HIV-1 clades. This was a double-blind, randomized, placebo-controlled phase 1 trial conducted across four clinical research centres in sub-Saharan Africa: Masaka (Uganda), Kilifi and Nairobi (Kenya), and Lusaka (Zambia). Between July 2021 and November 2022, 88 participants (57 men, 31 women; median age 30 years) received either vaccine (n=72) or placebo (n=16). Volunteers were assigned in a 9:2 ratio to receive the C1–M3M4 regimen or placebo. The C1 vaccine was administered intramuscularly at day 0, followed 28 days later by M3 and M4. Participants were followed for 40 weeks after the final vaccination. The regimen was safe and well tolerated, with no vaccine-related serious adverse events. Vaccine recipients mounted strong HIVconsvX-specific

responses, with 99% (70/71) of fully vaccinated individuals responding. Responses peaked at a median of 2,310 IFN-γ SFU per 10^6 PBMCs and recognised a median of 8 peptide pools out of 10. Vaccine-induced T-cells displayed proliferative capacity, polyfunctionality, and broad cross-clade inhibition of HIV-1 isolates [337].

Assessing immunogenicity and T-cell response breadth across these distinct settings is critical to determining the universal applicability and predicting efficacy of HIVconsvX vaccine strategy.

4.2 Aims

- To comprehensively map the breadth and distribution of T-cell responses induced by the HIVconsvX vaccine in participants from UK and African clinical trials.
- To identify and fine-map minimal optimal epitopes recognized by vaccine-elicited T-cells, and evaluate their HLA restriction**.**

4.3 Results

4.3.1 HIVconsvX vaccination induced broad, multi-epitope T-cell responses

We mapped vaccine-induced T-cell responses in 71 volunteers from two clinical trials: 10 participants from HIV-CORE 005.2 and 61 participants from HIV-CORE 006. Of these, 7 individuals received placebo. Epitope mapping covered all 399 15-mer peptides (overlapping by 11 amino acids) spanning the HIVconsvX immunogen. PBMCs collected at day 35 were expanded with the original 10 peptide pools and tested for IFN-γ release against each constituent peptide pair (each "peptide pair" denotes the mosaic 1 and mosaic 2 versions) by cultured ELISpot assay. For five peptides C047, C104, C141, C334, and C335 the mosaic-1 and mosaic-2 sequences are identical. The coded peptides C001 to C139 derive from Gag and C140 to C401 from Pol regions.

To establish a positivity cut-off, we calculated the median SFU count of the placebo recipients across all peptide pairs, then added three standard deviations to this value, yielding a threshold of ≥1000 SFU/10^6 short-term T-cell lines (STCL). The responses meeting or exceeding this threshold were considered positive.

The vaccinated participants recognised a median of 10 peptide pairs (range 0-70) out of the 203 tested pairs. Placebo recipients recognised a median of 0 (range 0-17) peptide pair (Figure 4.1). Responses were widely distributed across the HIVconsvX sequence, without restriction to a single immunodominant region. Of the 203 peptide pairs tested, 174 elicited at least one positive response in at least one volunteer, whereas 29 peptide pairs did not induce any responses above the positivity threshold in any participant (Figure 4.2). This pattern demonstrates that HIVconsvX vaccination induces multi-epitope recognition, which potentially enhances protective efficacy.

In addition to the broad distribution of responses, certain peptide pairs were recognised more frequently and with higher magnitude than others. Using the ≥1000 SFU/10^6 STCL cut-off, the most frequently recognised peptide pair was C082 VDRFFKTLRAEQATQ / C083

VDRFYKTLRAEQASQ, detected in 28 volunteers. The median magnitude across responders was 2069 SFU/10^6 STCL. This was followed by C256 NPEIVIYQYMDDLYV / C257 NPDIVIYQYMDDLYI and C258 VIYQYMDDLYVGSDL / C259 VIYQYMDDLYIGSDL, recognised by 24 and 26 volunteers, with median magnitudes of 3681 and 2265 SFU/10^6 STCL, respectively.

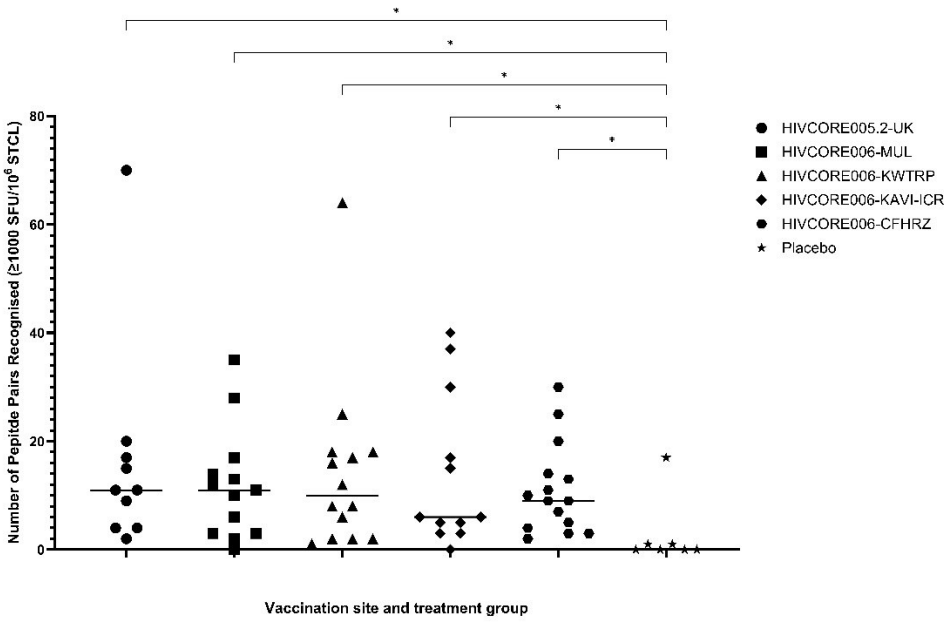

Figure 4.1 Breadth of HIVconsvX-induced T-cell responses across clinical trial sites and placebo group. Number of peptide pairs recognised at ≥1000 SFU/10^6 STCL in ELISpot assays for participants from HIV-CORE 005.2 (UK) and HIV-CORE 006 (sites: MUL, KWTRP, KAVI-ICR, CFHRZ) trials. Horizontal bars represent median values for each group. Statistical comparisons (Kruskal–Wallis with Dunn's multiple comparisons test) showed significantly greater breadth in all vaccinated groups compared with placebo: HIV-CORE 005.2-UK ($p = 0.0195$), HIV-CORE 006-MUL ($p = 0.0429$), HIV-CORE 006-KWTRP ($p = 0.0261$), HIV-CORE 006-KAVI-ICR ($p = 0.0382$), and HIV-CORE 006-CFHRZ ($p = 0.0334$).

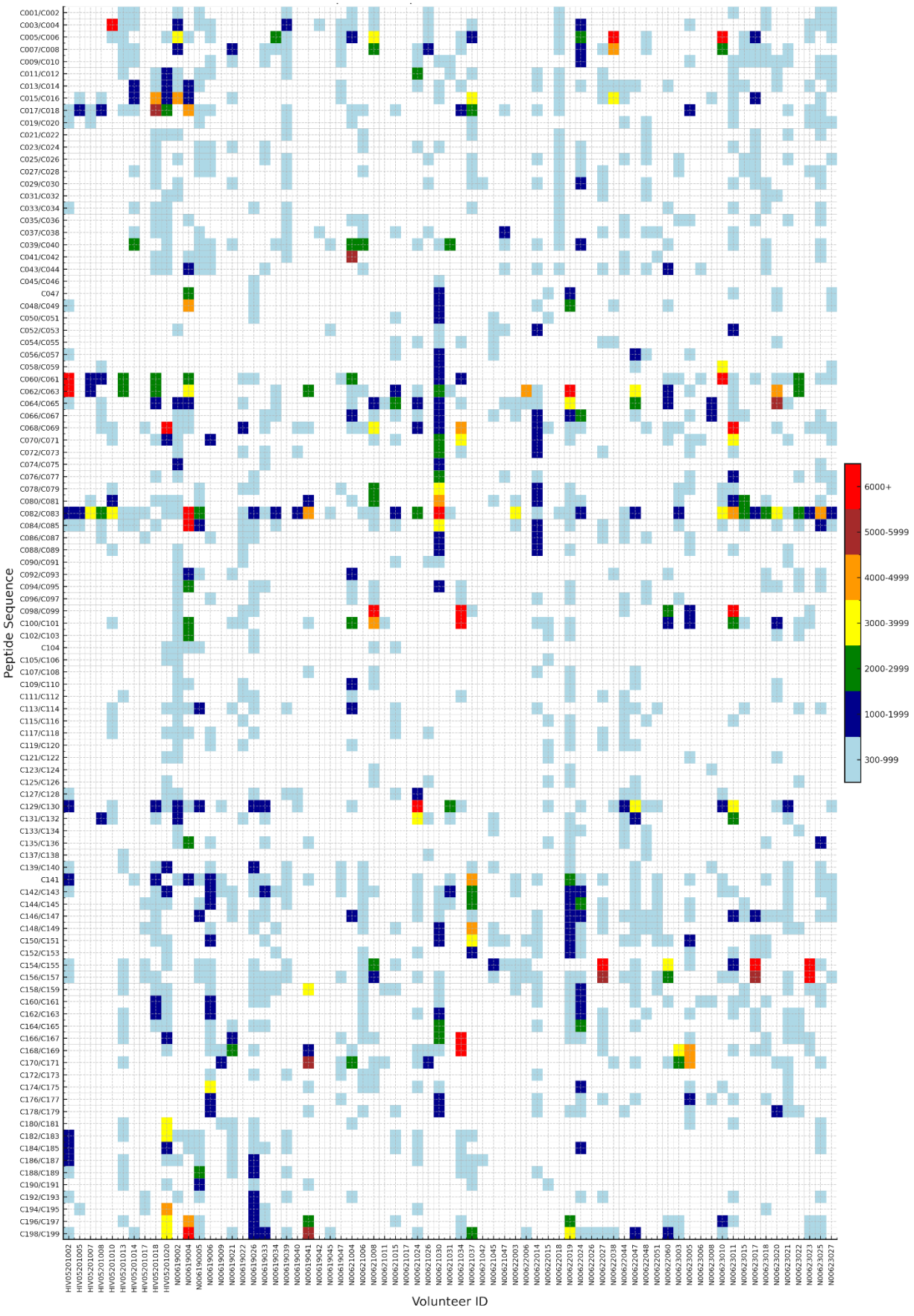
Peptide Sequence
C001/C002
C003/C004
C005/C006
C007/C008
C009/C010
C011/C012
C013/C014
C015/C016
C017/C018
C019/C020
C021/C022
C023/C024
C025/C026
C027/C028
C029/C030
C031/C032
C033/C034
C035/C036
C037/C038
C039/C040
C041/C042
C043/C044
C045/C046
C047
C048/C049
C050/C051
C052/C053
C054/C055
C056/C057
C058/C059
C060/C061
C062/C063
C064/C065
C066/C067
C068/C069
C070/C071
C072/C073
C074/C075
C076/C077
C078/C079
C080/C081
C082/C083
C084/C085
C086/C087
C088/C089
C090/C091
C092/C093
C094/C095
C096/C097
C098/C099
C100/C101
C102/C103
C104
C105/C106
C107/C108
C109/C110
C111/C112
C113/C114
C115/C116
C117/C118
C119/C120
C121/C122
C123/C124
C125/C126
C127/C128
C129/C130
C131/C132
C133/C134
C135/C136
C137/C138
C139/C140
C141
C142/C143
C144/C145
C146/C147
C148/C149
C150/C151
C152/C153
C154/C155
C156/C157
C158/C159
C160/C161
C162/C163
C164/C165
C166/C167
C168/C169
C170/C171
C172/C173
C174/C175
C176/C177
C178/C179
C180/C181
C182/C183
C184/C185
C186/C187
C188/C189
C190/C191
C192/C193
C194/C195
C196/C197
C198/C199
HIV05201002
HIV05201005
HIV05201007
HIV05201008
HIV05201010
HIV05201013
HIV05201014
HIV05201017
HIV05201018
HIV05201020
N00619002
N00619004
N00619005
N00619006
N00619009
N00619021
N00619022
N00619026
N00619033
N00619034
N00619039
N00619040
N00619041
N00619042
N00619045
N00619047
N00621004
N00621006
N00621008
N00621011
N00621015
N00621017
N00621024
N00621026
N00621030
N00621031
N00621034
N00621037
N00621042
N00621045
N00621047
N00622003
N00622006
N00622014
N00622015
N00622018
N00622019
N00622024
N00622026
N00622027
N00622038
N00622044
N00622047
N00622048
N00622051
N00622060
N00623003
N00623005
N00623006
N00623008
N00623010
N00623011
N00623015
N00623017
N00623018
N00623020
N00623021
N00623022
N00623023
N00623025
N00623027
Volunteer ID
6000+
5000-5999
4000-4999
3000-3999
2000-2999
1000-1999
300-999

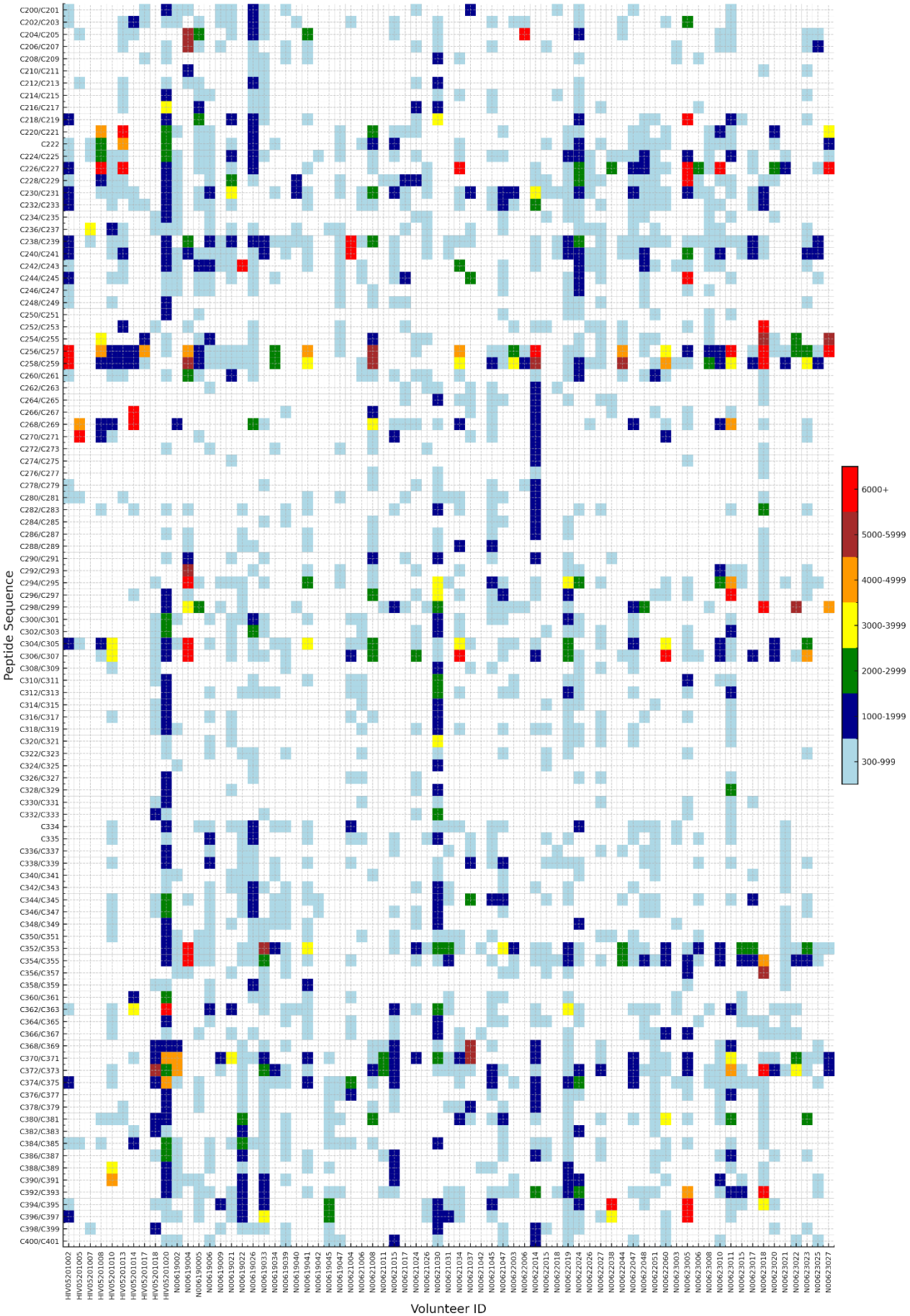
Peptide Sequence
C200/C201
C202/C203
C204/C205
C206/C207
C208/C209
C210/C211
C212/C213
C214/C215
C216/C217
C218/C219
C220/C221
C222
C224/C225
C226/C227
C228/C229
C230/C231
C232/C233
C234/C235
C236/C237
C238/C239
C240/C241
C242/C243
C244/C245
C246/C247
C248/C249
C250/C251
C252/C253
C254/C255
C256/C257
C258/C259
C260/C261
C262/C263
C264/C265
C266/C267
C268/C269
C270/C271
C272/C273
C274/C275
C276/C277
C278/C279
C280/C281
C282/C283
C284/C285
C286/C287
C288/C289
C290/C291
C292/C293
C294/C295
C296/C297
C298/C299
C300/C301
C302/C303
C304/C305
C306/C307
C308/C309
C310/C311
C312/C313
C314/C315
C316/C317
C318/C319
C320/C321
C322/C323
C324/C325
C326/C327
C328/C329
C330/C331
C332/C333
C334
C335
C336/C337
C338/C339
C340/C341
C342/C343
C344/C345
C346/C347
C348/C349
C350/C351
C352/C353
C354/C355
C356/C357
C358/C359
C360/C361
C362/C363
C364/C365
C366/C367
C368/C369
C370/C371
C372/C373
C374/C375
C376/C377
C378/C379
C380/C381
C382/C383
C384/C385
C386/C387
C388/C389
C390/C391
C392/C393
C394/C395
C396/C397
C398/C399
C400/C401
HIV05201002
HIV05201005
HIV05201007
HIV05201008
HIV05201010
HIV05201013
HIV05201014
HIV05201017
HIV05201018
HIV05201020
N00619002
N00619004
N00619005
N00619006
N00619009
N00619021
N00619022
N00619026
N00619033
N00619034
N00619039
N00619040
N00619041
N00619042
N00619045
N00619047
N00621004
N00621006
N00621008
N00621011
N00621015
N00621017
N00621024
N00621026
N00621030
N00621031
N00621034
N00621037
N00621042
N00621045
N00621047
N00622003
N00622006
N00622014
N00622015
N00622018
N00622019
N00622024
N00622026
N00622027
N00622038
N00622044
N00622047
N00622048
N00622051
N00622060
N00623003
N00623005
N00623006
N00623008
N00623010
N00623011
N00623015
N00623017
N00623018
N00623020
N00623021
N00623022
N00623023
N00623025
N00623027
Volunteer ID
6000+
5000-5999
4000-4999
3000-3999
2000-2999
1000-1999
300-999

Figure 4.2 Heatmap of HIVconsvX-induced T-cell responses to individual peptide pairs across all mapped volunteers. Cultured ELISpot mapping of IFN-γ responses to 399 overlapping 15-mer peptides (overlapping by 11 amino acids) spanning the HIVconsvX immunogen. Each row represents a peptide pair, and each column represents an individual volunteer (including vaccine and placebo recipients) from HIV-CORE 005.2 and HIV-CORE 006 trials. The colour scale indicates response magnitude in SFU per 10^6 STCL: light blue = 300-999 SFU, dark blue = 1000-1999 SFU, green = 2000–2999 SFU, yellow = 3000-3999 SFU, orange = 4000-4999 SFU, brown = 5000-5999 SFU and red = ≥6000 SFU. Responses <300 SFU are shown in white. Positivity was defined as ≥1000 SFU/10^6 STCL, set as placebo median + 3 SD; signals 300-999 SFU are shown as sub-threshold in figure. The heatmap illustrates that HIVconsvX vaccination elicited multi-epitope T-cell responses distributed across the immunogen, with variation in response magnitude and specificity among participants.

4.3.2 Fine mapping of HIVconsvX responses to minimal epitopes

Based on the initial 15-mer mapping, we selected peptide pairs that induced strong responses (≥2000 SFU/10^6 STCL) in HIV-CORE 005.2 trial participants. This selection yielded 40 high-responding 15-mer pairs. To define the minimal optimal $CD8^+$ T-cell epitopes, we identified 294 9-mer peptides (overlapping by 8 amino acids) spanning these 15-mers.

PBMCs from vaccinated volunteers were expanded *in vitro* and tested for IFN-γ release against each 9-mer peptide by cultured ELISpot assay. The breadth and magnitude of responses varied markedly between individuals, and certain 9-mers induced extremely high responses (>10,000 SFU/10^6 STCL). The magnitude of responses to 9-mer peptides often exceeded the corresponding 15-mer response. This pattern highlights the enhanced TCR engagement with optimally processed epitopes. In some cases, a single dominant 9-mer peak explained the 15-mer response. In some other cases, two adjacent 9-mers were co-dominant, indicating a possible shared either 8 or 10 aa core epitopes (Figure 4.3).

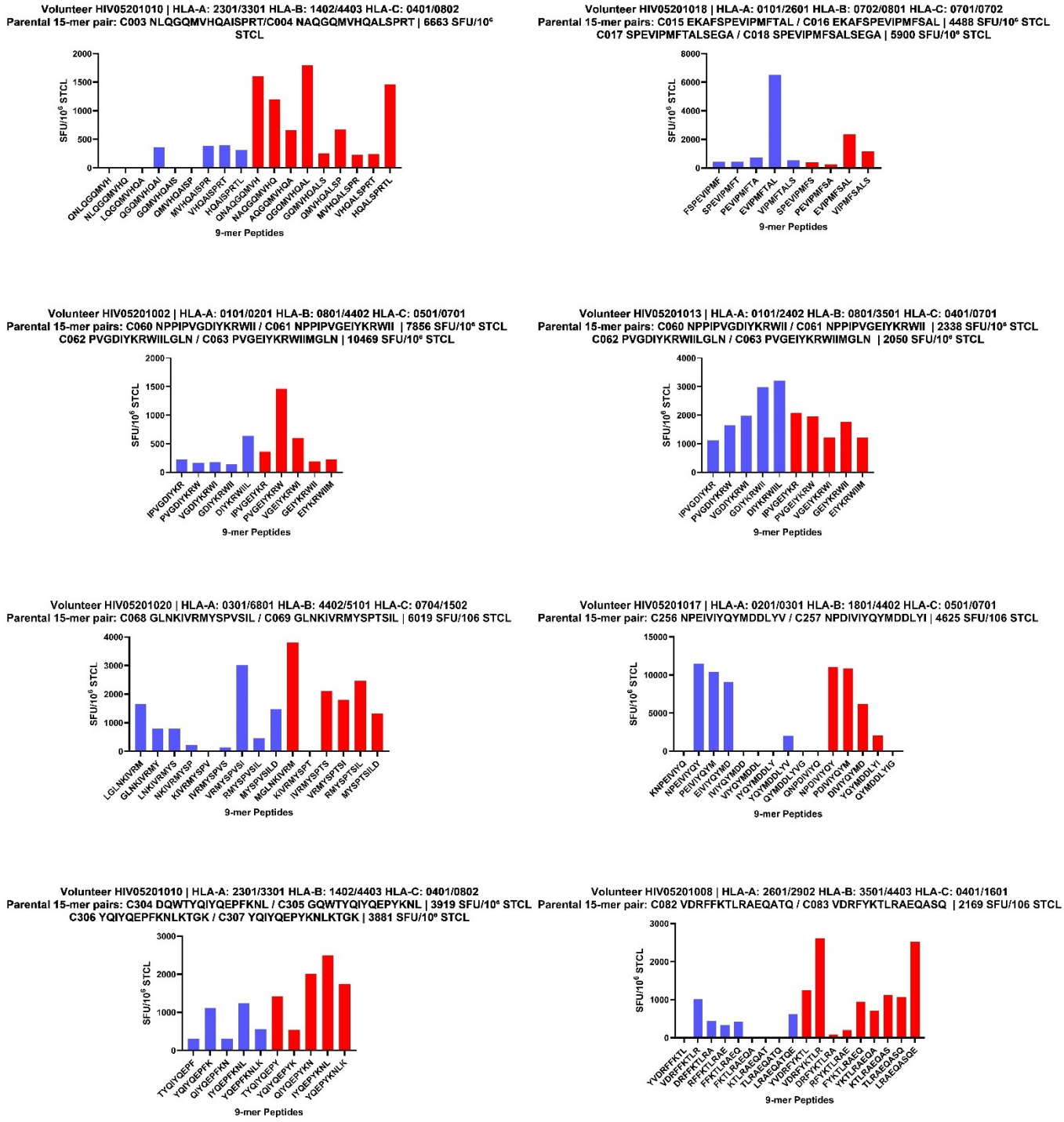

Figure 4.3 Fine mapping of HIVconsvX-induced responses to optimal 9-mer epitopes in selected volunteers. PBMCs from vaccinated volunteers were expanded with parental 15-mer peptides that previously induced strong responses (≥2000 SFU/10⁶ STCL) and tested against overlapping 9-mer peptides (overlapping by 8 amino acids) by cultured ELISpot. Each panel shows data from an individual volunteer, including HLA-I alleles, the parental 15-mer peptide pair(s) with their sequences and cultured ELISpot response magnitudes (SFU/10⁶ STCL). Bars represent IFN-γ responses to each 9-mer, colour-coded according to the mosaic immunogen origin: blue=Mosaic 1, red=Mosaic 2.

4.3.3 High-response 9-mer epitopes were compared with published entries in the database

From the 9-mer fine-mapping dataset, we focused on high-magnitude responses by selecting 9-mer peptides that elicited ≥2000 SFU/10^6 STCL in at least one HIV-CORE 005.2 volunteer. This yielded 23 distinct 9-mer epitopes. To see whether these epitopes had been reported before with the responding volunteers' HLA types, we searched the LANL Database. Of the 23 high-magnitude 9-mers, 6 had been previously reported with HLA restrictions that matched the responding volunteer's HLA types (Table 4.1). The remaining 17 9-mers were not found in the database with a matching HLA type and are therefore considered as unreported epitopes (Table 4.2).

Participant IDs	Participant's HLA types			Expanding 15-mers		Mapped Epitopes		SFU/10^6 STCL	Reported HLA	PMID
	HLA-A	HLA-B	HLA-C	ID	Sequence	Name	Sequence			
HIV05201013	HLA-A 01:01	HLA-B 08:01	HLA-C 04:01	C060	NPPIPVGDIYKRWII	GI9	GDIYKRWII	2975	HLA-B 08:01	9583596
	HLA-A 24:02	HLA-B 35:01	HLA-C 07:01	C061	NPPIPVGEIYKRWII					
				C062	PVGDIYKRWIILGLN					
				C063	PVGEIYKRWIIMGLN					
HIV05201017	HLA-A 02:01	HLA-B 18:01	HLA-C 05:01	C256	NPEIVIYQYMDDLYV	PM9	PEIVIYQYM	10400	HLA-B 18:01	28448594
	HLA-A 03:01	HLA-B 44:02	HLA-C 07:01	C257	NPDIVIYQYMDDLYI	ED9	EIVIYQYMD	9100	HLA-B 18:01	28448594
						YV9	YQYMDDLYV	2013	HLA-A 02:01	10982378
HIV05201018	HLA-A 01:01	HLA-B 07:02	HLA-C 07:01	C015	EKAFSPEVIPMFTAL	EL9	EVIPMFTAL	6513	HLA-A 26:01	17173051
	HLA-A 26:01	HLA-B 08:01	HLA-C 07:02	C016	EKAFSPEVIPMFSAL	EL9	EVIPMFSAL	2350	HLA-A 26:01	8902082
				C017	SPEVIPMFTALSEGA					
				C018	SPEVIPMFSALSEGA					

Table 4.1 Previously reported 9-mer epitopes ≥2000 SFU with corresponding HLA types. Columns: 9-mer sequence; parental 15-mer pair; responding volunteer(s); HLA type(s); SFU/10^6 STCL; publication reference PMID.

	Participant's HLA types			Expanding 15-mers		Mapped Epitopes		SFU/10^6 STCL	Predicted HLA
	HLA-A	HLA-B	HLA-C	ID	Sequence	Name	Sequence		
HIV05201008	HLA-A 26:01	HLA-B 35:01	HLA-C 04:01	C082	VDRFFKTLRAEQATQ	VR9	VDRFYKTLR	2613	HLA-B*44:03
	HLA-A 29:02	HLA-B 44:03	HLA-C 16:01	C083	VDRFYKTLRAEQASQ	LE9	LRAEQASQE	2525	HLA-B*44:03
HIV05201010	HLA-A 23:01	HLA-B 14:02	HLA-C 04:01	C304	DQWTYQIYQEPFKNL	QN9	QIYQEPYKN	2013	HLA-A*33:03
	HLA-A 33:01	HLA-B 44:03	HLA-C 08:02	C305	GQWTYQIYQEPYKNL	IL9	IYQEPYKNL	2488	HLA-A*23:01
HIV05201013	HLA-A 01:01	HLA-B 08:01	HLA-C 04:01	C060	NPPIPVGDIYKRWII	DL9	DIYKRWIIL	3213	HLA-B*08:01
	HLA-A 24:02	HLA-B 35:01	HLA-C 07:01	C061	NPPIPVGEIYKRWII	IR9	IPVGEIYKR	2075	HLA-B*35:01
				C226	YFSVPLDESFRKYTA	PY9	PLDESFRKY	2063	HLA-A*01:01
				C227	YFSVPLDKDFRKYTA	AK9	AYFSVPLDK	2100	HLA-A*24:02
HIV05201017	HLA-A 02:01	HLA-B 18:01	HLA-C 05:01	C256	NPEIVIYQYMDDLYV	NY9a	NPEIVIYQY	11475	HLA-B*18:01
	HLA-A 03:01	HLA-B 44:02	HLA-C 07:01	C257	NPDIVIYQYMDDLYI	NY9b	NPDIVIYQY	11063	HLA-B*18:01
						PM9	PDIVIYQYM	10850	HLA-B*18:01
						DD9	DIVIYQYMD	6175	HLA-B*18:01
						YI9	YQYMDDLYI	2050	HLA-A*02:01
HIV05201020	HLA-A 03:01	HLA-B 44:02	HLA-C 07:04	C068	GLNKIVRMYSPVSIL	VI9	VRMYSPVSI	3013	HLA-C*07:04
	HLA-A 68:01	HLA-B 51:01	HLA-C 15:02	C069	GLNKIVRMYSPTSIL	MM9	MGLNKIVRM	3800	HLA-C*15:02
						IS9	IVRMYSPTS	2100	HLA-B*51:01
						RL9	RMYSPTSIL	2475	HLA-C*15:02

Table 4.2 Unreported 9-mer epitopes ≥2000 SFU. Columns: 9-mer sequence; parental 15-mer pair; responding volunteer(s); HLA type(s); SFU/10^6 STCL and predicted HLA types by LANL epitope prediction tool.

4.3.4 HLA restriction testing with 721.221 B lymphoblastoid cell lines provided modest signals

To confirm HLA restriction for unreported 9-mer epitopes we performed ICS using 721.221 B-cell lines transfected with single HLA class I alleles. Because of in-house availability, we tested only HLA-B*08:01 and HLA-B*35:01. Notably, HLA-B*08:01 was the LANL-predicted restriction for DIYKRWIIL (DL9), and HLA-B*35:01 was predicted for IPVGEIYKR (IR9) in volunteer HIV05201013. We also re-tested the reported HLA-B*08:01 restriction of DI8 (DIYKRWII), and we extended assays to HIV-CORE 006 volunteers who carried HLA-B*08:01 or HLA-B*35:01. For each assay, 721.221 targets were peptide-pulsed and then washed three times in R10 to remove unbound peptide. Peptide-pulsed 721.221-HLA-B*08:01 or 721.221-HLA-B*35:01 cells were co-cultured with parental peptide specific STCLs and analysed for IFN-γ and TNF-α release. Baseline was un-pulsed 721.221 + STCL, with a peptide-only + STCL control for presentation by cells within the STCL.

We observed moderate increases over baseline: in N00619004 with HLA-B*08:01–DL9, IFN-γ rose 3.27→4.13% and TNF-α 0.98→1.87%; in HIV05201013 with HLA-B*35:01–IR9, IFN-γ 7.62→8.66% and TNF-α 4.80→5.11%; and in N00623022 with HLA-B*08:01–DI8, IFN-γ

11.1→12.6% and TNF-α 1.05→5.31% (Figure 4.4). Consequently, these data are supportive of the HLA-B*08:01 restriction of DI8, DL9 and the HLA-B*35:01 restriction of IR9.

A.

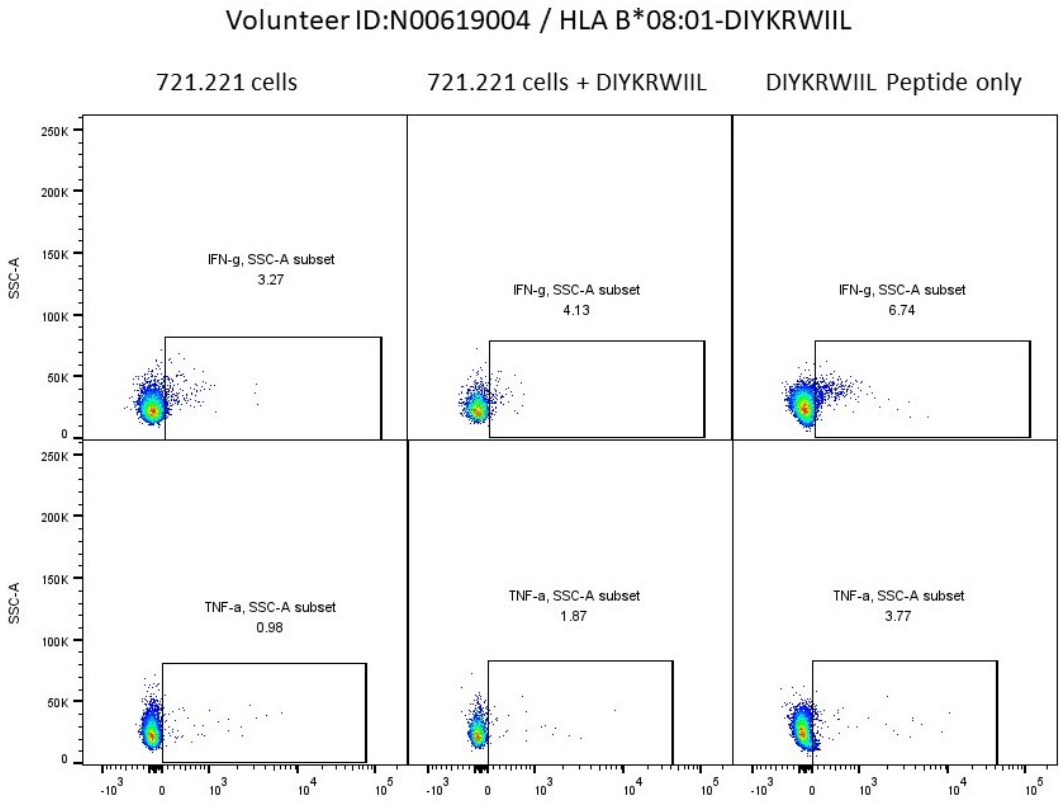

B.

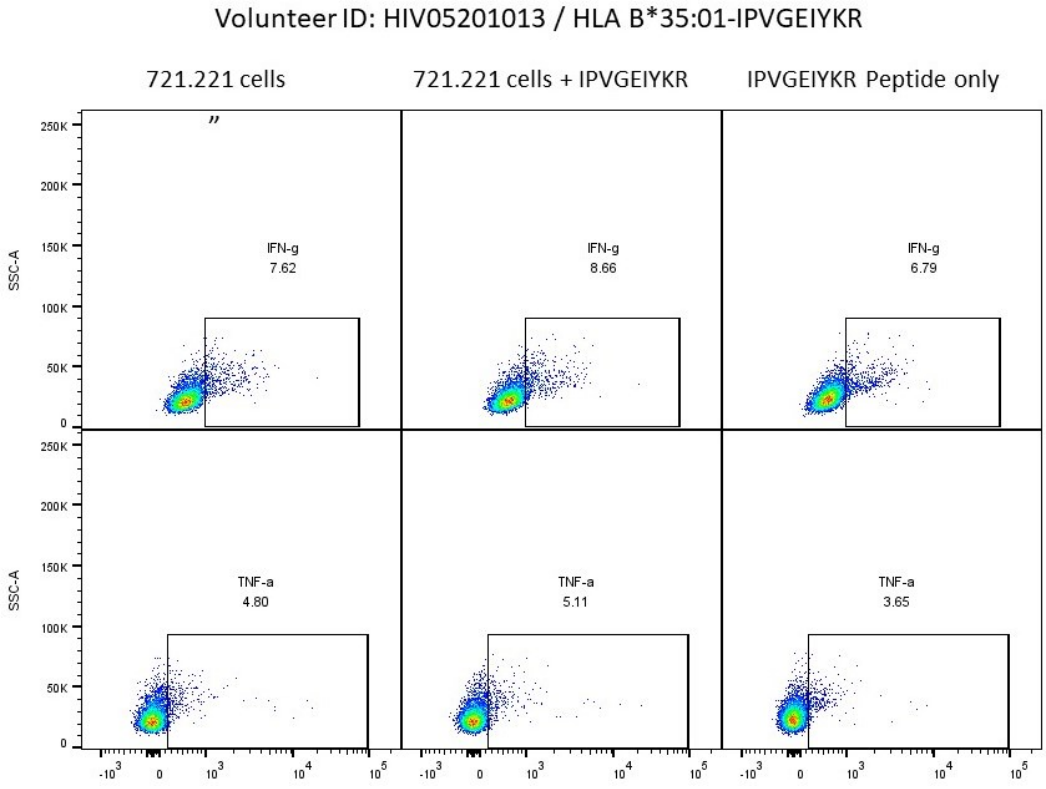

C.

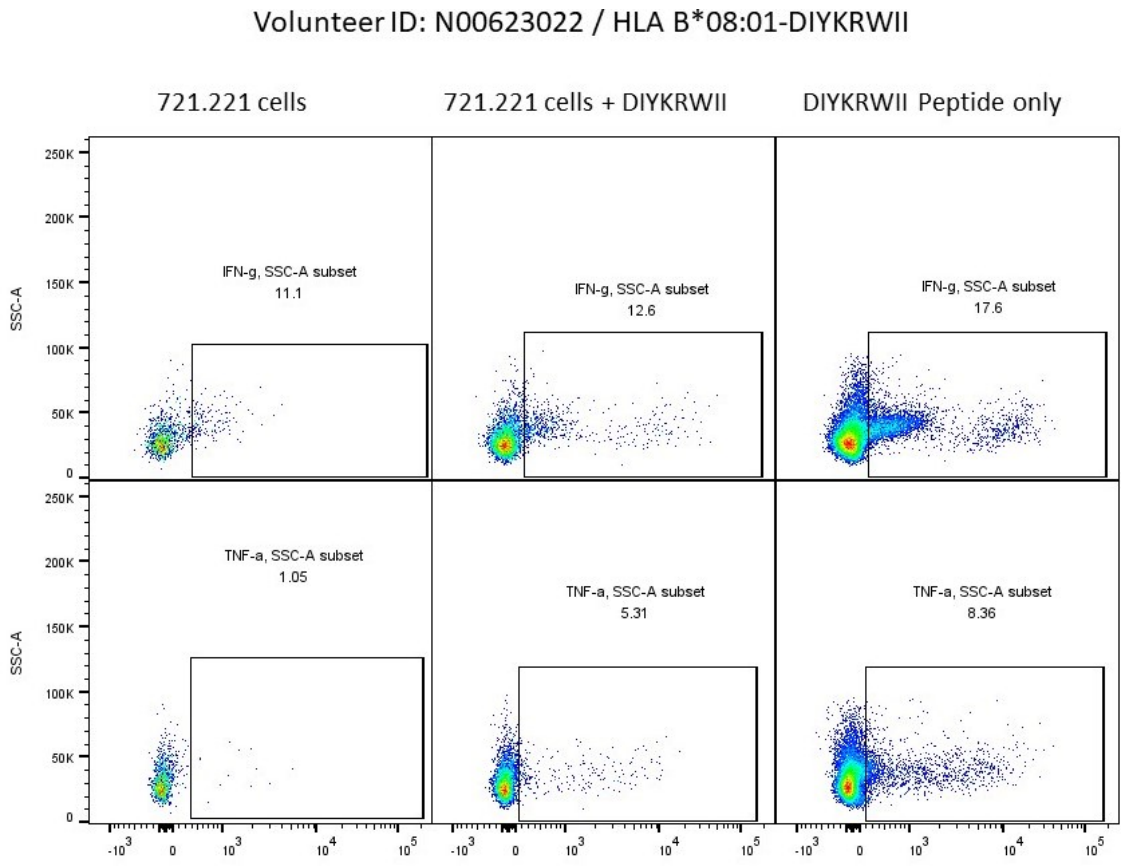

Figure 4.4 HLA restriction testing with HLA-transfected B cells by ICS. Un-pulsed 721.221 + STCL (baseline), peptide-pulsed 721.221 + STCL, and peptide only + STCL controls were shown. X-axis displays IFN-γ (top) and TNF-α (bottom) ICS readouts (percent cytokine-positive events within the SSC-A gate). (A) Volunteer N00619004; HLA-B*08:01; peptide DL9. (B) Volunteer HIV05201013; HLA-B*35:01; peptide IR9. (C) Volunteer N00623022; HLA-B*08:01; peptide DI8.

4.3.5 Cohort-level responder/HLA carrier analysis of parental 15-mer pairs supports several restricting HLA predictions

To complement single-allele assays, we used the full mapping dataset (71 volunteers from HIV-CORE 005.2 and HIV-CORE 006) to ask whether the LANL predicted restricting HLA for each 9-mer is supported at the HIVconsvX-vaccinated cohort level. For every unreported 9-mer, we stepped back to its parental 15-mer pair and assessed the cohort's response to that pair. We then searched across both trials for participants who responded ≥ 1000 SFU/10^6 STCL to that 15-mer pair. Finally, for each candidate allele, we counted responder/HLA carrier among the mapped volunteers. Thus, "3/3" means all three carriers of that allele in the cohort responded ≥1000 SFU to the relevant 15-mer pair.

This cohort analysis yielded several allele-epitope signals that either agree with LANL predictions and our ICS data or suggest alternative restrictions.

Across the cohort, responses to the C060 NPPIPVGDIYKRWII / C061 NPPIPVGEIYKRWII 15-mer pair were frequent among carriers of the LANL predicted alleles. In HIV-CORE 005.2, all four HLA-B*08:01 carriers responded; in HIV-CORE 006, two of three carriers responded (6/7 overall 86%). For HLA-B*35:01, both carriers in HIV-CORE 005.2 and one of three in HIV-CORE 006 responded (3/5 overall, 60%). The unreported 9-mers DL9 and IR9 were contained within this parental peptide pair. Their restriction by HLA-B*08:01 and HLA-B*35:01, respectively, was supported at the cohort level, consistent with the LANL predictions and with our single-allele 721.221 ICS data.

Responses to the C226 YFSVPLDESFRKYTA / C227 YFSVPLDKDFRKYTA 15-mer pair were consistently observed among carriers of HLA-B*35:01. In HIV-CORE 005.2, both HLA-B*35:01 carriers responded; in HIV-CORE 006, all three carriers responded (5/5 overall, 100%). The unreported 9-mers PY9 (PLDESFRKY) and AK9 (AYFSVPLDK) were within this parental peptide pair. Their restriction by HLA-B*35:01 was supported at the cohort level and is a strong candidate formal confirmation. LANL predictions were HLA-A*01:01 for PY9 and HLA-A*24:02 for AK9.

Responses to the C256 NPEIVIYQYMDDLYV / C257 NPDIVIYQYMDDLYI 15-mer pair were frequent among HLA-B*18:01 and HLA-C*05:01 carriers. In HIV-CORE 005.2, the single HLA-B*18:01 carrier responded, and in HIV-CORE 006 the single carrier also responded (1/1 and 1/1; 2/2 overall, 100%), consistent with the LANL-predicted restriction of 9-mer NY9a (NPEIVIYQY) within this peptide pair. For HLA-C*05:01, all three carriers in HIV-CORE 005.2 responded (3/3; there were no carriers in HIV-CORE 006). HLA-A*02:01 carriers also frequently responded to this 15-mer pair (3/3 in HIV-CORE 005.2 and 7/13 in HIV-CORE 006). Therefore, HLA-C*05:01 and HLA-A*02:01 are reasonable candidates for the restriction of NY9a and other overlapping 9-mers NY9b (NPDIVIYQY), PM9 (PDIVIYQYM), DD9 (DIVIYQYMD), and YI9 (YQYMDDLYI) within this peptide pair.

Each participant expresses multiple HLA class I alleles, and epitope presentation is a multistep process. The competition among peptides and constraints of the available TCR repertoire are also possible. Therefore, even if a given HLA allele is capable of presenting a peptide, it may not be presented in a particular individual or at a given time point. This biological variability explains why some carriers do not meet the ≥1000 SFU threshold and why our responder/HLA carrier analysis provides supportive rather than definitive evidence of restriction.

Participant ID's	Participant's HLA types			Expanding 15'mers		Mapped Epitopes		SFU/10^6 STCL	Predicted HLA's by Mapping data	052	006
	HLA-A	HLA-B	HLA-C	ID	Sequence	Name	Sequence				
HIV05201008	HLA-A 26:01	HLA-B 35:01	HLA-C 04:01	C082	VDRFFKTLRAEQATQ	VR9	VDRFYKTLR	2613	HLA-B 35:01	1/2	3/3
	HLA-A 29:02	HLA-B 44:03	HLA-C 16:01	C083	VDRFYKTLRAEQASQ	LE9	LRAEQASQE	2525	HLA-C 16:01	2/2	5/6
HIV05201013	HLA-A 01:01	HLA-B 08:01	HLA-C 04:01	C060	NPPIPVGDIYKRWII	DL9	DIYKRWIIL	3213	HLA-B 08:01	4/4	2/3
	HLA-A 24:02	HLA-B 35:01	HLA-C 07:01	C061	NPPIPVGEIYKRWII	IR9	IPVGEIYKR	2075	HLA-B 35:01	2/2	1/3
HIV05201013	HLA-A 01:01	HLA-B 08:01	HLA-C 04:01	C226	YFSVPLDESFRKYTA	PY9	PLDESFRKY	2063	HLA-B 35:01	2/2	3/3
	HLA-A 24:02	HLA-B 35:01	HLA-C 07:01	C227	YFSVPLDKDFRKYTA	AK9	AYFSVPLDK	2100	HLA-B 35:01	2/2	3/3
HIV05201017	HLA-A 02:01	HLA-B 18:01	HLA-C 05:01	C256	NPEIVIYQYMDDLYV	NY9	NPEIVIYQY	11475	HLA-B 18:01	1/1	1/1
	HLA-A 03:01	HLA-B 44:02	HLA-C 07:01	C257	NPDIVIYQYMDDLYI	NY9	NPDIVIYQY	11063	HLA-C 05:01	3/3	ND
						PM9	PDIVIYQYM	10850	HLA-A 02:01	3/3	7/13
						DD9	DIVIYQYMD	6175			
						YI9	YQYMDDLYI	2050			

Table 4.3 Cohort-level analysis of HLA-epitope interaction. For each predicted restricting HLA allele, we searched all mapped participants in HIV-CORE 005.2 and HIV-CORE 006 who carried that allele and identified how many of them showed a response ≥1000 SFU/10^6 STCL to the parental 15-mer peptide pair that contains the 9-mer. The two identical NY9 peptides are distinguished in the text as NY9a and NY9b. The numbers are shown as responder/HLA carrier.

4.4 Discussion

The present study provides a comprehensive mapping and highlights the breadth and specificity of HIVconsvX-induced T-cell responses across two distinct clinical trial populations in the UK and Africa. The findings demonstrate that HIVconsvX vaccination elicits broad, multi-epitope T-cell responses targeting conserved regions of the HIV-1 proteome.

Targeting multiple HIV-1 epitopes is considered a key prerequisite for improved control of the virus [393]. Prior studies, including the STEP and APPROACH trials, consistently showed that recognition of multiple epitopes correlates with superior control of plasma viral loads and successful virus inhibition respectively [387, 397]. For example, STEP trial participants recognizing three or more Gag epitopes exhibited lower viral loads than those with narrower epitope targeting [397]. In the APPROACH trial, in vaccinees, the number of HIV-1 isolates inhibited positively correlated with how broadly participants recognized peptide pools [387]. In this present study, the vaccinated participants recognised a median of 10 peptide pairs (range 0-70), after the *in vitro* expansion. The strength of the HIVconsvX vaccine is that, epitopes are conserved and, therefore, all likely contribute to protection [204, 336]. The mosaic immunogen design intends to maximize the coverage of 9-mer potential T-cell epitopes across globally diverse HIV-1 sequences, which expands the breadth and depth of cellular responses and is expected to improve coverage in HLA-diverse populations [333]. Importantly, the vaccine-induced responses mapped here were widely distributed across the HIVconsvX mosaic and not restricted to a single cluster of immunodominant regions.

Our study aimed to fine map to minimal, optimal 9-mer $CD8^+$ T-cell epitopes. Of the 23 peptides eliciting high-magnitude responses, 17 were classified as previously undescribed and further analysed for predicted HLA restriction, using both experimental single-allele *in vitro* assays and cohort-level responder/HLA carrier analyses. This dual validation supports the confirmation of several predicted HLA-epitope pairs. Mapping unreported epitopes and correlating their presentation with cohort HLA frequencies is critical for ensuring population-level vaccine coverage, given substantial global HLA diversity.

The present work demonstrates that HIVconsvX vaccination in diverse human populations elicits broad, multi-epitope T-cell responses targeting conserved regions of HIV-1. The identification and mapping of both known and unreported minimal epitopes, alongside confirmation of predicted HLA restrictions, establishes a robust foundation for future epitope-centric vaccine strategies. The findings confirm and extend prior literature suggesting that such approaches enhance immunological breadth, minimize escape, and may improve the prospects for universal HIV vaccine efficacy.

4.5 Limitations

Although *in vitro* cultured ELISpot assays offer high sensitivity for detecting antigen-specific T-cell responses, the STCL and expansion process may alter the magnitude of responses.

The experimental validation of HLA restriction was constrained by limited availability of HLA-transfected 721.221 cell lines and participants' frozen PBMCs. As a result, only a subset of predicted HLA-epitope pairs could be functionally tested, and the remainder relied on computational prediction and cohort-level correlation analyses. These indirect methods provide supportive but not definitive evidence of restriction.

Although the trials included participants from both the UK and multiple African sites, the sample size remains limited relative to global HLA diversity. Broader evaluation across additional geographic regions and HLA backgrounds will be necessary to confirm the identified epitopes for global vaccine coverage.

CHAPTER 5: MUCOSAL DELIVERY OF THE HIVCONSVX IMMUNOGENS USING PARAINFLUENZA-VIRUS IN A MURINE MODEL

5.1. Introduction

Preclinical and early clinical studies using viral vectors such as ChAdOx1 and MVA have shown that HIVconsvX vaccines can induce potent, broad, and multifunctional T-cell responses in systemic compartments [332, 382].

Since HIV transmission mainly occurs at mucosal sites, it is important to develop vaccine strategies that not only elicit systemic immunity but also target the mucosal immunity, where the virus first enter. Intranasal vaccination offers a needle-free route of immunization and has the potential to induce strong mucosal T-cell responses. In this context, Parainfluenza virus 5 (PIV5) has emerged as a promising vector [372]. PIV5 is a non-pathogenic canine respiratory virus with the ability to efficiently deliver heterologous genes and stimulate immune responses without being affected by pre-existing immunity [398].

This chapter investigates the use of PIV5 as a delivery platform for HIVconsvX immunogens in a murine model. Both stand-alone and heterologous prime-boost regimens combining PIV5 with ChAdOx1 or MVA are evaluated in order to determine their capacity to enhance systemic and mucosal T-cell responses. Furthermore, the study examines the effectiveness of a bi-valent mosaic design in extending epitope recognition to variants beyond those encoded in the vaccine constructs. These experiments aim to assess the potential of intranasal PIV5-vectored HIVconsvX vaccines to broaden and strengthen protective cellular immunity against HIV-1.

5.1.1 The Role of Mucosal Immunity in HIV-1 Defence

Mucosal immunity is the first line of defence against HIV-1 transmission and infection [399]. Recent research has highlighted how both innate and adaptive immune responses within these compartments are critical in limiting virus dissemination and preventing establishment of systemic infection [399, 400]. Upon exposure to HIV-1, the mucosal epithelium acts as a physical barrier, with tightly joined epithelial cells, antimicrobial peptides, and a protective mucus layer enriched with secretory IgA and other innate defence proteins such as beta-defensins, lactoferrin, lysozyme, serine and cysteine proteases [401]. The majority of the body's lymphocytes reside within these tissues, including the gastrointestinal, genital, and respiratory tracts, which are highly relevant during the initial phase of HIV-1 infection [399]. Beyond these local responses, mucosal immunity operates as an interconnected system across anatomical sites. Activation of mucosal immune cells in the lung, for example, can lead to the mobilization of activated T-cells via the mucosal-specific trafficking pathways regulated by chemokines and adhesion molecules. These lymphocytes express mucosal homing receptors (e.g., CCR9, α4β7 integrin) to migrate and exert protective functions in distal mucosal compartments, including the genital and gut mucosae [401, 402]. This phenomenon explains how pulmonary mucosal immunization can achieve protection at the genital and gastrointestinal mucosal surfaces, a concept supported by preclinical studies in HIV-1 vaccine development [403].

5.1.2 The HIVconsvX presentation to the immune system

We continue to explore alternative platforms to ChAdOx1-MVA in order to broaden HIVconsvX delivery options, enhance T-cell induction, improve protection in low responders, sustain long-term immunity, and reach anatomical sites of HIV-1 transmission. To date, an integration-deficient lentiviral vector, recombinant BCG, BioNTech's self-amplifying mRNA, and Moderna's lipid

nanoparticle (LNP)-formulated mRNA have been evaluated for delivery of HIVconsvX immunogens [404-407].

The integration-deficient lentiviral vector expressing ZVex.tHIVconsv1 and ZVex.tHIVconsv2 candidates was tested in a preclinical study. Each mosaic vaccine alone was immunogenic, and when combined in heterologous prime-boost regimens with chimpanzee adenovirus and/or MVA vectors in BALB/c and outbred CD1-Swiss mice, they elicited median frequencies exceeding 6,000 T cells per million splenocytes. These T cells were polyfunctional, broadly specific, and cross-reactive [404].

In another study, mice primed with recombinant BCG expressing HIVconsv1&2 and boosted with ChAdOx1.tHIVconsv5&6 exhibited significantly higher numbers of IFN-γ and TNF-α-secreting $CD8^+$ T cells than those receiving ChAdOx1.tHIVconsv5&6 alone ($p = 0.0380$), demonstrating the benefit of the BCG prime [405].

The delivery of HIVconsvX via self-amplifying mRNA induced durable, broadly specific $CD8^+$ and $CD4^+$ T-cell responses that remained at high frequencies for at least 22 weeks post-immunization in both BALB/c and outbred mice [406].

Finally, the bivalent mRNA-LNP vaccines elicited comparable responses to heterologous ChAdOx1 prime-MVA boost regimen. The LNP-formulated tetravalent conserved mosaic immunogens (HIVconsvM), induced higher T-cell frequencies than bivalent formulations [407].

5.2 Aims

- To evaluate the efficiency of the bi-valent mosaic design of HIVconsvX for inducing mucosal T-cell responses that are capable of recognizing epitope variants beyond these present in the vaccines.
- To investigate the elicitation of immune responses following PIV5-vectored HIVconsvX administration, within a prime-boost regimen alongside ChAdOx1 or MVA vectored HIVconsvX vaccines.

5.3 Results

5.3.1 Intranasal PIV5 combined with intramuscular ChAdOx1/MVA synergistically enhances mucosal T-cell responses

The work presented in this chapter is part of our collaborative study with Ashley C. Beavis and Biao He from Department of Infectious Diseases, College of Veterinary Medicine, University of Georgia, United States. The study aims to broaden strategies for inducing strong, protective HIV-1–specific T cell responses, with a focus on mucosal sites where HIV enters the body. Current leading regimens use ChAdOx1 prime-MVA boost, delivering bi-valent conserved mosaic HIVconsvX immunogens.

Parainfluenza virus 5 (PIV5) was introduced as a new viral vector, which can be administered intranasally (IN) due to its natural respiratory tropism. We tested if PIV5 alone and combining with ChAdOx1 and MVA vectors, through intramuscular (IM) and IN routes, can synergistically boost

mucosal and systemic T-cell responses in mice. ChAdOx1.tHIVconsv1 (C1) and ChAdOx1.HIVconsv6.2 (C62), MVA.tHIVconsv3 (M3) and MVA.tHIVconsv4 (M4), PIV5.HIVconsv5 (P5) and PIV5.HIVconsv2 (P2) vaccines were tested in 6 weeks old BALB/c mice. The cells from spleen, lung, Peyer's patches (PP), and female reproductive tract (FRT) were analysed. HIVconsvX immunogens were cloned into PIV5 genomes by our collaborators.

The following important findings were obtained in experiments and analyses performed by our co-authors. IN administration of the PIV5 vector was highly effective, eliciting robust HIV-specific T-cell responses in the lung tissue. When PIV5 was combined with either ChAdOx1 or MVA vectors, a significant synergistic effect was observed, resulting in dramatic increases in lung T-cell frequencies, sometimes exceeding 14,000 IFN-γ-producing cells per million lung cells (Table 5.1).

Spleen			Lungs		
Prime	Boost	SFU/10^6 cells	Prime	Boost	SFU/10^6 cells
C1(IM)	M3(IM)	3855 (3/6)	M3(IM)	P5(IN)	14095 (2/7)
C1(IM)+P5(IN)	M3(IM)	3245 (2/7)	C1(IN)	M3(IN)	10600 (2/5)
C1(IM)	M3(IM)+P5(IN)	2821 (2/7)	C1(IN)		9746 (2/7)
C1(IM)+P5(IN)	M3(IM)+P5(IN)	2493 (2/7)	C1(IM)	M3(IM)+P5(IN)	8825 (2/7)
C1(IM)+P5(IN)		1943 (2/5)	C1(IM)+P5(IN)	M3(IM)+P5(IN)	8730 (2/7)
M3(IM)	P5(IN)	1787 (2/7)	M3(IM)+P5(IN)		7517 (1/2)
C1(IM)		1467 (4/8)	C1(IM)+P5(IN)	M3(IM)	7397 (2/7)
C1(IM)	P5(IN)	1414 (1/2)	C1(IM)	P5(IN)	7265 (1/2)
C1(IN)	M3(IN)	1200 (2/5)	C1(IM)+P5(IN)		7227 (2/5)
M3(IM)+P5(IN)		1189 (1/2)	C1(IM)	M3(IM)	4200 (3/7)
M3(IM)		765 (3/6)	C1(IN)	P5(IN)	3050 (2/4)
C1(IN)		811 (2/7)	C1(IM)		2708 (4/8)
C1(IN)	P5(IN)	478 (2/4)	M3(IN)		2050 (1/2)
P5(IN)		275 (2/5)	P5(IN)	P5(IN)	1468 (2/5)
M3(IN)		275 (1/2)	P5(IN)	P5(IN) P5(IN)	905 (1/3)
P5(IN)	P5(IN)	187 (2/5)	M3(IM)		767 (3/6)
P5(IN)	P5(IN) P5(IN)	145 (1/3)	P5(IN)		758 (3/8)
P5(IM)		90 (1/2)	P5(IM)		66 (1/2)

Table 5.1 Sequential Ranking of Regimens by Vaccine-Induced CD8 T Cell Frequencies Targeting Dominant Epitope VLV. The data presented in this table illustrates the ordering of regimens based on the frequencies of T-cells elicited by the vaccine, specifically targeting the immunodominant epitope VLV. The results are depicted as the median frequencies of cells producing IFN-γ across all experiments in our collaborative publication (number of independent experiments/number of animals). The majority of the experiments included in this table were conducted by Edmund Wee.

5.3.2 Bi-valent mosaic vaccine approach enhances the variant-specific T-Cell responses

To evaluate the immunological benefits of bi-valent mosaic immunization over single-mosaic approaches, groups of three BALB/c mice were vaccinated with PIV5-vectored mosaic 1 (P5), mosaic 2 (P2), or a combination of both (P5+P2). Nine days post-boost, lung cells were isolated and T-cell responses were quantified by IFN-γ ELISPOT assay (Figure 5.1). We evaluated antigen-specific

responses to each vaccine epitope, building on the detailed epitope mapping previously performed by Wee *et al*. In those studies, key H-2d-restricted CD8+ T cell epitopes, VLVGPTPVNI, VLIGPTPVNI, AMQMLKDTI, and AMQMLKETI, were shown to be strongly immunogenic. In addition, we included analysis of the three most prevalent non-vaccine epitope variants identified from the Los Alamos National Laboratory HIV Sequence Database (LANL-HSD; Table 5.2).

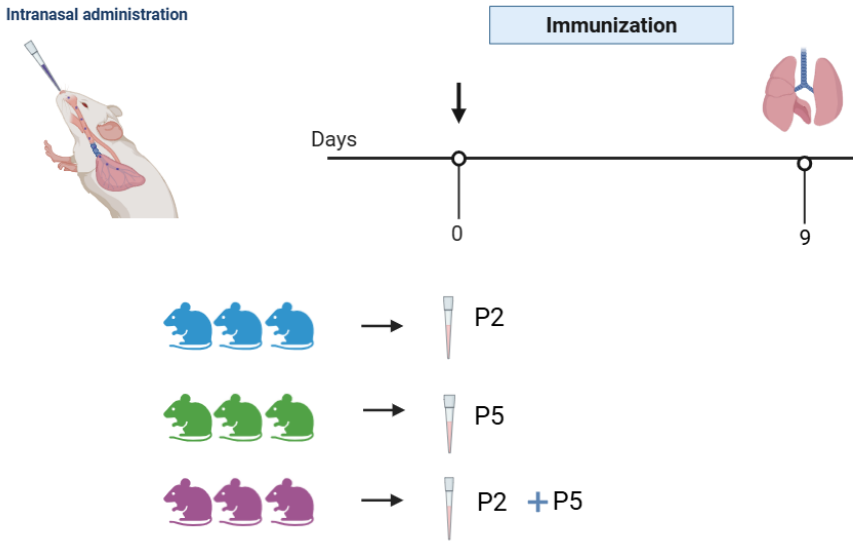

Figure 5.1 The experimental design of intranasal immunization. Three groups of BALB/c mice (n=3 per group) were immunized intranasally with PIV5-vectored HIVconsvX vaccines expressing either mosaic 2 (P2, blue), mosaic 1 (P5, green), or a combination of both (P2 + P5, purple). Nine days after immunization, mice were sacrificed, lungs were harvested, and lung cells were isolated for assessment of T-cell responses by IFN-γ ELISPOT assay. (BioRender.com)

Epitope Variant	f (%)
VLVGPTPVNI	76.97
VL**I**GPTPVNI	14.56
VLVGPTP**I**NI	5.01
VLVGPTP**A**NI	0.58
VL**I**GPTP**I**NI	0.52
AMQMLKDTI	44.09
AMQMLK**E**TI	43.4
AMQ**I**LKDTI	4.34
AMQ**I**LK**E**TI	0.97
A**L**Q**V**I**L**K**E**V**I**	0.59
AMQMLKD**A**I	0.15
AMQ**I**LK**E**V**I**	0.23

Table 5.2 Variants of immunodominant H-2^{d}-restricted HIV-1 epitopes used in this study. Red shows mosaic 1, blue shows mosaic 2, and black shows sequences that are not included in the vaccine. The amino acid differences from mosaic 1 were indicated as bold letters. f (%), percentage of HIV-1 isolates in the LANL-HSD with the indicated epitope variant (August 2025).

When the combined responses to both VLV and AMQ epitope variants were analysed, a significant difference among the vaccination groups was observed. The bi-valent P5+P2 regimen induced significantly higher IFN-γ responses compared to the group receiving the mono-valent P2 vaccine alone (P = 0.0373 for P2 vs. P5+P2) (Figure 5.2 A). Despite considerable variation among individual epitope variants, co-administration of both mosaic immunogens (P5+P2) increased the frequencies of IFN-γ–producing T-cells in 7 out of 10 tested epitopes compared to single-mosaic vaccination. Notably, this difference reached statistical significance only for the VLVGPTPINI variant, while the remaining six displayed a trend towards higher responses, but without reaching significance (Figure 5.2 B). The small group size in this pilot experiment likely limited our power to detect significant differences for all epitopes. Overall, these results show that PIV5-based bivalent HIVconsvX vaccine administration leads to deeper T-cell responses, which could improve the immune coverage against HIV-1 diversity.

A.

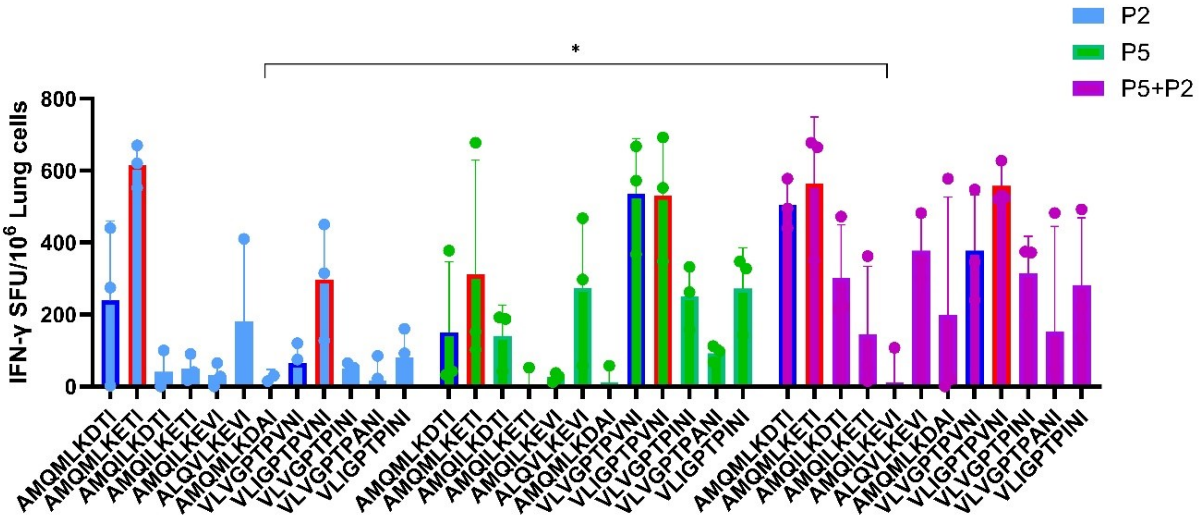

B.

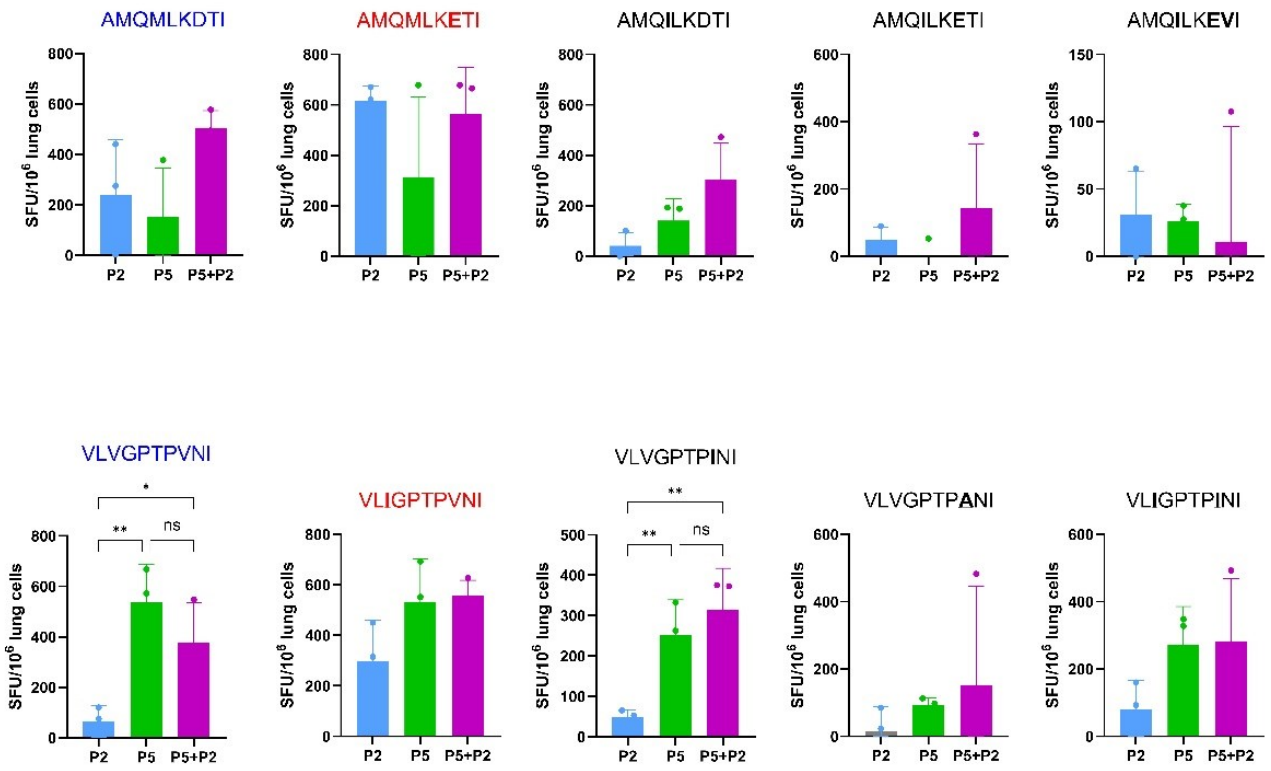

Figure 5.2 The magnitude and breadth of IFN-γ-secreting T-cell responses. Results are shown as a median with individual values plotted (n = 3). A) Responses to individual epitope variants are shown together in a single graph. Epitope variants derived from mosaic 1 are indicated with blue borders, while those from mosaic 2 are shown with red borders. IFN-γ SFU per million lung cells are presented for each vaccination group: P2 (blue), P5 (green), and P5+P2 (purple) (p = 0.0373, Kruskal-Wallis with Dunn's multiple comparisons test). B) Individual data for each epitope variant. For VLVGPTPVNI **p = 0.0081; *p = 0.0225, and for VLVGPTPINI **p=0.0049; **p=0.0025. If no asterisk or horizontal bar is shown, the difference is not statistically significant.

5.3.3 Optimal combination of PIV5, ChAdOx1 and MVA vectored HIVconsvX vaccines maximizes systemic and mucosal T-cell Responses

To evaluate the effect of combining IM administration of C62 or M4 with IN delivery of P2 on T-cell responses, six groups of BALB/c mice (n=5 per group) were immunized. The five experimental regimens used in this section were deliberately selected on the basis of prior findings to represent the optimal combinations of vaccine vectors for the induction of robust mucosal (lung) and systemic (spleen) T-cell responses. Vaccinations via IM (C62 or M4) and IN (P2) routes were administered as either single agents or in combination, with a control group included for the baseline comparison. Spleens and lungs were harvested two weeks after the last immunization and IFN-γ ELISPOT assays were performed (Figure 5.3).

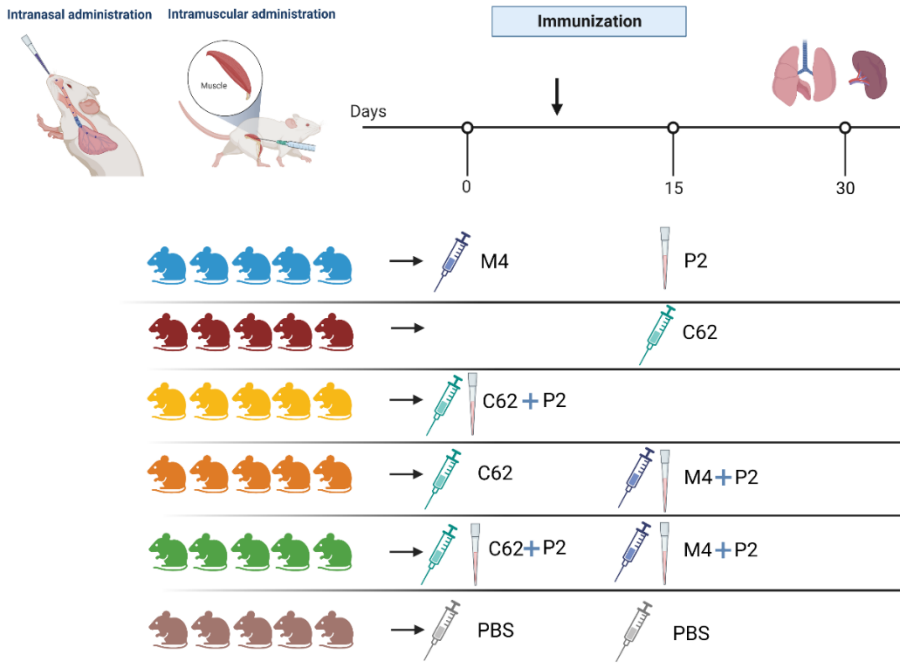

Figure 5.3 The experimental design of immunization. Six groups of BALB/c mice (n = 5) were immunized with mosaic2 HIVconsvX immunogen in the best five regimens or PBS. Two weeks after the second immunization, mice were sacrificed, lungs and spleens were harvested, and isolated for assessment of T-cell responses by IFN-γ ELISPOT assay. (BioRender.com)

In this experiment, only vaccines containing the mosaic 2 HIVconsvX immunogen were used; however, in a parallel study, Edmund Wee conducted an identical experimental design employing vectors carrying mosaic 1 HIVconsvX. The results from that study are also presented here to provide a comprehensive comparison.

Splenocytes and lung cells were restimulated *in vitro* with three immunodominant mosaic 1 HIVconsvX peptides (VLVGPTPVNI, AMQMLKDTI, IFQSSMTKI) in the mosaic 1 experiment, and mosaic 2 HIVconsvX peptides (VLIGPTPVNI, AMQMLKETI, IFQCSMTKI) in the mosaic 2 experiment. T-cell responses for each peptide were presented separately in the graphs. The highest

responses in mosaic 1 vaccinated groups were observed following stimulation with VLV-VLI peptides, whereas the most robust responses in mosaic 2 vaccinated groups were detected after stimulation with AMQ peptides. IFQCSMTKI responses were low across all groups.

For systemic T-cell responses in the mosaic 1 experiment, the regimens that combined C1 and P5 - whether P5 was administered as a prime or as a boost- namely C1+P5/M3 and C1/M3+P5 elicited the highest frequencies of IFN-γ–producing splenocytes. Specifically, both groups achieved median responses exceeding 8,000 SFU/10^6 splenocytes for the VLV epitope and over 2,000 SFU/10^6 splenocytes for the AMQ epitope. These responses were significantly higher than those observed with the C1 single immunization group (VLVGPTPVNI: ***p=0.0002, AMQMLKDTI: ***p=0.0003). Notably, there was no significant difference between the two combination strategies, indicating that PIV5 can be effectively incorporated as either a priming or boosting vector to enhance the magnitude of T-cell responses. Notably, the group receiving P5 in both the prime and boost stages exhibited lower responses than these two regimens, although the difference did not reach statistical significance (Figure 5.4 A).

We observed consistent findings in the mosaic 2 experiment. The most effective regimens were C62+P2/M4 and C62/M4+P2. Both of these strategies induced robust IFN-γ–producing T-cell responses, with median frequencies reaching 2,000 SFU/10^6 splenocytes for the VLI epitope and over 4,000 SFU/10^6 splenocytes for the AMQ epitope. These groups exhibited significantly higher responses compared to the C62-only immunization group (VLIGPTPVNI: ***p=0.0003, AMQMLKETI: **p=0.0036) (Figure 5.4 B).

A.

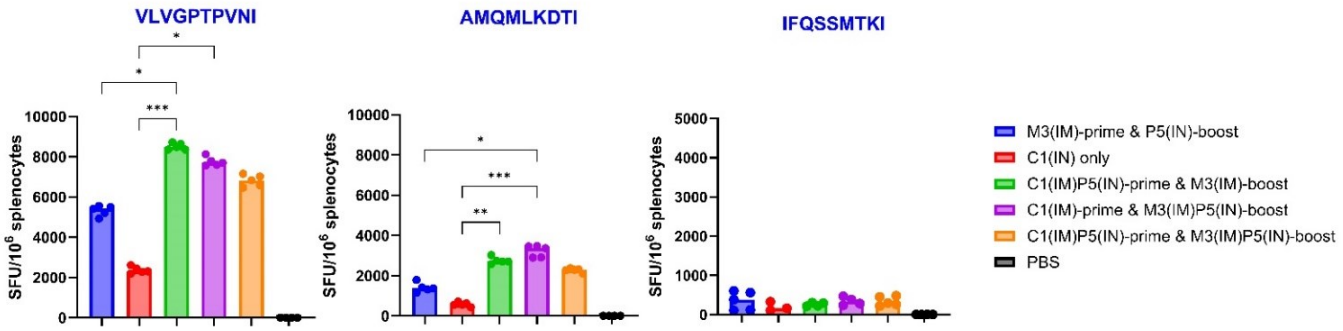

B.

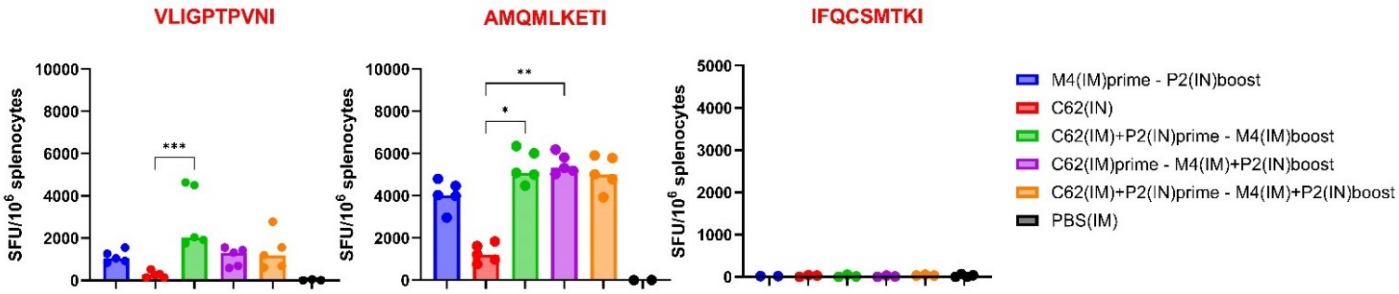

Figure 5.4 Systemic HIV-1-Specific T-Cell Induction using Heterologous and Homologous Mosaic 1 and Mosaic 2 Vaccine Regimens. BALB/c mice (n=5 per group) were vaccinated with optimal regimens A) ChAdOx1.HIVconsv1 (C1), MVA.HIVconsv3 (M3), and PIV5.HIVconsv5 (P5) mosaic 1 vaccines B) ChAdOx1.HIVconsv62 (C62), MVA.HIVconsv4 (M4), and PIV5.HIVconsv2 (P2) mosaic 2 vaccines or PBS. Immune cells were assessed against mosaic 1 (blue) and mosaic 2 (red)-derived peptide variants. Bar graphs represent median IFN-γ ELISPOT frequencies, with individual animal values indicated. Significance of group differences, determined by Dunn's multiple comparisons tests for the most immunodominant epitope, is denoted by asterisks: * $p<0.05$, ** $p<0.01$, **** $p<0.0001$ (Prism 10.5.0).

For lung T-cell responses, the group that received M3 prime followed by P5 boost exhibited the strongest immunogenicity, achieving approximately 30,000 SFU/10^6 lung cells for the VLV epitope in the mosaic 1 experiment and over 17,000 SFU/10^6 lung cells for the AMQ epitope in the mosaic 2 experiment. These responses were consistently and significantly higher than those observed in the group receiving the combined C1(IM)+P5(IN) prime with M3(IM)+P5(IN) boost regimen (VLVGPTPVNI: ***p=0.0006, AMQMLKETI: *p=0.0184) (Figure 5.5 A and B).

A.

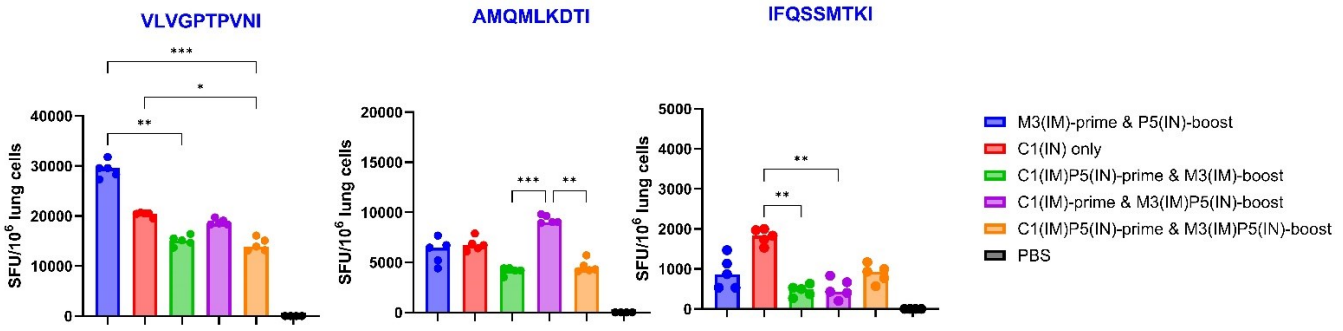

B.

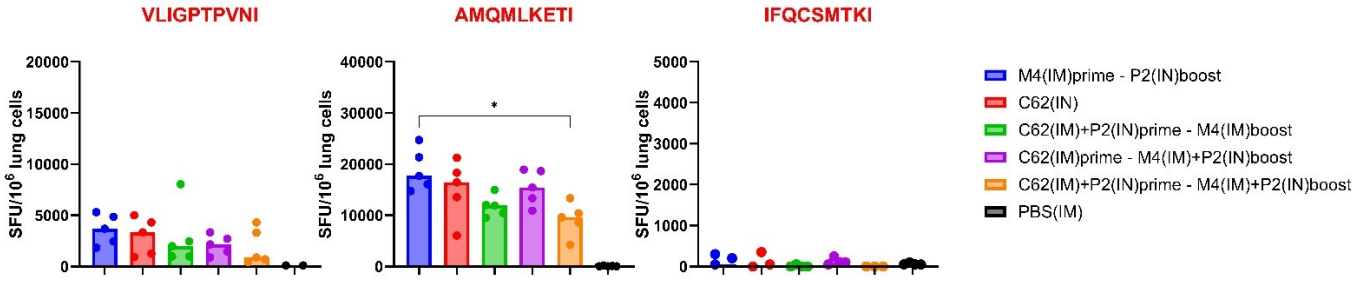

Figure 5.5 Mucosal HIV-1-Specific T-Cell Induction using Heterologous and Homologous Mosaic 1 and Mosaic 2 Vaccine Regimens. BALB/c mice (n=5 per group) were vaccinated with optimal regimens A) ChAdOx1.HIVconsv1 (C1), MVA.HIVconsv3 (M3), and PIV5.HIVconsv5 (P5) mosaic 1 vaccines B) ChAdOx1.HIVconsv62 (C62), MVA.HIVconsv4 (M4), and PIV5.HIVconsv2 (P2) mosaic 2 vaccines or PBS. Immune cells were assessed against mosaic 1 (blue) and mosaic 2 (red)-derived peptide variants. Bar graphs represent median IFN-γ ELISPOT frequencies, with individual animal values indicated. Significance of group differences, determined by Dunn's multiple comparisons tests for the most immunodominant epitope, is denoted by asterisks: * $p<0.05$, ** $p<0.01$, **** $p<0.0001$ (Prism 10.5.0).

5.4 Discussion

The HIVconsvX vaccines have demonstrated the ability to induce robust and polyfunctional T-cell responses in both preclinical and clinical settings, especially using established ChAdOx1-MVA regimens [336, 337, 382]. Nevertheless, expanding the repertoire of vaccine platforms is essential for achieving broader and more durable protection, particularly for individuals with suboptimal immune responses. Since HIV mainly transmitted through mucosal barriers, boosting mucosal immunity is essential for successful vaccine protection against HIV-1 [399].

The results presented in this thesis chapter provide evidence that IN delivery of PIV5-vectored HIVconsvX immunogens, especially when combined in heterologous prime-boost regimens with ChAdOx1 and MVA, significantly enhances mucosal T-cell responses in mice.

Recent studies in nonhuman primate models confirmed that IN PIV5-based HIV vaccines are safe, immunogenic, and can induce polyfunctional T-cell and antibody responses in both systemic and mucosal compartments [408]. Particularly, boosting with adjuvanted VLPs enhanced both humoral (neutralizing antibody, ADCC) and cellular immunity [408]. These findings mirror the robust mucosal T-cell responses and synergy observed when combining IN PIV5 with intramuscular ChAdOx1/MVA in the present murine experiments.

Intranasal vaccination offers ease of administration [409]. Moreover, mucosal vaccination was found more effective than systemic approaches for mobilizing immune cells to local, regional, and distal mucosal tissues in response to both HIV and non-HIV (including SIV) antigens [409-413]. In parallel with our findings in this chapter, studies with other viral vectors and DC-targeted HIV vaccines also support that the intranasal route enhances the magnitude and functionality of mucosal CD8+ and CD4+ T cells in both respiratory and distal mucosal tissues, often outperforming systemic routes in inducing mucosal immunity [409, 413].

Building on prior research, this chapter demonstrates that the bi-valent mosaic design of HIVconsvX substantially enhances the induction of T-cells able to recognize epitope variants beyond those encoded in the vaccine constructs, and provides broader immune coverage than monovalent formulations [382, 414].

These findings validate the high potential of PIV5-vectored HIVconsvX immunogens, especially when used in bivalent mosaic designs and in prime-boost regimens with ChAdOx1 or MVA, to induce robust mucosal T-cell responses, advancing our understanding of optimal strategies for HIV-1 vaccine development.

5.5 Limitations

The use of the BALB/c murine model might not fully capture the complexity of human immune responses to the HIVconsvX vaccines. Results observed in mice may not directly translate to humans due to species-specific differences in immune system and vaccine responses.

While the chapter focuses on the induction of T-cell responses in the lungs and spleen, other mucosal tissues, such as the genital and intestinal tracts, are also important in HIV-1 infection.

The sample size used in certain experiments (e.g., groups of three mice) might limit the statistical power of the study and the ability to draw robust conclusions.

The study primarily focuses on short-term immune responses after vaccination. Long-term immune persistence and memory responses are critical for vaccine efficacy and require further investigation.

CHAPTER 6: DEVELOPMENT OF TRIPLE TANDEM TRIMER SPYTAG/SPYCATCHER VIRUS-LIKE PARTICLES

6.1. Introduction

In this chapter, we evaluate a vaccine strategy that couples a stabilized HIV-1 Envelope Triple Tandem Trimer (TTT) to Hepatitis B surface antigen (HBsAg) virus-like particles (VLPs) using the SpyTag/SpyCatcher covalent binding. For multivalent display, we present TTT on pre-formed HBsAg VLPs via SpyTag (on TTT) and SpyCatcher (on VLP). Our study engineers TTT.HBsAg conjugates and assesses their assembly and antigenicity, and provides a path to induction of broadly neutralizing antibodies.

6.1.1 Strategies Toward Broadly Neutralizing Antibody Induction

A central goal of HIV-1 vaccine development is the induction of broadly neutralizing antibodies (bnAbs), which can protect against diverse circulating strains. However, eliciting bnAbs remains one of vaccinology's greatest challenges due to the extensive sequence variability of Env, the dense glycan shield, and the unusual structural requirements of bnAbs, such as long HCDR3 loops and high levels of somatic hypermutation [273]. Only ~20% of people living with HIV naturally develop potent bnAbs, typically after years of virus-antibody co-evolution [115, 273].

Early recombinant Env immunogens were unstable and exposed non-neutralizing epitopes, which diverted immune responses away from desired neutralizing sites[415]. They also failed to present several quaternary-structure dependent epitopes [416].

After years of iterative design, soluble native-like Env trimers such as SOSIP were developed. The term "SOSIP" comes from the engineered SOS disulphide bond (linking gp120 and gp41) and the IP substitution (I559P) that stabilizes Env in the prefusion state [417]. The design was pioneered by John P. Moore and Rogier W. Sanders and colleagues with the BG505 SOSIP.664 prototype [418]. Key SOSIP features also include the insertion of an RRRRRR motif to enhance furin cleavage, and the removal of hydrophobic MPER to improve solubility [419, 420]. The furin site (where protease recognizes and cleaves, usually REKR sequence) is between gp120 and gp41 in the gp160 precursor in wild-type Env [419]. Another SOSIP inspired format, single-chain (SC) trimers connect gp120 and gp41 with a flexible linker to achieve native-like conformation without furin cleavage [421]. Since many Env sequences do not yield fully native-like SOSIP trimers, the clade A transmitted/founder Env BG505, identified from a Kenyan infant, was selected for SOSIP.664 design. BG505 SOSIP.664 has a stable, native-like conformation, presents nearly all known bnAb epitopes while only weakly engaging certain non-NAbs, and carries a glycan shield enriched for native-like high-mannose structures [420].

6.1.2 The Triple Tandem Trimer (TTT) Design

The TTT design was introduced by del Moral-Sánchez *et al*. as a trimer format that links three Env protomers in a single open reading frame with flexible linkers. TTT expression is almost exclusively as native-like trimers and minimizes monomers/dimers that can misdirect antibody responses [283].

In TTT, each protomer is an uncleaved single-chain format where the furin site is replaced by a 15-aa Gly-Ser linker (GGSGGGGSGGGGSGG) to ensure furin independence. The adjacent protomers are connected gp41 C-terminus to gp120 N-terminus with an 11-aa flexible linker (GSGGSGGSGSG) to allow rotational freedom for correct assembly (Figure 6.1).

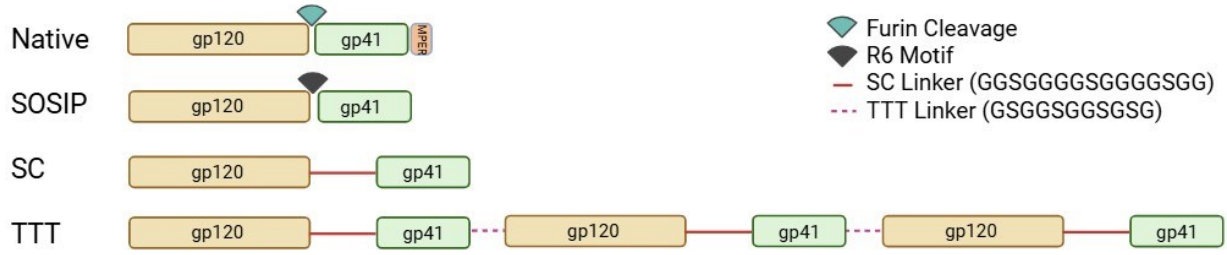

Figure 6.1 Linear schematic of HIV-1 Env formats: Native, SOSIP, SC, and TTT. Env protomers were shown as gp120 (yellow) followed by gp41 (green); small boxes labelled N and C indicate termini. In Native Env, the green wedge marks the furin cleavage site (usually REKR) between gp120 and gp41. In SOSIP, the black wedge denotes the engineered R6 motif that enhances furin cleavage (other stabilizing features of SOSIP, e.g., SOS disulfide and I559P, are not depicted). In SC, gp120 and gp41 are linked by a flexible SC linker (red; GGSGGGGSGGGGSGG). In TTT, three SC are arranged in a single open reading frame; within each protomer gp120–gp41 are joined by the same GS(15) linker (red), while TTT linkers (magenta dashed; GSGGSGGSGSG) connect the gp41 C-terminus of one protomer to the gp120 N-terminus of the next. Schematic is not to scale. This figure was made using Biorender.com.

6.1.3 HBsAg VLPs as the display platform

HBsAg VLPs are well established vaccine in humans [298]. Recombinant HBsAg, produced in yeast, self-assembles into ~22-nm lipoprotein particles [300]. They mimic the native virion surface and are safe, effective hepatitis B vaccines for decades [302].

HBsAg VLPs were also clinically validated as carrier for heterologous antigens. The first WHO-recommended malaria vaccine, RTS,S/AS01, presents a fusion of Plasmodium falciparum circumsporozoite protein (CSP) on HBsAg particles [305]. More recently, R21/Matrix-M refined this concept and achieved >70–75% efficacy against clinical malaria in African children in a phase 3 trial [306]. These successes demonstrate that HBsAg VLPs can safely and effectively display non-HBV antigens at human scale.

The repetitive structure of HBsAg VLPs presents epitopes at high density, and promotes efficient B-cell receptor engagement and successful recognition by IgM antibodies. This triggers the classical complement pathway, leading to antigen deposition on follicular dendritic cells, enhancing germinal centre formation and inducing durable, long-lived plasma cell responses [422-427]. HBsAg VLPs also offer practical advantages for translational vaccine development. They are readily manufactured at scale in yeast fermentation (including *Saccharomyces cerevisiae* and *Pichia pastoris*) with well-characterized purification processes and quality controls, with a cost-effective production [299].

6.1.4 SpyTag/SpyCatcher technology

SpyTag/SpyCatcher is a genetically encoded peptide-protein pair that forms a spontaneous, covalent isopeptide bond simply on mixing, without enzymes or chemicals [310, 311]. This technology was derived from the CnaB2 domain of the fibronectin-binding protein from *Streptococcus pyogenes* [310]. SpyTag/SpyCatcher-based VLP decoration has been used for the display of diverse antigens, including those from SARS-CoV-2, plasmodium spp., influenza A virus, cancer cells (PD-L1) and HIV-1 [312, 313].

The split-protein conjugation system has advanced from concept to human testing on AP205 capsid VLPs (ABNCoV2), demonstrating that Tag/Catcher-mediated VLP display can meet regulatory and manufacturing requirements. This AP205 capsid VLPs platform uses a similar Tag/Catcher conjugation system to the SpyTag/SpyCatcher technology [428, 429].

HBsAg particles can be engineered as “plug-and-display” carriers [304]. SpyCatcher.HBsAg VLPs displaying the Pfs25 malaria antigen elicit stronger antibody responses and greater transmission-reducing activity in mice than soluble Pfs25. This superiority is evident even at low antigen loading: with only ~10% VLP occupancy (molar ratio). Higher coupling levels (50% and 90%) further boost immunogenicity. This study also showed that the vaccination induces anti-HBsAg IgG without diminishing the Pfs25-specific response. Moreover, pre-existing anti-HBsAg immunity does not reduce the response to Pfs25.SpyTagSpyCatcherHBsAg, supporting the broad utility of this VLP platform [304].

6.1.5 TTT.SpyTag Conjugation to SpyCatcher.HBsAg

In our design, we couple TTT.SpyTag with pre-formed SpyCatcher.HBsAg particles (hereafter abbreviated as VLP.TTT). This strategy combines a trimer format that enriches native-like Env and minimizes off-target monomers/dimers with a human-validated VLP carrier that can present many copies of antigen. The goal is to amplify B-cell response while retaining correct Env quaternary structure (Figure 6.2).

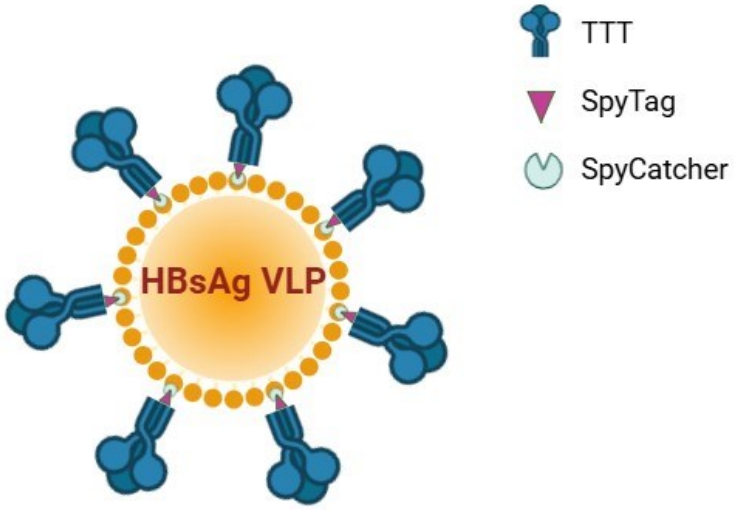

Figure 6.2 Design of the VLP.TTT vaccine using SpyTag/SpyCatcher technology. Schematic of an HBsAg virus-like particle (VLP; orange) used as a nanoparticle structure to multivalently display TTT Env trimers (blue). SpyCatcher peptides on the VLP subunits (mint) react covalently with SpyTag peptides on the TTT (magenta triangles), forming irreversible isopeptide bonds. Schematic is not to scale. This figure was made using Biorender.com.

6.1.6 Material Transfer of HBsAg VLPs from SpyBiotech

SpyCatcher.HBsAg VLPs used in this study were provided by SpyBiotech Ltd. (Oxford, UK) under a formal Materials Transfer Agreement (MTA) (reference R95167/CN001) between SpyBiotech and the University of Oxford. This agreement enabled the supply of HBsAg VLPs specifically for our collaborative research. In accordance with the terms of the MTA, all supplied materials were handled exclusively for non-clinical, preclinical research purposes under the supervision of the designated investigators at the University of Oxford. The agreement states secure use, restrictions on redistribution or commercial use, and appropriate acknowledgment of SpyBiotech Ltd. as the source of these materials in any resulting publications.

6.2 Aims

- To engineer TTT Env constructs fused with SpyTag for coupling to SpyCatcher.HBsAg VLPs.
- To optimize SpyTag/SpyCatcher-mediated conjugation of TTT to HBsAg VLPs and confirm the VLP.TTT formation by negative staining electron microscopy (EM).
- To verify the VLP.TTT binding to bnAbs.
- To assess the immunogenicity of VLP.TTT in mice, compare soluble TTT and SMAA-TTT, and determine adjuvant contribution.

6.3 Results

6.3.1 Cloning, Expi293F Expression, and GNL Purification of TTT.PkSpyTag/SpyTag002 Constructs

Using gene-specific primers that added a C-terminal Pk tag, GSG linker and either SpyTag or SpyTag002 together with a NotI site, we amplified the TTT.Pk open reading frame from p5848 plasmid. PCR yielded a product of ~6 kb for both designs (TTT.PkSpyTag and TTT.PkSpyTag002), which was gel-excised and purified (Figure 6.3 A). The inserts and the pTH (p71) vector were double-digested with KpnI-HF and NotI-HF and set up in overnight ligations. The expected plasmid sizes after ligation were ~10.88 kb for both constructs (Figure 6.3 B). Ligated constructs were transformed into Stellar (HST08) *E. coli*. Colony plasmid isolates were screened by diagnostic digestion with SalI-HF (Figure 6.3 C). One positive clone from each construct was selected for Sanger sequencing to verify the presence of SpyTag/SpyTag002 at the TTT C-terminus. Transient transfection of Expi293F cells with pTH.TTTPkSpyTag and pTH.TTTPkSpyTag002 yielded secreted Env proteins. Glycosylated proteins were captured from clarified supernatants by Galanthus nivalis lectin (GNL) agarose beads and eluted with α-methyl-D-mannopyranoside. This process provided purified TTT.PkSpyTag and TTT.PkSpyTag002 proteins for downstream conjugation and antigenicity/immunogenicity assays.

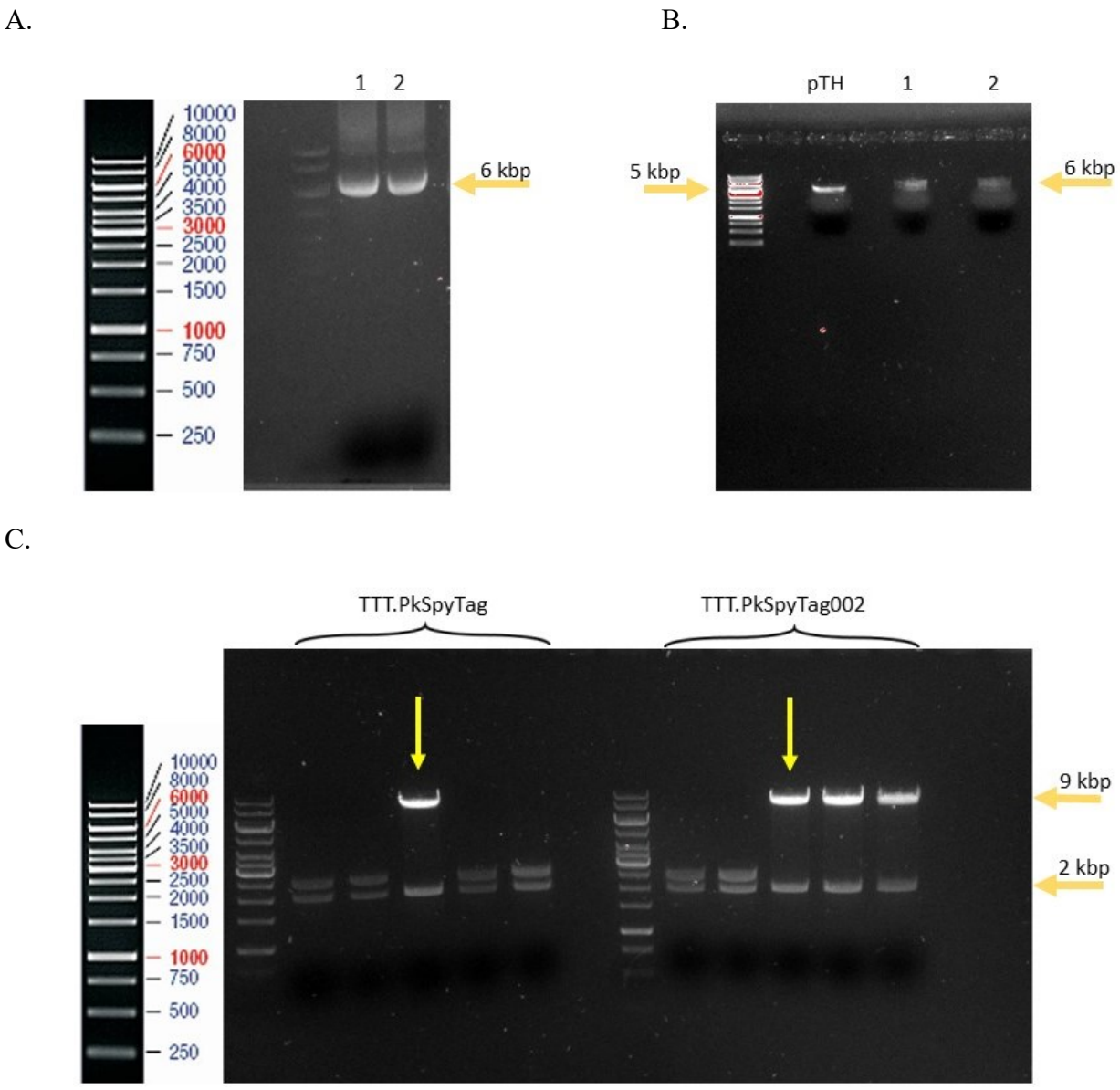

Figure 6.3 Cloning and transformation of TTT.PkSpyTag/SpyTag002 constructs. A) PCR from p5848 yielded the expected ~6 kbp amplicons for lane 1: TTT.PkSpyTag and lane 2: TTT.PkSpyTag002. B) KpnI/NotI digestion of pTH and the inserts (lanes 1, 2 as above) shows the ~5 kbp vector and ~6 kbp insert fragments. C) SalI diagnostic digests of colony plasmid isolates; arrows mark selected positive clones with the predicted two-band pattern (~9 kbp and ~2 kbp) for TTT.PkSpyTag (left) and TTT.PkSpyTag002 (right).

6.3.2 TTT.PkSpyTag Conjugation to SpyCatcher.HBsAg VLPs was confirmed

To confirm conjugation of TTT.PkSpyTag with SpyCatcher.HBsAg VLPs, we first performed western blotting using anti-Pk tag and anti-C tag antibodies. In the anti-Pk tag blot (Figure 6.4 A, left panel), a band corresponding to TTT.Pk.SpyTag was detected at the expected size of ~400 kDa. Due to the large size of TTT, no clear shift was observed following conjugation with VLPs. In the anti-C tag blot (Figure 6.4 A, right panel), conjugation was clearly detected: while TTT.PkSpyTag alone showed no C tag reactivity, incubation with SpyCatcher.HBsAg VLPs (includes C tag) produced a strong positive band, confirming the conjugation. Negative-stain EM showed multiple TTTs coating each HBsAg VLP, consistent with multivalent display. (Figure 6.4 B).

A.

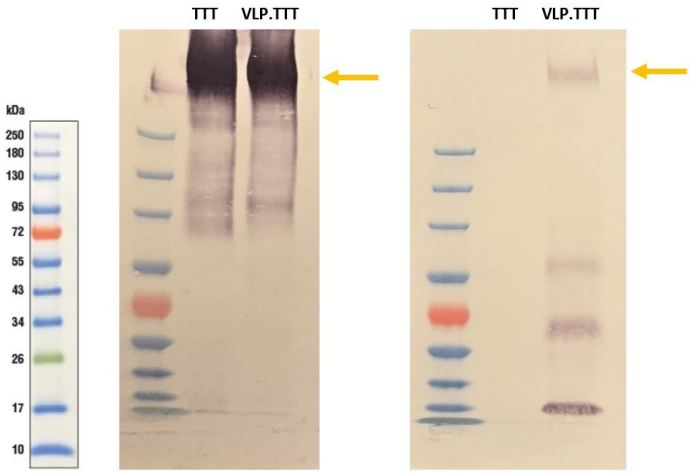

B.

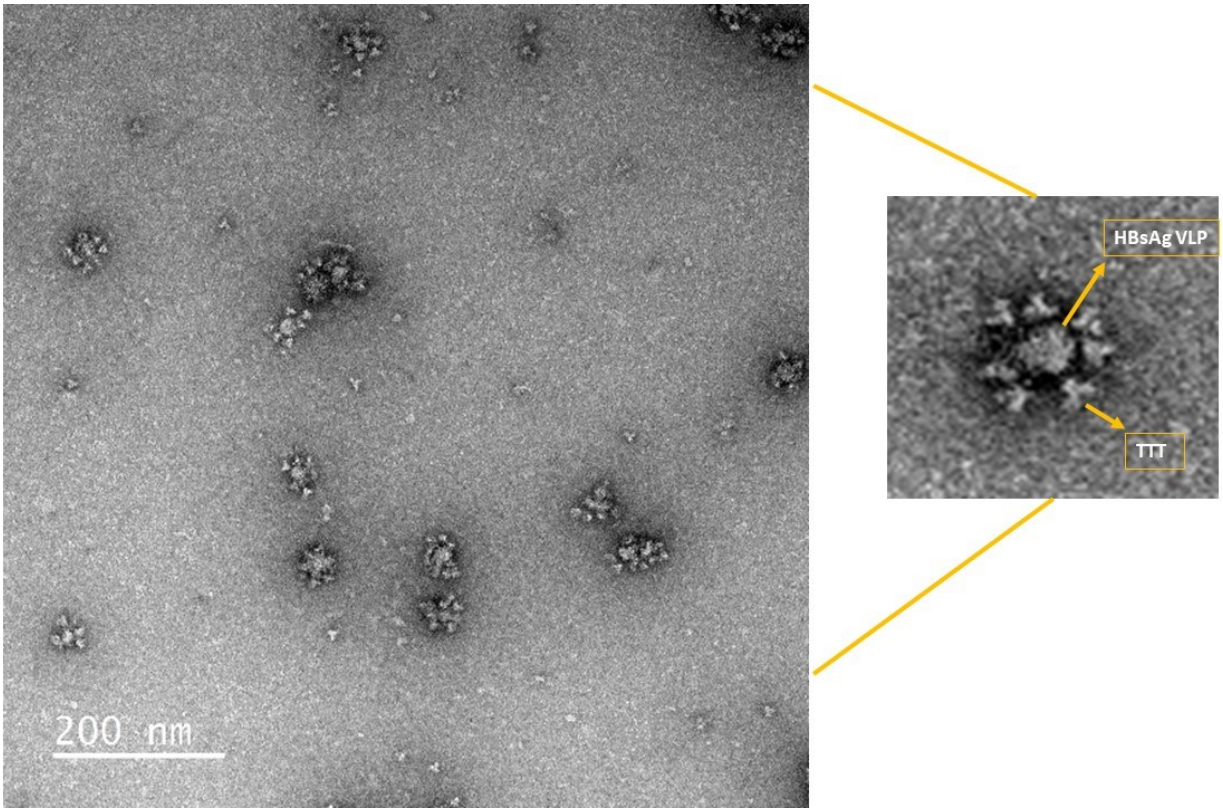

Figure 6.4 Confirmation of TTT.PkSpyTag conjugation to SpyCatcher.HBsAg VLPs. A) Western blot analysis using anti-Pk tag (left) and anti-C tag (right) antibodies. Anti-Pk blot detected TTT.PkSpyTag at the expected size (~400 kDa), with no shift upon conjugation to VLPs. Anti-C blot confirmed conjugation: while free TTT.PkSpyTag showed no signal, incubation with SpyCatcher.HBsAg VLPs (containing a C tag) produced a strong band. B) Negative-stain electron microscopy of conjugated particles, revealing HBsAg VLPs coated with multiple TTT trimers, consistent with efficient SpyTag/SpyCatcher coupling (scale bar: 200 nm).

6.3.3 Conjugation efficiency peaks at the 0.5 TTT:VLP molar ratio with 3 h shaking followed by overnight incubation

To further optimise conjugation efficiency, we tested a range of molar ratios and reaction conditions using High-performance liquid chromatography (HPLC). In the HPLC profiles, the major peak eluting between 14-16 minutes corresponded to the largest assembled particles, consistent with VLP.TTT conjugates under size-exclusion principles. Subsequent later-eluting peaks represented smaller components, including unbound TTT trimers, VLPs and fragments. The assay design included molar ratios of 0.08, 0.15, 0.3, 0.5, and 0.8 (TTT:VLP), with the VLP amount kept constant, along with controls of TTT.SpyTag alone and SpyCatcher.HBsAg VLP alone (Figure 6.5 A). The conjugation efficiency increased with higher molar ratios. The 0.5 ratio produced the largest under first peak area with 48.14%. The 0.8 ratio also produced a similar under peak area with 47.3% but, this was accompanied by excess unbound antigen (second and third peaks) (Table 6.1).

We also tested different incubation conditions, 3 hours vs. overnight, static vs. shaking, and acidic vs. neutral pH (Figure 6.5 B). Among the incubation conditions tested, overnight incubation, acidic pH and shaking further improved conjugation with 60.17%, 63.39% and 57.74% peak areas respectively (Table 6.1). Notably, acidic (pH 5) condition was excluded from immunisation studies due to *in vivo* physiological compatibility.

These results established that a 0.5 molar ratio of TTT.PkSpyTag to SpyCatcher.HBsAg VLPs, with 3 hours shaking following by overnight incubation at neutral pH, represented the optimal condition for efficient conjugation. This condition was selected for immunogenicity experiments.

A.

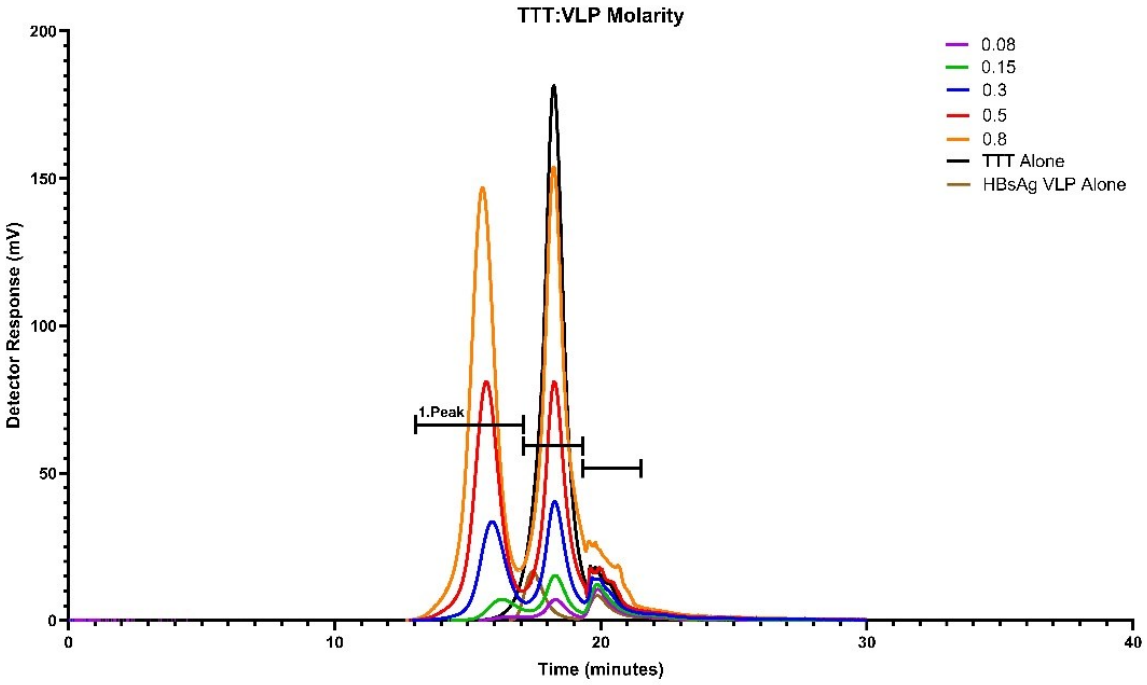

B.

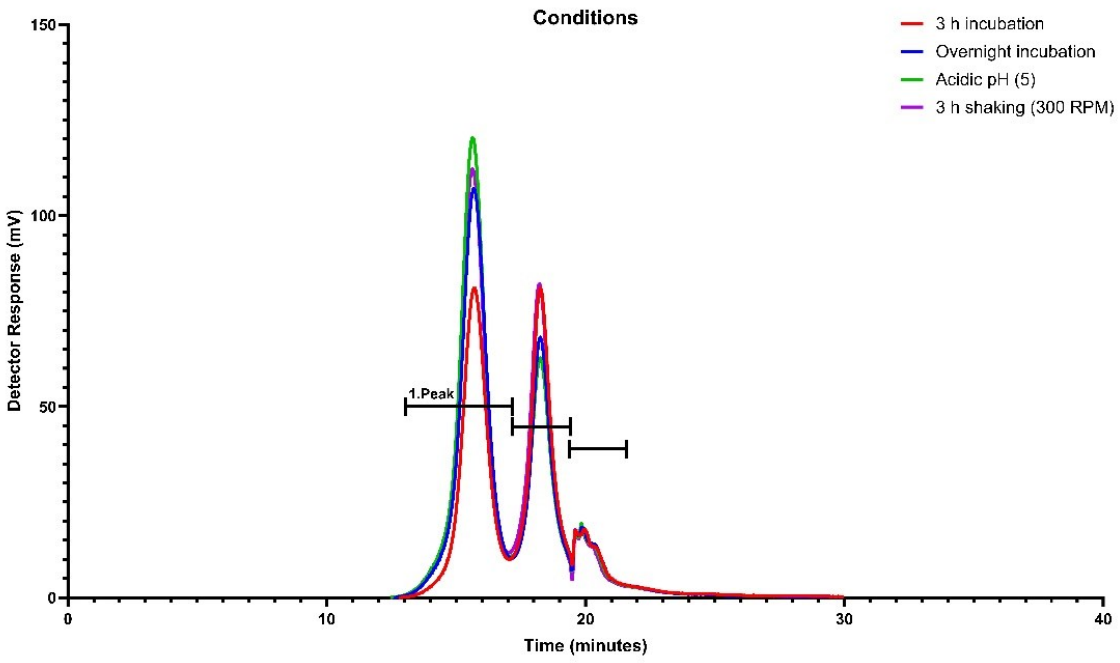

Figure 6.5 HPLC analysis of TTT.PkSpyTag conjugation to SpyCatcher.HBsAg VLPs. A) Representative chromatograms (UV 280 nm) of conjugation reactions at different TTT:VLP molar ratios and controls. The major peak (1.Peak) eluting at 14-16 minutes corresponds to the largest assembled particles, consistent with VLP.TTT conjugates. Subsequent later-eluting peaks reflect smaller species, including unbound TTT trimers, free VLPs, and fragments. TTT.SpyTag alone and SpyCatcher.HBsAg VLP alone served as controls. B) Conjugation reactions at different conditions, 3 hours incubation, overnight incubation, shaking (300 RPM), acidic pH at 0.5 molar ratio.

Samples	Region Number	Trace	Start (mins)	End (mins)	Peak Max RT (mins)	Peak Height (mV)	Peak Height (%)	Peak Area (mV.s)	Peak Area (%)
TTT.SpyTag Alone	Peak 1	UV 280nm	15.95167	19.49833	18.23	181.673	90.69	11317.71	91
	Peak 2	UV 280nm	19.4983	21.16833	19.60333	18.641	9.31	1119.983	9
SpyCatcher.HBsAg Alone	Peak 1	UV 280nm	16.30333	19.18667	17.4167	16.898	65.71	957.844	63.91
	Peak 2	UV 280nm	19.18667	21.19333	19.87833	8.818	34.29	540.887	36.09
TTT.SpyTag+SpyCatcher.HBsAg VLP **0.08 Molarity**	Peak 1	UV 280nm	15.25667	17.23333	16.675	1.352	7.01	102.632	**8.6**
	Peak 2	UV 280nm	17.32667	19.25667	18.29333	2.707	37.35	430.852	36.1
	Peak 3	UV 280nm	19.30333	21.83333	19.91333	81.48	55.64	1210.215	79.1
TTT.SpyTag+SpyCatcher.HBsAg VLP **0.15 Molarity**	Peak 1	UV 280nm	14.75833	17.31833	16.2	7.195	20.71	585.092	**25.48**
	Peak 2	UV 280nm	17.34167	19.30167	18.27667	8.823	44.25	543.621	24.26
	Peak 3	UV 280nm	19.34833	21.585	19.86667	23.854	35.05	1318.867	58.87
TTT.SpyTag+SpyCatcher.HBsAg VLP **0.3 Molarity**	Peak 1	UV 280nm	14.06667	17.17833	15.92	33.564	37.97	2501.29	**42.08**
	Peak 2	UV 280nm	17.225	19.37	18.37667	17.7367	45.63	2540.811	41.23
	Peak 3	UV 280nm	19.39333	21.58333	19.96667	66.298	16.4	9917.756	16.69
TTT.SpyTag+SpyCatcher.HBsAg VLP **0.5 Molarity**	Peak 1	UV 280nm	14.08667	16.95	15.705	80.716	45.11	570.701	**48.14**
	Peak 2	UV 280nm	17.04	19.50833	18.25333	80.676	45.09	5072.176	42.31
	Peak 3	UV 280nm	19.555	21.23833	19.96333	17.538	9.8	144.96	9.55
TTT.SpyTag+SpyCatcher.HBsAg VLP **0.8 Molarity**	Peak 1	UV 280nm	14.06667	16.94833	15.55833	93.898	44.99	10421.683	**47.63**
	Peak 2	UV 280nm	17.01833	19.36667	18.32333	140.602	47.11	90497.577	45.08
	Peak 3	UV 280nm	19.45167	21.28333	19.96667	1264.257	7.9	94002.499	97.77
TTT.SpyTag+SpyCatcher.HBsAg VLP 0.5 Molarity **Overnight Incubation**	Peak 1	UV 280nm	14.05	17.18	15.68667	106.477	55.7	7972.854	**60.17**
	Peak 2	UV 280nm	17.22667	19.49333	18.255	67.2	35.17	4157.871	31.38
	Peak 3	UV 280nm	19.49833	21.19167	19.91667	118.7	9.13	85231.256	98.51
TTT.SpyTag+SpyCatcher.HBsAg VLP 0.5 Molarity **pH:5**	Peak 1	UV 280nm	14.05	17.065	15.63333	119.434	60.04	8655.775	**63.39**
	Peak 2	UV 280nm	17.08833	19.43	18.06667	61.418	30.88	3992.362	29.24
	Peak 3	UV 280nm	19.475	21.005	19.86667	1264.414	9.08	72364.686	98.18
TTT.SpyTag+SpyCatcher.HBsAg VLP 0.5 Molarity **Shaking Incubation**	Peak 1	UV 280nm	14.02667	16.97	15.63333	111.315	53.26	8162.815	**57.74**
	Peak 2	UV 280nm	17.04	19.45167	18.21667	45.487	38.77	48835.35	37.45
	Peak 3	UV 280nm	19.49833	20.88333	19.87667	1263.952	7.97	65067.033	97.87

Table 6.1 HPLC quantification of TTT.PkSpyTag conjugation to SpyCatcher.HBsAg VLPs under different molar ratios and incubation conditions. The table summarises chromatographic peak parameters, including retention times (RT), peak heights, and peak areas, for reactions performed at varying TTT:VLP molar ratios (0.08-0.8) and different incubation settings (3 hours vs overnight, shaking vs static, neutral vs acidic pH). Conjugation efficiency increased with higher molar ratios, and the 0.5 molar ratio achieved the highest conjugation yield (48.14% peak area). Overnight incubation, acidic pH and shaking further improved conjugation with 60.17%, 63.39% and 57.74% peak areas respectively.

6.3.4 TTT Conjugation to VLPs Preserves Recognition by BnAbs

To evaluate whether TTT still presents its key conformational epitopes in the correct way so that specific antibodies can bind after conjugation to SpyCatcher.HBsAg VLPs, we performed an antigenicity ELISA with a panel of bnAbs. The assay was carried out using a GNL-capture format, in which VLP.TTT or unconjugated TTT proteins were immobilized on plates and probed with serial dilutions of bnAbs.

The selected bnAbs included 2G12, which targets a high-mannose glycan cluster on the outer domain of gp120; VRC01, which recognizes the CD4-binding site on gp120; PGT121, which engages a glycan-dependent epitope in the V3 loop region; and PGT145, which binds a quaternary apex epitope in the V1/V2 region of gp120 [430-433].

Across all four bnAbs, VLP.TTT and unconjugated TTT trimers displayed similar antigenicity profiles (Figure 6.7). The binding curves exhibited dose-dependent increases in OD450, and saturated at higher antibody concentrations. No loss of recognition indicated the maintained structural presentation of key bnAb epitopes after conjugation to VLPs. At lower antibody concentrations, VLP.TTT showed slightly enhanced binding compared to unconjugated TTT, likely reflecting the multivalent display of Env trimers on the VLP surface.

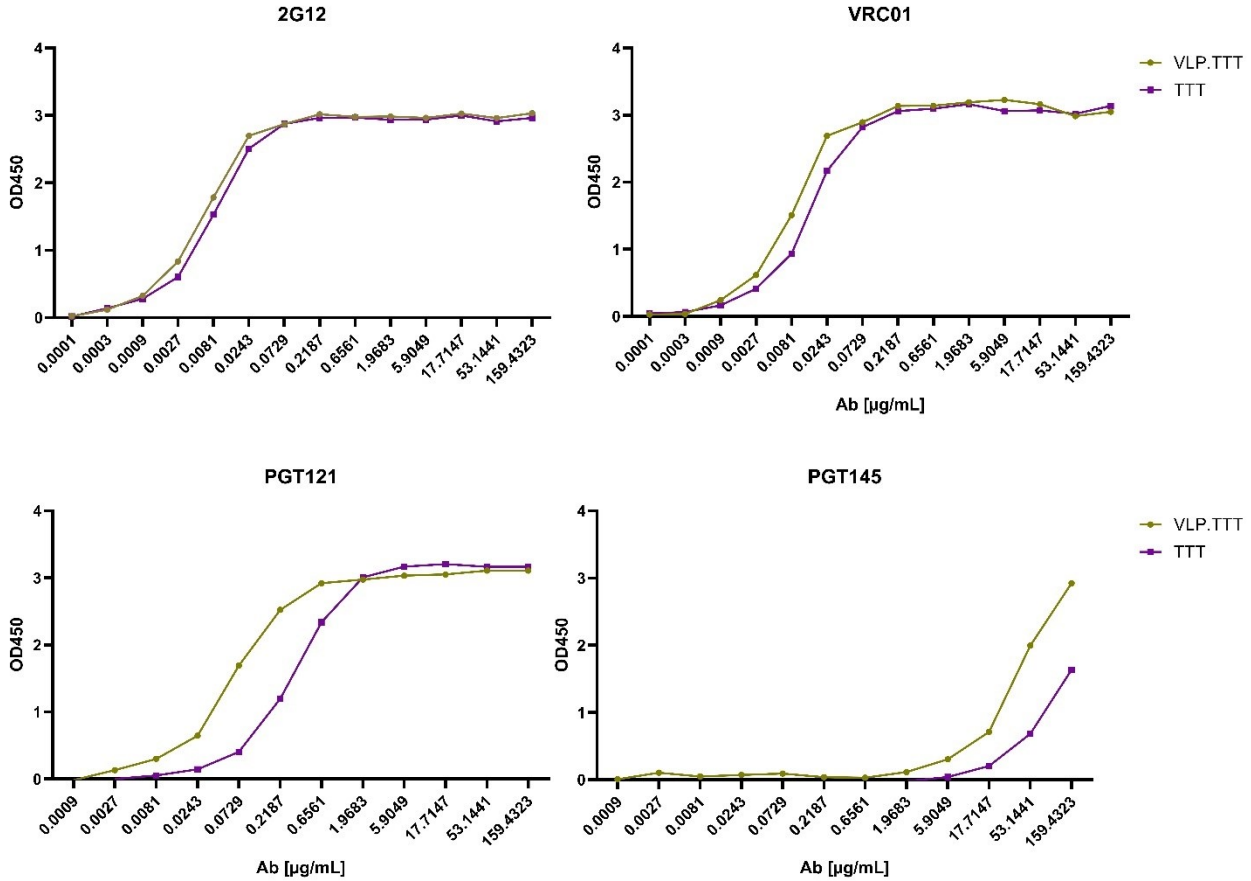

Figure 6.7 The antigenicity of TTT and VLP.TTT. Binding of bnAbs 2G12, VRC01, PGT121, and PGT145 to TTT alone (purple) or TTT conjugated to SpyCatcher.HBsAg VLPs (green) was measured by ELISA. Serial dilutions of each antibody were tested against immobilized antigens, and binding was detected at OD450.

6.3.5 Multivalent display of TTT on HBsAg VLPs accelerates antibody induction but results in titres comparable to soluble TTT after boosting

To evaluate the immunogenicity of TTT presentation formats, we performed a first pilot study in BALB/c mice (n=3 per group). The experimental design included four immunisation groups: TTT alone (soluble trimeric TTT protein), VLP.TTT, SMAA.TTT (TTT complexed with *Staphylococcus Aureus* protein A, an alternative multivalent display format), and HBsAg VLP alone (empty VLP carrier without TTT). All formulations, except SMAA.TTT, were administered with AddaVax

adjuvant. Mice were immunised at weeks 0, 4, and 8, and blood was collected at defined intervals (Figure 6.8). Antibody responses were quantified by endpoint titre ELISA using plates coated with TTT antigen.

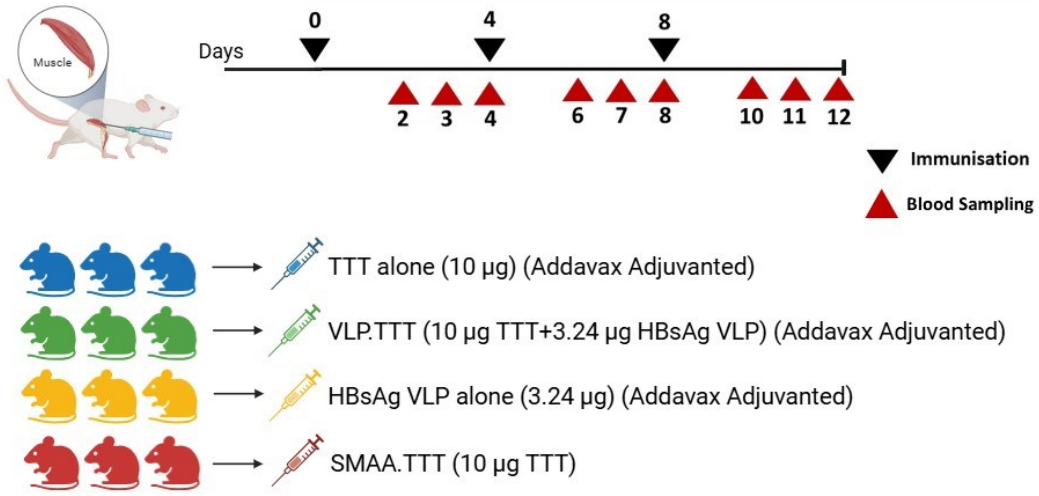

Figure 6.8 Immunisation schedule and experimental groups. BALB/c mice (n=3 per group) were immunised intramuscularly at weeks 0, 4, and 8 (black triangles) with one of four formulations: TTT alone (10 µg, AddaVax-adjuvanted), VLP.TTT (10 µg TTT + 3.24 µg HBsAg VLP, AddaVax-adjuvanted), HBsAg VLP alone (3.24 µg, AddaVax-adjuvanted), or SMAA.TTT (10 µg, non-adjuvanted). Blood samples (red triangles) were collected at weeks 2, 3, 4, 6, 7, 8, 10, 11, and 12 for ELISA. This figure was made using biorender.com.

Two weeks after the first immunisation, VLP.TTT and soluble TTT elicited low titres, which rose at week 3 and became substantially higher by week 4. In contrast, SMAA.TTT showed an earlier peak at week 2 and then remained stable thereafter. At both weeks 3 and 4, responses in the VLP.TTT group exceeded those in soluble TTT and SMAA.TTT (Figure 6.9 A). Following the second immunisation, all three TTT-containing groups (VLP.TTT, TTT alone, and SMAA.TTT) showed antibody boosting. At weeks 6 to 8, endpoint titres in both the VLP.TTT and TTT alone groups were at similarly high levels (Figure 6.9 B), which were sustained through weeks 10 to 12 (Figure 6.9 B). The HBsAg VLP alone group remained at background OD450 across all timepoints, confirming that the empty VLP showed no reactivity with TTT. This pilot study demonstrated that VLP.TTT elicits robust TTT-specific antibody responses, with evidence of accelerated induction compared to soluble TTT. After repeated immunisations, titres between VLP.TTT and TTT alone became comparable.

A.

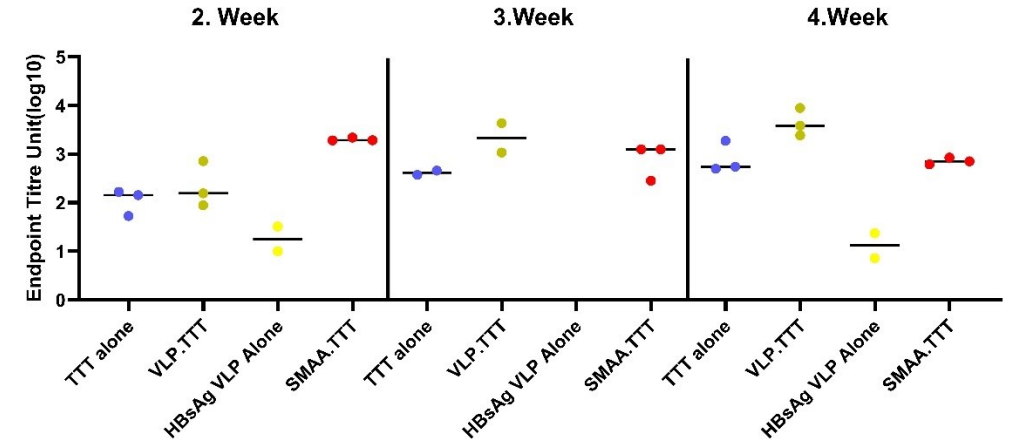

B.

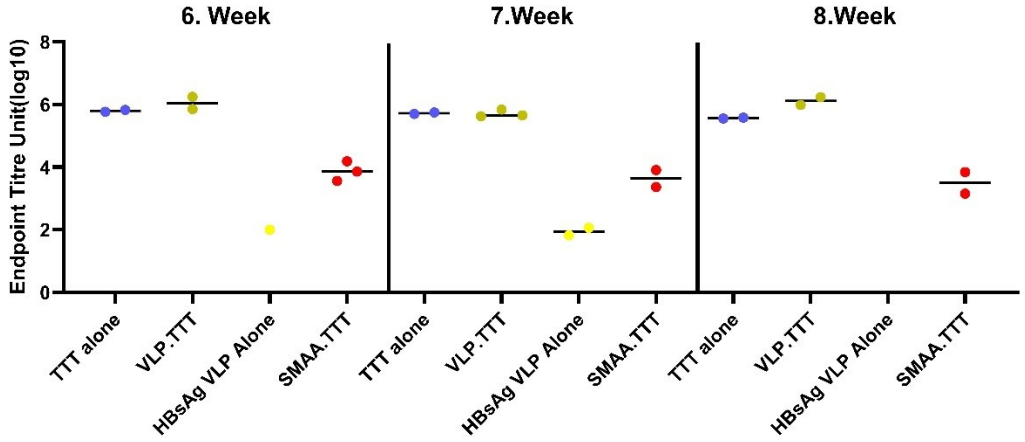

C.

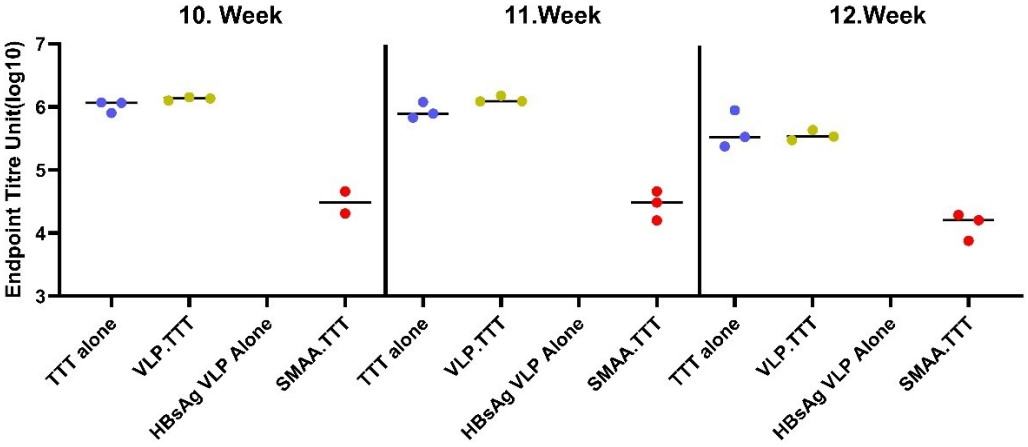

Figure 6.9 Antibody responses following immunisation with different TTT formats and VLP alone in mice. Sera were collected at three timepoints after each immunisation. The antigen-specific IgG endpoint titres were measured by ELISA. Individual mouse titres are shown with TTT alone (blue), VLP.TTT (green), HBsAg VLP alone (yellow), or SMAA.TTT (red) and horizontal lines indicates group medians. A) Antibody responses at weeks 2, 3, and 4. B) Antibody responses at weeks

6, 7, and 8. C) Antibody responses at weeks 10, 11, and 12. Statistical analysis revealed no significant differences ($p > 0.05$).

6.3.6 Adjuvant further enhances the immunogenicity of VLP.TTT

To further evaluate the immunogenicity of the VLP.TTT formulation, we performed a second experiment (n = 6 per group) comparing adjuvanted and non-adjuvanted conditions (Figure 6.10). Mice received either TTT alone or VLP.TTT, with or without AddaVax, and sera were collected at two timepoints after each immunisation. To control potential batch effects, soluble TTT was in the TTT.SpyTag format, and in the same batch that used for VLP.TTT coupling.

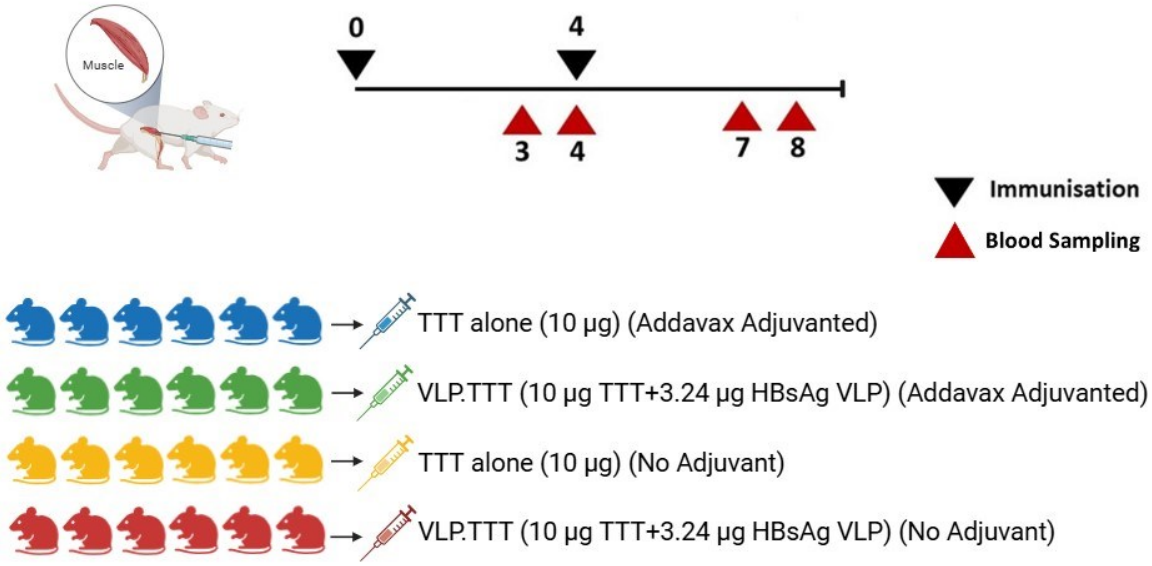

Figure 6.10 Immunisation schedule and experimental groups of the second experiment. Mice (n=6 per group) were immunised intramuscularly on days 0 and 4 with one of four formulations: TTT alone (10 µg, AddaVax adjuvanted), VLP.TTT (10 µg + 3.24 µg, AddaVax adjuvanted), TTT alone without adjuvant (10 µg), or VLP.TTT without adjuvant (10 µg + 3.24 µg). Blood samples were collected at weeks 3, 4, 7, and 8 (red triangles) for ELISA. This figure was made using biorender.com.

At week 3, adjuvanted groups showed clear antibody responses, with VLP.TTT+AddaVax inducing significantly higher titres compared to TTT+AddaVax ($p < 0.01$, Figure 6.11 A). In contrast, non-adjuvanted formulations elicited minimal responses, only one mouse in the VLP.TTT group showing detectable titres. This demonstrates the strong dependence of both TTT and VLP.TTT on adjuvant for early antibody induction. By week 4, antibody titres further increased in the adjuvanted groups, and VLP.TTT+AddaVax maintained superior titres compared to TTT+AddaVax ($p < 0.01$, Figure 6.11 B). Non-adjuvanted groups showed low-level responses.

Consistent with previous experiment, in the adjuvanted groups, titres between VLP.TTT and TTT alone became comparable after the second immunization. Although the difference is not statistically

significant, in non-adjuvanted groups, VLP.TTT induced higher titres compared to soluble TTT at weeks 7 and 8 (Figure 6.11 C, D).

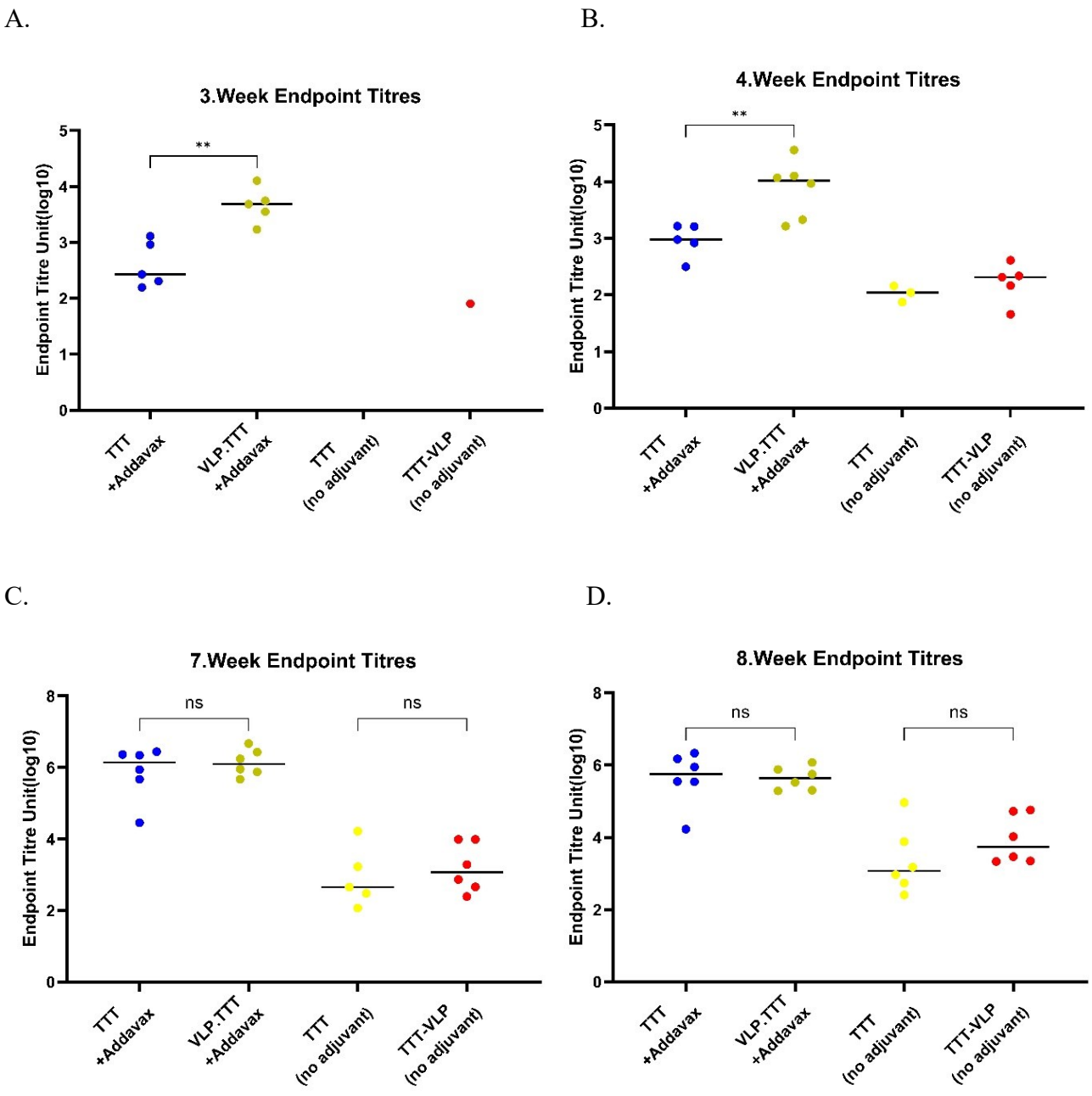

Figure 6.11 Endpoint antibody titres following immunisation with TTT or VLP.TTT with or without adjuvant. Serum samples were collected at weeks 3 (A), 4 (B), 7(C) and 8(D) endpoint antibody titres were measured by ELISA. Data points represent individual mice, TTT alone (blue), VLP.TTT (green), TTT without adjuvant (yellow), or VLP.TTT without adjuvant (red) and horizontal lines indicate group medians. At weeks 3 and 4 timepoints, adjuvanted VLP.TTT immunisation elicited significantly higher titres than adjuvanted TTT alone (**p = 0.0079, and **p=0.0087, at 3. And 4. Weeks respectively, Mann–Whitney U test). At weeks 7 and 8, statistical analysis revealed no significant differences ($p > 0.05$).

6.4 Discussion

HIV-1 continues to evade simple vaccine solutions. Maintaining Class I fusion proteins, such as HIV-1 Env, influenza HA, Mers-CoV and RSV F spike antigens, in the prefusion state is important for vaccine development because this conformation, found on infectious virions, presents the neutralizing epitopes necessary for protective antibody responses [417, 434, 435]. These proteins tend to form dimers/monomers or spontaneously form into the post-fusion conformation when their transmembrane domain is removed [283, 436]. HIV-1 vaccine efforts have long struggled to present the native-like Env trimers to elicit bnAbs. Many trimerization motifs have been fused to the C-terminus of gp140 to stabilize the Env trimer formation, such as GCN4 transcription factor, bacteriophage T4 fibritin, and a soluble trimerization domain of chicken cartilage matrix protein [437-439] The presence of these motifs results in the elicitation of undesirable motif-specific antibody responses [440]. The TTT design promotes the formation of stable trimers and does not affect the function or conformation of the protein. Gly-Ser flexible linkers provide the spacing necessary for independent folding, and they are thought to be poorly immunogenic [283]. These linkers have been widely used in the design of fusion proteins such as Brolucizumab and Blinatumomab [441, 442].

TTT format sits alongside two major Env vaccine strategies: (i) soluble native-like trimers such as BG505 SOSIP trimers that have been further multimerized on protein nanoparticles such as I53-50 to boost B-cell activation and autologous Tier-2 neutralization [280]. Germline targeting BG505 SOSIP GT1.1 immunogen is currently undergoing clinical evaluation (NCT04224701) [418]. (ii) Un-cleaved prefusion-optimized (UFO) group M consensus immunogens developed by Shattock's group, including ConSOSL.UFO.664 and membrane-anchored ConSOSL.UFO.750, which induced autologous tier 2 neutralization after DNA or protein immunizations in animals [443]. Subsequent work showed that ConSOSL.UFO Env trimers delivered by self-amplifying mRNA induced Env-specific IgG response in guinea pig, rabbit, and macaque models [444]. Two consensus Env immunogens, ConM SOSIP and ConS UFO were tested in a Phase I clinical trial. The ConM SOSIP trimer included disulphide linkages between the gp120 and gp41 and the I559P mutation to stabilize gp41 in its pre-fusion conformation. ConS UFO included a short flexible amino acid linker between gp120 and gp41 subunits A433C + I201C mutations that stabilize the CD4 binding site and V570D mutation that stabilizes gp41. Immunogens were co-formulated with MPLA adjuvant. Env trimers were found immunogenic in a prime-boost schedule, but they were insufficient to induce broad neutralizing antibody titers [445]. However, these immunogens have the potential in a sequential immunization with a germline-targeting immunogen for the induction of bNAbs.

The TTT design, as introduced by del Moral-Sánchez *et al*., genetically links three Env protomers in a single reading frame. This design is compatible with nucleic-acid platforms, and promotes trimeric assembly while minimizing immune-distracting oligomers [283]. The present chapter extends this innovation, displaying TTT in a VLP format.

Platforms able to present preserved quaternary epitopes in a multivalent, immune-stimulating context are at the leading edge [446, 447]. This work demonstrates that the multivalent display of TTT on VLP is a promising addition to the field. We confirmed that key conformational bnAb epitopes remain accessible after VLP conjugation. VLP.TTT multivalent display further advances the binding to bnAbs.

We described the design of a VLP.TTT vaccine using SpyTag/SpyCatcher conjugation to multivalently display Env trimers while preserving their native-like conformation to elicit robust

humoral immune response. We verified and optimised the efficient conjugation of TTT.SpyTag with SpyCatcher.HBsAg VLP at 0.5 molar ratio, with shaking and overnight incubation.

VLP-based display is a validated approach for improving immunogenicity via dense, repetitive surface epitope presentation, with several licensed vaccines (e.g., hepatitis B, HPV) and notable malaria vaccine success (RTS,S/AS01, R21/Matrix-M)[286, 303, 305, 307]. Displaying trimeric Env on VLPs, either through co-expression, or plug-and-display conjugation, has been shown to increase antibody titres and enhance B-cell activation compared to soluble forms [289, 304]. SOSIP-I53-50NPs displaying SOSIP trimers on self-assembling protein nanoparticles induced 41-fold higher autologous Tier-2 neutralizing antibody titres in rabbits compared to soluble trimers [280]. In our study, the use of HBsAg as a carrier is particularly notable for high-density, scalable production, and for its proven safety and efficacy profile [299, 305, 307].

This chapter's application of the SpyTag/SpyCatcher conjugation system offers stable, site-specific coupling, and recently validated for malaria and SARS-CoV-2 antigens on HBsAg VLPs [304, 312]. Preclinical studies demonstrated that pre-existing anti-carrier immunity does not hamper the target response [304]. Facilitating this system's plug-and-display modularity, VLP.TTT design can be enhanced to cover diverse HIV-1 envelope trimers.

HIV-1 displays a very low density of Env spikes, about 7-14 per virion, far fewer than many viruses and well below SIV, which has ~70 per particle [36]. This low-density arrangement is considered an evolved immune-evasion tactic that limits bivalent antibody binding, lowers avidity and hampers neutralization [448]. The density of Env spikes is important for an effective B-cell receptors cross-linking, which contributes B-cell expansion, affinity maturation, and the generation of broadly neutralizing antibodies [449]. In line with this principle, VLP.TTT represents a promising vaccine design, displaying multiple TTT per particle as confirmed by electron microscopy.

Our mouse studies show that multivalent display of TTT on HBsAg VLPs boosts early antibody responses after the first immunisation and achieves higher titres than soluble TTT when adjuvanted, aligning with observations for VLP-based COVID-19 and malaria vaccines [304, 312]. However, following secondary and tertiary immunization, titre differences between VLP.TTT and soluble TTT diminished, consistent with Pfs25.SpyTagSpyCatcherVLP and SOSIP-I53-50NPs vaccine studies [447, 450]. This suggests the main advantage of VLP display lies in speed of antibody induction and priming efficiency. Once memory and germinal centre responses are established, booster doses expand these populations even with soluble antigen. Therefore, the differences between formats are minimized. In contrast, in the absence of adjuvant, the particulate nature of VLP.TTT provides intrinsic immunostimulatory advantages, and higher titres than soluble TTT sustain after the booster dose. This pattern is also in line with the Pfs25.SpyTagSpyCatcherVLP study, where in the non-adjuvanted groups the VLP formulation continued to outperform soluble antigen after boosting, and the gap was larger than the difference between adjuvanted VLP.Pfs25 and adjuvanted Pfs25 soluble antigen [450].

Adjuvant (AddaVax) is essential for robust responses. The dependence on adjuvant highlights the need to explore alternative adjuvants (e.g., saponin-based or TLR agonists) to induce robust innate immunity.

Despite the progress, further work is needed to improve VLP.TTT vaccine platform. Titres are robust but not yet shown to be broadly neutralizing against global viral diversity. The next phase should include functional assays in rabbits and non-human primates, and may benefit from incorporating sequence-diverse Env immunogens. Investigating T-cell responses and fine mapping of B-cell epitopes

post-vaccination, optimising dosing schedules and adjuvant choices, and combinatorial approaches with T-cell vaccines in prime-boost regimens will advance this platform.

6.5 Limitations

Small pilot study (n = 3) in mice limits statistical power and generalizability.

Immunogenicity assessed mainly by Endpoint ELISA. Avidity, neutralization breadth, durability were not evaluated.

Conjugation analyses (EM, HPLC) provided qualitative/indirect evidence rather than precise quantification of antigen density per VLP.

Only one adjuvant (AddaVax) was tested; alternative adjuvants were not explored.

CHAPTER 7: CONCLUDING REMARKS

Despite four decades of intensive research, an efficacious HIV-1 vaccine remains elusive. The failures of several efficacy trials, such as RV144, HVTN 702 (Uhambo), HVTN 705 (Imbokodo), and HVTN 706 (Mosaico) showed the complexity of inducing durable protection against this rapidly mutating virus [142, 274-276]. Current HIV vaccine and cure strategies are commonly grouped into two principal classes: (i) antibody-based vaccines that aim to elicit bnAbs, and (ii) T-cell–based vaccines designed to induce potent cytotoxic and helper responses. A growing number of regimens now explore combination of T-cell and B-cell vaccine designs, and passive bnAb infusion either alone or together with active immunization to induce 'vaccinal effect' [451]. Therapeutic strategies are also advancing, including latency-reversing agents, immune modulators, therapeutic vaccine-bnAb combinations that aim to reduce the viral reservoir and promote durable immune control.

A preventive HIV-1 vaccine will likely require combined strategies that induce both the cellular and humoral arms of the immune system to achieve effective and durable protection [452]. Arunachalam *et al*. immunized macaques with a BG505 SOSIP.664 trimer formulated with a TLR7/8-agonist adjuvant together with a heterologous series of viral vectors expressing SIVmac239 Gag, vesicular stomatitis virus, vaccinia virus and Ad5, eliciting high-magnitude Gag-specific $CD8^+$ effector and tissue-resident memory T-cell responses. The co-immunization of two vaccines provided superior protection against homologous SHIV challenge in rhesus macaques compared with either modality alone. Additionally, the combined B- and T-cell vaccine regimen reduced the neutralising-antibody titre required for protection, and enhanced the durability of protection [453]. In this thesis, the sequential research steps were designed with this immune duality as a core principle. The initial aim was to induce robust, broad T-cell responses with bivalent HIVconsvX mosaics. We subsequently aimed to advance HIVconsvX delivery with PIV5, which enhanced mucosal immunity. Subsequent work aimed to induce humoral immunity using a VLP platform displaying stabilized HIV Env trimers. These arms could ultimately be harnessed within a prime-boost regimen in which T-cell priming vaccines are followed by antibody-inducing boosters. Across four main chapters, the thesis offers a coherent advancement of novel vaccine modalities.

Selectively targeting multiple conserved regions of HIV-1 represents a rational T-cell vaccine strategy, as supported by several human studies [332, 454-456]. This approach focuses T-cell responses on the virus's most conserved regions, thereby restricting its ability to mutate without a substantial loss in viral fitness [327]. One such approach, the conserved elements (CE) immunogen, was developed by Mullins, and colleagues. It focuses on short segments within the HIV Gag protein that are remarkably well conserved across HIV group M [323]. In a Phase I trial involving people living without HIV-1/2, the heterologous prime/boost CE/CE+p55Gag DNA vaccination demonstrated immunogenicity [457]. Building on this, to elicit multiple arms of the immune response, interleukin-12 adjuvanted CE-based T-cell vaccine was tested together with bnAbs infusions and toll-like receptor 9 agonist lefitolimod in UCSF-AmfAR study. Rutishauser *et al*. presented findings from this single-arm, proof-of-concept trial in ten individuals living with HIV [458]. Following ART interruption, one participant remained aviremic for over 18 months, while six others exhibited persistently low viral load setpoints for 3-6 months [458]. Earlier randomized, placebo-controlled study by Gunst *et al*. using bNAb and lefitolimod in eCLEAR study, suggests that part of the virological control in the UCSF-AmfAR study might be due to the bnAbs infusion [459]. The first-generation conserved mosaic HIVconsv immunogen was designed to provide broad coverage across major HIV-1 clades (A, B, C, and D). HIVconsv immunogen delivered by a combination of plasmid DNA, non-replicating simian adenovirus (ChAdV63), and MVA regimens, was evaluated in clinical trials involving people living without HIV in Europe and Africa [330, 331, 460]. These studies demonstrated a favourable safety

profile and induced high frequencies of $CD8^+$ T cells capable of inhibiting HIV-1 *in vitro* [330, 331, 460]. In a phase I clinical trial, enrolling 15 early-treated individuals living with HIV, MVA.HIVconsv vaccine was tested with the combination of latency-reversing agent romidepsin. The sustained suppression of viremia was observed in 23% of individuals up to 32 weeks [454]. The next-generation conserved mosaic vaccines, HIVconsvX, incorporate two complementary mosaic sequences composed of six functionally conserved regions from the Gag and Pol sub-proteins [332]. The amino acid sequences of mosaic 1 and mosaic 2 differ by roughly 10% [332]. Together, these two mosaics achieve an exact 9/9-amino acid match with at least 80% of potential T-cell epitope variants found among diverse HIV-1 strains in the LANL-HSD database alignments [332, 333].

In our study, we demonstrated the immunogenicity of the experimental HIVconsvX vaccines in people living without HIV-1/2 in the UK (HIV-CORE 005.2). The HIVconsvX vaccine, delivered using the ChAdOx1-MVA regimen, provided more potent heterologous vector delivery compared with the STEP and Mosaico study vaccines [276, 318]. ChAdOx1 was selected for ChAd vectors' low pre-existing seroprevalence in humans [461], thereby mitigating limitations associated with certain human adenovirus-vectored vaccines [462]. MVA was used as the boost because poxvirus vectors have been shown to effectively amplify existing $CD8^+$ T-cell responses and its established safety profile [353, 354, 463]. Although rare adverse events such as vaccine-induced immune thrombotic thrombocytopenia, capillary leak syndrome, and Guillain-Barré syndrome have been reported with widespread ChAdOx1 use, this platform remains notable for its strong safety record, ability to elicit robust immune responses, and scalability for mass production [347]. In many cases, the heterologous approach was found to be more effective than the homologous prime-boost regimen [376, 385]. A recent clinical study demonstrated that a heterologous vaccination regimen, using the BBIBP-CorV vaccine for priming followed by the Ad26.COV2.S vaccine as a booster induced a stronger humoral immune response compared to a homologous vaccination schedule [377]. The heterologous prime-boost strategy employing chimpanzee adenoviruses for priming and MVA for boosting is a well-established and clinically validated platform. A heterologous ChAdOx1-MVA prime-boost platform has shown a consistent safety profile and strong cellular immunogenicity across multiple clinical studies. In influenza, ChAdOx1-NP+M1 priming followed by MVA-NP+M1 boosting significantly increased cross-reactive T-cells and responses were maintained 18 months after vaccination [379]. In tuberculosis, ChAdOx1-85A priming with MVA85A boost was well tolerated and induced Ag85A-specific, polyfunctional $CD8^+$ and $CD4^+$ responses and serum Ag85A IgG responses beyond single-dose regimens [385]. A second dose of ChAdOx1-85A did not further boost these responses, however they were significantly boosted with MVA85A vaccination [385]. In a prostate cancer study, a ChAdOx1.5T4 prime followed by an MVA.5T4 boost showed excellent safety. Among the participants, 64% responded to the vaccination, with response magnitudes ranging from 30 to 1,025 SFU/10^6 PBMCs.

In the HIV-CORE 005.2 study, C1-M3M4 vectored HIVconsvX vaccine elicited IFN-γ-producing T-cells in all (100%) vaccine recipients with median (IQR) = 4,432 (2,750-5,820) SFU/10^6 PBMCs at peak time point. At the end of the monitoring period, on day 140, the vaccine-induced response was still detectable although lower than earlier time points, with a total net frequency of median (IQR) = 595 (320-1,495) SFU/10^6 PBMCs. These responses were broadly HIV-1–specific and recognized epitope variants beyond those encoded in the immunogens. The vaccine-induced T cells were polyfunctional, a characteristic repeatedly associated with improved viral control [172, 179]. Overall, the immunogenicity was comparable to that observed with the prototype HIVconsv vaccine. In the

STEP study, the median magnitude of the total response (Gag + Pol + Nef) was 625 SFU/10^6 PBMCs at the Fred Hutchinson laboratory and 886 SFU/10^6 PBMCs at the Merck laboratory [397].

In HIV-CORE 006 clinical study, we evaluated the safety and immunogenicity of the same HIVconsvX vaccines in healthy adults living without HIV-1/2 across four clinical research centres in sub-Saharan Africa, where clades A, C, and D circulate. 88 participants received study injections, 72 vaccine and 16 placebos, with 57 (65%) men and 31 (35%) women. The C1, M3, and M4 vaccines were well tolerated and induced HIVconsvX-specific responses in 70 of 71 (99%) participants who completed all doses. Vaccine-induced T cells peaked at a median of 2,310 (IQR 1,080-4,480) IFN-γ SFU/10^6 PBMCs and recognized a median of 8 (5-10) of the 10 peptide pools spanning the HIVconsvX immunogen. Vaccine-induced T-cells were polyfunctional and inhibited HIV-1 representatives from clades A, B, C, and D [337].

Broad targeting of multiple HIV-1 epitopes is considered essential for better viral control [393]. STEP and APPROACH trials have consistently linked wider epitope recognition with improved outcomes. In STEP study, participants recognizing three or more Gag epitopes had lower plasma viral loads, and in APPROACH study, the breadth of peptide-pool recognition correlated with the number of HIV-1 isolates inhibited [387, 397]. In our study, after *in vitro* expansion, vaccine recipients recognized a median of 10 15-mer peptide pairs (range 0-70). A key advantage of the HIVconsvX vaccine is that its targeted epitopes are conserved, and thus each is likely to contribute to protection [204].

Although HIV has the most extensively mapped T-cell epitope landscape of any human pathogen, many such responses fail to provide effective antiviral immunity [464]. To better prioritize functional targets, Mothe *et al*. defined "beneficial epitopes" based on associations with lower viral loads in approximately 1,000 individuals living with HIV-1 clade B or C [334]. The HIVconsvX design includes 33 of these 48 beneficial epitopes. Env was deliberately excluded because despite a short-conserved region, it contains none of the beneficial epitopes [332]. Based on the Mothe *et al*.'s study, the multiepitope HIVACAT T-cell immunogen (HTI) was designed and has been evaluated in four human trials in people with and without HIV. In the first-in-human, placebo-controlled AELIX-002 study, 40% of vaccine recipients completed the 24-week ATI versus 8% in the placebo arm, providing an encouraging efficacy signal [321]. A recently completed Phase I, placebo-controlled trial (BCN03, NCT05208125) assessed a regimen including single doses of ChAdOx1.HTI and MVA.HTI given between three vaccinations of the B-cell immunogen ConM SOSIP.v7 gp140 in 30 ART-treated individuals living with HIV-1 [465-467]. In BCN03, T-cell responses to the ConM SOSIP immunogen positively correlated with SOSIP-binding antibody titres, whereas HTI-directed immunity was markedly lower than in AELIX-002/003, possibly due to the study population being composed of individuals treated during later stages of HIV infection [465]. Notably, the same vaccination scheme (ChAdOx1.HTI followed by MVA.HTI) elicited responses in HIV-negative individuals exceeding a median of 8,300 SFU/10^6 PBMCs, with a median of 16 individual epitopes targeted [466].

We are aware of the HIV-CORE 005.2 limitations, such as small sample size and single location. The longevity of responses was limited. From peak, the responses declined by ~60%, reaching a median of 1,690 (IQR 1,212.5-2,755) SFU/10^6 PBMCs two weeks after the MVA boost (D42). Another limitation of our study is its exclusive focus on PBMCs, even though the most critical immune activity and clearance of HIV-1-infected cells occur within lymphoid tissues and organs [388].

The clinical development of HIVconsvX vaccines includes completed and ongoing trials across varied populations and regions, with Phase 1- or Phase-2 studies to evaluate safety and immunogenicity in individuals living with or without HIV-1. DC-HIV04 and the M&M studies focus on therapeutic

vaccination. The M&M Study is a Phase I trial investigating the MVA.HIVconsvX vaccine in people living with HIV on ART. The study examined the impact of age on immune responses to the vaccine. The results showed that while older age was associated with a reduced T-cell response, the vaccine was safe and induced T-cell responses across all age groups [380]. Ongoing trials, IMPAACT 2039 A-B, AbVax, and RV630 expand the pipeline by testing HIVconsvX in children, adolescents, and adults in combination with bnabs. The clinical evaluation of HIVconsvX vaccines indicate encouraging immunogenicity and safety, while ongoing work is expected to further clarify vaccines' role in cure and prevention strategies for HIV-1.

We are continuing to evaluate alternatives to the ChAdOx1-MVA platform to expand HIVconsvX delivery options, improve T-cell induction in low responders, sustain long-term immunity, and target the anatomical sites of HIV-1 transmission. Thus far, an integration-deficient lentiviral vector, recombinant BCG, BioNTech's self-amplifying mRNA, and Moderna's lipid-nanoparticle mRNA have been tested for delivering HIVconsvX immunogens [404-407]. PIV5 offers several advantages as a vaccine platform, including a strong safety record, broad tissue tropism, and potent systemic and mucosal immunogenicity [368, 369].

Mucosal immunity constitutes the first line of defence against HIV-1 transmission and infection [399]. Mucosal lymphocytes express homing receptors (e.g., CCR9, α4β7 integrin) that guide them to distal mucosal sites, such as the genital and gut mucosa, where they can exert protective functions [401, 402]. In a preclinical work, intranasal immunization of mice with HIV gp140 elicited antigen-specific antibodies in vaginal secretions [468, 469]. In humans, nasal immunization with cholera toxin B subunit has been linked to vaginal antibody responses and produced stronger responses than direct intravaginal immunization [470]. The MUCOVAC, a Phase I study in healthy women living without HIV-1/2, evaluated the safety and immunogenicity of three HIV-1 clade C gp140 immunizations delivered by intramuscular, intranasal, and intravaginal routes, with a particular emphasis on gp140-specific antibodies in cervico-vaginal secretions and serum. Notably, the strongest $CD4^+$ T-cell responses were observed after intranasal, not intramuscular, administration. Intranasal vaccination also served as an effective prime for an intramuscular boost, whereas intravaginal delivery had no detectable effect on either systemic or mucosal responses [471].

Our study showed that intranasal delivery of PIV5-vectored HIVconsvX immunogens, especially when combined in heterologous prime-boost regimens with ChAdOx1 and MVA, significantly enhances mucosal T-cell responses in mice. Incorporating bivalent mosaic HIVconsvX immunogens further broadened recognition, enhancing responses to epitope variants that are not encoded in the vaccine. Another PIV5-vectored HIV vaccine study demonstrated humoral immunity induced by vaccination [408]. In a non-human primate model, intranasal PIV5 vaccines expressing HIV Env and SIV Gag followed by a boost with virus-like particles coated with HIV Env generated robust, durable systemic and mucosal Env-specific antibody titres with functional activity, including ADCC [408]. Growing evidence indicates that Fcγ receptor-mediated effector functions, such as ADCC, contribute to protection [142, 258, 472, 473].

Intranasal, mucosa-targeted vaccines are used beyond HIV. For example, the live-attenuated influenza vaccine Fluenz Tetra nasal spray is licensed in the UK [474]. Meanwhile, five mucosal vaccines for SARS-CoV-2 have received approval for human use in China, Morocco, Indonesia, India, Iran, and Russia (iNCOVACC®, Convidecia Air®, Sputnik V, Pneucolin®, RAZI-COV PARS) [475-479]. Intranasal vaccination offers non-invasive administration and strong patient adherence [480].

The last result chapter details the novel design of VLP.TTT vaccine, engineered virus-like particles displaying stabilized HIV Env trimers using the SpyTag/SpyCatcher plug-and-display technology. This approach preserves native-like Env formation and key quaternary neutralizing epitopes, and achieves multivalent display. The natural instability of the Env spike has significant implications for its production as a vaccine antigen for bNAb induction strategies [281]. Several trimer-based immunogen design strategies aim to minimize the induction of non-NAbs to monomeric gp120 and gp41 subunits and focus the response on NAb epitopes [281, 481]. The majority of bnAbs recognize epitopes that are influenced by the quaternary structure of the trimer [281]. The key rationale for the development of recombinant trimer-based immunogens is that trimers present multiple bNAb epitopes in ways that best mimic how these epitopes appear on the native Env spike [281]. One of these trimer-based immunogen designs is the BG505 SOSIP trimers, which have been further multimerized on protein nanoparticles such as I53-50 to boost B-cell activation and autologous Tier-2 neutralization [280]. Germline targeting BG505 SOSIP GT1.1 immunogen is currently undergoing clinical evaluation (NCT04224701) [418]. Another approach is un-cleaved prefusion-optimized (UFO) group-M consensus immunogens, ConSOSL.UFO.664 and the membrane-anchored ConSOSL.UFO.750, which elicited autologous tier-2 neutralization in animals following DNA or protein immunization, but did not achieve breadth in neutralizing antibodies [443, 445]. However, these immunogens have the potential in a sequential immunization with a germline-targeting immunogen for the induction of bnAbs. To promote stable trimeric assembly while minimizing immune-distracting oligomers, the TTT design introduced by del Moral-Sánchez *et al*. genetically links three Env protomers within a single open reading frame. Del Moral-Sánchez *et al*. showed that TTT consisted of trimers exclusively, while SOSIP.v8 and Single Chain controls also contained substantial amounts of dimers and monomers. Additionally, viral vectored TTT induced similar neutralization titres but with a higher proportion of trimer-specific responses compared to SOSIP.664 [283]. In our approach, we combined the TTT design with VLPs' repetitive display to enhance B-cell receptor engagement and strengthen humoral immunity. This design also has the advantage of HBsAg VLP's safety and well-established scalable production. We confirmed that key conformational bnAb epitopes remain accessible after VLP conjugation. In our murine immunization studies, adjuvanted VLP.TTTs induced significantly higher antibody titres after priming. However, booster immunizations brought titres in line with soluble TTT, suggesting the main advantage of VLP display is possibly the speed of antibody induction and priming efficiency. The SpyTag/SpyCatcher conjugation system offers modular, stable, site-specific coupling, and recently validated for malaria and SARS-CoV-2 antigens on HBsAg VLPs [304, 312]. The next stage for this VLP approach will require rabbit and non-human primate studies to assess the breadth and potency of neutralizing antibody responses across global HIV-1 clades. This design has a modular potential to incorporate sequence-diverse Env immunogens for future strategies.

In summary, these advances present a comprehensive strategy for modern HIV vaccine design, combining rational T-cell epitope selection, systemic and mucosal delivery optimization, and the development of innovative platforms to stimulate both cellular and humoral arms of adaptive immunity. This work advances the strategies to achieve a vaccine that is globally applicable, and protective across a wide spectrum of HIV-1 variants.

1. Bekker, L.G., *et al*., *Advancing global health and strengthening the HIV response in the era of the Sustainable Development Goals: the International AIDS Society-Lancet Commission.* Lancet, 2018. **392**(10144): p. 312-358.
2. *UNAIDS 2024 Report*. 2024; Available from: https://www.unaids.org/sites/default/files/media_asset/new-hiv-infections-data-among-key-populations-proportions_en.pdf.
3. Dwyer-Lindgren, L., *et al*., *Mapping HIV prevalence in sub-Saharan Africa between 2000 and 2017.* Nature, 2019. **570**(7760): p. 189-193.
4. Sharp, P.M. and B.H. Hahn, *Origins of HIV and the AIDS pandemic.* Cold Spring Harb Perspect Med, 2011. **1**(1): p. a006841.
5. Barre-Sinoussi, F., *et al*., *Isolation of a T-lymphotropic retrovirus from a patient at risk for acquired immune deficiency syndrome (AIDS).* Science, 1983. **220**(4599): p. 868-71.
6. Jacobs, M.M., *HIV or HTLV-III?* Arch Surg, 1987. **122**(8): p. 959.
7. Fauci, A.S. and H.C. Lane, *Four Decades of HIV/AIDS - Much Accomplished, Much to Do.* N Engl J Med, 2020. **383**(1): p. 1-4.
8. Alexander, T.S., *Human Immunodeficiency Virus Diagnostic Testing: 30 Years of Evolution.* Clin Vaccine Immunol, 2016. **23**(4): p. 249-53.
9. Mitsuya, H., *et al*., *3'-Azido-3'-deoxythymidine (BW A509U): an antiviral agent that inhibits the infectivity and cytopathic effect of human T-lymphotropic virus type III/lymphadenopathy-associated virus in vitro.* Proc Natl Acad Sci U S A, 1985. **82**(20): p. 7096-100.
10. Maeda, K., *et al*., *Discovery and Development of Anti-HIV Therapeutic Agents: Progress Towards Improved HIV Medication.* Curr Top Med Chem, 2019. **19**(18): p. 1621-1649.
11. Graves, M.C., *et al*., *An 11-kDa form of human immunodeficiency virus protease expressed in Escherichia coli is sufficient for enzymatic activity.* Proc Natl Acad Sci U S A, 1988. **85**(8): p. 2449-53.
12. Sever, B., *et al*., *A Review of FDA-Approved Anti-HIV-1 Drugs, Anti-Gag Compounds, and Potential Strategies for HIV-1 Eradication.* Int J Mol Sci, 2024. **25**(7).
13. *Latest Global Results & Projections Factsheet*. 2024; Available from: https://www.state.gov/pepfar-latest-global-results-factsheet-dec-2024/.
14. Chisumpa, V.H., C.O. Odimegwu, and N. Saikia, *Adult mortality in sub-Saharan Africa: cross-sectional study of causes of death in Zambia.* Trop Med Int Health, 2019. **24**(10): p. 1208-1220.
15. Hontelez, J.A., *et al*., *Changing HIV treatment eligibility under health system constraints in sub-Saharan Africa: investment needs, population health gains, and cost-effectiveness.* AIDS, 2016. **30**(15): p. 2341-50.
16. Julien, A., *et al*., *Health Care Providers' Challenges to High-Quality HIV Care and Antiretroviral Treatment Retention in Rural South Africa.* Qual Health Res, 2021. **31**(4): p. 722-735.
17. Van Damme, W., K. Kober, and M. Laga, *The real challenges for scaling up ART in sub-Saharan Africa.* AIDS, 2006. **20**(5): p. 653-6.
18. Meintjes, G., *et al*., *HIV-Related Medical Admissions to a South African District Hospital Remain Frequent Despite Effective Antiretroviral Therapy Scale-Up.* Medicine (Baltimore), 2015. **94**(50): p. e2269.
19. Veenstra, N. and A. Oyier, *The burden of HIV-related illness on outpatient health services in KwaZulu-Natal, South Africa.* AIDS Care, 2006. **18**(3): p. 262-8.
20. Naidoo, K., S. Rampersad, and S.A. Karim, *Improving survival with tuberculosis & HIV treatment integration: A mini-review.* Indian J Med Res, 2019. **150**(2): p. 131-138.
21. Goldstein, D., *et al*., *Integrating global HIV services with primary health care: a key step in sustainable HIV epidemic control.* Lancet Glob Health, 2023. **11**(7): p. e1120-e1124.

22. Sweeney, S., *et al*., *Costs and efficiency of integrating HIV/AIDS services with other health services: a systematic review of evidence and experience.* Sex Transm Infect, 2012. **88**(2): p. 85-99.
23. Abdool Karim, S.S., *et al*., *Timing of initiation of antiretroviral drugs during tuberculosis therapy.* N Engl J Med, 2010. **362**(8): p. 697-706.
24. Wanni Arachchige Dona, S., *et al*., *Added socioeconomic burden of non-communicable disease on HIV/AIDS affected households in the Asia Pacific region: A systematic review.* Lancet Reg Health West Pac, 2021. **9**: p. 100111.
25. Alkenbrack Batteh, S.E., *et al*., *Confirming the impact of HIV/AIDS epidemics on household vulnerability in Asia: the case of Cambodia.* AIDS, 2008. **22 Suppl 1**: p. S103-11.
26. *The Social-Economic Impact of HIV/AIDS at Individual and Household Level in China*. 2013.
27. *Gender impact of HIV and AIDS in India*. Available from: http://www.undp.org/content/dam/india/docs/gender.pdf.
28. *The Socio-Economic Impact of People Living with HIV at the Household Level in Myanmar*. 2017; Available from: https://www.undp.org/myanmar/publications/socio-economic-impact-people-living-hiv-household-level-myanmar#:~:text=The%20Socio-Economic%20Impact%20of%20People%20Living%20with%20HIV,level%20across%20all%20States%20and%20Regions%20in%20Myanmar.
29. Poudel, A.N., D. Newlands, and P. Simkhada, *The economic burden of HIV/AIDS on individuals and households in Nepal: a quantitative study.* BMC Health Serv Res, 2017. **17**(1): p. 76.
30. Ilinigumugabo, A., *[The economic consequences of AIDS in Africa].* Afr J Fertil Sexual Reprod Heal, 1996. **1**(2): p. 153-61.
31. Bor, J., *et al*., *In a study of a population cohort in South Africa, HIV patients on antiretrovirals had nearly full recovery of employment.* Health Aff (Millwood), 2012. **31**(7): p. 1459-69.
32. Ajithkumar, K., *et al*., *Impact of antiretroviral therapy on vocational rehabilitation.* AIDS Care, 2007. **19**(10): p. 1310-2.
33. Thirumurthy, H., *et al*., *Two-year impacts on employment and income among adults receiving antiretroviral therapy in Tamil Nadu, India: a cohort study.* AIDS, 2011. **25**(2): p. 239-46.
34. German Advisory Committee Blood, S.A.o.P.T.b.B., *Human Immunodeficiency Virus (HIV).* Transfus Med Hemother, 2016. **43**(3): p. 203-22.
35. Gelderblom, H.R., *Assembly and morphology of HIV: potential effect of structure on viral function.* AIDS, 1991. **5**(6): p. 617-37.
36. Stano, A., *et al*., *Dense Array of Spikes on HIV-1 Virion Particles.* J Virol, 2017. **91**(14).
37. Troyano-Hernaez, P., R. Reinosa, and A. Holguin, *HIV Capsid Protein Genetic Diversity Across HIV-1 Variants and Impact on New Capsid-Inhibitor Lenacapavir.* Front Microbiol, 2022. **13**: p. 854974.
38. Zhao, G., *et al*., *Mature HIV-1 capsid structure by cryo-electron microscopy and all-atom molecular dynamics.* Nature, 2013. **497**(7451): p. 643-6.
39. Zurnic Bonisch, I., *et al*., *Capsid-Labelled HIV To Investigate the Role of Capsid during Nuclear Import and Integration.* J Virol, 2020. **94**(7).
40. Watts, J.M., *et al*., *Architecture and secondary structure of an entire HIV-1 RNA genome.* Nature, 2009. **460**(7256): p. 711-6.
41. Rein, A., *RNA Packaging in HIV.* Trends Microbiol, 2019. **27**(8): p. 715-723.
42. Manavi, K., *A review on infection with human immunodeficiency virus.* Best Pract Res Clin Obstet Gynaecol, 2006. **20**(6): p. 923-40.
43. Tekeste, S.S., *et al*., *Interaction between Reverse Transcriptase and Integrase Is Required for Reverse Transcription during HIV-1 Replication.* J Virol, 2015. **89**(23): p. 12058-69.
44. Dwivedi, R., *et al*., *HIV-1 capsid and viral DNA integration.* mBio, 2024. **15**(1): p. e0021222.

45. Prabakaran, P., *et al*., *Structure and function of the HIV envelope glycoprotein as entry mediator, vaccine immunogen, and target for inhibitors.* Adv Pharmacol, 2007. **55**: p. 33-97.
46. Gramberg, T., N. Sunseri, and N.R. Landau, *Accessories to the crime: recent advances in HIV accessory protein biology.* Curr HIV/AIDS Rep, 2009. **6**(1): p. 36-42.
47. Rose, K.M., *et al*., *The viral infectivity factor (Vif) of HIV-1 unveiled.* Trends Mol Med, 2004. **10**(6): p. 291-7.
48. Popov, S., *et al*., *Viral protein R regulates nuclear import of the HIV-1 pre-integration complex.* EMBO J, 1998. **17**(4): p. 909-17.
49. Khan, N. and J.D. Geiger, *Role of Viral Protein U (Vpu) in HIV-1 Infection and Pathogenesis.* Viruses, 2021. **13**(8).
50. Neil, S.J., T. Zang, and P.D. Bieniasz, *Tetherin inhibits retrovirus release and is antagonized by HIV-1 Vpu.* Nature, 2008. **451**(7177): p. 425-30.
51. Jabbar, M.A. and D.P. Nayak, *Intracellular interaction of human immunodeficiency virus type 1 (ARV-2) envelope glycoprotein gp160 with CD4 blocks the movement and maturation of CD4 to the plasma membrane.* J Virol, 1990. **64**(12): p. 6297-304.
52. Willey, R.L., *et al*., *Human immunodeficiency virus type 1 Vpu protein induces rapid degradation of CD4.* J Virol, 1992. **66**(12): p. 7193-200.
53. Magadan, J.G., *et al*., *Multilayered mechanism of CD4 downregulation by HIV-1 Vpu involving distinct ER retention and ERAD targeting steps.* PLoS Pathog, 2010. **6**(4): p. e1000869.
54. Garcia, J.V. and A.D. Miller, *Serine phosphorylation-independent downregulation of cell-surface CD4 by nef.* Nature, 1991. **350**(6318): p. 508-11.
55. Stove, V., *et al*., *Human immunodeficiency virus Nef induces rapid internalization of the T-cell coreceptor CD8alphabeta.* J Virol, 2005. **79**(17): p. 11422-33.
56. Swigut, T., N. Shohdy, and J. Skowronski, *Mechanism for down-regulation of CD28 by Nef.* EMBO J, 2001. **20**(7): p. 1593-604.
57. Schwartz, O., *et al*., *Endocytosis of major histocompatibility complex class I molecules is induced by the HIV-1 Nef protein.* Nat Med, 1996. **2**(3): p. 338-42.
58. Schindler, M., *et al*., *Down-modulation of mature major histocompatibility complex class II and up-regulation of invariant chain cell surface expression are well-conserved functions of human and simian immunodeficiency virus nef alleles.* J Virol, 2003. **77**(19): p. 10548-56.
59. Geyer, M., O.T. Fackler, and B.M. Peterlin, *Structure--function relationships in HIV-1 Nef.* EMBO Rep, 2001. **2**(7): p. 580-5.
60. Li, L., *et al*., *Roles of HIV-1 auxiliary proteins in viral pathogenesis and host-pathogen interactions.* Cell Res, 2005. **15**(11-12): p. 923-34.
61. Zheng, Y.H., *et al*., *Nef increases the synthesis of and transports cholesterol to lipid rafts and HIV-1 progeny virions.* Proc Natl Acad Sci U S A, 2003. **100**(14): p. 8460-5.
62. Berkhout, B., R.H. Silverman, and K.T. Jeang, *Tat trans-activates the human immunodeficiency virus through a nascent RNA target.* Cell, 1989. **59**(2): p. 273-82.
63. Zhou, Q. and P.A. Sharp, *Novel mechanism and factor for regulation by HIV-1 Tat.* EMBO J, 1995. **14**(2): p. 321-8.
64. Truman, C.T., *et al*., *HIV Rev-isited.* Open Biol, 2020. **10**(12): p. 200320.
65. Coyle, J.H., *et al*., *The Tpr protein regulates export of mRNAs with retained introns that traffic through the Nxf1 pathway.* RNA, 2011. **17**(7): p. 1344-56.
66. Katahira, J., *Nuclear export of messenger RNA.* Genes (Basel), 2015. **6**(2): p. 163-84.
67. Purcell, D.F. and M.A. Martin, *Alternative splicing of human immunodeficiency virus type 1 mRNA modulates viral protein expression, replication, and infectivity.* J Virol, 1993. **67**(11): p. 6365-78.
68. Henderson, B.R. and P. Percipalle, *Interactions between HIV Rev and nuclear import and export factors: the Rev nuclear localisation signal mediates specific binding to human importin-beta.* J Mol Biol, 1997. **274**(5): p. 693-707.

69. Malim, M.H., *et al*., *HIV-1 structural gene expression requires binding of the Rev trans-activator to its RNA target sequence.* Cell, 1990. **60**(4): p. 675-83.
70. Pereira, L.A., *et al*., *A compilation of cellular transcription factor interactions with the HIV-1 LTR promoter.* Nucleic Acids Res, 2000. **28**(3): p. 663-8.
71. Gaynor, R., *Cellular transcription factors involved in the regulation of HIV-1 gene expression.* AIDS, 1992. **6**(4): p. 347-63.
72. Fred C. Krebs, T.H.H., Shane Quiterio, Suzanne Gartner, and Brian Wigdahl. *Lentiviral LTR-directed Expression, Sequence Variation, and Disease Pathogenesis*. 2001; Available from: https://www.hiv.lanl.gov/content/sequence/HIV/COMPENDIUM/2001/partI/Wigdahl.pdf#:~:text=LTR%20function%20has%20a%20direct%20impact%20on%20%28i%29,the%20peripheral%20circulation%2C%20lymphatic%20system%2C%20brain%2C%20and%20lungs.
73. Masenga, S.K., *et al*., *HIV-Host Cell Interactions.* Cells, 2023. **12**(10).
74. Xiao, T., Y. Cai, and B. Chen, *HIV-1 Entry and Membrane Fusion Inhibitors.* Viruses, 2021. **13**(5).
75. Hu, W.S. and S.H. Hughes, *HIV-1 reverse transcription.* Cold Spring Harb Perspect Med, 2012. **2**(10).
76. Craigie, R. and F.D. Bushman, *HIV DNA integration.* Cold Spring Harb Perspect Med, 2012. **2**(7): p. a006890.
77. Campbell, E.M. and T.J. Hope, *HIV-1 capsid: the multifaceted key player in HIV-1 infection.* Nat Rev Microbiol, 2015. **13**(8): p. 471-83.
78. Peng, K., *et al*., *Quantitative microscopy of functional HIV post-entry complexes reveals association of replication with the viral capsid.* Elife, 2014. **3**: p. e04114.
79. Koh, Y., *et al*., *Differential effects of human immunodeficiency virus type 1 capsid and cellular factors nucleoporin 153 and LEDGF/p75 on the efficiency and specificity of viral DNA integration.* J Virol, 2013. **87**(1): p. 648-58.
80. Francis, A.C. and G.B. Melikyan, *Single HIV-1 Imaging Reveals Progression of Infection through CA-Dependent Steps of Docking at the Nuclear Pore, Uncoating, and Nuclear Transport.* Cell Host Microbe, 2018. **23**(4): p. 536-548 e6.
81. Rozera, G., *et al*., *Intact provirus and integration sites analysis in acute HIV-1 infection and changes after one year of early antiviral therapy.* J Virus Erad, 2022. **8**(4): p. 100306.
82. Ott, M., M. Geyer, and Q. Zhou, *The control of HIV transcription: keeping RNA polymerase II on track.* Cell Host Microbe, 2011. **10**(5): p. 426-35.
83. Karn, J. and C.M. Stoltzfus, *Transcriptional and posttranscriptional regulation of HIV-1 gene expression.* Cold Spring Harb Perspect Med, 2012. **2**(2): p. a006916.
84. Ramdas, P., *et al*., *From Entry to Egress: Strategic Exploitation of the Cellular Processes by HIV-1.* Front Microbiol, 2020. **11**: p. 559792.
85. Berkowitz, R.D., *et al*., *Retroviral nucleocapsid domains mediate the specific recognition of genomic viral RNAs by chimeric Gag polyproteins during RNA packaging in vivo.* J Virol, 1995. **69**(10): p. 6445-56.
86. Kuzembayeva, M., *et al*., *Life of psi: how full-length HIV-1 RNAs become packaged genomes in the viral particles.* Virology, 2014. **454-455**: p. 362-70.
87. Nikolaitchik, O.A., *et al*., *Dimeric RNA recognition regulates HIV-1 genome packaging.* PLoS Pathog, 2013. **9**(3): p. e1003249.
88. Cochrane, A.W., M.T. McNally, and A.J. Mouland, *The retrovirus RNA trafficking granule: from birth to maturity.* Retrovirology, 2006. **3**: p. 18.
89. Engelman, A. and P. Cherepanov, *The structural biology of HIV-1: mechanistic and therapeutic insights.* Nat Rev Microbiol, 2012. **10**(4): p. 279-90.
90. Guha, D. and V. Ayyavoo, *Innate immune evasion strategies by human immunodeficiency virus type 1.* ISRN AIDS, 2013. **2013**: p. 954806.

91. O'Neil, P.K., *et al*., *Mutational analysis of HIV-1 long terminal repeats to explore the relative contribution of reverse transcriptase and RNA polymerase II to viral mutagenesis.* J Biol Chem, 2002. **277**(41): p. 38053-61.
92. Lu, L., *et al*., *Tactics used by HIV-1 to evade host innate, adaptive, and intrinsic immunities.* Chin Med J (Engl), 2013. **126**(12): p. 2374-9.
93. Peterlin, B.M. and D. Trono, *Hide, shield and strike back: how HIV-infected cells avoid immune eradication.* Nat Rev Immunol, 2003. **3**(2): p. 97-107.
94. Lane, H.C., *et al*., *Abnormalities of B-cell activation and immunoregulation in patients with the acquired immunodeficiency syndrome.* N Engl J Med, 1983. **309**(8): p. 453-8.
95. Shirai, A., *et al*., *Human immunodeficiency virus infection induces both polyclonal and virus-specific B cell activation.* J Clin Invest, 1992. **89**(2): p. 561-6.
96. Martinez-Maza, O. and E.C. Breen, *B-cell activation and lymphoma in patients with HIV.* Curr Opin Oncol, 2002. **14**(5): p. 528-32.
97. Moir, S., *et al*., *Evidence for HIV-associated B cell exhaustion in a dysfunctional memory B cell compartment in HIV-infected viremic individuals.* J Exp Med, 2008. **205**(8): p. 1797-805.
98. Cagigi, A., *et al*., *B cell immunopathology during HIV-1 infection: lessons to learn for HIV-1 vaccine design.* Vaccine, 2008. **26**(24): p. 3016-25.
99. Vidya Vijayan, K.K., *et al*., *Pathophysiology of CD4+ T-Cell Depletion in HIV-1 and HIV-2 Infections.* Front Immunol, 2017. **8**: p. 580.
100. Brenchley, J.M., *et al*., *CD4+ T cell depletion during all stages of HIV disease occurs predominantly in the gastrointestinal tract.* J Exp Med, 2004. **200**(6): p. 749-59.
101. Brooks, D.G., *et al*., *Intrinsic functional dysregulation of CD4 T cells occurs rapidly following persistent viral infection.* J Virol, 2005. **79**(16): p. 10514-27.
102. Chun, T.W., *et al*., *Early establishment of a pool of latently infected, resting CD4(+) T cells during primary HIV-1 infection.* Proc Natl Acad Sci U S A, 1998. **95**(15): p. 8869-73.
103. McCune, J.M., *The dynamics of CD4+ T-cell depletion in HIV disease.* Nature, 2001. **410**(6831): p. 974-9.
104. Doitsh, G., *et al*., *Abortive HIV infection mediates CD4 T cell depletion and inflammation in human lymphoid tissue.* Cell, 2010. **143**(5): p. 789-801.
105. Doitsh, G., *et al*., *Cell death by pyroptosis drives CD4 T-cell depletion in HIV-1 infection.* Nature, 2014. **505**(7484): p. 509-14.
106. Fevrier, M., K. Dorgham, and A. Rebollo, *CD4+ T cell depletion in human immunodeficiency virus (HIV) infection: role of apoptosis.* Viruses, 2011. **3**(5): p. 586-612.
107. Cossarizza, A., *Apoptosis and HIV infection: about molecules and genes.* Curr Pharm Des, 2008. **14**(3): p. 237-44.
108. Gonzalez, S.M., *et al*., *Mucosa: Key Interactions Determining Sexual Transmission of the HIV Infection.* Front Immunol, 2019. **10**: p. 144.
109. Kawamura, T., *et al*., *The role of Langerhans cells in the sexual transmission of HIV.* J Dermatol Sci, 2005. **40**(3): p. 147-55.
110. Cohen, O.J. and A.S. Fauci, *Host factors that affect sexual transmission of HIV.* Int J Infect Dis, 1998. **2**(4): p. 182-5.
111. Huang, Y., *et al*., *The role of a mutant CCR5 allele in HIV-1 transmission and disease progression.* Nat Med, 1996. **2**(11): p. 1240-3.
112. Szabo, R. and R.V. Short, *How does male circumcision protect against HIV infection?* BMJ, 2000. **320**(7249): p. 1592-4.
113. Konrad, B.P., *et al*., *On the duration of the period between exposure to HIV and detectable infection.* Epidemics, 2017. **20**: p. 73-83.
114. Geijtenbeek, T.B., *et al*., *DC-SIGN, a dendritic cell-specific HIV-1-binding protein that enhances trans-infection of T cells.* Cell, 2000. **100**(5): p. 587-97.

115. McMichael, A.J., *et al*., *The immune response during acute HIV-1 infection: clues for vaccine development.* Nat Rev Immunol, 2010. **10**(1): p. 11-23.
116. Schacker, T.W., *et al*., *Biological and virologic characteristics of primary HIV infection.* Ann Intern Med, 1998. **128**(8): p. 613-20.
117. Price, D.A., *et al*., *Positive selection of HIV-1 cytotoxic T lymphocyte escape variants during primary infection.* Proc Natl Acad Sci U S A, 1997. **94**(5): p. 1890-5.
118. Andrew McMichael, L.D., *The immune response to HIV.* Medicine, 2009. **Volume 37**(Issue 7).
119. Mellors, J.W., *et al*., *Prognosis in HIV-1 infection predicted by the quantity of virus in plasma.* Science, 1996. **272**(5265): p. 1167-70.
120. Rustagi, A. and M. Gale, Jr., *Innate antiviral immune signaling, viral evasion and modulation by HIV-1.* J Mol Biol, 2014. **426**(6): p. 1161-77.
121. Cologne, G.I.f.Q.a.E.i.H.C.I. *In brief: The innate and adaptive immune systems*. 2023; Available from: https://www.ncbi.nlm.nih.gov/books/NBK279396/.
122. Freed, E.O. and M. Gale, Jr., *Antiviral innate immunity: editorial overview.* J Mol Biol, 2014. **426**(6): p. 1129-32.
123. Loo, Y.M. and M. Gale, Jr., *Viral regulation and evasion of the host response.* Curr Top Microbiol Immunol, 2007. **316**: p. 295-313.
124. Martin-Moreno, A. and M.A. Munoz-Fernandez, *Dendritic Cells, the Double Agent in the War Against HIV-1.* Front Immunol, 2019. **10**: p. 2485.
125. Worbs, T., S.I. Hammerschmidt, and R. Forster, *Dendritic cell migration in health and disease.* Nat Rev Immunol, 2017. **17**(1): p. 30-48.
126. Ugur, M. and S.N. Mueller, *T cell and dendritic cell interactions in lymphoid organs: More than just being in the right place at the right time.* Immunol Rev, 2019. **289**(1): p. 115-128.
127. Manches, O., D. Frleta, and N. Bhardwaj, *Dendritic cells in progression and pathology of HIV infection.* Trends Immunol, 2014. **35**(3): p. 114-22.
128. Sabado, R.L., *et al*., *Evidence of dysregulation of dendritic cells in primary HIV infection.* Blood, 2010. **116**(19): p. 3839-52.
129. Villadangos, J.A. and L. Young, *Antigen-presentation properties of plasmacytoid dendritic cells.* Immunity, 2008. **29**(3): p. 352-61.
130. Secchi, M., *et al*., *Combination of the CCL5-derived peptide R4.0 with different HIV-1 blockers reveals wide target compatibility and synergic cobinding to CCR5.* Antimicrob Agents Chemother, 2014. **58**(10): p. 6215-23.
131. Manches, O., *et al*., *HIV-activated human plasmacytoid DCs induce Tregs through an indoleamine 2,3-dioxygenase-dependent mechanism.* J Clin Invest, 2008. **118**(10): p. 3431-9.
132. Kruize, Z. and N.A. Kootstra, *The Role of Macrophages in HIV-1 Persistence and Pathogenesis.* Front Microbiol, 2019. **10**: p. 2828.
133. Woottum, M., *et al*., *Macrophages: Key Cellular Players in HIV Infection and Pathogenesis.* Viruses, 2024. **16**(2).
134. Igarashi, T., *et al*., *Macrophage are the principal reservoir and sustain high virus loads in rhesus macaques after the depletion of CD4+ T cells by a highly pathogenic simian immunodeficiency virus/HIV type 1 chimera (SHIV): Implications for HIV-1 infections of humans.* Proc Natl Acad Sci U S A, 2001. **98**(2): p. 658-63.
135. Hendricks, C.M., *et al*., *The Interplay of HIV-1 and Macrophages in Viral Persistence.* Front Microbiol, 2021. **12**: p. 646447.
136. Kanitakis, J., P. Petruzzo, and J.M. Dubernard, *Turnover of epidermal Langerhans' cells.* N Engl J Med, 2004. **351**(25): p. 2661-2.
137. Zhang, L. and M.B. Bansal, *Role of Kupffer Cells in Driving Hepatic Inflammation and Fibrosis in HIV Infection.* Front Immunol, 2020. **11**: p. 1086.

138. Cribbs, S.K., K. Crothers, and A. Morris, *Pathogenesis of HIV-Related Lung Disease: Immunity, Infection, and Inflammation.* Physiol Rev, 2020. **100**(2): p. 603-632.
139. Prager, I. and C. Watzl, *Mechanisms of natural killer cell-mediated cellular cytotoxicity.* J Leukoc Biol, 2019. **105**(6): p. 1319-1329.
140. Jiang, Y., *et al*., *KIR3DS1/L1 and HLA-Bw4-80I are associated with HIV disease progression among HIV typical progressors and long-term nonprogressors.* BMC Infect Dis, 2013. **13**: p. 405.
141. Cohen, G.B., *et al*., *The selective downregulation of class I major histocompatibility complex proteins by HIV-1 protects HIV-infected cells from NK cells.* Immunity, 1999. **10**(6): p. 661-71.
142. Haynes, B.F., *et al*., *Immune-correlates analysis of an HIV-1 vaccine efficacy trial.* N Engl J Med, 2012. **366**(14): p. 1275-86.
143. Lam, N., Y. Lee, and D.L. Farber, *A guide to adaptive immune memory.* Nat Rev Immunol, 2024. **24**(11): p. 810-829.
144. Bonilla, F.A. and H.C. Oettgen, *Adaptive immunity.* J Allergy Clin Immunol, 2010. **125**(2 Suppl 2): p. S33-40.
145. Scott N. Mueller, B.T.R., *Immune responses to viruses.* Clinical Immunology (Third Edition), 2008: p. 421-431.
146. Hoffman, W., F.G. Lakkis, and G. Chalasani, *B Cells, Antibodies, and More.* Clin J Am Soc Nephrol, 2016. **11**(1): p. 137-54.
147. Nutt, S.L., *et al*., *The generation of antibody-secreting plasma cells.* Nat Rev Immunol, 2015. **15**(3): p. 160-71.
148. Basu, R. and M. Huse, *Mechanical Communication at the Immunological Synapse.* Trends Cell Biol, 2017. **27**(4): p. 241-254.
149. Roche, P.A. and K. Furuta, *The ins and outs of MHC class II-mediated antigen processing and presentation.* Nat Rev Immunol, 2015. **15**(4): p. 203-16.
150. Mak, T.W., *et al*., *Costimulation through the inducible costimulator ligand is essential for both T helper and B cell functions in T cell-dependent B cell responses.* Nat Immunol, 2003. **4**(8): p. 765-72.
151. Chalasani, G. and D. Rothstein, *Non-Antibody Mediated Roles of B Cells in Allograft Survival.* Current Transplantation Reports, 2014. **1**(3): p. 155-165.
152. Murin, C.D., I.A. Wilson, and A.B. Ward, *Antibody responses to viral infections: a structural perspective across three different enveloped viruses.* Nat Microbiol, 2019. **4**(5): p. 734-747.
153. Burton, D.R., *Antiviral neutralizing antibodies: from in vitro to in vivo activity.* Nat Rev Immunol, 2023. **23**(11): p. 720-734.
154. Burton, D.R., *Antibodies, viruses and vaccines.* Nat Rev Immunol, 2002. **2**(9): p. 706-13.
155. Johnson, W.E. and R.C. Desrosiers, *Viral persistence: HIV's strategies of immune system evasion.* Annu Rev Med, 2002. **53**: p. 499-518.
156. Koch, M., *et al*., *Structure-based, targeted deglycosylation of HIV-1 gp120 and effects on neutralization sensitivity and antibody recognition.* Virology, 2003. **313**(2): p. 387-400.
157. Burton, D.R., *et al*., *Broadly neutralizing antibodies present new prospects to counter highly antigenically diverse viruses.* Science, 2012. **337**(6091): p. 183-6.
158. Burton, D.R. and L. Hangartner, *Broadly Neutralizing Antibodies to HIV and Their Role in Vaccine Design.* Annu Rev Immunol, 2016. **34**: p. 635-59.
159. Swain, S.L., K.K. McKinstry, and T.M. Strutt, *Expanding roles for CD4(+) T cells in immunity to viruses.* Nat Rev Immunol, 2012. **12**(2): p. 136-48.
160. Crotty, S., *T follicular helper cell differentiation, function, and roles in disease.* Immunity, 2014. **41**(4): p. 529-42.

161. Locci, M., *et al*., *Human circulating PD-1+CXCR3-CXCR5+ memory Tfh cells are highly functional and correlate with broadly neutralizing HIV antibody responses.* Immunity, 2013. **39**(4): p. 758-69.
162. Kervevan, J. and L.A. Chakrabarti, *Role of CD4+ T Cells in the Control of Viral Infections: Recent Advances and Open Questions.* Int J Mol Sci, 2021. **22**(2).
163. Vetter, M.L. and R.T. D'Aquila, *Cytoplasmic APOBEC3G restricts incoming Vif-positive human immunodeficiency virus type 1 and increases two-long terminal repeat circle formation in activated T-helper-subtype cells.* J Virol, 2009. **83**(17): p. 8646-54.
164. Vingert, B., *et al*., *HIV controllers maintain a population of highly efficient Th1 effector cells in contrast to patients treated in the long term.* J Virol, 2012. **86**(19): p. 10661-74.
165. McKinstry, K.K., *et al*., *Memory CD4+ T cells protect against influenza through multiple synergizing mechanisms.* J Clin Invest, 2012. **122**(8): p. 2847-56.
166. Soghoian, D.Z., *et al*., *HIV-specific cytolytic CD4 T cell responses during acute HIV infection predict disease outcome.* Sci Transl Med, 2012. **4**(123): p. 123ra25.
167. Phetsouphanh, C., *et al*., *Maintenance of Functional CD57+ Cytolytic CD4+ T Cells in HIV+ Elite Controllers.* Front Immunol, 2019. **10**: p. 1844.
168. Koh, C.H., *et al*., *CD8 T-cell subsets: heterogeneity, functions, and therapeutic potential.* Exp Mol Med, 2023. **55**(11): p. 2287-2299.
169. Wherry, E.J. and R. Ahmed, *Memory CD8 T-cell differentiation during viral infection.* J Virol, 2004. **78**(11): p. 5535-45.
170. Walker, B. and A. McMichael, *The T-cell response to HIV.* Cold Spring Harb Perspect Med, 2012. **2**(11).
171. Goonetilleke, N., *et al*., *The first T cell response to transmitted/founder virus contributes to the control of acute viremia in HIV-1 infection.* J Exp Med, 2009. **206**(6): p. 1253-72.
172. Collins, D.R., G.D. Gaiha, and B.D. Walker, *CD8(+) T cells in HIV control, cure and prevention.* Nat Rev Immunol, 2020. **20**(8): p. 471-482.
173. Frucht, D.M., *et al*., *IFN-gamma production by antigen-presenting cells: mechanisms emerge.* Trends Immunol, 2001. **22**(10): p. 556-60.
174. Harris, D.P., *et al*., *Regulation of IFN-gamma production by B effector 1 cells: essential roles for T-bet and the IFN-gamma receptor.* J Immunol, 2005. **174**(11): p. 6781-90.
175. Roff, S.R., E.N. Noon-Song, and J.K. Yamamoto, *The Significance of Interferon-gamma in HIV-1 Pathogenesis, Therapy, and Prophylaxis.* Front Immunol, 2014. **4**: p. 498.
176. Koirala, J., *et al*., *Interferon-gamma receptors in HIV-1 infection.* AIDS Res Hum Retroviruses, 2008. **24**(8): p. 1097-102.
177. Lane, B.R., *et al*., *TNF-alpha inhibits HIV-1 replication in peripheral blood monocytes and alveolar macrophages by inducing the production of RANTES and decreasing C-C chemokine receptor 5 (CCR5) expression.* J Immunol, 1999. **163**(7): p. 3653-61.
178. Kedzierska, K. and S.M. Crowe, *Cytokines and HIV-1: interactions and clinical implications.* Antivir Chem Chemother, 2001. **12**(3): p. 133-50.
179. Betts, M.R., *et al*., *HIV nonprogressors preferentially maintain highly functional HIV-specific CD8+ T cells.* Blood, 2006. **107**(12): p. 4781-9.
180. Kiepiela, P., *et al*., *CD8+ T-cell responses to different HIV proteins have discordant associations with viral load.* Nat Med, 2007. **13**(1): p. 46-53.
181. Deng, K., *et al*., *Broad CTL response is required to clear latent HIV-1 due to dominance of escape mutations.* Nature, 2015. **517**(7534): p. 381-5.
182. Perdiguero, B., *et al*., *Induction of Broad and Polyfunctional HIV-1-Specific T Cell Responses by the Multiepitopic Protein TMEP-B Vectored by MVA Virus.* Vaccines (Basel), 2019. **7**(3).
183. Ryan, S.O. and B.A. Cobb, *Roles for major histocompatibility complex glycosylation in immune function.* Semin Immunopathol, 2012. **34**(3): p. 425-41.

184. Campbell, E.C., A.N. Antoniou, and S.J. Powis, *The multi-faceted nature of HLA class I dimer molecules.* Immunology, 2012. **136**(4): p. 380-4.
185. Zhang, Y., E. Baig, and D.B. Williams, *Functions of ERp57 in the folding and assembly of major histocompatibility complex class I molecules.* J Biol Chem, 2006. **281**(21): p. 14622-31.
186. Paquet, M.E., *et al*., *Bap29/31 influences the intracellular traffic of MHC class I molecules.* J Immunol, 2004. **172**(12): p. 7548-55.
187. Androlewicz, M.J. and P. Cresswell, *How selective is the transporter associated with antigen processing?* Immunity, 1996. **5**(1): p. 1-5.
188. Josephs, T.M., E.J. Grant, and S. Gras, *Molecular challenges imposed by MHC-I restricted long epitopes on T cell immunity.* Biol Chem, 2017. **398**(9): p. 1027-1036.
189. Olson, E., J. Geng, and M. Raghavan, *Polymorphisms of HLA-B: influences on assembly and immunity.* Curr Opin Immunol, 2020. **64**: p. 137-145.
190. Rajapaksa, U.S., *et al*., *HLA-B may be more protective against HIV-1 than HLA-A because it resists negative regulatory factor (Nef) mediated down-regulation.* Proc Natl Acad Sci U S A, 2012. **109**(33): p. 13353-8.
191. Carrington, M., *et al*., *HLA and HIV-1: heterozygote advantage and B*35-Cw*04 disadvantage.* Science, 1999. **283**(5408): p. 1748-52.
192. Goulder, P.J. and B.D. Walker, *HIV and HLA class I: an evolving relationship.* Immunity, 2012. **37**(3): p. 426-40.
193. Goulder, P.J. and D.I. Watkins, *Impact of MHC class I diversity on immune control of immunodeficiency virus replication.* Nat Rev Immunol, 2008. **8**(8): p. 619-30.
194. Leslie, A., *et al*., *Differential selection pressure exerted on HIV by CTL targeting identical epitopes but restricted by distinct HLA alleles from the same HLA supertype.* J Immunol, 2006. **177**(7): p. 4699-708.
195. Neefjes, J., *et al*., *Towards a systems understanding of MHC class I and MHC class II antigen presentation.* Nat Rev Immunol, 2011. **11**(12): p. 823-36.
196. Reith, W. and B. Mach, *The bare lymphocyte syndrome and the regulation of MHC expression.* Annu Rev Immunol, 2001. **19**: p. 331-73.
197. Sarri, C.A., *et al*., *HLA class II peptide-binding-region analysis reveals funneling of polymorphism in action.* Immunol Lett, 2021. **238**: p. 75-95.
198. Ferre, A.L., *et al*., *HIV controllers with HLA-DRB1*13 and HLA-DQB1*06 alleles have strong, polyfunctional mucosal CD4+ T-cell responses.* J Virol, 2010. **84**(21): p. 11020-9.
199. Borghans, J.A., *et al*., *HLA alleles associated with slow progression to AIDS truly prefer to present HIV-1 p24.* PLoS One, 2007. **2**(9): p. e920.
200. Brumme, Z.L., *et al*., *Marked Epitope- and Allele-Specific Differences in Rates of Mutation in Human Immunodeficiency Type 1 (HIV-1) Gag, Pol, and Nef Cytotoxic T-Lymphocyte Epitopes in Acute/Early HIV-1 Infection.* Journal of Virology, 2008. **82**(18): p. 9216-9227.
201. Gorin, A.M., *et al*., *HIV-1 epitopes presented by MHC class I types associated with superior immune containment of viremia have highly constrained fitness landscapes.* PLoS Pathog, 2017. **13**(8): p. e1006541.
202. Chen, W., *et al*., *Dissecting the multifactorial causes of immunodominance in class I-restricted T cell responses to viruses.* Immunity, 2000. **12**(1): p. 83-93.
203. Kloverpris, H., *et al*., *Induction of novel CD8+ T-cell responses during chronic untreated HIV-1 infection by immunization with subdominant cytotoxic T-lymphocyte epitopes.* AIDS, 2009. **23**(11): p. 1329-1340.
204. Frahm, N., *et al*., *Control of human immunodeficiency virus replication by cytotoxic T lymphocytes targeting subdominant epitopes.* Nat Immunol, 2006. **7**(2): p. 173-8.
205. Gallimore, A., *et al*., *Protective immunity does not correlate with the hierarchy of virus-specific cytotoxic T cell responses to naturally processed peptides.* J Exp Med, 1998. **187**(10): p. 1647-57.

206. Holtappels, R., *et al*., *Subdominant CD8 T-cell epitopes account for protection against cytomegalovirus independent of immunodomination.* J Virol, 2008. **82**(12): p. 5781-96.
207. Friedrich, T.C., *et al*., *Subdominant CD8⁺ T-Cell Responses Are Involved in Durable Control of AIDS Virus Replication.* Journal of Virology, 2007. **81**(7): p. 3465-3476.
208. Mothe, B., *et al*., *Therapeutic Vaccination Refocuses T-cell Responses Towards Conserved Regions of HIV-1 in Early Treated Individuals (BCN 01 study).* EClinicalMedicine, 2019. **11**: p. 65-80.
209. Fiore-Gartland, A., *et al*., *Pooled-Peptide Epitope Mapping Strategies Are Efficient and Highly Sensitive: An Evaluation of Methods for Identifying Human T Cell Epitope Specificities in Large-Scale HIV Vaccine Efficacy Trials.* PLoS One, 2016. **11**(2): p. e0147812.
210. Wang, L., *et al*., *Identification of virus epitopes and reactive T-cell receptors from memory T cells without peptide synthesis.* Communications Biology, 2024. **7**(1): p. 1432.
211. Schmittel, A., U. Keilholz, and C. Scheibenbogen, *Evaluation of the interferon-gamma ELISPOT-assay for quantification of peptide specific T lymphocytes from peripheral blood.* J Immunol Methods, 1997. **210**(2): p. 167-74.
212. Roider, J., *et al*., *Comparison of experimental fine-mapping to in silico prediction results of HIV-1 epitopes reveals ongoing need for mapping experiments.* Immunology, 2014. **143**(2): p. 193-201.
213. Klohe, E.P., *et al*., *Analysis of the molecular specificities of anti-class II monoclonal antibodies by using L cell transfectants expressing HLA class II molecules.* J Immunol, 1988. **141**(6): p. 2158-64.
214. Constantin, C.M., *et al*., *Major histocompatibility complex (MHC) tetramer technology: an evaluation.* Biol Res Nurs, 2002. **4**(2): p. 115-27.
215. Hamidinia, M., *et al*., *Occlusion of TCR binding to HLA-A*11:01 by a non-pathogenic human alloantibody.* Cellular and Molecular Life Sciences, 2025. **82**(1): p. 94.
216. Borthwick, N., *et al*., *Novel, in-natural-infection subdominant HIV-1 CD8+ T-cell epitopes revealed in human recipients of conserved-region T-cell vaccines.* PLoS One, 2017. **12**(4): p. e0176418.
217. Deeks, S.G., S.R. Lewin, and D.V. Havlir, *The end of AIDS: HIV infection as a chronic disease.* Lancet, 2013. **382**(9903): p. 1525-33.
218. Samji, H., *et al*., *Closing the gap: increases in life expectancy among treated HIV-positive individuals in the United States and Canada.* PLoS One, 2013. **8**(12): p. e81355.
219. Cohen, M.S., *et al*., *Prevention of HIV-1 infection with early antiretroviral therapy.* N Engl J Med, 2011. **365**(6): p. 493-505.
220. De Clercq, E. and G. Li, *Approved Antiviral Drugs over the Past 50 Years.* Clin Microbiol Rev, 2016. **29**(3): p. 695-747.
221. *Antiretroviral Clinical Guidelines*. 2024 2024 29.04.2025]; Available from: https://clinicalinfo.hiv.gov/en/guidelines/hiv-clinical-guidelines-adult-and-adolescent-arv/what-start-initial-combination.
222. Markham, A., *Ibalizumab: First Global Approval.* Drugs, 2018. **78**(7): p. 781-785.
223. Chahine, E.B. and S.H. Durham, *Ibalizumab: The First Monoclonal Antibody for the Treatment of HIV-1 Infection.* Ann Pharmacother, 2021. **55**(2): p. 230-239.
224. Ramgopal, M.N., *et al*., *Efficacy, safety, and tolerability of switching to long-acting cabotegravir plus rilpivirine versus continuing fixed-dose bictegravir, emtricitabine, and tenofovir alafenamide in virologically suppressed adults with HIV, 12-month results (SOLAR): a randomised, open-label, phase 3b, non-inferiority trial.* Lancet HIV, 2023. **10**(9): p. e566-e577.
225. Ford, S.L., *et al*., *Thigh Injections of Cabotegravir + Rilpivirine in Virally Suppressed Adults With Human Immunodeficiency Virus Type 1: A Substudy of the Phase 3b ATLAS-2M Study.* Clin Infect Dis, 2025.

226. McKellar, M.S., *Lenacapavir: a first-in-class capsid inhibitor for HIV treatment and prevention.* Curr Opin Infect Dis, 2025. **38**(3): p. 208-213.
227. Cohen, J., *The long shot.* Science, 2024. **386**(6727): p. 1208-1209.
228. Bekker, L.G., *et al*., *Twice-Yearly Lenacapavir or Daily F/TAF for HIV Prevention in Cisgender Women.* N Engl J Med, 2024. **391**(13): p. 1179-1192.
229. Kelley, C.F., *et al*., *Twice-Yearly Lenacapavir for HIV Prevention in Men and Gender-Diverse Persons.* N Engl J Med, 2025. **392**(13): p. 1261-1276.
230. Segal-Maurer, S., *et al*., *Capsid Inhibition with Lenacapavir in Multidrug-Resistant HIV-1 Infection.* N Engl J Med, 2022. **386**(19): p. 1793-1803.
231. Ogbuagu, O., *et al*., *Efficacy and safety of the novel capsid inhibitor lenacapavir to treat multidrug-resistant HIV: week 52 results of a phase 2/3 trial.* Lancet HIV, 2023. **10**(8): p. e497-e505.
232. Gupta, S.K., *et al*., *Lenacapavir administered every 26 weeks or daily in combination with oral daily antiretroviral therapy for initial treatment of HIV: a randomised, open-label, active-controlled, phase 2 trial.* Lancet HIV, 2023. **10**(1): p. e15-e23.
233. Temereanca, A. and S. Ruta, *Strategies to overcome HIV drug resistance-current and future perspectives.* Front Microbiol, 2023. **14**: p. 1133407.
234. Gakhar, H., A. Kamali, and M. Holodniy, *Health-related quality of life assessment after antiretroviral therapy: a review of the literature.* Drugs, 2013. **73**(7): p. 651-72.
235. Carr, A. and D.A. Cooper, *Adverse effects of antiretroviral therapy.* Lancet, 2000. **356**(9239): p. 1423-30.
236. Kalra, D.K., *et al*., *Dyslipidemia in Human Immunodeficiency Virus Disease: JACC Review Topic of the Week.* J Am Coll Cardiol, 2023. **82**(2): p. 171-181.
237. Feinstein, M.J., *et al*., *Patterns of Cardiovascular Mortality for HIV-Infected Adults in the United States: 1999 to 2013.* Am J Cardiol, 2016. **117**(2): p. 214-20.
238. Hong, F.F. and J.W. Mellors, *Changes in HIV reservoirs during long-term antiretroviral therapy.* Curr Opin HIV AIDS, 2015. **10**(1): p. 43-8.
239. Bartlett, J.A. and J.F. Shao, *Successes, challenges, and limitations of current antiretroviral therapy in low-income and middle-income countries.* Lancet Infect Dis, 2009. **9**(10): p. 637-49.
240. Kalichman, S.C., *et al*., *Adherence to antiretroviral therapy and HIV transmission risks: implications for test-and-treat approaches to HIV prevention.* AIDS Patient Care STDS, 2010. **24**(5): p. 271-7.
241. Fauci, A.S., G.K. Folkers, and H.D. Marston, *Ending the global HIV/AIDS pandemic: the critical role of an HIV vaccine.* Clin Infect Dis, 2014. **59 Suppl 2**(Suppl 2): p. S80-4.
242. Corey, L., *et al*., *Two Randomized Trials of Neutralizing Antibodies to Prevent HIV-1 Acquisition.* N Engl J Med, 2021. **384**(11): p. 1003-1014.
243. Fauci, A.S., *25 years of HIV.* Nature, 2008. **453**(7193): p. 289-90.
244. Barouch, D.H., *Challenges in the development of an HIV-1 vaccine.* Nature, 2008. **455**(7213): p. 613-9.
245. Hatziioannou, T. and D.T. Evans, *Animal models for HIV/AIDS research.* Nat Rev Microbiol, 2012. **10**(12): p. 852-67.
246. Victor Garcia, J., *Humanized mice for HIV and AIDS research.* Curr Opin Virol, 2016. **19**: p. 56-64.
247. Van Rompay, K.K., *Evaluation of antiretrovirals in animal models of HIV infection.* Antiviral Res, 2010. **85**(1): p. 159-75.
248. Hessell, A.J. and N.L. Haigwood, *Animal models in HIV-1 protection and therapy.* Curr Opin HIV AIDS, 2015. **10**(3): p. 170-6.
249. De Cock, K.M., H.W. Jaffe, and J.W. Curran, *Reflections on 40 Years of AIDS.* Emerg Infect Dis, 2021. **27**(6): p. 1553-1560.

250. Bbosa, N., P. Kaleebu, and D. Ssemwanga, *HIV subtype diversity worldwide.* Curr Opin HIV AIDS, 2019. **14**(3): p. 153-160.
251. Rashid, A., *et al*., *HIV-1 genetic diversity a challenge for AIDS vaccine development: a retrospective bibliometric analysis.* Hum Vaccin Immunother, 2022. **18**(1): p. 2014733.
252. Hemelaar, J., *et al*., *Global and regional molecular epidemiology of HIV-1, 1990-2015: a systematic review, global survey, and trend analysis.* Lancet Infect Dis, 2019. **19**(2): p. 143-155.
253. Buonaguro, L., M.L. Tornesello, and F.M. Buonaguro, *Human immunodeficiency virus type 1 subtype distribution in the worldwide epidemic: pathogenetic and therapeutic implications.* J Virol, 2007. **81**(19): p. 10209-19.
254. Nair, M., *et al*., *Global and regional genetic diversity of HIV-1 in 2010-21: systematic review and analysis of prevalence.* Lancet Microbe, 2024. **5**(11): p. 100912.
255. Robertson, D.L., *et al*., *HIV-1 nomenclature proposal.* Science, 2000. **288**(5463): p. 55-6.
256. Hemelaar, J., *et al*., *Country Level Diversity of the HIV-1 Pandemic between 1990 and 2015.* J Virol, 2020. **95**(2).
257. Plotkin, S.A., *Correlates of protection induced by vaccination.* Clin Vaccine Immunol, 2010. **17**(7): p. 1055-65.
258. Rerks-Ngarm, S., *et al*., *Vaccination with ALVAC and AIDSVAX to prevent HIV-1 infection in Thailand.* N Engl J Med, 2009. **361**(23): p. 2209-20.
259. Yates, N.L., *et al*., *Vaccine-induced Env V1-V2 IgG3 correlates with lower HIV-1 infection risk and declines soon after vaccination.* Sci Transl Med, 2014. **6**(228): p. 228ra39.
260. Lin, L., *et al*., *COMPASS identifies T-cell subsets correlated with clinical outcomes.* Nat Biotechnol, 2015. **33**(6): p. 610-6.
261. Tomaras, G.D. and S.A. Plotkin, *Complex immune correlates of protection in HIV-1 vaccine efficacy trials.* Immunol Rev, 2017. **275**(1): p. 245-261.
262. Lieberman, P.M., *Epigenetics and Genetics of Viral Latency.* Cell Host Microbe, 2016. **19**(5): p. 619-28.
263. Fidler, S., *et al*., *Antiretroviral therapy alone versus antiretroviral therapy with a kick and kill approach, on measures of the HIV reservoir in participants with recent HIV infection (the RIVER trial): a phase 2, randomised trial.* Lancet, 2020. **395**(10227): p. 888-898.
264. Saunders, K.O., R.S. Rudicell, and G.J. Nabel, *The design and evaluation of HIV-1 vaccines.* AIDS, 2012. **26**(10): p. 1293-302.
265. Harmon, T.M., *et al*., *Exploring the Potential Health Impact and Cost-Effectiveness of AIDS Vaccine within a Comprehensive HIV/AIDS Response in Low- and Middle-Income Countries.* PLoS One, 2016. **11**(1): p. e0146387.
266. Daniel, M.D., *et al*., *Protective effects of a live attenuated SIV vaccine with a deletion in the nef gene.* Science, 1992. **258**(5090): p. 1938-41.
267. Baba, T.W., *et al*., *Pathogenicity of live, attenuated SIV after mucosal infection of neonatal macaques.* Science, 1995. **267**(5205): p. 1820-5.
268. Murphey-Corb, M., *et al*., *A formalin-inactivated whole SIV vaccine confers protection in macaques.* Science, 1989. **246**(4935): p. 1293-7.
269. Flynn, N.M., *et al*., *Placebo-controlled phase 3 trial of a recombinant glycoprotein 120 vaccine to prevent HIV-1 infection.* J Infect Dis, 2005. **191**(5): p. 654-65.
270. *Clinical Trials*. Available from: https://clinicaltrials.gov/uk.
271. Ahmed, S. and A. Herschhorn, *Insights from HIV-1 vaccine and passive immunization efficacy trials.* Trends Mol Med, 2024. **30**(10): p. 908-912.
272. Plotkin, S.A., *Updates on immunologic correlates of vaccine-induced protection.* Vaccine, 2020. **38**(9): p. 2250-2257.
273. Haynes, B.F., *et al*., *Strategies for HIV-1 vaccines that induce broadly neutralizing antibodies.* Nat Rev Immunol, 2023. **23**(3): p. 142-158.

274. Gray, G.E., *et al*., *Vaccine Efficacy of ALVAC-HIV and Bivalent Subtype C gp120-MF59 in Adults.* N Engl J Med, 2021. **384**(12): p. 1089-1100.
275. Gray, G.E., *et al*., *Mosaic HIV-1 vaccine regimen in southern African women (Imbokodo/HVTN 705/HPX2008): a randomised, double-blind, placebo-controlled, phase 2b trial.* Lancet Infect Dis, 2024. **24**(11): p. 1201-1212.
276. Nkolola, J.P. and D.H. Barouch, *Prophylactic HIV-1 vaccine trials: past, present, and future.* Lancet HIV, 2024. **11**(2): p. e117-e124.
277. Violari, A., *et al*., *Safety and implementation of a phase 1 randomized GLA-SE-adjuvanted CH505TF gp120 HIV vaccine trial in newborns.* medRxiv, 2024.
278. Leggat, D.J., *et al*., *Vaccination induces HIV broadly neutralizing antibody precursors in humans.* Science, 2022. **378**(6623): p. eadd6502.
279. Murji, A.A., *et al*., *Elicitation of Neutralizing Antibody Responses to HIV-1 Immunization with Nanoparticle Vaccine Platforms.* Viruses, 2021. **13**(7).
280. Brouwer, P.J.M., *et al*., *Immunofocusing and enhancing autologous Tier-2 HIV-1 neutralization by displaying Env trimers on two-component protein nanoparticles.* NPJ Vaccines, 2021. **6**(1): p. 24.
281. Sanders, R.W. and J.P. Moore, *Native-like Env trimers as a platform for HIV-1 vaccine design.* Immunol Rev, 2017. **275**(1): p. 161-182.
282. Goo, L., *et al*., *Early development of broadly neutralizing antibodies in HIV-1-infected infants.* Nat Med, 2014. **20**(6): p. 655-8.
283. Del Moral-Sanchez, I., *et al*., *Triple tandem trimer immunogens for HIV-1 and influenza nucleic acid-based vaccines.* NPJ Vaccines, 2024. **9**(1): p. 74.
284. Bugude Laxmi, P.U.M.D., Thanjavur Naveen, Viswanath Buddolla, *Virus-like particles: Innovative strategies for combatting emerging and re-emerging viral threats.* The Microbe, 2025. **7**.
285. Martins, S.A., *et al*., *How promising are HIV-1-based virus-like particles for medical applications.* Front Cell Infect Microbiol, 2022. **12**: p. 997875.
286. Nooraei, S., *et al*., *Virus-like particles: preparation, immunogenicity and their roles as nanovaccines and drug nanocarriers.* J Nanobiotechnology, 2021. **19**(1): p. 59.
287. Bednarska, J., *et al*., *Rapid formation of human immunodeficiency virus-like particles.* Proc Natl Acad Sci U S A, 2020. **117**(35): p. 21637-21646.
288. Fernandes, B., *et al*., *Adaptive laboratory evolution of stable insect cell lines for improved HIV-Gag VLPs production.* J Biotechnol, 2020. **307**: p. 139-147.
289. Zhang, P., *et al*., *A multiclade env-gag VLP mRNA vaccine elicits tier-2 HIV-1-neutralizing antibodies and reduces the risk of heterologous SHIV infection in macaques.* Nat Med, 2021. **27**(12): p. 2234-2245.
290. Peters, B.S., *et al*., *A pilot phase II study of the safety and immunogenicity of HIV p17/p24:VLP (p24-VLP) in asymptomatic HIV seropositive subjects.* J Infect, 1997. **35**(3): p. 231-5.
291. Weber, J., *et al*., *Immunogenicity of the yeast recombinant p17/p24:Ty virus-like particles (p24-VLP) in healthy volunteers.* Vaccine, 1995. **13**(9): p. 831-4.
292. Coler, R.N., *et al*., *Adjuvants for malaria vaccines.* Parasite Immunol, 2009. **31**(9): p. 520-8.
293. Reed, S.G., *et al*., *New horizons in adjuvants for vaccine development.* Trends Immunol, 2009. **30**(1): p. 23-32.
294. Burke, B., *et al*., *Neutralizing antibody responses to subtype B and C adjuvanted HIV envelope protein vaccination in rabbits.* Virology, 2009. **387**(1): p. 147-56.
295. Carter, D. and S.G. Reed, *Role of adjuvants in modeling the immune response.* Curr Opin HIV AIDS, 2010. **5**(5): p. 409-13.
296. O'Hagan, D.T., *et al*., *The mechanism of action of MF59 - an innately attractive adjuvant formulation.* Vaccine, 2012. **30**(29): p. 4341-8.

297. Barnett, S.W., *et al*., *Antibody-mediated protection against mucosal simian-human immunodeficiency virus challenge of macaques immunized with alphavirus replicon particles and boosted with trimeric envelope glycoprotein in MF59 adjuvant.* J Virol, 2010. **84**(12): p. 5975-85.
298. Moradi Vahdat, M., *et al*., *Hepatitis B core-based virus-like particles: A platform for vaccine development in plants.* Biotechnol Rep (Amst), 2021. **29**: p. e00605.
299. Valenzuela, P., *et al*., *Synthesis and assembly of hepatitis B virus surface antigen particles in yeast.* Nature, 1982. **298**(5872): p. 347-50.
300. Hosseini, S.N., *et al*., *Assessing virus like particles formation and r-HBsAg aggregation during large scale production of recombinant hepatitis B surface antigen from Pichia pastoris.* Int J Biol Macromol, 2019. **139**: p. 697-711.
301. Lehky, M., *et al*., *A novel method for recombinant mammalian-expressed S-HBsAg virus-like particle production for assembly status analysis and improved anti-HBs serology.* Protein Sci, 2025. **34**(1): p. e5251.
302. McAleer, W.J., *et al*., *Human hepatitis B vaccine from recombinant yeast.* Nature, 1984. **307**(5947): p. 178-80.
303. Meireles, L.C., R.T. Marinho, and P. Van Damme, *Three decades of hepatitis B control with vaccination.* World J Hepatol, 2015. **7**(18): p. 2127-32.
304. Marini, A., *et al*., *A Universal Plug-and-Display Vaccine Carrier Based on HBsAg VLP to Maximize Effective Antibody Response.* Front Immunol, 2019. **10**: p. 2931.
305. *Malaria: Phase 3 trial results for vaccine RTS,S/AS01*. 2017; Available from: https://www.who.int/news-room/questions-and-answers/item/phase-3-trial-results-for-malaria-vaccine-rtss-as01.
306. Collins, K.A., *et al*., *Enhancing protective immunity to malaria with a highly immunogenic virus-like particle vaccine.* Sci Rep, 2017. **7**: p. 46621.
307. Datoo, M.S., *et al*., *Safety and efficacy of malaria vaccine candidate R21/Matrix-M in African children: a multicentre, double-blind, randomised, phase 3 trial.* Lancet, 2024. **403**(10426): p. 533-544.
308. Kotiw, M., *et al*., *Immunological response to parenteral vaccination with recombinant hepatitis B virus surface antigen virus-like particles expressing Helicobacter pylori KatA epitopes in a murine H. pylori challenge model.* Clin Vaccine Immunol, 2012. **19**(2): p. 268-76.
309. Dooley, L., *et al*., *Chimeric hepatitis B surface antigen virus-like particles expressing the strep A epitope p*17 elicit a humoral immune response in mice.* Heliyon, 2024. **10**(9): p. e30606.
310. Zakeri, B., *et al*., *Peptide tag forming a rapid covalent bond to a protein, through engineering a bacterial adhesin.* Proc Natl Acad Sci U S A, 2012. **109**(12): p. E690-7.
311. Yilan Chen, P.D., Minghui Li, Siyuan Liu, Zejie Chang, Dongna Ren, Ruiqi Li, Ning Zhang, Xueke Sun, Gaiping Zhang, *Spy&IAC enables specific capture of SpyTagged proteins for rapid assembly of plug-and-display nanoparticle vaccines.* International Journal of Biological Macromolecules, 2023. **226**: p. 240-253.
312. Tan, T.K., *et al*., *A COVID-19 vaccine candidate using SpyCatcher multimerization of the SARS-CoV-2 spike protein receptor-binding domain induces potent neutralising antibody responses.* Nat Commun, 2021. **12**(1): p. 542.
313. Escolano, A., *et al*., *Immunization expands B cells specific to HIV-1 V3 glycan in mice and macaques.* Nature, 2019. **570**(7762): p. 468-473.
314. Thrane, S., *et al*., *Bacterial superglue enables easy development of efficient virus-like particle based vaccines.* J Nanobiotechnology, 2016. **14**: p. 30.
315. Korber, B. and W. Fischer, *T cell-based strategies for HIV-1 vaccines.* Hum Vaccin Immunother, 2020. **16**(3): p. 713-722.

316. Hammer, S.M., *et al*., *Efficacy trial of a DNA/rAd5 HIV-1 preventive vaccine.* N Engl J Med, 2013. **369**(22): p. 2083-92.
317. Janes, H.E., *et al*., *Higher T-Cell Responses Induced by DNA/rAd5 HIV-1 Preventive Vaccine Are Associated With Lower HIV-1 Infection Risk in an Efficacy Trial.* J Infect Dis, 2017. **215**(9): p. 1376-1385.
318. Buchbinder, S.P., *et al*., *Efficacy assessment of a cell-mediated immunity HIV-1 vaccine (the Step Study): a double-blind, randomised, placebo-controlled, test-of-concept trial.* Lancet, 2008. **372**(9653): p. 1881-1893.
319. Gray, G.E., *et al*., *Recombinant adenovirus type 5 HIV gag/pol/nef vaccine in South Africa: unblinded, long-term follow-up of the phase 2b HVTN 503/Phambili study.* Lancet Infect Dis, 2014. **14**(5): p. 388-96.
320. Brander, C. and D. Hartigan-O'Connor, *HIV T-cell immunogen design and delivery.* Curr Opin HIV AIDS, 2022. **17**(6): p. 333-337.
321. Bailon, L., *et al*., *Safety, immunogenicity and effect on viral rebound of HTI vaccines in early treated HIV-1 infection: a randomized, placebo-controlled phase 1 trial.* Nat Med, 2022. **28**(12): p. 2611-2621.
322. Mothe, B., *et al*., *A human immune data-informed vaccine concept elicits strong and broad T-cell specificities associated with HIV-1 control in mice and macaques.* J Transl Med, 2015. **13**: p. 60.
323. Rolland, M., D.C. Nickle, and J.I. Mullins, *HIV-1 group M conserved elements vaccine.* PLoS Pathog, 2007. **3**(11): p. e157.
324. Hu, X., *et al*., *Gag and env conserved element CE DNA vaccines elicit broad cytotoxic T cell responses targeting subdominant epitopes of HIV and SIV Able to recognize virus-infected cells in macaques.* Hum Vaccin Immunother, 2018. **14**(9): p. 2163-2177.
325. McMichael, A.J. and M. Carrington, *Topological perspective on HIV escape.* Science, 2019. **364**(6439): p. 438-439.
326. Gaiha, G.D., *et al*., *Structural topology defines protective CD8(+) T cell epitopes in the HIV proteome.* Science, 2019. **364**(6439): p. 480-484.
327. Letourneau, S., *et al*., *Design and pre-clinical evaluation of a universal HIV-1 vaccine.* PLoS One, 2007. **2**(10): p. e984.
328. Ondondo, B., *et al*., *Absence of systemic toxicity changes following intramuscular administration of novel pSG2.HIVconsv DNA, ChAdV63.HIVconsv and MVA.HIVconsv vaccines to BALB/c mice.* Vaccine, 2013. **31**(47): p. 5594-601.
329. Hanke, T., *Aiming for protective T-cell responses: a focus on the first generation conserved-region HIVconsv vaccines in preventive and therapeutic clinical trials.* Expert Rev Vaccines, 2019. **18**(10): p. 1029-1041.
330. Hayton, E.J., *et al*., *Safety and tolerability of conserved region vaccines vectored by plasmid DNA, simian adenovirus and modified vaccinia virus ankara administered to human immunodeficiency virus type 1-uninfected adults in a randomized, single-blind phase I trial.* PLoS One, 2014. **9**(7): p. e101591.
331. Borthwick, N., *et al*., *Vaccine-elicited human T cells recognizing conserved protein regions inhibit HIV-1.* Mol Ther, 2014. **22**(2): p. 464-475.
332. Ondondo, B., *et al*., *Novel Conserved-region T-cell Mosaic Vaccine With High Global HIV-1 Coverage Is Recognized by Protective Responses in Untreated Infection.* Mol Ther, 2016. **24**(4): p. 832-42.
333. Fischer, W., *et al*., *Polyvalent vaccines for optimal coverage of potential T-cell epitopes in global HIV-1 variants.* Nat Med, 2007. **13**(1): p. 100-6.
334. Mothe, B., *et al*., *Definition of the viral targets of protective HIV-1-specific T cell responses.* J Transl Med, 2011. **9**: p. 208.

335. Ondondo, B. and S. Abdul-Jawad, *Vector Delivery-Dependant Effect of Human Tissue Plasminogen Activator Signal Peptide on Vaccine Induction of T Cells.* Journal of HIV and AIDS, 2016. **2**.
336. Borthwick, N., *et al*., *Safety and immunogenicity of the ChAdOx1-MVA-vectored conserved mosaic HIVconsvX candidate T-cell vaccines in HIV-CORE 005.2, an open-label, dose-escalation, first-in-human, phase 1 trial in adults living without HIV-1 in the UK.* Lancet Microbe, 2025. **6**(3): p. 100956.
337. Chanda, C., *et al*., *Safety and broad immunogenicity of HIVconsvX conserved mosaic candidate T-cell vaccines vectored by ChAdOx1 and MVA in HIV-CORE 006: a double-blind, randomised, placebo-controlled phase 1 trial in healthy adults living without HIV-1 in eastern and southern Africa.* Lancet Microbe, 2025. **6**(6): p. 101041.
338. Ondondo, B.O., *The influence of delivery vectors on HIV vaccine efficacy.* Front Microbiol, 2014. **5**: p. 439.
339. Olvera, A., *et al*., *Impact of ChAdOx1 or DNA Prime Vaccination on Magnitude, Breadth, and Focus of MVA-Boosted Immunogen-Specific T Cell Responses.* Vaccines (Basel), 2024. **12**(3).
340. Ewer, K.J., *et al*., *Viral vectors as vaccine platforms: from immunogenicity to impact.* Curr Opin Immunol, 2016. **41**: p. 47-54.
341. Lasaro, M.O. and H.C. Ertl, *New insights on adenovirus as vaccine vectors.* Mol Ther, 2009. **17**(8): p. 1333-9.
342. Pillai, V.K., *et al*., *Different patterns of expansion, contraction and memory differentiation of HIV-1 Gag-specific CD8 T cells elicited by adenovirus type 5 and modified vaccinia Ankara vaccines.* Vaccine, 2011. **29**(33): p. 5399-406.
343. Folegatti, P.M., *et al*., *Safety and immunogenicity of the ChAdOx1 nCoV-19 vaccine against SARS-CoV-2: a preliminary report of a phase 1/2, single-blind, randomised controlled trial.* Lancet, 2020. **396**(10249): p. 467-478.
344. Zhou, D., *et al*., *A chimpanzee-origin adenovirus vector expressing the rabies virus glycoprotein as an oral vaccine against inhalation infection with rabies virus.* Mol Ther, 2006. **14**(5): p. 662-72.
345. Jia, W., *et al*., *Single intranasal immunization with chimpanzee adenovirus-based vaccine induces sustained and protective immunity against MERS-CoV infection.* Emerg Microbes Infect, 2019. **8**(1): p. 760-772.
346. Morris, S.J., *et al*., *Simian adenoviruses as vaccine vectors.* Future Virol, 2016. **11**(9): p. 649-659.
347. Folegatti, P.M., *et al*., *Vaccines based on the replication-deficient simian adenoviral vector ChAdOx1: Standardized template with key considerations for a risk/benefit assessment.* Vaccine, 2022. **40**(35): p. 5248-5262.
348. Travieso, T., *et al*., *The use of viral vectors in vaccine development.* NPJ Vaccines, 2022. **7**(1): p. 75.
349. Ewer, K.J., *et al*., *T cell and antibody responses induced by a single dose of ChAdOx1 nCoV-19 (AZD1222) vaccine in a phase 1/2 clinical trial.* Nat Med, 2021. **27**(2): p. 270-278.
350. Volz, A. and G. Sutter, *Modified Vaccinia Virus Ankara: History, Value in Basic Research, and Current Perspectives for Vaccine Development.* Adv Virus Res, 2017. **97**: p. 187-243.
351. Carroll, M.W. and B. Moss, *Host range and cytopathogenicity of the highly attenuated MVA strain of vaccinia virus: propagation and generation of recombinant viruses in a nonhuman mammalian cell line.* Virology, 1997. **238**(2): p. 198-211.
352. Meyer, H., G. Sutter, and A. Mayr, *Mapping of deletions in the genome of the highly attenuated vaccinia virus MVA and their influence on virulence.* J Gen Virol, 1991. **72 (Pt 5)**: p. 1031-8.
353. Mahnel, H. and A. Mayr, *[Experiences with immunization against orthopox viruses of humans and animals using vaccine strain MVA].* Berl Munch Tierarztl Wochenschr, 1994. **107**(8): p. 253-6.

354. Draper, S.J., *et al*., *Effective induction of high-titer antibodies by viral vector vaccines.* Nat Med, 2008. **14**(8): p. 819-21.
355. Barouch, D.H., *et al*., *Vaccine protection against acquisition of neutralization-resistant SIV challenges in rhesus monkeys.* Nature, 2012. **482**(7383): p. 89-93.
356. McConkey, S.J., *et al*., *Enhanced T-cell immunogenicity of plasmid DNA vaccines boosted by recombinant modified vaccinia virus Ankara in humans.* Nat Med, 2003. **9**(6): p. 729-35.
357. Anderson, R.J., *et al*., *Enhanced CD8+ T cell immune responses and protection elicited against Plasmodium berghei malaria by prime boost immunization regimens using a novel attenuated fowlpox virus.* J Immunol, 2004. **172**(5): p. 3094-100.
358. Sheehy, S.H., *et al*., *Phase Ia clinical evaluation of the Plasmodium falciparum blood-stage antigen MSP1 in ChAd63 and MVA vaccine vectors.* Mol Ther, 2011. **19**(12): p. 2269-76.
359. Scriba, T.J., *et al*., *A phase IIa trial of the new tuberculosis vaccine, MVA85A, in HIV- and/or Mycobacterium tuberculosis-infected adults.* Am J Respir Crit Care Med, 2012. **185**(7): p. 769-78.
360. Tameris, M.D., *et al*., *Safety and efficacy of MVA85A, a new tuberculosis vaccine, in infants previously vaccinated with BCG: a randomised, placebo-controlled phase 2b trial.* Lancet, 2013. **381**(9871): p. 1021-8.
361. Guimaraes-Walker, A., *et al*., *Lessons from IAVI-006, a phase I clinical trial to evaluate the safety and immunogenicity of the pTHr.HIVA DNA and MVA.HIVA vaccines in a prime-boost strategy to induce HIV-1 specific T-cell responses in healthy volunteers.* Vaccine, 2008. **26**(51): p. 6671-7.
362. Gomez, C.E., *et al*., *The HIV/AIDS vaccine candidate MVA-B administered as a single immunogen in humans triggers robust, polyfunctional, and selective effector memory T cell responses to HIV-1 antigens.* J Virol, 2011. **85**(21): p. 11468-78.
363. Garcia, F., *et al*., *Safety and immunogenicity of a modified pox vector-based HIV/AIDS vaccine candidate expressing Env, Gag, Pol and Nef proteins of HIV-1 subtype B (MVA-B) in healthy HIV-1-uninfected volunteers: A phase I clinical trial (RISVAC02).* Vaccine, 2011. **29**(46): p. 8309-16.
364. Bakari, M., *et al*., *Broad and potent immune responses to a low dose intradermal HIV-1 DNA boosted with HIV-1 recombinant MVA among healthy adults in Tanzania.* Vaccine, 2011. **29**(46): p. 8417-28.
365. Wang, T., *et al*., *Parainfluenza virus 5 is a next-generation vaccine vector for human infectious pathogens.* J Med Virol, 2023. **95**(3): p. e28622.
366. Chatziandreou, N., *et al*., *Relationships and host range of human, canine, simian and porcine isolates of simian virus 5 (parainfluenza virus 5).* J Gen Virol, 2004. **85**(Pt 10): p. 3007-3016.
367. Azetaka, M. and S. Konishi, *Kennel cough complex: confirmation and analysis of the outbreak in Japan.* Nihon Juigaku Zasshi, 1988. **50**(4): p. 851-8.
368. He, B., *et al*., *Recovery of infectious SV5 from cloned DNA and expression of a foreign gene.* Virology, 1997. **237**(2): p. 249-60.
369. Phan, S.I., *et al*., *Genetic Stability of Parainfluenza Virus 5-Vectored Human Respiratory Syncytial Virus Vaccine Candidates after In Vitro and In Vivo Passage.* J Virol, 2017. **91**(19).
370. Chen, Z., *Parainfluenza virus 5-vectored vaccines against human and animal infectious diseases.* Rev Med Virol, 2018. **28**(2).
371. Li, Z., *et al*., *Recombinant parainfluenza virus 5 expressing hemagglutinin of influenza A virus H5N1 protected mice against lethal highly pathogenic avian influenza virus H5N1 challenge.* J Virol, 2013. **87**(1): p. 354-62.
372. Huang, Y., *et al*., *Parainfluenza virus 5 expressing the G protein of rabies virus protects mice after rabies virus infection.* J Virol, 2015. **89**(6): p. 3427-9.

373. Spearman, P., *et al*., *Intranasal parainfluenza virus type 5 (PIV5)-vectored RSV vaccine is safe and immunogenic in healthy adults in a phase 1 clinical study.* Sci Adv, 2023. **9**(43): p. eadj7611.
374. Spearman, P., *et al*., *Safety and immunogenicity of intranasal parainfluenza virus type 5 (PIV5)-vectored COVID-19 vaccine in adults and teens in an open-label phase 1 trial.* Sci Adv, 2025. **11**(27): p. eadw0896.
375. Kardani, K., A. Bolhassani, and S. Shahbazi, *Prime-boost vaccine strategy against viral infections: Mechanisms and benefits.* Vaccine, 2016. **34**(4): p. 413-423.
376. Lu, S., *Heterologous prime-boost vaccination.* Curr Opin Immunol, 2009. **21**(3): p. 346-51.
377. Ramgi, P., *et al*., *Immunogenicity and Safety of Heterologous Versus Homologous Prime-Boost Regimens With BBIBP-CorV and Ad26.COV2.S COVID-19 Vaccines: A Multicentric, Randomized, Observer-Blinded Non-inferiority Trial in Madagascar and Mozambique.* Clin Infect Dis, 2025. **80**(Supplement_1): p. S37-S46.
378. Reyes-Sandoval, A., *et al*., *Prime-boost immunization with adenoviral and modified vaccinia virus Ankara vectors enhances the durability and polyfunctionality of protective malaria CD8+ T-cell responses.* Infect Immun, 2010. **78**(1): p. 145-53.
379. Coughlan, L., *et al*., *Heterologous Two-Dose Vaccination with Simian Adenovirus and Poxvirus Vectors Elicits Long-Lasting Cellular Immunity to Influenza Virus A in Healthy Adults.* EBioMedicine, 2018. **29**: p. 146-154.
380. Sophia Abene, N.G. *The M&M Study: Age-Related T Cell Response in People with HIV on ART in MVA.HIVconsvX Vaccine Trial*. 2025; Available from: https://www.contagionlive.com/view/the-m-m-study-age-related-t-cell-response-in-people-with-hiv-on-art-in-mva-hivconsvx-vaccine-trial
381. Beavis, A.C., *et al*., *Combined intranasal and intramuscular parainfluenza 5-, simian adenovirus ChAdOx1- and poxvirus MVA-vectored vaccines induce synergistically HIV-1-specific T cells in the mucosa.* Front Immunol, 2023. **14**: p. 1186478.
382. Wee, E.G., *et al*., *Effect of epitope variant co-delivery on the depth of CD8 T cell responses induced by HIV-1 conserved mosaic vaccines.* Mol Ther Methods Clin Dev, 2021. **21**: p. 741-753.
383. de Taeye, S.W., *et al*., *Immunogenicity of Stabilized HIV-1 Envelope Trimers with Reduced Exposure of Non-neutralizing Epitopes.* Cell, 2015. **163**(7): p. 1702-15.
384. Keeble, A.H., *et al*., *Evolving Accelerated Amidation by SpyTag/SpyCatcher to Analyze Membrane Dynamics.* Angew Chem Int Ed Engl, 2017. **56**(52): p. 16521-16525.
385. Wilkie, M., *et al*., *A phase I trial evaluating the safety and immunogenicity of a candidate tuberculosis vaccination regimen, ChAdOx1 85A prime - MVA85A boost in healthy UK adults.* Vaccine, 2020. **38**(4): p. 779-789.
386. Barouch, D.H., *et al*., *Mosaic HIV-1 vaccines expand the breadth and depth of cellular immune responses in rhesus monkeys.* Nat Med, 2010. **16**(3): p. 319-23.
387. van Duijn, J., *et al*., *Mosaic HIV-1 vaccination induces anti-viral CD8(+) T cell functionality in the phase 1/2a clinical trial APPROACH.* J Virol, 2023. **97**(10): p. e0112623.
388. Buggert, M., A.S. Japp, and M.R. Betts, *Everything in its right place: resident memory CD8+ T cell immunosurveillance of HIV infection.* Curr Opin HIV AIDS, 2019. **14**(2): p. 93-99.
389. Akbari, E., M. Seyedinkhorasani, and A. Bolhassani, *Conserved multiepitope vaccine constructs: A potent HIV-1 therapeutic vaccine in clinical trials.* Braz J Infect Dis, 2023. **27**(3): p. 102774.
390. Guardo, A.C., *et al*., *Preclinical evaluation of an mRNA HIV vaccine combining rationally selected antigenic sequences and adjuvant signals (HTI-TriMix).* AIDS, 2017. **31**(3): p. 321-332.
391. Reguzova, A.Y., *et al*., *Peptide-MHC multimer-based monitoring of CD8 T-cells in HIV-1 infection and AIDS vaccine development.* Expert Rev Vaccines, 2015. **14**(1): p. 69-84.

392. Kaseke, C., *et al*., *The Emerging Role for CTL Epitope Specificity in HIV Cure Efforts.* J Infect Dis, 2021. **223**(12 Suppl 2): p. 32-37.
393. Hayes, P., *et al*., *Breadth of CD8 T-cell mediated inhibition of replication of diverse HIV-1 transmitted-founder isolates correlates with the breadth of recognition within a comprehensive HIV-1 Gag, Nef, Env and Pol potential T-cell epitope (PTE) peptide set.* PLoS One, 2021. **16**(11): p. e0260118.
394. Ritz, D., *et al*., *High-sensitivity HLA class I peptidome analysis enables a precise definition of peptide motifs and the identification of peptides from cell lines and patients' sera.* Proteomics, 2016. **16**(10): p. 1570-80.
395. *HIV databases*. Available from: https://www.hiv.lanl.gov/content/index.
396. Anuska Llano, S.C., Sandra Silva Arrieta, and Christian Brander, *Optimal CTL Review*. 2019.
397. Janes, H., *et al*., *Vaccine-induced gag-specific T cells are associated with reduced viremia after HIV-1 infection.* J Infect Dis, 2013. **208**(8): p. 1231-9.
398. Chen, Z., *et al*., *Evaluating a parainfluenza virus 5-based vaccine in a host with pre-existing immunity against parainfluenza virus 5.* PLoS One, 2012. **7**(11): p. e50144.
399. Shacklett, B.L., *Mucosal immunity in acute HIV: a review of recent work.* Curr Opin HIV AIDS, 2025. **20**(3): p. 193-198.
400. Caputo, V., *et al*., *The initial interplay between HIV and mucosal innate immunity.* Front Immunol, 2023. **14**: p. 1104423.
401. Demberg, T. and M. Robert-Guroff, *Mucosal immunity and protection against HIV/SIV infection: strategies and challenges for vaccine design.* Int Rev Immunol, 2009. **28**(1): p. 20-48.
402. Gallichan, W.S. and K.L. Rosenthal, *Long-term immunity and protection against herpes simplex virus type 2 in the murine female genital tract after mucosal but not systemic immunization.* J Infect Dis, 1998. **177**(5): p. 1155-61.
403. Gherardi, M.M., *et al*., *Induction of HIV immunity in the genital tract after intranasal delivery of a MVA vector: enhanced immunogenicity after DNA prime-modified vaccinia virus Ankara boost immunization schedule.* J Immunol, 2004. **172**(10): p. 6209-20.
404. Wee, E.G., *et al*., *HIV-1 Conserved Mosaics Delivered by Regimens with Integration-Deficient DC-Targeting Lentiviral Vector Induce Robust T Cells.* Mol Ther, 2017. **25**(2): p. 494-503.
405. Kilpelainen, A., *et al*., *Priming With Recombinant BCG Expressing Novel HIV-1 Conserved Mosaic Immunogens and Boosting With Recombinant ChAdOx1 Is Safe, Stable, and Elicits HIV-1-Specific T-Cell Responses in BALB/c Mice.* Front Immunol, 2019. **10**: p. 923.
406. Moyo, N., *et al*., *Efficient Induction of T Cells against Conserved HIV-1 Regions by Mosaic Vaccines Delivered as Self-Amplifying mRNA.* Mol Ther Methods Clin Dev, 2019. **12**: p. 32-46.
407. Moyo, N., *et al*., *Tetravalent Immunogen Assembled from Conserved Regions of HIV-1 and Delivered as mRNA Demonstrates Potent Preclinical T-Cell Immunogenicity and Breadth.* Vaccines (Basel), 2020. **8**(3).
408. Xiao, P., *et al*., *Parainfluenza Virus 5 Priming Followed by SIV/HIV Virus-Like-Particle Boosting Induces Potent and Durable Immune Responses in Nonhuman Primates.* Front Immunol, 2021. **12**: p. 623996.
409. Ruane, D., *et al*., *A dendritic cell targeted vaccine induces long-term HIV-specific immunity within the gastrointestinal tract.* Mucosal Immunol, 2016. **9**(5): p. 1340-52.
410. Yanagita, M., *et al*., *Nasopharyngeal-associated lymphoreticular tissue (NALT) immunity: fimbriae-specific Th1 and Th2 cell-regulated IgA responses for the inhibition of bacterial attachment to epithelial cells and subsequent inflammatory cytokine production.* J Immunol, 1999. **162**(6): p. 3559-65.
411. Langermann, S., *et al*., *Systemic and mucosal immunity induced by BCG vector expressing outer-surface protein A of Borrelia burgdorferi.* Nature, 1994. **372**(6506): p. 552-5.

412. Velge-Roussel, F., *et al*., *Intranasal immunization with Toxoplasma gondii SAG1 induces protective cells into both NALT and GALT compartments.* Infect Immun, 2000. **68**(2): p. 969-72.
413. Cokarić Brdovčak, M., *et al*., *ChAdOx1-S adenoviral vector vaccine applied intranasally elicits superior mucosal immunity compared to the intramuscular route of vaccination.* Eur J Immunol, 2022. **52**(6): p. 936-945.
414. Abdul-Jawad, S., *et al*., *Increased Valency of Conserved-mosaic Vaccines Enhances the Breadth and Depth of Epitope Recognition.* Mol Ther, 2016. **24**(2): p. 375-384.
415. Del Moral-Sanchez, I. and K. Sliepen, *Strategies for inducing effective neutralizing antibody responses against HIV-1.* Expert Rev Vaccines, 2019. **18**(11): p. 1127-1143.
416. Julien, J.P., *et al*., *Asymmetric recognition of the HIV-1 trimer by broadly neutralizing antibody PG9.* Proc Natl Acad Sci U S A, 2013. **110**(11): p. 4351-6.
417. Sanders, R.W., *et al*., *A next-generation cleaved, soluble HIV-1 Env trimer, BG505 SOSIP.664 gp140, expresses multiple epitopes for broadly neutralizing but not non-neutralizing antibodies.* PLoS Pathog, 2013. **9**(9): p. e1003618.
418. Medina-Ramirez, M., *et al*., *Design and crystal structure of a native-like HIV-1 envelope trimer that engages multiple broadly neutralizing antibody precursors in vivo.* J Exp Med, 2017. **214**(9): p. 2573-2590.
419. Binley, J.M., *et al*., *Enhancing the proteolytic maturation of human immunodeficiency virus type 1 envelope glycoproteins.* J Virol, 2002. **76**(6): p. 2606-16.
420. de Taeye, S.W., J.P. Moore, and R.W. Sanders, *HIV-1 Envelope Trimer Design and Immunization Strategies To Induce Broadly Neutralizing Antibodies.* Trends Immunol, 2016. **37**(3): p. 221-232.
421. Kong, L., *et al*., *Uncleaved prefusion-optimized gp140 trimers derived from analysis of HIV-1 envelope metastability.* Nat Commun, 2016. **7**: p. 12040.
422. Bachmann, M.F., *et al*., *The influence of antigen organization on B cell responsiveness.* Science, 1993. **262**(5138): p. 1448-51.
423. Mohsen, M.O., G. Augusto, and M.F. Bachmann, *The 3Ds in virus-like particle based-vaccines: "Design, Delivery and Dynamics".* Immunol Rev, 2020. **296**(1): p. 155-168.
424. Mohsen, M.O., *et al*., *Interaction of Viral Capsid-Derived Virus-Like Particles (VLPs) with the Innate Immune System.* Vaccines (Basel), 2018. **6**(3).
425. Link, A., *et al*., *Innate immunity mediates follicular transport of particulate but not soluble protein antigen.* J Immunol, 2012. **188**(8): p. 3724-33.
426. Zinkhan, S., *et al*., *The impact of size on particle drainage dynamics and antibody response.* J Control Release, 2021. **331**: p. 296-308.
427. Mohsen, M.O. and M.F. Bachmann, *Virus-like particle vaccinology, from bench to bedside.* Cell Mol Immunol, 2022. **19**(9): p. 993-1011.
428. Aves, K.L. and A.F. Sander, *Design and Purification of Tag/Catcher AP205-Based Capsid Virus-Like Particle Vaccines.* Methods Mol Biol, 2024. **2720**: p. 127-141.
429. Smit, M.J., *et al*., *First-in-human use of a modular capsid virus-like vaccine platform: an open-label, non-randomised, phase 1 clinical trial of the SARS-CoV-2 vaccine ABNCoV2.* Lancet Microbe, 2023. **4**(3): p. e140-e148.
430. Scanlan, C.N., *et al*., *The Broadly Neutralizing Anti-Human Immunodeficiency Virus Type 1 Antibody 2G12 Recognizes a Cluster of α1→2 Mannose Residues on the Outer Face of gp120.* Journal of Virology, 2002. **76**(14): p. 7306-7321.
431. Zhou, T., *et al*., *Structural basis for broad and potent neutralization of HIV-1 by antibody VRC01.* Science, 2010. **329**(5993): p. 811-7.
432. Julien, J.P., *et al*., *Broadly neutralizing antibody PGT121 allosterically modulates CD4 binding via recognition of the HIV-1 gp120 V3 base and multiple surrounding glycans.* PLoS Pathog, 2013. **9**(5): p. e1003342.

433. Lee, J.H., *et al*., *A Broadly Neutralizing Antibody Targets the Dynamic HIV Envelope Trimer Apex via a Long, Rigidified, and Anionic beta-Hairpin Structure.* Immunity, 2017. **46**(4): p. 690-702.
434. Crank, M.C., *et al*., *A proof of concept for structure-based vaccine design targeting RSV in humans.* Science, 2019. **365**(6452): p. 505-509.
435. Pallesen, J., *et al*., *Immunogenicity and structures of a rationally designed prefusion MERS-CoV spike antigen.* Proc Natl Acad Sci U S A, 2017. **114**(35): p. E7348-E7357.
436. Sanders, R.W., *et al*., *Stabilization of the soluble, cleaved, trimeric form of the envelope glycoprotein complex of human immunodeficiency virus type 1.* J Virol, 2002. **76**(17): p. 8875-89.
437. Selvarajah, S., *et al*., *Focused dampening of antibody response to the immunodominant variable loops by engineered soluble gp140.* AIDS Res Hum Retroviruses, 2008. **24**(2): p. 301-14.
438. Yang, X., *et al*., *Characterization of stable, soluble trimers containing complete ectodomains of human immunodeficiency virus type 1 envelope glycoproteins.* J Virol, 2000. **74**(12): p. 5716-25.
439. Yang, X., *et al*., *Highly stable trimers formed by human immunodeficiency virus type 1 envelope glycoproteins fused with the trimeric motif of T4 bacteriophage fibritin.* J Virol, 2002. **76**(9): p. 4634-42.
440. Sliepen, K., *et al*., *Immunosilencing a highly immunogenic protein trimerization domain.* J Biol Chem, 2015. **290**(12): p. 7436-42.
441. *DRUG: Brolucizumab*. Available from: https://www.kegg.jp/entry/D11083.
442. Meckler, J.F., *et al*., *A Novel bispecific T-cell engager (BiTE) targeting CD22 and CD3 has both in vitro and in vivo activity and synergizes with blinatumomab in an acute lymphoblastic leukemia (ALL) tumor model.* Cancer Immunol Immunother, 2023. **72**(9): p. 2939-2948.
443. Aldon, Y., *et al*., *Rational Design of DNA-Expressed Stabilized Native-Like HIV-1 Envelope Trimers.* Cell Rep, 2018. **24**(12): p. 3324-3338 e5.
444. Aldon, Y., *et al*., *Immunogenicity of stabilized HIV-1 Env trimers delivered by self-amplifying mRNA.* Mol Ther Nucleic Acids, 2021. **25**: p. 483-493.
445. Pollock, K.M., *et al*., *Experimental medicine study with stabilised native-like HIV-1 Env immunogens drives long-term antibody responses, but lacks neutralising breadth.* EBioMedicine, 2025. **112**: p. 105544.
446. Sok, D., *et al*., *Recombinant HIV envelope trimer selects for quaternary-dependent antibodies targeting the trimer apex.* Proc Natl Acad Sci U S A, 2014. **111**(49): p. 17624-9.
447. Brouwer, P.J.M., *et al*., *Enhancing and shaping the immunogenicity of native-like HIV-1 envelope trimers with a two-component protein nanoparticle.* Nat Commun, 2019. **10**(1): p. 4272.
448. Klein, J.S. and P.J. Bjorkman, *Few and far between: how HIV may be evading antibody avidity.* PLoS Pathog, 2010. **6**(5): p. e1000908.
449. Schiller, J. and B. Chackerian, *Why HIV virions have low numbers of envelope spikes: implications for vaccine development.* PLoS Pathog, 2014. **10**(8): p. e1004254.
450. Brune, K.D., *et al*., *Plug-and-Display: decoration of Virus-Like Particles via isopeptide bonds for modular immunization.* Sci Rep, 2016. **6**: p. 19234.
451. Tipoe, T., S. Fidler, and J. Frater, *An exploration of how broadly neutralizing antibodies might induce HIV remission: the 'vaccinal' effect.* Curr Opin HIV AIDS, 2022. **17**(3): p. 162-170.
452. Maciel, M., Jr., *et al*., *Exploring synergies between B- and T-cell vaccine approaches to optimize immune responses against HIV-workshop report.* NPJ Vaccines, 2024. **9**(1): p. 39.
453. Arunachalam, P.S., *et al*., *T cell-inducing vaccine durably prevents mucosal SHIV infection even with lower neutralizing antibody titers.* Nat Med, 2020. **26**(6): p. 932-940.

454. Mothe, B., *et al*., *HIVconsv Vaccines and Romidepsin in Early-Treated HIV-1-Infected Individuals: Safety, Immunogenicity and Effect on the Viral Reservoir (Study BCN02).* Front Immunol, 2020. **11**: p. 823.
455. Gunst, J.D., *et al*., *Early intervention with 3BNC117 and romidepsin at antiretroviral treatment initiation in people with HIV-1: a phase 1b/2a, randomized trial.* Nat Med, 2022. **28**(11): p. 2424-2435.
456. Zou, C., *et al*., *Effective Suppression of HIV-1 Replication by Cytotoxic T Lymphocytes Specific for Pol Epitopes in Conserved Mosaic Vaccine Immunogens.* J Virol, 2019. **93**(7).
457. Kalams, S.A., *et al*., *Focusing HIV-1 Gag T cell responses to highly conserved regions by DNA vaccination in HVTN 119.* JCI Insight, 2024. **9**(18).
458. Peluso, M.J., *et al*., *Combination immunotherapy induces post-intervention control of HIV.* Res Sq, 2025.
459. Gunst, J.D., *et al*., *Impact of a TLR9 agonist and broadly neutralizing antibodies on HIV-1 persistence: the randomized phase 2a TITAN trial.* Nat Med, 2023. **29**(10): p. 2547-2558.
460. Mutua, G., *et al*., *Broad HIV-1 inhibition in vitro by vaccine-elicited CD8(+) T cells in African adults.* Mol Ther Methods Clin Dev, 2016. **3**: p. 16061.
461. Colloca, S., *et al*., *Vaccine vectors derived from a large collection of simian adenoviruses induce potent cellular immunity across multiple species.* Sci Transl Med, 2012. **4**(115): p. 115ra2.
462. Gray, G., S. Buchbinder, and A. Duerr, *Overview of STEP and Phambili trial results: two phase IIb test-of-concept studies investigating the efficacy of MRK adenovirus type 5 gag/pol/nef subtype B HIV vaccine.* Curr Opin HIV AIDS, 2010. **5**(5): p. 357-61.
463. Hanke, T., A.J. McMichael, and L. Dorrell, *Clinical experience with plasmid DNA- and modified vaccinia virus Ankara-vectored human immunodeficiency virus type 1 clade A vaccine focusing on T-cell induction.* J Gen Virol, 2007. **88**(Pt 1): p. 1-12.
464. *HIV Molecular Immunology 2024, Editors: Jennifer L. Mamrosh, Elizabeth-Sharon David-Fung, Bette T. M. Korber, Christian Brander, Dan Barouch, Rob de Boer, Barton F. Haynes, P. J. Klasse, Richard Koup, Bjoern Peters, Michael Seaman, and Bruce D. Walker. 2024. Publisher: Los Alamos National Laboratory, Theoretical Biology and Biophysics, Los Alamos, New Mexico. LA-UR-24-32444.*
465. Mothe, B. *Future design and conduct of vaccine and bNAb clinical trials SY01 symposium vaccines and bNAbs*. in *Research for Prevention Conference/R4P*. 2024.
466. Mothe, B. and C. Brander, *Prospects for therapeutic T-cell vaccine strategies for HIV cure.* Curr Opin HIV AIDS, 2025. **20**(5): p. 463-471.
467. IrsiCaixa. *A Phase I, Randomized, Double-Blind, Placebo-Controlled Safety, Tolerability and Immunogenicity Study of Candidate HIV-1 Vaccines ChAdOx1.HTI and MVA.HTI With Recombinant HIV-1 Envelope Protein ConM SOSIP.v7 gp140 Vaccine, Adjuvanted With MPLA Liposomes in ART-Suppressed HIV-1 Positive Individuals*. 2024; Available from: https://ichgcp.net/clinical-trials-registry/NCT05208125.
468. Buffa, V., *et al*., *Evaluation of TLR agonists as potential mucosal adjuvants for HIV gp140 and tetanus toxoid in mice.* PLoS One, 2012. **7**(12): p. e50529.
469. Arias, M.A., *et al*., *Glucopyranosyl Lipid Adjuvant (GLA), a Synthetic TLR4 agonist, promotes potent systemic and mucosal responses to intranasal immunization with HIVgp140.* PLoS One, 2012. **7**(7): p. e41144.
470. Kozlowski, P.A., *et al*., *Differential induction of mucosal and systemic antibody responses in women after nasal, rectal, or vaginal immunization: influence of the menstrual cycle.* J Immunol, 2002. **169**(1): p. 566-74.
471. Cosgrove, C.A., *et al*., *Comparative Immunogenicity of HIV-1 gp140 Vaccine Delivered by Parenteral, and Mucosal Routes in Female Volunteers; MUCOVAC2, A Randomized Two Centre Study.* PLoS One, 2016. **11**(5): p. e0152038.

472. Hessell, A.J., *et al*., *Fc receptor but not complement binding is important in antibody protection against HIV.* Nature, 2007. **449**(7158): p. 101-4.
473. Xiao, P., *et al*., *Multiple vaccine-elicited nonneutralizing antienvelope antibody activities contribute to protective efficacy by reducing both acute and chronic viremia following simian/human immunodeficiency virus SHIV89.6P challenge in rhesus macaques.* J Virol, 2010. **84**(14): p. 7161-73.
474. *Fluenz® intranasal live attenuated influenza vaccine: EU summary of product characteristics*. Available from: http://www.ema.europa.eu/docs/%0Aen_GB/document_library/EPAR and https://www.medicines.org.uk/emc/files/pil.15790.pdf.
475. CanSinoBIO. *CanSinoBIO's convidecia air™ approved for emergency use in Morocco*. 2022; Available from: http://47.99.161.107/detail-3927.
476. CanSinoBIO. *CanSinoBIO's Convidecia Air® Receives Approval in Indonesia*. 2023; Available from: http://47.99.161.107/detail-3941.
477. Biotech, B. *Bharat Biotech's iNCOVACC world's first Intra Nasal vaccine receives approval for emergency use in India*. 2022; Available from: https://bharatbiotech.com/images/press/Bharat-Biotech-iNCOVACC-Worlds-First-Intra-Nasal-Vaccine-Receives-Approval.pdf.
478. Tukhvatulin, A.I., *et al*., *Immunogenicity and protectivity of intranasally delivered vector-based heterologous prime-boost COVID-19 vaccine Sputnik V in mice and non-human primates.* Emerg Microbes Infect, 2022. **11**(1): p. 2229-2247.
479. *Two homegrown vaccines receive emergency use license*. 2021; Available from: https://www.tehrantimes.com/news/466570/Two-homegrown-vaccines-receive-emergency-use-license.
480. Skwarczynski, M. and I. Toth, *Non-invasive mucosal vaccine delivery: advantages, challenges and the future.* Expert Opin Drug Deliv, 2020. **17**(4): p. 435-437.
481. Parren, P.W., D.R. Burton, and Q.J. Sattentau, *HIV-1 antibody--debris or virion?* Nat Med, 1997. **3**(4): p. 366-7.